

Migration of phenolic compounds from cork to wine: reactivity and sensory implications

Joana Filomena da Costa Azevedo

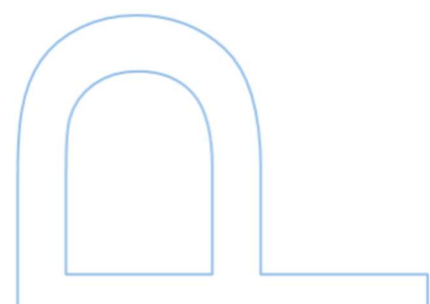
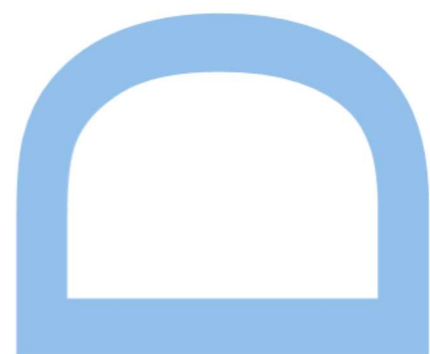
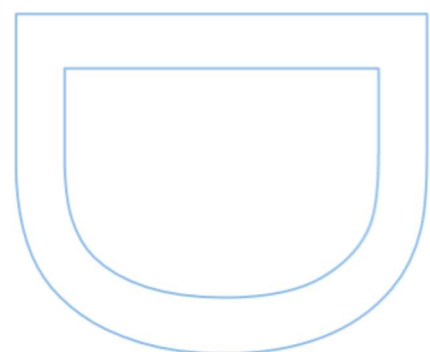
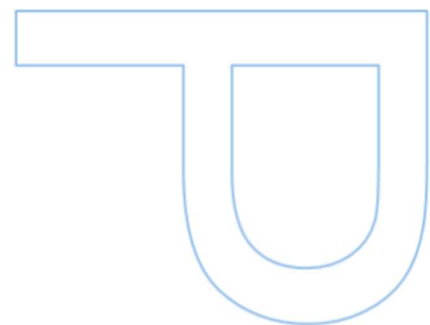
Programa Doutoral em Química
Departamento Química e Bioquímica da Universidade do Porto
2023

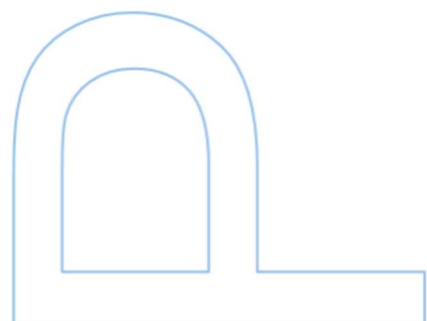
Orientador

Doutor Vítor de Freitas, Professor Catedrático, Faculdade de Ciências da Universidade do Porto

Coorientador

Doutor Paulo Dinis Lopes, Doutorando Viticultura e Enologia, Amorim & Irmãos





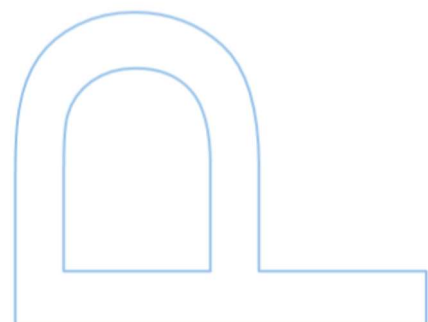
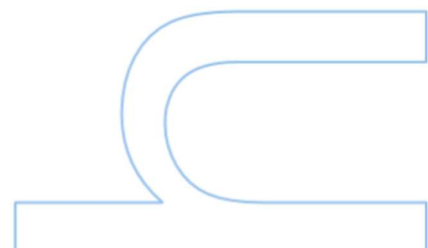
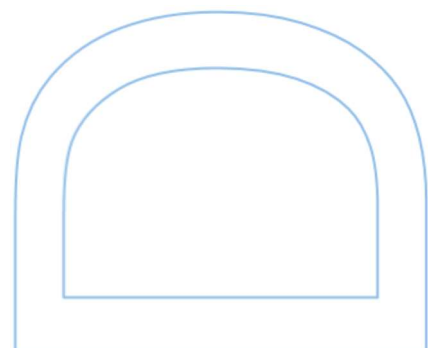
Nota: A presente página só deverá ser incluída no caso de o júri aprovar a tese com recomendação de correção, pelo estudante, dos erros, imprecisões ou incorreções formais identificados e expressamente referidos durante as provas.

Todas as correções determinadas pelo júri, e só essas, foram efetuadas.

A/O Orientadora(o),

Victor Augusto Pereira de Freitas

Porto, 03 / 04 / 2023



Declaração de Honra

Eu, Joana Filomena da Costa Azevedo, inscrito(a) no Programa Doutoral em Química da Faculdade de Ciências da Universidade do Porto declaro, nos termos do disposto na alínea a) do artigo 14.º do Código Ético de Conduta Académica da U.Porto, que o conteúdo da presente tese reflete as perspetivas, o trabalho de investigação e as minhas interpretações no momento da sua entrega.

Ao entregar esta tese, declaro, ainda, que a mesma é resultado do meu próprio trabalho de investigação e contém contributos que não foram utilizados previamente noutros trabalhos apresentados a esta ou outra instituição.

Mais declaro que todas as referências a outros autores respeitam escrupulosamente as regras da atribuição, encontrando-se devidamente citadas no corpo do texto e identificadas na secção de referências bibliográficas. Não são divulgados na presente tese quaisquer conteúdos cuja reprodução esteja vedada por direitos de autor.

Tenho consciência de que a prática de plágio e auto-plágio constitui um ilícito académico.

Joana Filomena da Costa Azevedo

17 janeiro 2023

Agradecimentos

Em primeiro lugar tenho a agradecer à Fundação Para a Ciência e Tecnologia (FCT) pelo financiamento deste trabalho na forma de uma bolsa de Doutoramento (SFRH/BD/139709/2018) sem a qual a realização deste trabalho seria impossível. Gostava de agradecer também Departamento de Química e Bioquímica da Faculdade de Ciências da Universidade do Porto especialmente à Linha de Investigação QUINOA/LAQV do REQUIMTE pelos diversos apoios logísticos e financeiros concedidos.

Gostava de agradecer ao meu orientador Professor Doutor Victor de Freitas e coorientador Doutor Paulo Lopes por todo interesse, disponibilidade, compreensão e ajuda sempre que as dúvidas surgiam ao longo do trabalho. Foram fundamentais para o desenvolvimento e evolução de todo o trabalho. Gostava também de agradecer ao Professor Doutor Nuno Mateus pela ajuda, pelo incentivo, e com o seu humor característico me ter ajudado nos momentos de maior desânimo.

A todos os meus amigos do FoodPhenolLAB em especial às “velhas guardas” que me acompanham desde sempre: Iva, Ana Luísa, Susana, Luís, Rosa, Natércia, pelo companheirismo, ajuda e compreensão. Estamos juntos há uma vida! E claro a Joana Oliveira, pela qual nunca terei palavras suficientes para agradecer tudo que me ensina, ajuda, me faz crescer todos os dias, não esquecendo também a Dra. Zélia por toda a ajuda nas análises de massa.

Aos que vieram mais tarde Paulinha, Elsa, Patrícia, Rita, Hélder, Ricardo, Carlos, Sofia, Alexandra, Ana, Leonor, José, Mónica e Vânia (minha companheira de aflições nestes 4 anos). Todos eles sempre tiveram uma palavra de ânimo nos dias mais cinzentos, sempre me ajudaram nas minhas dúvidas e me fizeram crescer com o seu conhecimento e ajuda.

À minha família, pais, irmãos e sobrinhos pelo apoio sempre que necessário.

Ao Celestino, marido, amigo, confidente, namorado, companheiro de uma vida que me faz acreditar que os nossos sonhos vão mesmo se realizar.

Ao Duarte e ao Francisco, que sem saberem, são a minha força de todos os dias.

A ti avô, um exemplo de trabalho e dedicação à família. Ensinaste me que o trabalho sério e dedicado nos leva longe e acredito que terias muito orgulho se cá estivesses.

Obrigado!

“Porque os que passam por nós, nunca nos deixam sós, deixam um pouco de si e levam um pouco de nós.”

Antoine de Saint-Exupery

The work presented in this thesis was developed at:

QUINOA-LAQV-REQUIMTE laboratory at Chemistry and Biochemistry Department in Faculty of Science of University of Porto, Portugal;



Nutrition and Bromatology Group, Department of Analytical and Food Chemistry, Faculty of Food Science and Technology, University of Vigo, Ourense Campus, Spain;

Universidade de Vigo

Financial support from Fundação para a Ciência e Tecnologia (FCT)

PhD Grant SFRH/BD/139709/2018

FCT

Fundação para a Ciência e a Tecnologia

Publications List

This thesis includes results already published or submitted in international peer-reviewed scientific journals and scientific conferences through oral and poster communications.

Publications in international peer-reviewed scientific journals

Joana Azevedo, Elsa Brandão, Susana Soares, Joana Oliveira, Paulo Lopes, Nuno Mateus and Victor de Freitas. Polyphenolic Characterization of Nebbiolo Red Wines and Their Interaction with Salivary Proteins, *Foods*, **2020**, **DOI:** 10.3390/foods9121867;

Joana Oliveira, Joana Azevedo, Natércia Teixeira, Paula Araújo, Victor de Freitas, Nuno Basílio and Fernando Pina. On the Limits of Anthocyanins Co-Pigmentation Models and Respective Equations, *Journal of Agricultural and Food Chemistry*, **2021**, **DOI:** 10.1021/acs.jafc.0c05954;

Joana Azevedo, João Pissarra, Filipa Amaro, Luís Guido, Joana Oliveira, Paulo Lopes, Paula Guedes de Pinho, Nuno Mateus and Victor de Freitas. Development of a new procedure for the determination of the reactivity of brandies used in wine fortification, *OENO One*, **2021**, **DOI:** 10.20870/oeno-one.2021.55.3.4676;

Joana Oliveira, Joana Azevedo, André Seco, Johan Mendoza, Nuno Basílio, Victor de Freitas and Fernando Pina, Copigmentation of anthocyanins with copigments possessing an acid-base equilibrium in moderately acidic solution, *Dyes and Pigments*, **2021**, **DOI:** 10.1016/j.dyepig.2021.109438;

Joana Azevedo, Mónica Jesus, Elsa Brandão, Susana Soares, Joana Oliveira, Paulo Lopes, Nuno Mateus and Victor de Freitas, Interaction between salivary proteins and cork phenolic compounds able to migrate to wine model solution, *Food Chemistry*, **2022**, **DOI:** 10.1016/j.foodchem.2021.130607;

Joana Azevedo, Paulo Lopes, Nuno Mateus and Victor de Freitas, Cork, a Natural Choice to Wine? *Foods*, **2022**, **DOI:** 10.3390/foods11172638;

Joana Azevedo, Joana Pinto; Natércia Teixeira; Joana Oliveira; Miguel Cabral; Paula Guedes de Pinho; Paulo Lopes; Nuno Mateus; Victor de Freitas, The Impact of Storage Conditions and Bottle Orientation on the Evolution of Phenolic and Volatile Compounds of Vintage Port Wine, *Foods*, **2022**, **DOI:** 10.3390/foods11182770;

Joana Azevedo, Lucia Cassani, Joana Oliveira, Franklim Chamorro, Jesus Simal-Gandara, Paulo Lopes, Nuno Mateus, Victor de Freitas, Miguel Prieto, and Rosa Perez-Gregorio, Ultrasound-assisted extraction optimization for maximum recovery of bioactive phenolic compounds from cork industry waste, *Submitted*

Joana Azevedo, Joana Oliveira, Franklim Chamorro, Paulo Lopes, Nuno Mateus, Rosa Perez-Gregorio, Victor de Freitas, Jesus Simal-Gandara, Miguel Prieto and Lucia Cassani, Sustainable valorization of cork waste through an efficient microwave-assisted extraction of bioactive phenolic compounds, *In preparation*

Joana Azevedo, Joana Oliveira, Luís Cruz, Paulo Lopes, Nuno Mateus and Victor de Freitas, Identification and structural characterization of a novel (+)-catechin-caffeic acid adduct present in wines, *In preparation*.

Oral Communications

Joana Azevedo, João Pissarra, Luís Guido, Joana Oliveira, Paulo Lopes, Nuno Mateus, Victor de Freitas. O10- Development of a methodology for the determination of the reactivity of brandies used in wine fortification, XXVII Encontro Nacional SPQ, 14 - 16 July 2021, Braga, Portugal;

Joana Azevedo, Natércia Teixeira, Joana Oliveira, Paulo Lopes, Nuno Mateus, Victor de Freitas. FC23- The impact of bottle position during storage on phenolic compounds evolution of Port Wines, XV Encontro Nacional Química Alimentos, 5 - 8 September 2021, Funchal, Portugal;

Joana Azevedo, Joana Oliveira, Paulo Lopes, Nuno Mateus, Victor de Freitas. OC11- Reactivity between Cork and wine compounds, 14TH National Organic Chemistry Meeting & 7TH National Medicinal Chemistry Meeting, 20 - 22 April 2022, Caparica, Portugal;

Joana Azevedo, Joana Oliveira, Paulo Lopes, Nuno Mateus, Victor de Freitas. S2.21- Cork and Wine: interactions and newly formed compounds, In *Vino Analytica Scientia* 2022, 4 - 7 July 2022, Neustadt, Germany;

Joana Azevedo, Lucia Cassani, Joana Oliveira, Franklin Chamorro, Rosa Perez-Gregorio, Jesus Simal-Gandara, Paulo Lopes, Nuno Mateus, Victor de Freitas and Miguel Prieto. AMB26- Screening of the main factors affecting the microwave-assisted extraction (MAE) of phenolic compounds from cork industry waste, XXVITH Encontro Galego Português de Química, 16 - 18 November 2022, Santiago de Compostela, Spain.

Posters in conferences

Joana Azevedo, Joana Oliveira, Paulo Lopes, Miguel Cabral, Nuno Mateus e Vítor Freitas. Characterization of the cork polyphenolic fraction from different regions of the Iberian Peninsula able to migrate to wine model solutions, 1st Science and Wine Word Congress, 8 - 10 May 2019, Porto, Portugal;

Joana Azevedo, Joana Oliveira, Paulo Lopes, Miguel Cabral, Nuno Mateus e Vítor Freitas. Corklins in Wine, Oeno2019 - 11th International Symposium of Enology of Bordeaux/11th Edition IVAS, 25 - 28 June 2019, Bordeaux, France;

Joana Azevedo, Mónica Jesus, Elsa Brandão, Susana Soares, Joana Oliveira, Paulo Lopes, Nuno Mateus, Victor de Freitas. Interaction between salivary proteins and cork phenolic compounds able to migrate to wine model solutions, ICP 2020 XXX International Conference on Polyphenols, 13 - 15 July 2021, Turku, Finland.

Outline of the thesis

This thesis is organized into an Introduction, three Parts of experimental work, and a final remark. This is a formal organization and does not reflect the order of the experimental work. It is an author option in order to simplify the overall reading of this work and to better present the works developed.

In the general introduction, the topics necessary for the broad comprehension of this thesis are described. It is a brief definition of cork, its structure, the cork stoppers used in the wine industry, the compounds that can migrate and interact with the wine matrix, and finally the way that this industry contributes to sustainability. Nonetheless, in each chapter, a small introduction is included related to the work presented.

The experimental work is divided into **three parts**.

The **first part** exploits the different ways of extraction of phenolic compounds from cork, with three works described, divided into **Chapter 1, 2, and 3**. The **chapter 1** starts with the characterization of the cork polyphenolic fraction from different regions of the Iberian Peninsula able to migrate to wine model solutions with a study that characterized the polyphenolic content and the antioxidant capability of 33 cork samples (*Quercus suber*) obtained from eleven different regions from the Iberian Peninsula. **Chapter 2** describes the optimization of the ultrasound-assisted extraction for the maximized recovery of bioactive phenolic compounds from cork industry waste and **Chapter 3** a sustainable valorization of cork waste through an efficient microwave-assisted extraction of bioactive phenolic compounds. All these works allowed us to identify, quantify and describe the nature of compounds that can be obtained from cork samples.

The **second part** reports the way that the characteristics of the compounds from cork can interact with salivary proteins and interfere with copigmentation phenomena, distributed in **Chapter 1, 2, and 3**, constituting three works. **Chapter 1** reports the interaction of human salivary proteins (SP) with phenolic compounds that migrate from cork stoppers to wine. This yielded valuable data to understand the influence that these compounds may have on the sensory perception of wine from an astringency perspective. **Chapter 2** describes the co-pigmentation phenomena of malvidin-3-glucoside with pentagalloyl glucose (PGG). **Chapter 3** describes how compounds

present in cork (cinnamic acids, more specifically sinapic acid) may influence the copigmentation process.

The **last part** describes the chemical impact of cork in wines. Divided into three chapters, different types of analysis were made aiming to understand how different factors may influence the sensorial properties of bottled wine. **Chapter 1** starts with a study of the influence of bottle position and cellar conditions in bottled Port wine, and the search for compounds that can result from the interaction between cork compounds that can be able to pass to the wine and the wine's main constituents. In the same line, **Chapter 2** describes a new (+)-catechin-caffeic acid adduct present in wines. **Chapter 3** correlates how the phenolic composition of wines is responsible for salivary proteins' precipitation process and impact on a sensorial perception.

Finally, this work presents final remarks on the main results obtained concerning the abstract of this thesis, and some indications for future work activities are also presented.

Resumo

Neste trabalho procurou-se compreender de que modo a composição química de cortiças, nas rolhas de cortiça, afeta as características químicas e sensoriais dos vinhos. Para atingir este objetivo, o trabalho focou-se em três partes distintas começando pela caracterização química da cortiça sobretudo ao nível da composição fenólica, seguindo-se o modo como alguns compostos presentes na cortiça podem afetar a cor e o sabor do vinho e, por último, a deteção destes compostos em vinhos brancos e tintos:

Parte A) avaliar qualitativamente e quantitativamente a composição em compostos fenólicos na cortiça. Para isso recorreu-se a diferentes técnicas de extração, desde a maceração tradicional (contacto da cortiça com uma solução modelo de vinho 12% etanol) até à extração assistida por micro-ondas e ultrassons, com solução a diferentes percentagens de etanol, de forma a potenciar a extração e reduzir o tempo, volume de solventes e energia com o intuito de tornar o processo de extração mais sustentável; procedeu-se também ao fracionamento em coluna de um extrato de cortiça de modo a obter frações separadas por diferentes pesos moleculares e ao isolamento de compostos puros por HPLC preparativo;

Parte B) foram feitos estudos de interação das frações e/ou compostos puros com: a) proteínas salivares de modo a compreender melhor o seu impacto no processo de adstringência; b) e copigmentação por interação com antocianinas (malvidina-3-O-glucósido). Estes estudos permitem perceber de que forma os compostos da cortiça poderão influenciar sensorialmente os vinhos;

Parte C) por fim, passou-se à caracterização química de vinhos engarrafados com diferentes classes de cortiça natural, rolhas colmatadas, aglomeradas, técnicas e vedantes sintéticas/plásticas. Foram analisados vinhos tintos, brancos e espumantes. Os vinhos que tiveram em contacto com a cortiça foram alvo de pesquisa de novos compostos resultantes da interação dos compostos da cortiça com os do vinho e estudadas as diferenças cromáticas entre os vinhos.

Estes estudos envolveram diferentes técnicas, nomeadamente cromatografia líquida de alta eficiência (HPLC), espectrofotometria UV-vis, espectrometria de massa, extração por ultrassons (UAE) e micro-ondas (MAE), turbidimetria e ressonância magnética nuclear (RMN).

Os resultados obtidos na primeira parte do trabalho mostraram que foi possível a extração de compostos fenólicos da cortiça, tanto por maceração tradicional como pelas duas técnicas de extração usadas (UAE e MAE). Foi possível identificar dezanove compostos dos quais fazem parte diferentes ácidos fenólicos como o ácido gálico, ácido protocatecuico, ácido cafeico, ácido ferúlico, ácido sinápico e ácido elágico, os aldeídos protocatecuico e vanilina e taninos elágicos como a castalagina, a vescalagina, a pentagalóilglucose (PGG), entre outros.

Seguiu-se o estudo da reatividade de diferentes frações de cortiça, de diferente peso molecular, com as proteínas salivares. Este estudo demonstrou que todas elas têm capacidade de precipitar as proteínas salivares e contribuir para fenômenos de adstringência. Além disso, também parece haver um efeito de matriz (presença de outros compostos) na capacidade de interação destes compostos com as proteínas. Passando para o processo de copigmentação, a PGG e ácido sinápico foram escolhidos como compostos de referência na cortiça para serem utilizados como copigmentos, e ambos demonstraram uma grande capacidade de complexação com a malvidina-3-O-glucosido, sendo possível a determinação das respectivas constantes de copigmentação: $K_{AH+CP} = 914 \pm 10 \text{ M}^{-1}$ (PGG) e $K_{CP} = 243 \text{ M}^{-1}$, $K_{CB CP} = 53 \text{ M}^{-1}$ and $K_{CB CP (-)} = 78 \text{ M}^{-1}$ (ácido sinápico)

Finalmente, passando ao impacto no vinho, os resultados revelaram que as condições da adega e a orientação da garrafa fechada com rolha cortiça natural tem impacto na composição química do vinho do Porto correspondente. As amostras armazenadas na adega tradicional, com maiores amplitudes térmicas, apresentaram maior tonalidade amarela, menor reatividade com taninos e maiores teores de furfural e 5-metilfurfural (marcadores de oxidação). Além disso, as amostras armazenadas na posição horizontal revelaram níveis significativamente mais altos de proantocianidinas totais e maior reatividade com taninos do que as amostras armazenadas na posição vertical. Foi também detetado nos vinhos armazenados na posição horizontal, um derivado de elagitaninos (Corklina), que resulta da reação de compostos da cortiça com os compostos fenólicos presentes nos vinhos. Em linha com a procura de compostos que possam ser formados pela interação entre os componentes do vinho e os componentes da rolha, foi identificado com sucesso um novo aduto catequina-ácido cafeico. A caracterização estrutural completa deste novo composto e os estudos realizados em soluções modelo revelaram que resulta da interação entre o ácido cafeico e a (+)-catequina.

Foi também estudada a composição polifenólica de dois vinhos tintos e a sua capacidade de interagir com as proteínas salivares. Verificou-se que ambos os vinhos foram muito reativos com as proteínas da saliva, o que poderá justificar o seu elevado carácter adstringente. O vinho que apresentou maior interação com as proteínas salivares tinha também valores mais elevados de fenólicos totais, proantocianidinas totais e reatividade com taninos.

De uma forma geral, este trabalho permitiu aumentar o conhecimento acerca da capacidade dos compostos que migram da cortiça para o vinho e de que forma podem afetar as características sensoriais destes.

Esta informação pode ser de grande utilidade para a indústria corticeira e vinícola pois pode direcionar a classe de rolhas mais adequado ao tipo de envelhecimento que o produtor quer para seu vinho.

Palavras-chave: Polifenóis, taninos, ácidos fenólicos, aldeídos, extração, interações, vinho, rolha, cortiça, proteínas salivares, adstringência, copigmentação.

Abstract

This work sought to understand how the chemical composition of cork, in cork stoppers, affects the chemical and sensory characteristics of wines. To achieve this objective, the work focused on three distinct parts, starting with the chemical characterization of cork, particularly in terms of its phenolic composition, followed by the way in which some compounds present in cork can affect the color and flavor of the wine, and finally the detection of these compounds in white and red wines:

Part A) qualitatively and quantitatively evaluate the composition of phenolic compounds from cork. To this end, different extraction techniques were used, from traditional maceration (contact of the cork with a model wine solution 12% ethanol) to microwave and ultrasound-assisted extraction, using different ethanol percentage, in order to enhance extraction and reduce time, solvents volume and energy with the aim of making the extraction process more sustainable; a cork extract was also fractionated in a column in order to obtain fractions separated by different molecular weights and the isolation of pure compounds by preparative HPLC;

Part B) interaction studies of fractions and/or pure compounds with: a) salivary proteins in order to better understand their impact on the astringency process; b) and copigmentation by interaction with anthocyanins (malvidin-3-O-glucoside). These studies make it possible to understand how cork compounds can have a sensory influence on wines;

Part C) finally, the chemical characterization of bottled wines with different classes of natural cork, colmated and agglomerated stoppers, techniques and synthetic/plastic closures was carried out. Red, white and sparkling wines were analyzed. The wines that came into contact with cork were the subject of research into new compounds resulting from the interaction of the compounds in cork with those in the wine, and the chromatic differences between the wines were studied.

These studies involved different techniques, namely high performance liquid chromatography (HPLC), UV-vis spectrophotometry, mass spectrometry, ultrasonic (UAE) and microwave (MAE) extraction, turbidimetry and nuclear magnetic resonance (NMR).

The results obtained in the first part of the work showed that it was possible to extract phenolic compounds from cork, both by traditional maceration and by the two extraction techniques used (UAE and MAE). It was possible to identify nineteen compounds comprising different phenolic acids such as gallic acid, protocatechuic acid, caffeic acid, ferulic acid, sinapic acid and ellagic acid, protocatechuic and vanillin aldehydes and ellagic tannins such as castalagin, vescalagin, pentagalloylglucose (PGG), among others.

This was followed by the study of the reactivity of different fractions of cork, of different molecular weight, with salivary proteins. This study demonstrated that all of them have the capacity to precipitate salivary proteins and contribute to astringency phenomena. Furthermore, there also seems to be a matrix effect (presence of other compounds) on the ability of these compounds to interact with proteins. Moving on to the co-pigmentation process, PGG and sinapic acid were chosen as reference compounds in cork to be used as co-pigments, and both showed a great ability to complex with malvidin-3-*O*-glucoside, making it possible to determine the respective copigmentation constants: $K_{AH+CP} = 914 \pm 10 \text{ M}^{-1}$ (PGG) and $K_{CP} = 243 \text{ M}^{-1}$, $K_{CBCP} = 53 \text{ M}^{-1}$ and $K_{CBCP(-)} = 78 \text{ M}^{-1}$ (sinapic acid)

Finally, moving on to the impact on the wine, the results revealed that the cellar conditions and the orientation of the bottle closed with a natural cork stopper have an impact on the chemical composition of the corresponding Port wine. The samples stored in the traditional cellar, with greater temperature ranges, showed a greater yellow hue, less tannin specific activity and higher levels of furfural and 5-methylfurfural (oxidation markers). In addition, samples stored horizontally showed significantly higher levels of total proanthocyanidins and higher tannin specific activity than samples stored vertically. A derivative of ellagitannins (Corklin) was also detected in wines stored in a horizontal position, which results from the reaction of cork compounds with the phenolic compounds present in wines. In line with the search for compounds that can be formed by the interaction between wine components and cork stopper components, a new catechin-caffeic acid adduct was successfully identified. The complete structural characterization of this new compound and the studies carried out in model solutions revealed that it results from the interaction between caffeic acid and (+)-catechin.

The polyphenolic composition of two red wines and their ability to interact with salivary proteins were also studied. It was found that both wines were very reactive with saliva proteins, which could explain their high astringent character. The wine that showed

greater interaction with salivary proteins also had higher values of total phenolics, total proanthocyanidins and tannin specific activity.

In general, this work allowed us to increase knowledge about the capacity of the compounds that migrate from cork to wine and how they can affect their sensory characteristics.

This information can be of great use to the cork and wine industry as it can direct the class of stoppers that are most suitable for the type of aging that the producer wants for his wine.

Keywords: Phenolic compounds, tannins, phenolic acids, aldehydes, extraction, interactions, wine, cork, stopper, salivary proteins, astringency phenomena, copigmentation phenomena.

Table of Contents

Introduction	3
Part A. Extraction and Phenolic Characterization	31
Chapter 1- Characterization of the cork polyphenolic fraction from different regions of the Iberian Peninsula able to migrate to wine model solutions.....	33
Chapter 2- Optimization of the ultrasound-assisted extraction for the maximized recovery of bioactive phenolic compounds from cork industry waste	47
Chapter 3- Sustainable valorization of cork waste through an efficient microwave-assisted extraction of bioactive phenolic compounds	71
Part B. Sensory Implications: molecular interactions between cork compounds and their impact in astringency and copigmentation phenomena’s	93
Chapter 1- Interaction between salivary proteins and cork phenolic compounds able to migrate to wine model solution	95
Chapter 2- On the Limits of Anthocyanins Co-Pigmentation Models and Respective Equations	121
Chapter 3- Copigmentation of Anthocyanins with Copigments Possessing an Acid-Base Equilibrium in Moderately Acidic Solutions.	155
Part C. Wine Impact	189
Chapter 1- The Impact of Storage Conditions and Bottle Orientation on the Evolution of Phenolic and Volatile Compounds of Vintage Port Wine.....	191
Chapter 2- Identification and structural characterization of a novel (+)-catechin-caffeic acid adduct present in wines	211

Chapter 3- Polyphenolic Characterization of Nebbiolo Red Wines and Their Interaction with Salivary Proteins	223
Final Remarks and Future work	237

List of abbreviations

ACN- Acetonitrile

ANOVA- Analysis of Variance

aPRPs- Acidic proline-rich proteins

bPRPs- Basic proline-rich proteins

BSA- Bovine serum albumin

COSY- Correlation spectroscopy

DAD- Diode Array Detector

DMACA- *para*-dimethylaminocinamaldehyde

ESI- Electrospray Ionization

EtOH- Ethanol

EY- Yield

GA- Gallic Acid

GAE- Gallic Acid equivalents

GC- Gas chromatography

Glc- Glucose

gPRPs- Glycosylated proline-rich proteins

HHDP- Hexahydroxydiphenyl moiety

HMBC- Heteronuclear Multiple Bond Correlation

HPLC- High Pressure Liquid Chromatography

HSQC- Heteronuclear Single Quantum Correlation

MAE- Microwave assisted extraction

MS- Mass Spectrometry

MW- Molecular weight

NaOH- Sodium Hydroxide

NMR- Nuclear Magnetic Resonance

PGG- Pentagalactoglucose

PRP (s)- Proline-rich proteins

RSM- Response surface methodology

SP- Salivary proteins

UAE- Ultrasound assisted extraction

UV/Vis- Ultraviolet/Visible

TPC- Total phenolics contents

Introduction

Adapted from: Joana Azevedo, Paulo Lopes, Nuno Mateus and Victor de Freitas

Cork, a Natural Choice to Wine? *Foods*, **2022**, *DOI*: 10.3390/foods11172638

All the bibliographical research and writing in this part was carried out by the author.

Abstract

This review presents the most recent data on the state of the art of the main compounds present in cork, their interaction with wine, and the impact that natural stoppers may have on wines' physical-chemical and sensory properties. Several aspects will be reviewed according to the recent scientific literature, including the chemical composition of cork and the scientific relevance of the compounds extracted from cork to wine over time. Furthermore, the effect of cork compounds transferred into wines during post-bottling will also be discussed, as well as their impact to the organoleptic (color and taste) of wines. This knowledge is essential for the decision-making process undertaken by wine producers to select the stopper most suitable for their wines. In addition, sustainability is also a topic addressed since it is a natural product that generates some waste and the way in which this industry is adapting to the closure of the waste cycle.

Keywords: Wine, Cork Stoppers, Interactions, Polyphenols, Corklins

Introduction

The Cork oak tree is very important for Portugal, and in 2011 the Portuguese Parliament declared this tree Portugal's National Tree, reinforcing the protection acquired by law since the 13th century. Historically, cork was first used by Greeks, Romans, and Egyptians as a closure for amphoras (Van Damme 2019). In the early 1600s, Dom Pérignon innovated by starting to use cork stoppers instead of the traditional wooden stoppers (wood wrapped in hemp soaked in olive oil). With that decision, the wine industry was never the same, with cork stoppers still being used in wine closures (Amorim 2021). Nowadays, natural cork stoppers are used for in all types of wines, from centenary to the most recent ones (Jové, Pareras et al. 2021).

For instance, the Port wine industry developed faster when it started to age wines in bottles sealed with cork stoppers. This natural material adapts itself correctly to the bottleneck, filling the irregularities and closing perfectly even if the glass expands or contracts, which can happen with a change in the temperature of storage or during transportation. For a long time, cork was claimed to be an inert material as a natural product; however, cork's chemical inertness has been called into question due to the number of potential compounds that can be extracted. (Mazzoleni, Caldentey et al. 1994, Conde, Cadahía et al. 1997, Fernandes, Sousa et al. 2011, Azevedo, Fernandes et al. 2014, Pereira 2015).

Wine closures have an interest to be investigated in detail (different types of corks are discussed later in section 2), including the relationship between the closure's permeability and the chemical reactions that can occur in wines during bottle storage aging. Ultimately, such work would be crucial to obtaining a predictive tool to improve wine production and quality (Karbowski, Gougeon et al. 2009). Several reviews have already focused on the wine's evolution and the main characteristics of cork. However, none of them showed the correlation that may exist between the wine aging under a natural cork stopper and the compounds that can be extracted from cork. Thus, the main purpose of this review is to discuss the impact of cork stoppers on wine's physical-chemical and sensorial properties during aging in bottles.

Cork from the cork oak, *Quercus suber*, has been substantially studied, mostly because of its economic impact and the worldwide utilization of cork products (Leite and Pereira 2017). The main commercial product is the natural cork stopper. According to the statistical report of the International Organization of Vine and Wine (OIV), the annual world wine production is around 275 million hectoliters (292 MhL in 2018), and 70% of the bottled wines are closed with cork stoppers (Mislata, Puxeu et al. 2020).

When the cork is in direct contact with an alcoholic solution such as bottled wine, some cork components can be extracted into the wine (Conde, Cadahía et al. 1997, Varea, Garcia-Vallejo et al. 2001, Azevedo, Fernandes et al. 2014). Hydrocarbons, alcohols, ketones, phenolic compounds including tannins, and other soluble in ethanol/water compounds have been shown to pass from cork to wine and may have a putative contribution to the wine sensory properties of color, flavor, astringency, and bitterness (Soares, Mateus et al. 2012, Azevedo, Brandão et al. 2020, Watrelot, Heymann et al. 2020, Azevedo, Jesus et al. 2021).

Cork structure

Cork is a natural cellular material with a combination of properties that make it perfect to be used as a wine closure. Hooke (Hooke, Allestry et al. 1665), first studied the cellular structure of cork, followed by Brugnatelli (Brugnatelli 1787) who discovered that cork is composed by aliphatic, terpenic, and phenolic compounds. These compounds can be obtained by traditional methods or green technologies with organic and aqueous solvents (Snackers, Nepveu et al. 2000).

Pereira et al. described the chemical composition of cork from *Quercus suber L.* as 0.7% ash, 15.3% total extractives, 38.6% suberin, 21.7% lignin, and 18.2% polysaccharides. The carbohydrate composition analysis showed that glucose represents 50.6% of all monosaccharides, xylose 35.0%, arabinose 7.0%, and galactose and mannose, respectively, 3.6% and 3.4% (Pereira 1988). Furthermore, they described cork as a foam with closed cells with cells being formed by the phellogen, with cell division capability (meristematic layer) that produces the bark periderm. The biological tissue is compact with a regular honeycomb arrangement (**Figure 1**).

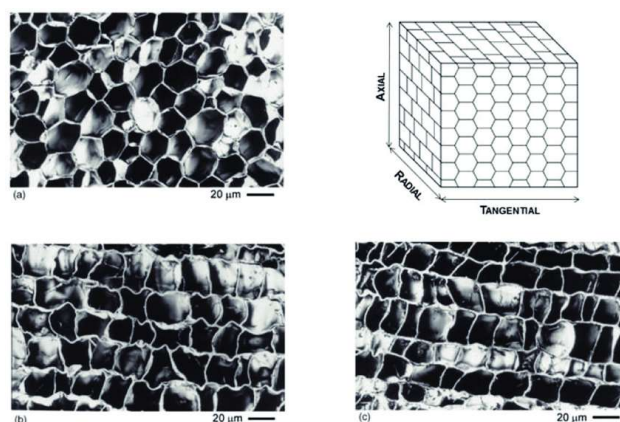


Figure 1. Schematic representation of the cellular structure of cork with scanning electron micrographs of sections of reproduction cork: (a) tangential, (b) radial, and (c) transverse sections, from (Oliveira and Pereira 2020).

The tissue is homogeneous, and cells are constituted by dead parenchymatous cells with hollow, air-filled interiors. The characteristics of the two main chemical components (suberin and lignin, which represent 53% and 26%, respectively, of the cell wall) are responsible for the unique characteristics of cork: impermeability to fluids, low density, buoyancy, low thermal coefficient, high elasticity and deformation behaviour without fracturing if compressed, long durability (Pereira 2015). However, cork composition varies with geographic origin, climate, soil conditions, genetic origin, tree dimensions, age (virgin or reproduction), and growth conditions (Pinto, Oliveira et al. 2019, Reis, Teixeira et al. 2020). Recently, it has been described that the variability associated with the tree is much more relevant than the effect of the scarcity of water. In practical terms, the climatic changes seem to have a low impact on the performance of cork as a closure for wine bottles (Leite, Oliveira et al. 2020).

Cork stoppers production and classification

Portugal, Spain, and Morocco are the main suppliers of cork around the world. The cork industry is divided into two main areas: i) the natural cork industry with natural cork stoppers and natural cork discs; and ii) the granulate/agglomerated industry that includes technical stoppers, floors, wall coverings, and, boards. Natural cork accounts for 70% of the value added by the whole industry. However, more than 70% of the raw material used to make natural cork stoppers is converted into industrial by-products used in the second sector (granulate-agglomerate industry), improving by this way the total use of the raw material (Rives, Fernandez-Rodriguez et al. 2012).

During bottling, four types of cork can be used: i) natural cork; ii) colmated cork; iii) agglomerated; and iv) technical closures (**Figure 2**).



Figure 2. Types of cork closures that can be used for wine bottling (<https://www.corklink.com/index.php/natural-wine-cork-classification/>).

The natural cork stoppers are obtained by the direct cutting off from planks of cork wood obtained from cork oak trees. However, despite being only one piece, they can be graded in different categories. The external surface homogeneity/heterogeneity of the natural cork stoppers will determine the commercial grade and the quality classes (Oliveira,

Knapić et al. 2013). The homogeneity of the cork surface is given by the absence of voids or defects (the presence of lenticular channels), which is recognized as the porosity of cork (Pereira, Lopes et al. 1996).

The commercial grade and quality classes may go up to nine grades, such as, “flor”, which is less porous and the most homogenous, “extra”, “superior”, “1st to 6th”, with the last ones presenting a higher porosity and more heterogeneity (**Figure 3**). However, a three-class system, i.e., premium, good, and standard, is a more realistic way to meet the performance requirements (Oliveira, Knapić et al. 2012).



Figure 3. Natural cork stoppers

Colmated cork stoppers are made from natural cork where lenticels have been covered with cork powder and glue (Suffo, Sales et al. 2022). The origin of cork powder is from the manufacturing process of improving the performance of the closure since the size of the cork particles and the presence of micro-spheres or other additives in the composition of stoppers are variables that could affect their mechanical behaviour (Chanut, Lagorce et al. 2020). The agglomerated cork stoppers are made with granulated cork of different dimensions (offcuts of cork from the punching process) and a food-grade binder. This food-grade binder is particularly relevant in the context of this review because, at least in theory, migrations can not only take place from cork to wine but also be derived from the use of these synthetic products. Studies of potential migration of adhesives and surfaces were made and a methodology for primary aromatic amines was described as a potential migrant that might be associated with polyurethane adhesives (Six and Feigenbaum 2003). Another study described twelve neo-formed compounds (amines, amides, and urethane) as a result of the reaction of isocyanates with acetic acid and ethanol used as food simulants, and the levels formed were found to exceed the specific migration limit established (Canellas, Vera et al. 2021). The inorganic elements potentially migrating from cork to a food simulant (a hydroalcoholic solution containing 12 and 20% ethanol) were tested. In all cases, cork met the general safety criteria applicable to food contact materials (Corona, Iglesias et al. 2014). To avoid direct contact between wine and glue, the technical cork stoppers are constituted of cork granules in the body and natural cork discs in the tops. In this solution, the stoppers

maintained the good characteristics of agglomerated closures, and in this case, the wine is in contact with natural cork. Moreover, synthetic stoppers or plastic have been commercialized since the end of the 20th century and with the main proposal to guarantee wines without “cork taint”. They are designed to look like natural cork and are produced as compressed plastic. For that reason, it is much cheaper than natural cork. Nowadays, this type represents a negative point because it is made of non-biodegradable material (Dwivedi, Mishra et al. 2019). They can be obtained by two techniques: extrusion and injection molding, using polymers that are usually used for food packaging. Generally, low density polyethylene (LDPE) for co-extruded stoppers and styrene-butadiene-styrene (SBS) or styrene-ethylene-butylene-styrene (SEBS) for molded ones (Gardner 2008). The screw cap is a metal cap that screws onto threads on the neck of a bottle, applying a metal skirt down the neck to become more like the traditional wine capsule. Created in the 70’s, it was the first option to prevent the “cork taint” problem and to reduce the oxygen permeation, especially for wines sensitive to oxidation. They are made of aluminium with an inner joint to ensure the barrier property. Two joints are mainly used: the Saran joint, composed of consecutive layers of expanded polyethylene (PEE), polyethylene (PE), tin, and polyvinylidene chloride (PVDC); Saranex joint composed of PEE inserted between two PE/PVDC/PE multilayers (Silva, Julien et al. 2011). All these components have different purposes: PVDC is used for its good barrier property to oxygen, PE as a water vapour barrier and PEE for the mechanical property of the joint. The tin layer ensures a good sealing of the system. Finally, the crown capsules are used during the bottle fermentation and ageing of sparkling wines. This type uses as a barrier property to gas transfer the gasket composed of an LDPE/ethylene vinyl acetate (EVA) blend (White 1999). Altogether, per year, it was estimated to be around 17 billion closures sold (Amorim 2017). Take note that 86% of global consumers prefer cork stoppers and, in their opinion, screw caps as well as synthetic closures dedicated to inexpensive wine (Mateus, Bordado et al. 2017). Knowing that cork represents a natural material that can be in direct contact with wine for years, it is of great importance to understand the impact of cork compounds on wine sensory properties. Azevedo et al. quantified the phenolic compounds that were able to be extracted from different classes of cork stoppers (“Flor”, “Third”, and micro-agglomerated), with and without treatment, to wine model solutions. It was observed that natural corks (3rd quality and Flor) were the ones that, at the end of 27 months, allowed a higher quantity of phenolic compounds to be extracted into wine model solution when compared to agglomerated corks without surface treatment (Azevedo, Fernandes et al. 2014). These results showed that the wine model solution bottled with 3rd quality cork

stoppers presented the highest levels of phenolic compounds, which may be related to the highest level of porosity/wooden parts of these stoppers. To clarify how porosity influences the profile of volatile organic compounds, a methodology was developed and applied to natural cork stoppers with different levels of porosity: group 1 (low porosity), group 2 (intermediate porosity) and group 3 (high porosity). The differences were found between cork stoppers of low and intermediate porosity when compared with those of high porosity (group 1 vs. 3 and group 2 vs. 3) (Furtado, Oliveira et al. 2020). The intermediate and low porosity presented higher levels of volatile compounds when compared with group 3. Furthermore, 2-pentylfuran, cyclene, camphene, limonene, eucalyptol, camphor, furfural, and 5-methyl-2-furfural were compounds responsible for defining the highest level of homogeneity within each group, which made possible the subgroups 'creation. Another goal was the development and validation of a HS-SPME-GC-MS/MS method for the quantification of compounds able to differentiate subgroups within each porosity level in wine model solution. This method constitutes a proof-of-concept tool to fine tune the current selection of stoppers in the cork industry (Furtado, Oliveira et al. 2021). The primary goal of all of these studies is to identify and quantify the compounds that pass from cork into wine. The main compounds found within the different phenolic classes were phenolic acids and aldehydes, namely gallic and protocatechuic acid amounts of around 3.5 mg/L, and the aldehydes vanillin and protocatechuic quantified in 2.5 and 1.5 mg/L after 27 months of bottling, respectively. More complex polyphenols, namely hydrolysable tannins such as castalagin/vescalagin and mongolícain A/B, were also detected in trace amounts (Azevedo, Fernandes et al. 2014). However, it is possible that hydrolysable tannins could be underestimated and unidentified since this study was focused on low molecular weight polyphenols. According to Reis et al. 2019, hydrolysable ellagitannins are present in cork in the same amounts as low molecular weight phenolic compounds. (Reis, Lopes et al. 2019).

Cork oxygen permeability

In the middle of the 19th century, Pasteur was the first scientist to consider the importance of oxygen for wine production and ageing. He wrote: "There exists a period...during which the wine must pass from a permeable container [the barrel] to one nearly impermeable [the bottle]" (Pasteur 1873).

The micro-permeability of cork stoppers to oxygen is considered to be the most important property that influences wine sensorial properties during post-bottling. Lopes et al. described that oxygen diffusion varies with the type of closure and material used (Lopes, Saucier et al. 2005). The oxygen input through different stoppers was determined by the

closure type and was independent of bottle storage position for the generality of the closures tested (during the first 24 months). The oxygen entry rates into bottles were lower in screw caps and “technical” corks, moderate in natural cork stoppers, and higher in the synthetic closures (Lopes, Saucier et al. 2006). In natural corks, during the first 12 months, oxygen desorbs slowly and continuously from the cell structure into the bottles during storage. In addition, technical cork stoppers are shown to be impermeable to oxygen from the atmosphere during the first 24 months of storage. On the other hand, synthetic closures were permeable to oxygen, mainly after the first month of storage (Lopes, Saucier et al. 2007). It seems that the screwcaps are the most airtight systems, followed by technical stoppers, natural corks and synthetic stoppers, in line with previous reports (Crouvisier-Urien, Bellat et al. 2018) (**Figure 4**).

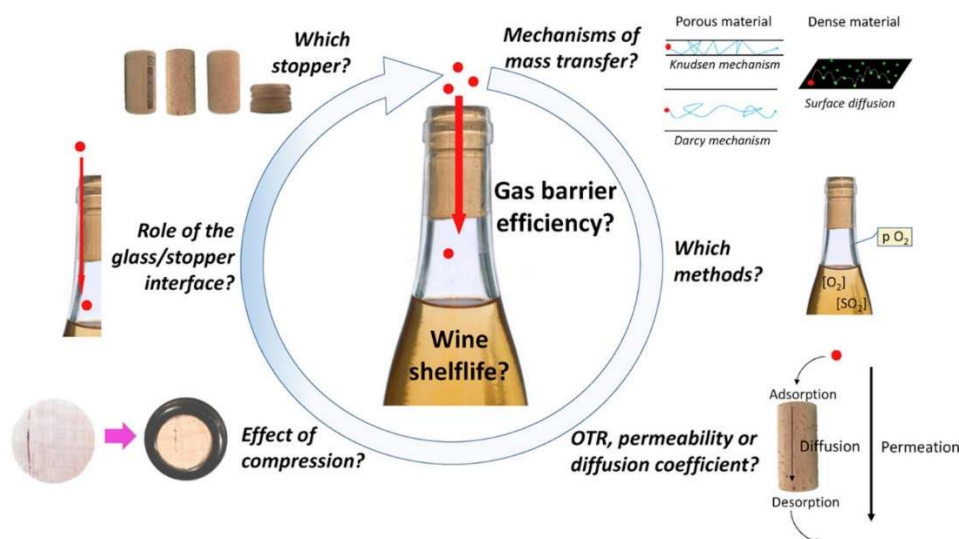


Figure 4. Graphical abstract in (Crouvisier-Urien, Bellat et al. 2018)

Furthermore, the quantity of oxygen in contact with wine can cause oxidation or reduction, which changes the wine aroma (Karbowiak, Gougeon et al. 2010). In a study correlating the impact of oxygen in a bottled Bordeaux Sauvignon Blanc wine with commercially available closures, it was observed that wines with higher exposition to oxygen at bottling and sealed with a synthetic with a higher permeability to oxygen, presented an oxidized aroma, low in volatile compounds and brown in color, when compared to wines sealed with other types of closures. On the other hand, wines bottles sealed with cork stoppers and screw cap saranex presented very low levels of reduced and oxidized characteristics (Lopes, Silva et al. 2009). However, due to the fact that the quantities of oxygen in cork stoppers are so low, oxygen transfer from cork stoppers cannot fully explain the evolution of wines after bottling, (Lopes, Silva et al. 2009). In fact, in the case of red wines, higher amounts of phenolic compounds make wine easier to oxidize, but at the same time, wines with higher amounts (despite oxidation) become

more oxygen resistant. In the case of white wines, the impact is usually perceived as it causes detrimental changes in the aroma, color, and taste.

But oxygen permeability has been investigated by different authors using a screw cap closure, two different natural corks, a synthetic closure, and a glass ampoule. The Waters group's work detailed the results of Riesling and a wooded Chardonnay wine over five years. The main findings were that the synthetic closure produced wines that were relatively oxidized in aroma, brown in color, and low in sulfur dioxide compared to those held under the other closures. The wines sealed with screw caps or in glass ampoules had a characteristic reduced aroma. This study's wines sealed with natural corks barely had any reduced aroma. In the circumstances of this study, bottle orientation during storage had no discernible effects on the composition and sensory characteristics of the wines under evaluation (SKOUROUMOUNIS, KWIATKOWSKI et al. 2005). Another work concerning the consistency of 'alternative' closures was developed by Brotto et al. (Brotto, Battistutta et al. 2010) that described a technique used to assess the variation among the lot of 20 various types of stoppers regarding oxygen permeability. The synthetic closure performed more consistently while the natural cork stopper displayed low homogeneity within the batch, notably in the first month following bottling (Brotto, Battistutta et al. 2010). Focus only on cork natural stoppers and the capacity of oxygen ingress capabilities. Oliveira et al studied 600 natural cork stoppers made from cork boards, in order to evaluate various quality classes. They are examined in order to account for the cork's inherent variability with relation to oxygen intrusion into the bottle. All examples had similar oxygen transport kinetics that could be adapted to logarithmic models. A substantial variation was discovered in the oxygen entry into the bottles sealed with natural cork stoppers. The findings imply that variations in oxygen intrusion are caused by the stopper's structure's naturally occurring variations in cell size and air volume (Oliveira, Lopes et al. 2013).

But technological advances allow creating novel types of closures, so the ranking related to oxygen permeability of different closures is modified. More recent work by (Pons, Lavigne et al. 2021) over a ten-year period, examined the chemical alterations in the strength of the oxidation odor in three Sauvignon blanc wines sealed with natural cork and various closures that had varied known oxygen transfer rates. Free SO₂ and 3-sulfanylhexanol loss during aging were connected with closure oxygen transfer rate levels, as were increases in dissolved O₂, OD420, and sotolon. Following a 10-year aging period, sensory analysis was carried out, accompanied by additional chemical analysis of fragrance effect markers, and it was discovered that some Sauvignon blanc wines

were protected from oxidation as long as the closing oxygen transfer rate did not surpass 0.3 mg/year.

It is also worth considering that the high inconsistency of cork oxygen ingress has been reported to cause variable levels of dissolved oxygen in the wine during bottle storage, which in turn has been associated with variable levels of sotolon, a well-known oxidation marker (Pons, Lavigne et al. 2010). Seven years after bottling, the sotolon and oxygen contents of various bottles of the same white wine were studied. The sotolon content in wine continued to be below its perceptibility threshold at the range of dissolved oxygen concentrations typically observed. Only in wines with oxygen contents exceeding 500 g/L was the perceptual threshold surpassed. The amount of free sulphur dioxide in the wine samples under study decreased as a result of the presence of dissolved oxygen (Lavigne, Pons et al. 2008).

Therefore, the impact of oxygen on bottled wine is going to differ depending on the type of wine (Tarko, Duda-Chodak et al. 2020). Moreover, since the 1960s, industry and scientists have been working together to identify compounds present in wines, especially phenolic compounds, involved in the mechanisms of oxidation occurring in wines (Karbowiak, Gougeon et al. 2009).

Phenolic compounds in wine

Phenolic compounds are plant secondary metabolism compounds with over 8000 compounds identified (Pérez-Jiménez, Neveu et al. 2010). Chemically, they have a general structure with at least one benzene ring and one hydroxyl group attached. Moreover, they can be divided into different families depending on structural differences (phenol rings number or/and the substitution groups). The two major families of phenolic compounds are flavonoids and non-flavonoids (**figure 5**).

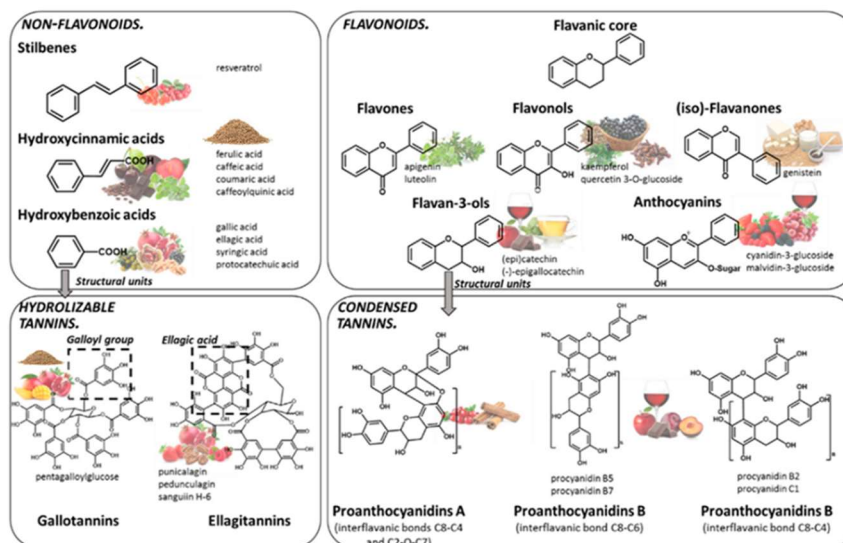


Figure 5: Chemical structure of the main families of polyphenols adapted from (Pérez-Gregorio, Soares et al. 2020)

Non flavonoids include stilbenes, lignins, coumarins, hydroxycinnamic acids and, hydroxybenzoic acids, these compounds have one or more benzene ring and different substitution patterns. Hydroxybenzoic acids are the simplest phenolic acids found in nature, and hydroxycinnamic acids are more common than the first ones. On the other hand, flavonoids are characterized by a flavanic core (**Figure 5**), two benzopyran rings and benzene. The methoxylation and/or hydroxylation pattern and linkage between the benzopyran and benzene rings define the subclasses. They can exist either in glycosylated or aglycone forms.

In wines, anthocyanins (in red wines), flavan-3-ols, and tannins are the phenolic compounds present in higher amounts. Tannins can be divided into hydrolyzable or condensed tannins. Their constitution is based on monosaccharide esters derived from gallic acid or units of flavan-3-ols, respectively (Pérez-Gregorio, Soares et al. 2020). Among these compounds, catechin (Flavan-3-ol) and malvidin-3-O-glucoside (Anthocyanin) in line with tannins are model compounds used in the works reported herein.

Phenolic compounds in cork

Since 1990, several studies have characterized the chemical composition of cork, mainly on phenolic compounds (**Table 1**) (Conde, Cadahía et al. 1997, Conde, Cadahía et al. 1998, Fernandes, Fernandes et al. 2009, Santos, Pinto et al. 2010, Fernandes, Sousa et al. 2011, Santos, Villaverde et al. 2013, Azevedo, Fernandes et al. 2014, Azevedo, Jesus et al. 2021) The first compounds that were identified in cork samples were gallic, sinapic, and caffeic acids, and vanillin (Conde, Cadahía et al. 1997, Santos, Pinto et al.

2010, Touati, Santos et al. 2015). Ten years later, the ellagitannins vescalagin and castalagin (isomers), grandinin, and roburin were reported as the main compounds that were extracted from a wine model solution after 24 h of contact with cork stoppers (Varea, Garcia-Vallejo et al. 2001). Furthermore, the structures of thirty-three compounds present in cork from *Quercus suber* L. were tentatively identified by LC-MS after being extracted into hydroalcoholic solutions (Table 1) (Fernandes, Sousa et al. 2011).

Table 1. Compounds found in cork.

Compound	First Described in <i>Quercus Suber</i>
Gallic acid	(Conde, Cadahía et al. 1997)
Protocatechuic acid	(Conde, Cadahía et al. 1997)
Protocatechuic aldehyde	(Conde, Cadahía et al. 1997)
Coniferaldehyde	(Conde, Cadahía et al. 1997)
Caffeic acid	(Conde, Cadahía et al. 1997)
Ferulic acid	(Conde, Cadahía et al. 1997)
Vanillin	(Conde, Cadahía et al. 1997)
Sinapic acid	(Conde, Cadahía et al. 1997)
Ellagic acid	(Conde, Cadahía et al. 1997)
Ellagic acid-pentose	(Conde, Cadahía et al. 1998)
Ellagic acid-deoxyhexose	(Conde, Cadahía et al. 1997, Conde, Cadahía et al. 1998)
Ellagic acid-hexose	(Conde, Cadahía et al. 1998)
Valoneic acid dilactone	(Conde, Cadahía et al. 1997, Conde, Cadahía et al. 1998)
HHDP-glucose	(Cantos, Espín et al. 2003)
Valoneic acid	(Cantos, Espín et al. 2003)
Dehydrated tergallic-C-glucoside	(Cantos, Espín et al. 2003)
HHDP-galloyl-glucose	(Cantos, Espín et al. 2003)
Trigalloyl-glucose	(Cantos, Espín et al. 2003)
Di-HHDP-glucose	(Cantos, Espín et al. 2003)
HHDP-digalloyl-glucose	(Cantos, Espín et al. 2003)
Tetragalloyl-glucose	(Cantos, Espín et al. 2003)
Di-HHDP-galloyl-glucose	(Cantos, Espín et al. 2003)
Trigalloyl-HHDP-glucose	(Cantos, Espín et al. 2003)
Pentagalloyl-glucose	(Cantos, Espín et al. 2003)
Mongolicain	(Ito, Yamaguchi et al. 2002)
Dehydrocastalagin	(Azevedo, Jesus et al. 2021)
Ellagic acid rhamnoside	(Azevedo, Jesus et al. 2021)
Vescalagin	(Varea, Garcia-Vallejo et al. 2001)
Castalagin	(Varea, Garcia-Vallejo et al. 2001)

Vescalagin–ethanol derivative	(Azevedo, Fernandes et al. 2017)
Roburin A	(Conde, Cadahía et al. 1998, Varea, Garcia-Vallejo et al. 2001)
Roburin E	(Conde, Cadahía et al. 1998)
Granidin	(Varea, Garcia-Vallejo et al. 2001)
Ethyl-vescalagin	(Azevedo, Fernandes et al. 2017)
Acutissimin	(Azevedo, Fernandes et al. 2017)
salicylic acid	(Santos, Pinto et al. 2010)
eriodictyol	(Santos, Pinto et al. 2010)
naringenin	(Santos, Pinto et al. 2010)
quinic acid	(Santos, Pinto et al. 2010)
hydroxyphenyllactic acid	(Santos, Pinto et al. 2010)
vescalin	(Reis, Lopes et al. 2019)
castalin	(Reis, Lopes et al. 2019)
guajavin B/ eugenigrandinin A	(Reis, Lopes et al. 2019)
vescavalonic acid	(Reis, Lopes et al. 2019)
castavalonic acid	(Reis, Lopes et al. 2019)
Isorhamnetin-3-O-rutinoside	(Azevedo, Jesus et al. 2021)

*HHDP:hexahydriphenyl

The simpler phenolic compounds detected were phenolic acids and aldehydes and more complex like gallic acid derivatives, gallotannins (galloyl esters of glucose), combinations of galloyl and ellagitannins (hexahydroxydiphenoyl esters of glucose), dehydrated tergallic-C-glucosides or ellagic acid derivatives. In addition, Mongolicain (flavanoellagitannin with hydrolysable tannin and flavan-3-ol moieties are linked through a carbon–carbon bond) was also detected in cork from *Quercus suber L.* (Ito, Yamaguchi et al. 2002). These examples show how rich in phenolic compounds is cork (Fernandes, Sousa et al. 2011). Santos et al. 2010 reported for the first time salicylic acid, eriodictyol, naringenin, quinic acid and hydroxyphenyllactic acid as cork components (Santos, Pinto et al. 2010). Moreover, Reis et al 2019 described the presence of vescalin, castalin, guajavin B/eugenigrandinin A, vescavalonic, and castavalonic acids in cork samples (Reis, Lopes et al. 2019). Other ellagitannins such as the glycosylated structure of acutissimin A/B and guajavin B/eugenigrandinin A, oligomeric ellagitannins and a glycosylated dimer of galocatechin linked to vescalagin/castalagin were found to occur by MALDI-TOF (Reis, Lopes et al. 2019). In another work, a wine model solution extracted ellagitannins, proanthocyanidins, and pectic-derived polysaccharides from natural cork stoppers, with simple C-glycosidic, complex, and oligomeric ellagitannins being identified by HPLC–DAD/ESI-MS. In addition, MALDI-TOF-MS was used for the identification of ellagitannins linked to proanthocyanidins and some pectic-derived polysaccharides (Reis, Coelho et al. 2020).

Some studies were developed to evaluate the potential correlation between the composition of cork and its geographic region of origin. Cork stopper granulates from eleven geographical origins in Portugal and Spain were analyzed by HPLC-DAD/ESI-MS and near-infrared spectroscopy (NIRS) to assess geographical discrimination regarding polyphenol composition. NIRS technique showed to be a powerful tool to discriminate origins and predict the concentration of polyphenols. However, the variability in the phenolic compound composition of cork samples was high and it was not influenced by geographical location (Reis, Teixeira et al. 2020). Within the same regions, Guedes de Pinho et al. demonstrated three main clusters of regions according to their chemical similarity, however, a geographical proximity was not found (Pinto, Oliveira et al. 2019). Nineteen compounds were responsible for the clusters, including terpenes, polyphenols (vescalagin and castalagin) and others (pyrogallol, glucosan, sitost-4-en-3-one, *o*-cymene, quinic acid, and five unidentified compounds), with the authors concluding that the geographical location does not seem to be responsible for the variability in the polyphenol composition of cork stoppers, being more likely influenced by genetics or tree age (Pinto, Oliveira et al. 2019). The fact that there are no statistically differences between each of the regions studied may be due to the high amounts of gallic, protocatechuic, and ellagic acids present in samples from all regions (Fernandes, Fernandes et al. 2009, Touati, Santos et al. 2015).

Interaction between cork and wine

Cork stoppers are known to be the major cause of contamination in wines (Sefton and Simpson 2005). Cork taint is in fact a problem in this industry, and a recent review described in detail six compounds that have been found to contribute to this undesirable flavor. These are guaiacol, geosmin, 2-methylisoborneol (MIB), octen-3-ol, and octen-3-one; and the most important of them all, 2,4,6 trichloroanisole (Cravero 2020). Other authors described also 2-Methoxy-3,5-dimethylpyrazine (Simpson, Capone et al. 2004, Chatonnet, Fleury et al. 2010). The geosmin and 2-methylisoborneol (2-MIB) are responsible for earthy off-flavor; pyrazines cause vegetable odors, and guaiacol results in smoked, phenolic and medicinal defects and the 1-octen-3-ol and 1-octen-3-one caused off-odors of mushrooms in wines which are caused by grapes contaminated by bunch rot (Cravero 2020). Moreover, the best known and the most problematic off-flavor compound of the cork stopper is the 2,4,6-trichloroanisole (TCA), known specifically to yield a "cork taint" in wines (Pena-Neira, De Simón et al. 2000), and it is formed from the chlorination of lignin-related compounds during chlorine bleaching in the processing of cork (Buser, Zanier et al. 1982). About twenty years ago this problem in the wine industry originated losses of around 10 billion dollars per year (Taylor, Young et al. 2000). The

small amounts around ng/L of TCA can be extremely detrimental to the wine quality (Tarasov, Rauhut et al. 2017) derived from its high volatility and low perception threshold (1,5-2 ng/L) (Sefton and Simpson 2005). Other compounds from the same family can also be responsible for the designated cork taint but in a much less extension, the 2,4-dichloroanisole (2,4-DCA), 2,6-dichloroanisole (2,6-DCA), 2,3,4,6-tetrachloroanisole (TeCA) and pentachloroanisole (PCA). Furthermore, the 2,4,6-tribromoanisole (TBA) has a significant impact on the musty/moldy fault; however, this compound isn't found in cork (Chatonnet, Bonnet et al. 2004). The chlorophenols (2,4,6-trichlorophenol, 2,3,4,6-tetrachlorophenol, and pentachlorophenol (PCP)) were also described as “cork taint responsible compounds” (Peña-Neira, Fernández de Simón et al. 2000). Note that, not always, the sources of contamination are natural cork stoppers. The air pollution of the cellars, wood materials, barrels, and chips are also known as the sources of the problem (Cravero 2020).

In addition, several groups have been working on the identification of the main volatile compounds present in cork, such as aliphatic alcohols, monoterpenes, triterpenes, sterols, phenols, and fatty acids (Rocha, Delgadillo et al. 1996, Moreira, Lopes et al. 2016), described as the main compounds (**Table 2**). These compounds can be extracted from cork by a wine model solution in bottle (Pinto, Oliveira et al. 2019).

Table 2. Description of semi-volatile (GC-MS) and volatile (HS-SPME-GC-MS) compounds able to pass from cork by methanol and wine model solution (Pinto, Oliveira et al. 2019)

GC-MS profiling of semi-volatile compounds extracted from cork by methanol

<i>Alkenes</i>	<i>Carbohydrate</i>	<i>Fatty alcohols</i>
1-Pentacosene	Glucosan	1-Eicosanol
1-Heptacosene		1-Docosanol

<i>Fatty acids</i>	<i>Glycerolipids</i>
n-Hexadecanoic acid	Glycerol 1-hexadecanoate
cis-9,cis-12-Octadecadienoic acid	Glycerol 1-octadecanoate
cis-9-Octadecenoic acid	
n-Octadecanoic acid	
Eicosanoic acid	
Docosanoic acid	

<i>Phenols and derivatives</i>	<i>Sterols</i>	<i>Triterpenes</i>
Catechol	Stigmastan-3,5-diene	<i>trans</i> -Squalene
Pyrogallol	β-Sitosterol	Lupen-3-one
Vanillin	Sitost-4-en-3-one	Lupeol

trans-Coniferyl alcohol

Friedelin

Betulin

HS-SPME-GC-MS profiling of volatile compounds extracted from cork by wine model solution

<i>Aldehydes</i>	<i>Benzenoids</i>	<i>Esters</i>	<i>Monoterpenes</i>
Hexanal	<i>o</i> -Cymene	Ethyl hexanoate	α -Pinene
Heptanal	Naphthalene	Ethyl heptanoate	Camphene
Benzaldehyde		Ethyl nonanoate	β -Pinene
Octanal		Fenchyl acetate	1,4-Cineole
Nonanal		Isobornyl acetate	α -Terpinene
Decanal			Limonene
			Eucalyptol
			Terpinolene
			Fenchone
			Fenchol
			α -Campholenal
			(+)-Camphor
			<i>trans</i> - β -Terpineol
			<i>trans</i> -3-Pinanone
			Isoborneol
			<i>l</i> -Borneol
			<i>cis</i> -3-Pinanone
			1-Terpinen-4-ol
			α -Terpineol
			Monoterpene 1

Beside the volatile fraction, polyphenols can be extracted from cork to wine model solutions (Azevedo, Fernandes et al. 2014, Reis, Coelho et al. 2020). Therefore, it is important to understand the possible impact these compounds may have on the evolution of wine sealed with cork stoppers. A recent study showed that corks from different origins (suppliers) can impact differently on wine properties (Minnaar, Gerber et al. 2021) due to the phenolic acids susceptible to pass from cork to wine. Gallic, caffeic, and *p*-coumaric acids were studied in two-disc corks from three different commercial suppliers. Gallic acid was significantly higher in Cork A wines, which indicates the contribution of Cork A to the concentration of this compound in the wine. This may be due to differences in the surface roughness of cork that would increase the surface area in contact with the wine (Minnaar, Gerber et al. 2021). Moreover, a study evaluated the reactivity of phenolic compounds from cork stoppers and assayed their reaction with two major wine components, namely, (+)-catechin and malvidin-3-O-

glucoside. From these assays, several compounds already described in the literature were detected together with a new compound belonging to a family of ellagitannin-derived compounds, named corklins (**Figure 6**) (Azevedo, Fernandes et al. 2017). The interaction between ellagitannins in alcoholic solutions and catechins (cat) described this new family of compounds.

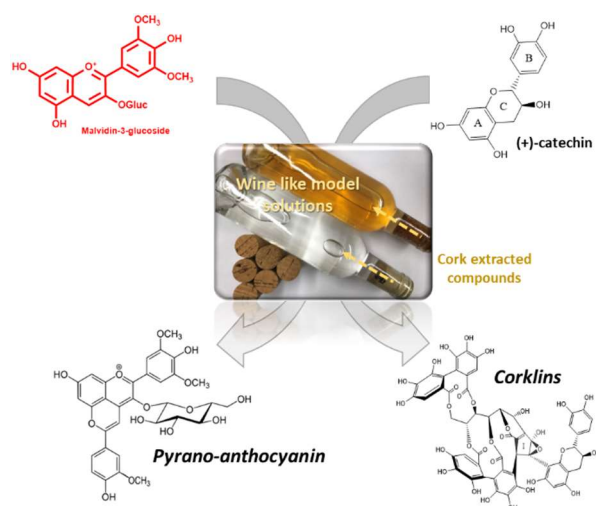


Figure 6. Bottling study scheme and compounds formed (graphical abstract from (Azevedo, Fernandes et al. 2017).

Other reactions yielded the formation of structures like pinotins (**Figure 6**) (Schwarz, Jerz et al. 2003), xanthylum salts (Es-Safi, Cheynier et al. 2000), and a dimer of cat-Vanillin-cat (Vivas, Nonier et al. 2016). All these compounds have different chromatic characteristics from their precursors and can thus have an impact on the final color of wines. Indeed, phenolic acids and aldehydes have been identified as the major compounds that pass through to bottled wine model solutions from various cork stopper grades (Azevedo, Fernandes et al. 2014). These phenolic acids did not influence directly the organoleptic properties of red wine but may be involved on white wine color evolution when oxidized to the respective quinones (Karbowiak, Gougeon et al. 2009). On the other hand, a recent work describes the influence that these compounds may have on the sensory perception of wine from an astringency perspective (Azevedo, Jesus et al. 2021).

In wine, tannins can undergo chemical transformations such as condensation with anthocyanins, pyranoanthocyanins, or other phenolic compounds, oxidation or hydrolysis reactions in a slow but continuous way (Quideau, Jourdes et al. 2005), yielding to the formation of more complex structures like portisins (Oliveira, de Freitas et al. 2007), flavano-ellagitannins and ethyl-vescalagin (Saucier, Jourdes et al. 2006) or corklins (ellagitannin derivate compounds) (Azevedo, Fernandes et al. 2017). While it is known

that grape seed tannins contribute to the structure of wines, they can also cause excessive astringency. When combined with polysaccharides and proteins, tannins contribute to wine's softness and roundness but can also impart herbaceous notes if grapes are not ripened (Soares, Brandao et al. 2017). These compounds have also been described as some of the compounds that pass from cork stopper to model wine solutions (Varea, Garcia-Vallejo et al. 2001, Azevedo, Fernandes et al. 2017).

From an astringency standpoint, a recent work (Azevedo, Jesus et al. 2021) explored for the first time the interaction between three cork fractions and salivary proteins. The results suggested that the ellagitannin castalagin was the most reactive with salivary proteins, while 4-dehydrocastalagin was the most precipitated compound. The fraction containing caffeic and sinapic acids showed the highest interaction with salivary proteins, mainly cystatins. Castalagin, 4-dehydrocastalagin, caffeic, and ellagic acids were almost always precipitated above their reported astringency thresholds, and by this, they may contribute to the astringency perception.

The wine's flavor undergoes changes during bottle aging, which can be induced by the type of closure (cork, synthetic, or screw cap). These changes are more noticeable when the storage period is longer than the five years described by Guedes de Pinho and co-workers (Furtado, Lopes et al. 2021). The permeation, sorption (scalping), or desorption phenomena among closures and wines were studied, and concluded that corks help to keep the aroma, as cork material has a low sorption capacity for some compounds, specifically non-polar ones, which are known to be directly correlated with wine fruity scents. (Furtado, Lopes et al. 2021). Moreover, the authors also reported for the first time the presence of two new compounds, *trans-4-tert-butylcyclohexanol* and *2,4-di-tert-butylphenol*, in wines sealed with specific micro-agglomerated cork stoppers with plastic microspheres and synthetic closures, respectively. Furthermore, wines with synthetic stoppers presented high levels of oxidative attributes, low levels of SO₂, and high color intensity, contrarily to cork stoppers that demonstrated higher scores in aroma intensity, aroma quality, and balance (Oliveira, Furtado et al. 2020).

As previously mentioned, cork stoppers as well as wood barrels could impact wine organoleptic properties (aroma, color, and taste) during ageing. Despite extensive knowledge on the subject, oenologists typically select cork stoppers or wood barrel varieties based on intuition rather than targeted chemical interactions. A recent study suggested that some polyphenols found in cork stoppers migrate to wine solutions, interacting with human salivary proteins linked to astringency. This could be positive or negative depending on the type of wine. This knowledge should be expanded for other

varieties of cork stoppers in order to allow the choice of stoppers to upgrade wine quality during storage and aging. Nowadays, numerous studies are trying to correlate the beneficial effect of cork on wine's physical-chemical and sensorial parameters.

Sustainability

Cork oak trees are natural retainers of CO₂, with a stripped cork oak absorbing on average five times more CO₂ during the regeneration than a regular cork oak (Amorim 2020). Moreover, these trees prevent soil degradation, regulate the hydrological cycle, combat desertification and contribute to biodiversity. Cork is a natural material that is both renewable and recyclable (Ritsche, Katzensteiner et al. 2021). Cork is not only used in the wine industry, and its application in other industries has been increasing, such as in footwear, automotive, and packaging industries. In the cork industry, there is no waste and everything is transformed into new products and solutions (Amorim 2021).

The cork industry's main byproducts are cork powder and granules. This product has a wide range of applications, from cork stoppers to incorporation in agglomerates and briquettes to use as an adsorbent in the treatment of gaseous emissions, waters, and wastewaters (Antxustegi, Corro et al. 2022). In its natural form, cork biomass has been used as a biosorbent for heavy metals and oils, and it is also a precursor of activated carbon for the removal of emerging organic pollutants in water. (Pintor, Ferreira et al. 2012).

Several research groups are looking for non-destructive methods to remove some undesirable volatile compounds from cork that could eventually end up contaminating the bottled wines (Khaw, Parat et al. 2017, Manrique 2017). These techniques have been developed with the propose to be clean, sustainable, and efficient process (Azmir, Zaidul et al. 2013). Supercritical fluids extraction in the cork industry has been applied to extract contaminants such as TCA, or bioactive compounds (Taylor, Young et al. 2000, Silva, Sabino et al. 2005, Manrique 2017). This methodology aims to produce clean cork granules, ensuring that microagglomerate cork is free of TCA and contaminants.

This knowledge is very important within the context of the circular economy, as the characterization of natural waste sources for reutilization leads to greater global sustainability (Dairi, Bellili et al. 2022). In general, cork stoppers and cork by-product extracts demonstrated high aromatic and antioxidant potential to be further reused in different industries, such as agricultural, cosmetic, and pharmaceutical industries (Quideau, Jourdes et al. 2005, Fernandes, Fernandes et al. 2009, Azevedo, Fernandes

et al. 2014, Manrique 2017, Carriço, Ribeiro et al. 2018, Reis, Lopes et al. 2019, Mislata, Puxeu et al. 2020).

In a similar vein, the work described by Freitas group (Freitas, Rocha et al. 2022) using natural deep eutectic solvents (NADES) as a solvent in order to eliminate or reduce the use of toxic chemicals. They used different natural compounds, such as lactic acid and glycerol. The results showed higher extraction capacity with acidic NADES, which extracted great quantities of aromatic compounds, terpenoids, and fatty acids. On the other hand, more basic eutectic mixtures extracted more quantities of low molecular weight polar compounds. This research, along with the associated nontoxicity, low cost, and ease of preparation, establishes NADES as a green approach to extracting high added-value compounds from cork (Freitas, Rocha et al. 2022).

When considering adsorption for water treatment, commercial activated carbon is typically the adsorbent of choice for the removal of pollutants from the aqueous phase, particularly pharmaceuticals. Attempts have been made to use wastes as raw materials for the production of alternative carbon adsorbents in order to reduce costs and conserve natural resources. This approach aims to improve efficiency and cost-effectiveness while also proposing an alternative and sustainable method for residue valorization and management (Silva, Jaria et al. 2018, Antxustegi, Corro et al. 2022). Cork has gained popularity in water remediation since it was first used as a precursor for the production of eco-friendly activated carbon through chemical and physical activation. The findings of this study show that lab-made carbons have adequate properties for removing pharmaceutical compounds from water (Mestre, Pires et al. 2014). Furthermore, cork powder biosorption is regarded as a promising method for heavy metal removal from industrial wastewaters, such as those from chromium tanning factories (Sfaksi, Azzouz et al. 2014).

In a circular economy approach, it is intended to close the energetic cycle. Despite the technical and safety difficulties presented by the use of cork powder as a low-density material, which complicates its transportation for industrial uses outside the area in which it is produced, the cork industry has attempted to take advantage of residues, primarily through direct energy recovery. As a result, cork pellets emerge as a safer and more easily transportable alternative for energy recovery from cork dust and other granulated types of cork waste, with the potential for wider application. These findings show that cork pellets have a higher calorific value than other biomass pellets (Nunes, Matias et al. 2013).

Conclusions

As a result, the recognition of cork as an excellent product used globally has piqued the interest of this research area. The heterogeneity of its chemical constitution and its remarkable properties give cork material with enormous potential and considerable importance. The wine industry and the scientific community have published a number of sensory studies that have reported that consumers believe that wines bottled with cork stoppers present an enhanced quality compared to wines sealed with other closures (Marin, Jorgensen et al. 2007).

There is also a valorization as a natural product from a sustainable perspective and also an accounting that its by-products can be regarded as a relevant source of bioactive components like phenolic acids, terpenoids, and tannins as already described in the literature (Manrique 2017, Carriço, Ribeiro et al. 2018, Reis, Lopes et al. 2019, Reis, Coelho et al. 2020).

The path of research seems to point to the cork stopper as an excellent closure. It is a fact for the cork industry that the ability to predict whether the cork may or may not influence the bottled wine will always be an asset. Ultimately, the cork stopper will always be a natural choice.

Acknowledgements

The authors thank the Science and Technology Foundation (FCT) for the scholarships SFRH/BD/139709/2018, UIDB/50006/2020 and UIDBP/50006/2020. This research had support by AGRIFOOD XXI - Development and consolidation of re-search in the agrifood sector in Northern Portugal. Funding Program. "Projetos Estruturados de I&D&I" - UNorte, Reference: NORTE-01-0145-FEDER-00004.

Funding

This research was funded by UIDB/50006/2020.

Conflicts of Interest: The authors declare no conflict of interest

Author Contributions: Conceptualization, J.A., P. L. and V.F.; investigation, J.A.; writing—original draft preparation, J.A.; writing—review and editing, P.L., N.M and V.F.; funding acquisition, N. M. and V.F. All authors have read and agreed to the published version of the manuscript.

References

- . Retrieved 24/5/2021 from <https://www.corklink.com/index.php/natural-wine-cork-classification/>
- Amorim. (2017). *About cork stoppers*. https://www.amorim.com/xms/files/Documentacao/About_cork_stoppers_final_LR.pdf.
- Amorim. (2020). *Cork Oak Forest*. <https://amorimcorkcomposites.com/en/why-cork/facts-and-curiosities/about-oak-forest/#section-HowImportantAreCorkOakForests-3651>
- Amorim. (2021). <https://www.amorim.com/en/cork/history/>
- Antxustegi, M., Corro, E., Baloch, M., Volpe, R., & Alriols, M. G. (2022). Production of Activated Bio-chars for Wastewater Treatment: Characterization, Activation and Evaluation of the Adsorption Capacity. *Chemical Engineering Transactions*, 92, 547-552. <https://doi.org/10.3303/CET2292092>
- Azevedo, J., Brandão, E., Soares, S., Oliveira, J., Lopes, P., Mateus, N., & de Freitas, V. (2020). Polyphenolic Characterization of Nebbiolo Red Wines and Their Interaction with Salivary Proteins. *Foods (Basel, Switzerland)*, 9(12). <https://doi.org/https://10.3390/foods9121867>
- Azevedo, J., Fernandes, A., Oliveira, J., Brás, N. F., Reis, S., Lopes, P., Roseira, I., Cabral, M., Mateus, N., & de Freitas, V. (2017). Reactivity of Cork Extracts with (+)-Catechin and Malvidin-3-O-glucoside in Wine Model Solutions: Identification of a New Family of Ellagitannin-Derived Compounds (Corklins). *J Agric and Food Chem*, 65(39), 8714-8726. <https://doi.org/https://doi.org/10.1021/acs.jafc.7b02845>
- Azevedo, J., Fernandes, I., Lopes, P., Roseira, I., Cabral, M., Mateus, N., & Freitas, V. (2014). Migration of phenolic compounds from different cork stoppers to wine model solutions: antioxidant and biological relevance [journal article]. *Eur Food Res and Techno*, 239(6), 951-960. <https://doi.org/https://doi.org/10.1007/s00217-014-2292-y>
- Azevedo, J., Jesus, M., Brandão, E., Soares, S., Oliveira, J., Lopes, P., Mateus, N., & de Freitas, V. (2021). Interaction between salivary proteins and cork phenolic compounds able to migrate to wine model solutions. *Food Chemistry*, 130607. <https://doi.org/https://doi.org/10.1016/j.foodchem.2021.130607>
- Azmir, J., Zaidul, I. S. M., Rahman, M. M., Sharif, K. M., Mohamed, A., Sahena, F., Jahurul, M. H. A., Ghafoor, K., Norulaini, N. A. N., & Omar, A. K. M. (2013). Techniques for extraction of bioactive compounds from plant materials: A review. *Journal of Food Engineering*, 117(4), 426-436. <https://doi.org/https://doi.org/10.1016/j.jfoodeng.2013.01.014>
- Brotto, L., Battistutta, F., Tat, L., Comuzzo, P., & Zironi, R. (2010). Modified Nondestructive Colorimetric Method To Evaluate the Variability of Oxygen Diffusion Rate through Wine Bottle Closures. *Journal of Agricultural and Food Chemistry*, 58(6), 3567-3572. <https://doi.org/10.1021/jf903846h>
- Brugnatelli, D. (1787). *Elementi di chimica. Tomo II* (Vol. Tomo II).
- Buser, H. R., Zanier, C., & Tanner, H. (1982). Identification of 2,4,6-trichloroanisole as a potent compound causing cork taint in wine. *Journal of Agricultural and Food Chemistry*, 30(2), 359-362. <https://doi.org/10.1021/jf00110a037>
- Canellas, E., Vera, P., Nerin, C., Goshawk, J., & Dreolin, N. (2021). The application of ion mobility time of flight mass spectrometry to elucidate neo-formed compounds derived from polyurethane adhesives used in champagne cork stoppers. *Talanta*, 234, 122632. <https://doi.org/https://doi.org/10.1016/j.talanta.2021.122632>
- Cantos, E., Espín, J. C., López-Bote, C., de la Hoz, L., Ordóñez, J. A., & Tomás-Barberán, F. A. (2003). Phenolic Compounds and Fatty Acids from Acorns (*Quercus* spp.), the Main Dietary Constituent of Free-Ranged Iberian Pigs. *J of Agric and Food Chem*, 51(21), 6248-6255. <https://doi.org/10.1021/jf030216v>
- Carrigo, C., Ribeiro, H. M., & Marto, J. (2018). Converting cork by-products to ecofriendly cork bioactive ingredients: Novel pharmaceutical and cosmetics applications. *Ind Crops and Prod*, 125, 72-84. <https://doi.org/https://doi.org/10.1016/j.indcrop.2018.08.092>
- Chanut, J., Lagorce, A., Lequin, S., Gougeon, R. D., Simon, J.-M., Bellat, J.-P., & Karbowiak, T. (2020). Fast manometric method for determining the effective oxygen diffusion coefficient through wine stopper. *Polymer Testing*, 106924. <https://doi.org/https://doi.org/10.1016/j.polymertesting.2020.106924>

- Chatonnet, P., Bonnet, S., Boutou, S., & Labadie, M.-D. (2004). Identification and responsibility of 2, 4, 6-tribromoanisole in musty, corked odors in wine. *Journal of Agricultural and Food Chemistry*, 52(5), 1255-1262.
- Chatonnet, P., Fleury, A., & Boutou, S. (2010). Origin and Incidence of 2-Methoxy-3,5-dimethylpyrazine, a Compound with a "Fungal" and "Corky" Aroma Found in Cork Stoppers and Oak Chips in Contact with Wines. *Journal of Agricultural and Food Chemistry*, 58(23), 12481-12490. <https://doi.org/10.1021/jf102874f>
- Conde, E., Cadahía, E., García-Vallejo, M. C., & De Simón, B. F. (1998). Polyphenolic Composition of Quercus suber Cork from Different Spanish Provenances [Article]. *Journal of Agricultural and Food Chemistry*, 46(8), 3166-3171. <https://doi.org/https://doi.org/10.1021/jf970863k>
- Conde, E., Cadahía, E., García-Vallejo, M. C., Fernández De Simón, B., & González Adrados, J. R. (1997). Low Molecular Weight Polyphenols in Cork of Quercus suber [Article]. *J of Agric and Food Chem*, 45(7), 2695-2700. <https://doi.org/https://doi.org/10.1021/jf960486w>
- Corona, T., Iglesias, M., & Anticó, E. (2014). Migration of Components from Cork Stoppers to Food: Challenges in Determining Inorganic Elements in Food Simulants. *Journal of Agricultural and Food Chemistry*, 62(24), 5690-5698. <https://doi.org/10.1021/jf500170w>
- Cravero, M. C. (2020). Musty and Moldy Taint in Wines: A Review. *Beverages*, 6(2), 41. <https://www.mdpi.com/2306-5710/6/2/41>
- Crouvisier-Urien, K., Bellat, J.-P., Gougeon, R. D., & Karbowski, T. (2018). Gas transfer through wine closures: A critical review. *Trends in Food Science & Technology*, 78, 255-269. <https://doi.org/https://doi.org/10.1016/j.tifs.2018.05.021>
- Dairi, B., Bellili, N., Hamour, N., Boulassel, A., Djidjelli, H., Boukerrou, A., & Bendib, R. (2022). Cork waste valorization as reinforcement in high-density polyethylene matrix. *Materials Today: Proceedings*. <https://doi.org/https://doi.org/10.1016/j.matpr.2021.12.420>
- Dwivedi, P., Mishra, P. K., Mondal, M. K., & Srivastava, N. (2019). Non-biodegradable polymeric waste pyrolysis for energy recovery. *Heliyon*, 5(8), e02198. <https://doi.org/https://doi.org/10.1016/j.heliyon.2019.e02198>
- Es-Safi, N.-E., Cheyner, V., & Moutounet, M. (2000). Study of the Reactions between (+)-Catechin and Furfural Derivatives in the Presence or Absence of Anthocyanins and Their Implication in Food Color Change. *Journal of Agricultural and Food Chemistry*, 48(12), 5946-5954. <https://doi.org/https://doi.org/10.1021/jf000394d>
- Fernandes, A., Fernandes, I., Cruz, L., Mateus, N., Cabral, M., & De Freitas, V. (2009). Antioxidant and biological properties of bioactive phenolic compounds from Quercus suber L [Article]. *J of Agric and Food Chem*, 57(23), 11154-11160. <https://doi.org/https://doi.org/10.1021/jf902093m>
- Fernandes, A., Sousa, A., Mateus, N., Cabral, M., & de Freitas, V. (2011). Analysis of phenolic compounds in cork from Quercus suber L. by HPLC–DAD/ESI–MS. *Food Chem*, 125(4), 1398-1405. <https://doi.org/https://doi.org/10.1016/j.foodchem.2010.10.016>
- Freitas, D. S., Rocha, D., Castro, T. G., Noro, J., Castro, V. I. B., Teixeira, M. A., Reis, R. L., Cavaco-Paulo, A., & Silva, C. (2022). Green Extraction of Cork Bioactive Compounds Using Natural Deep Eutectic Mixtures. *ACS Sustainable Chemistry & Engineering*. <https://doi.org/10.1021/acssuschemeng.2c01422>
- Furtado, I., Lopes, P., Oliveira, A. S., Amaro, F., Bastos, M. d. L., Cabral, M., Guedes de Pinho, P., & Pinto, J. (2021). The Impact of Different Closures on the Flavor Composition of Wines during Bottle Aging. *Foods (Basel, Switzerland)*, 10(9), 2070. <https://doi.org/10.3390/foods10092070>
- Furtado, I., Oliveira, A. S., Amaro, F., Lopes, P., Cabral, M., Bastos, M. d. L., Guedes de Pinho, P., & Pinto, J. (2021). Volatile profile of cork as a tool for classification of natural cork stoppers. *Talanta*, 223, 121698. <https://doi.org/https://doi.org/10.1016/j.talanta.2020.121698>
- Furtado, I., Oliveira, A. S., Amaro, F., Lopes, P., Cabral, M., de Lourdes Bastos, M., Guedes de Pinho, P., & Pinto, J. (2020). Volatile profile of cork as a tool for classification of natural cork stoppers. *Talanta*, 121698. <https://doi.org/https://doi.org/10.1016/j.talanta.2020.121698>
- Gardner, D. (2008). Innovative Packaging for the Wine Industry: A Look at Wine Closures. *Virginia Tech Food Science and Technology. Duck Pond, Dr Blacksburg, VA, 24061*, 2008.
- Hooke, R., Allestry, J., & Martyn, J. (1665). *Micrographia, or, Some physiological descriptions of minute bodies made by magnifying glasses :with observations and inquiries thereupon*. Printed by Jo. Martyn and Ja. Allestry, printers to the Royal Society ... <https://www.biodiversitylibrary.org/item/15485>

- Ito, H., Yamaguchi, K., Kim, T. H., Khenouf, S., Gharzouli, K., & Yoshida, T. (2002). Dimeric and trimeric hydrolyzable tannins from *Quercus coccifera* and *Quercus suber* [Article]. *Journal of Natural Products*, 65(3), 339-345. <https://doi.org/10.1021/np010465i>
- Jové, P., Pareras, A., De Nadal, R., & Verdum, M. (2021). Development and optimization of a quantitative analysis of main odorants causing off flavours in cork stoppers using headspace solid-phase microextraction gas chromatography tandem mass spectrometry [Article]. *Journal of Mass Spectrometry*, 56(5), Article e4728. <https://doi.org/10.1002/jms.4728>
- Karbowiak, T., Gougeon, R. D., Alinc, J.-B., Brachais, L., Debeaufort, F., Voilley, A., & Chassagne, D. (2009). Wine Oxidation and the Role of Cork. *Critical Reviews in Food Science and Nutrition*, 50(1), 20-52. <https://doi.org/10.1080/10408390802248585>
- Karbowiak, T., Gougeon, R. D., Alinc, J. B., Brachais, L., Debeaufort, F., Voilley, A., & Chassagne, D. (2010). Wine Oxidation and the Role of Cork [Review]. *Critical Reviews in Food Science and Nutrition*, 50(1), 20-52. <https://doi.org/10.1080/10408390802248585>
- Khaw, K.-Y., Parat, M.-O., Shaw, P. N., & Falconer, J. R. (2017). Solvent Supercritical Fluid Technologies to Extract Bioactive Compounds from Natural Sources: A Review. *Molecules (Basel, Switzerland)*, 22(7), 1186. <https://doi.org/10.3390/molecules22071186>
- Lavigne, V., Pons, A., Darriet, P., & Dubourdiou, D. (2008). Changes in the Sotolon Content of Dry White Wines during Barrel and Bottle Aging. *Journal of Agricultural and Food Chemistry*, 56(8), 2688-2693. <https://doi.org/10.1021/jf072336z>
- Leite, C., Oliveira, V., Miranda, I., & Pereira, H. (2020). Cork oak and climate change: Disentangling drought effects on cork chemical composition [Article]. *Scientific Reports*, 10(1), Article 7800. <https://doi.org/10.1038/s41598-020-64650-9>
- Leite, C., & Pereira, H. (2017). Cork-containing barks—a review [Review]. *Frontiers in Materials*, 3, Article 63. <https://doi.org/10.3389/fmats.2016.00063>
- Lopes, P., Saucier, C., & Glories, Y. (2005). Nondestructive Colorimetric Method To Determine the Oxygen Diffusion Rate through Closures Used in Winemaking. *Journal of Agricultural and Food Chemistry*, 53(18), 6967-6973. <https://doi.org/10.1021/jf0404849>
- Lopes, P., Saucier, C., Teissedre, P.-L., & Glories, Y. (2006). Impact of Storage Position on Oxygen Ingress through Different Closures into Wine Bottles. *Journal of Agricultural and Food Chemistry*, 54(18), 6741-6746. <https://doi.org/10.1021/jf0614239>
- Lopes, P., Saucier, C., Teissedre, P.-L., & Glories, Y. (2007). Main Routes of Oxygen Ingress through Different Closures into Wine Bottles. *Journal of Agricultural and Food Chemistry*, 55(13), 5167-5170. <https://doi.org/10.1021/jf0706023>
- Lopes, P., Silva, M. A., Pons, A., Tominaga, T., Lavigne, V., Saucier, C., Darriet, P., Teissedre, P.-L., & Dubourdiou, D. (2009). Impact of Oxygen Dissolved at Bottling and Transmitted through Closures on the Composition and Sensory Properties of a Sauvignon Blanc Wine during Bottle Storage. *Journal of Agricultural and Food Chemistry*, 57(21), 10261-10270. <https://doi.org/10.1021/jf9023257>
- Manrique, Y. J. A. (2017). Supercritical fluid extraction and fractionation of bioactive natural products from cork.
- Marin, A. B., Jorgensen, E. M., Kennedy, J. A., & Ferrier, J. (2007). Effects of bottle closure type on consumer perceptions of wine quality [Article]. *American Journal of Enology and Viticulture*, 58(2), 182-191. <Go to ISI>://WOS:000247979500004
- Mateus, M. M., Bordado, J. M., & dos Santos, R. G. (2017). Ultimate use of Cork—Unorthodox and innovative applications. *Ciência & Tecnologia dos Materiais*, 29(2), 65-72.
- Mazzoleni, V., Caldentey, P., Careri, M., Mangia, A., & Colagrande, O. (1994). Volatile components of cork used for production of wine stoppers. *American Journal of Enology and Viticulture*, 45(4), 401-406.
- Mestre, A. S., Pires, R. A., Aroso, I., Fernandes, E. M., Pinto, M. L., Reis, R. L., Andrade, M. A., Pires, J., Silva, S. P., & Carvalho, A. P. (2014). Activated carbons prepared from industrial pre-treated cork: Sustainable adsorbents for pharmaceutical compounds removal. *Chemical Engineering Journal*, 253, 408-417. <https://doi.org/https://doi.org/10.1016/j.cej.2014.05.051>
- Minnaar, P. P., Gerber, P., Booyse, M., & Jolly, N. (2021). Phenolic Compounds in Cork-Closed Bottle-Fermented Sparkling Wines [Article]. *South African J. Enol. Vitic.*, 42(1), 19-24. <https://doi.org/10.21548/42-1-4336>

- Mislata, A. M., Puxeu, M., & Ferrer-Gallego, R. (2020). Aromatic Potential and Bioactivity of Cork Stoppers and Cork By-Products. *Foods (Basel, Switzerland)*, 9(2), 133. <https://doi.org/10.3390/foods9020133>
- Moreira, N., Lopes, P., Cabral, M., & Guedes de Pinho, P. (2016). HS-SPME/GC-MS methodologies for the analysis of volatile compounds in cork material. *European Food Research and Technology*, 242(4), 457-466. <https://doi.org/10.1007/s00217-016-2636-x>
- Nunes, L. J. R., Matias, J. C. O., & Catalão, J. P. S. (2013). Energy recovery from cork industrial waste: Production and characterisation of cork pellets. *Fuel*, 113, 24-30. <https://doi.org/https://doi.org/10.1016/j.fuel.2013.05.052>
- Oliveira, A. S., Furtado, I., Bastos, M. d. L., Guedes de Pinho, P., & Pinto, J. (2020). The influence of different closures on volatile composition of a white wine. *Food Packaging and Shelf Life*, 23, 100465. <https://doi.org/https://doi.org/10.1016/j.foodpack.2020.100465>
- Oliveira, J., de Freitas, V., Silva, A. M. S., & Mateus, N. (2007). Reaction between hydroxycinnamic acids and anthocyanin-pyruvic acid adducts yielding new portisins [Article]. *Journal of Agricultural and Food Chemistry*, 55(15), 6349-6356. <https://doi.org/https://doi.org/10.1021/jf070968f>
- Oliveira, V., Knapic, S., & Pereira, H. (2012). Natural variability of surface porosity of wine cork stoppers of different commercial classes. *Journal International des Sciences de la Vigne et du Vin*, 46(4), 331-340. <http://www.scopus.com/inward/record.url?eid=2-s2.0-84880898069&partnerID=40&md5=dc7937e938ac9317ea11a293438648c9>
- Oliveira, V., Knapic, S., & Pereira, H. (2013). Classification modeling based on surface porosity for the grading of natural cork stoppers for quality wines. *Food and Bioprocess Technology*, 6(11), 1804-1811. <https://doi.org/http://dx.doi.org/10.1016/j.fbp.2013.11.004>
- Oliveira, V., Lopes, P., Cabral, M., & Pereira, H. (2013). Kinetics of Oxygen Ingress into Wine Bottles Closed with Natural Cork Stoppers of Different Qualities. *American Journal of Enology and Viticulture*, 64(3), 395. <https://doi.org/10.5344/ajev.2013.13009>
- Oliveira, V., & Pereira, H. (2020). Cork and Cork Stoppers: Quality and Performance. In. <https://doi.org/https://doi.org/10.5772/intechopen.92561>
- Pasteur, L. (1873). *Études sur le vin: ses maladies, causes qui les provoquent, procédés nouveaux pour le conserver et pour le vieillir*. Simon Raçon et Comp.
- Pena-Neira, A., De Simón, B. F., García-Vallejo, M., Hernández, T., Cadahía, E., & Suarez, J. (2000). Presence of cork-taint responsible compounds in wines and their cork stoppers. *European Food Research and Technology*, 211(4), 257-261.
- Peña-Neira, A., Fernández de Simón, B., García-Vallejo, M. C., Hernández, T., Cadahía, E., & Suarez, J. A. (2000). Presence of cork-taint responsible compounds in wines and their cork stoppers. *European Food Research and Technology*, 211(4), 257-261. <https://doi.org/10.1007/s002170000193>
- Pérez-Gregorio, R., Soares, S., Mateus, N., & de Freitas, V. (2020). Bioactive Peptides and Dietary Polyphenols: Two Sides of the Same Coin. *Molecules*, 25(15), 3443. <https://www.mdpi.com/1420-3049/25/15/3443>
- Pérez-Jiménez, J., Neveu, V., Vos, F., & Scalbert, A. (2010). Identification of the 100 richest dietary sources of polyphenols: an application of the Phenol-Explorer database. *European journal of clinical nutrition*, 64(3), S112-S120.
- Pereira, H. (1988). Chemical composition and variability of cork from *Quercus suber* L. *Wood Sci and Technol*, 22(3), 211-218. <https://doi.org/https://doi.org/10.1007/BF00386015>
- Pereira, H. (2015). The Rationale behind Cork Properties: A Review of Structure and Chemistry [Cork; *Quercus suber*; Suberin; Lignin; Cellular structure; Compression; Properties]. 2015, 10(3), 23. https://ojs.cnr.ncsu.edu/index.php/BioRes/article/view/BioRes_10_3_Review_Rationale_Cork_Properties
- Pereira, H., Lopes, F., & Graça, J. (1996). The evaluation of the quality of cork planks by image analysis. *Holzforchung*, 50(2), 111-115. <http://www.scopus.com/inward/record.url?eid=2-s2.0-0030353112&partnerID=40&md5=ed36dae44e30875d701744de0014d058>
- Pinto, J., Oliveira, A. S., Lopes, P., Roseira, I., Cabral, M., Bastos, M. L., & Guedes de Pinho, P. (2019). Characterization of chemical compounds susceptible to be extracted from cork by the wine using GC-MS and (1)H NMR metabolomic approaches. *Food Chem*, 271, 639-649. <https://doi.org/https://doi.org/10.1016/j.foodchem.2018.07.222>
- Pintor, A. M. A., Ferreira, C. I. A., Pereira, J. C., Correia, P., Silva, S. P., Vilar, V. J. P., Botelho, C. M. S., & Boaventura, R. A. R. (2012). Use of cork powder and granules for the adsorption of pollutants: A

- review. *Water Research*, **46**(10), 3152-3166. <https://doi.org/https://doi.org/10.1016/j.watres.2012.03.048>
- Pons, A., Lavigne, V., Landais, Y., Darriet, P., & Dubourdiou, D. (2010). Identification of a Sotolon Pathway in Dry White Wines. *Journal of Agricultural and Food Chemistry*, **58**(12), 7273-7279. <https://doi.org/10.1021/jf100150q>
- Pons, A., Lavigne, V., Thibon, C., Redon, P., Loisel, C., Dubourdiou, D., & Darriet, P. (2021). Impact of Closure OTR on the Volatile Compound Composition and Oxidation Aroma Intensity of Sauvignon Blanc Wines during and after 10 Years of Bottle Storage. *Journal of Agricultural and Food Chemistry*, **69**(34), 9883-9894. <https://doi.org/10.1021/acs.jafc.1c02635>
- Quideau, S., Jourdes, M., Lefeuvre, D., Montaudon, D., Saucier, C., Glories, Y., Pardon, P., & Pourquier, P. (2005). The Chemistry of Wine Polyphenolic C-Glycosidic Ellagitannins Targeting Human Topoisomerase II. *Chem. Eur. J.*, **11**(22), 6503-6513. <https://doi.org/https://doi.org/10.1002/chem.200500428>
- Reis, S. F., Coelho, E., Evtuguin, D. V., Coimbra, M. A., Lopes, P., Cabral, M., Mateus, N., & Freitas, V. (2020). Migration of Tannins and Pectic Polysaccharides from Natural Cork Stoppers to the Hydroalcoholic Solution. *Journal of Agricultural and Food Chemistry*, **68**(48), 14230-14242. <https://doi.org/10.1021/acs.jafc.0c02738>
- Reis, S. F., Lopes, P., Roseira, I., Cabral, M., Mateus, N., & Freitas, V. (2019). Recovery of added value compounds from cork industry by-products. *Ind Crops Prod.*, **140**, 111599. <https://doi.org/https://doi.org/10.1016/j.indcrop.2019.111599>
- Reis, S. F., Teixeira, T., Pinto, J., Oliveira, V., Lopes, P., Cabral, M., Mateus, N., Guedes de Pinho, P., Pereira, H., & de Freitas, V. (2020). Variation in the Phenolic Composition of Cork Stoppers from Different Geographical Origins. *J of Agri and Food Chem*, **68**(50), 14970-14977. <https://doi.org/10.1021/acs.jafc.0c00586>
- Ritsche, J., Katzensteiner, K., & Acácio, V. (2021). Tree regeneration patterns in cork oak landscapes of Southern Portugal: The importance of land cover type, stand characteristics and site conditions. *Forest Ecology and Management*, **486**, 118970. <https://doi.org/https://doi.org/10.1016/j.foreco.2021.118970>
- Rives, J., Fernandez-Rodriguez, I., Gabarrell Durany, X., & Rieradevall, J. (2012). Environmental analysis of cork granulate production in Catalonia – Northern Spain. *Resources, Conservation and Recycling*, **58**, 132–142. <https://doi.org/10.1016/j.resconrec.2011.11.007>
- Rocha, S., Delgadillo, I., & Correia, A. J. F. (1996). GC-MS study of volatiles of normal and microbiologically attacked cork from *Quercus suber* L [Article]. *Journal of Agricultural and Food Chemistry*, **44**(3), 865-871. <https://doi.org/10.1021/jf9500400>
- Santos, S., Pinto, P., Silvestre, A., & Neto, C. (2010). Chemical composition and antioxidant activity of phenolic extracts of cork from *Quercus suber* L. *Industrial Crops and Products*, **31**, 521-526. <https://doi.org/10.1016/j.indcrop.2010.02.001>
- Santos, S. A. O., Pinto, P. C. R. O., Silvestre, A. J. D., & Neto, C. P. (2010). Chemical composition and antioxidant activity of phenolic extracts of cork from *Quercus suber* L [Article]. *Industrial Crops and Products*, **31**(3), 521-526. <https://doi.org/https://doi.org/10.1016/j.indcrop.2010.02.001>
- Santos, S. A. O., Villaverde, J. J., Sousa, A. F., Coelho, J. F. J., Neto, C. P., & Silvestre, A. J. D. (2013). Phenolic composition and antioxidant activity of industrial cork by-products [Article]. *Ind Crops Prod.*, **47**, 262-269. <https://doi.org/https://doi.org/10.1016/j.indcrop.2013.03.015>
- Saucier, C., Jourdes, M., Glories, Y., & Quideau, S. (2006). Extraction, detection, and quantification of flavano-ellagitannins and ethylvescalagin in a Bordeaux red wine aged in oak barrels. *J Agric Food Chem*, **54**(19), 7349-7354. <https://doi.org/https://doi.org/10.1021/jf061724i>
- Schwarz, M., Jerz, G., & Winterhalter, P. (2003). Isolation and structure of Pinotin A, a new anthocyanin derivative from Pinotage wine [Article]. *Vitis*, **42**(2), 105-106.
- Sefton, M. A., & Simpson, R. F. (2005). Compounds causing cork taint and the factors affecting their transfer from natural cork closures to wine—a review. *Australian Journal of Grape and Wine Research*, **11**(2), 226-240.
- Sfaksi, Z., Azzouz, N., & Abdelwahab, A. (2014). Removal of Cr(VI) from water by cork waste. *Arabian Journal of Chemistry*, **7**(1), 37-42. <https://doi.org/https://doi.org/10.1016/j.arabjc.2013.05.031>
- Silva, C. P., Jaria, G., Otero, M., Esteves, V. I., & Calisto, V. (2018). Waste-based alternative adsorbents for the remediation of pharmaceutical contaminated waters: Has a step forward already been taken?

- Bioresource Technology*, 250, 888-901.
<https://doi.org/https://doi.org/10.1016/j.biortech.2017.11.102>
- Silva, M. A., Julien, M., Jourdes, M., & Teissedre, P.-L. (2011). Impact of closures on wine post-bottling development: a review. *European Food Research and Technology*, 233(6), 905-914.
<https://doi.org/10.1007/s00217-011-1603-9>
- Silva, S., Sabino, M., Fernandes, E., Correlo, V., Boesel, L., & Reis, R. L. (2005). Cork: Properties, capabilities and applications. *International Materials Reviews*, 50, 345-365.
<https://doi.org/10.1179/174328005x41168>
- Simpson, R. F., Capone, D. L., & Sefton, M. A. (2004). Isolation and identification of 2-methoxy-3,5-dimethylpyrazine, a potent musty compound from wine corks. *J Agric Food Chem*, 52(17), 5425-5430. <https://doi.org/10.1021/jf049484z>
- Six, T., & Feigenbaum, A. (2003). Mechanism of migration from agglomerated cork stoppers. Part 2: Safety assessment criteria of agglomerated cork stoppers for champagne wine cork producers, for users and for control laboratories. *Food Addit Contam*, 20(10), 960-971.
<https://doi.org/10.1080/02652030310001597583>
- SKOUROUMOUNIS, G. K., KWIATKOWSKI, M. J., FRANCIS, I. L., OAKLEY, H., CAPONE, D. L., DUNCAN, B., SEFTON, M. A., & WATERS, E. J. (2005). The impact of closure type and storage conditions on the composition, colour and flavour properties of a Riesling and a wooded Chardonnay wine during five years' storage. *Australian Journal of Grape and Wine Research*, 11(3), 369-377.
<https://doi.org/https://doi.org/10.1111/j.1755-0238.2005.tb00036.x>
- Snakkers, G., Nepveu, G., Guilley, E., & Cantagrel, R. (2000). Geographic, silvicultural and individual variabilities of extractive content for French sessile oaks (*Quercus petraea* Liebl.): polyphenols, octalactones and volatile phenols. *Annals of Forest Science*, 57(3), 251-260.
- Soares, S., Brandao, E., Mateus, N., & de Freitas, V. (2017). Sensorial properties of red wine polyphenols: Astringency and bitterness. *Crit Rev Food Sci Nutr*, 57(5), 937-948.
<https://doi.org/https://doi.org/10.1080/10408398.2014.946468>
- Soares, S., Mateus, N., & de Freitas, V. (2012). Interaction of different classes of salivary proteins with food tannins. *Food Research International*, 49(2), 807-813.
<https://doi.org/https://doi.org/10.1016/j.foodres.2012.09.008>
- Suffo, M., Sales, D. L., Cortés-Triviño, E., de la Mata, M., & Jiménez, E. (2022). Characterization and production of agglomerated cork stoppers for spirits based on a factor analysis method. *Food Packaging and Shelf Life*, 31, 100815. <https://doi.org/https://doi.org/10.1016/j.foodres.2022.100815>
- Tarasov, A., Rauhut, D., & Jung, R. (2017). "Cork taint" responsible compounds. Determination of haloanisoles and halophenols in cork matrix: A review. *Talanta*, 175, 82-92.
<https://doi.org/https://doi.org/10.1016/j.talanta.2017.07.029>
- Tarko, T., Duda-Chodak, A., Sroka, P., & Siuta, M. (2020). The Impact of Oxygen at Various Stages of Vinification on the Chemical Composition and the Antioxidant and Sensory Properties of White and Red Wines. *International Journal of Food Science*, 2020, 7902974.
<https://doi.org/10.1155/2020/7902974>
- Taylor, M. K., Young, T. M., Butzke, C. E., & Ebeler, S. E. (2000). Supercritical fluid extraction of 2,4,6-trichloroanisole from cork stoppers. *J Agric Food Chem*, 48(6), 2208-2211.
<https://doi.org/10.1021/jf991045q>
- Touati, R., Santos, S. A. O., Rocha, S. M., Belhamel, K., & Silvestre, A. J. D. (2015). The potential of cork from *Quercus suber* L. grown in Algeria as a source of bioactive lipophilic and phenolic compounds. *Ind Crops Prod.*, 76, 936-945. <https://doi.org/https://doi.org/10.1016/j.indcrop.2015.07.074>
- Van Damme, T. (2019). STOPPERS, TRANSPORT STIRRUP JARS AND WINE TRANSPORT, 1450–1150 bc. *The Annual of the British School at Athens*, 114, 93-117.
<https://doi.org/10.1017/S0068245419000108>
- Varea, S., Garcia-Vallejo, M. C., Cadahia, E., & de Simon, B. F. (2001). Polyphenols susceptible to migrate from cork stoppers to wine. *European Food Research and Technology*, 213(1), 56-61.
<https://doi.org/https://doi.org/10.1007/s002170100327>
- Vivas, N., Nonier, M. F. B., Absalon, C., Abad, V. L., Jamet, F., Gaulejac, N. V. D., Vitry, C., & Fouquet, E. (2016). Formation of Flavanol-aldehyde Adducts in Barrel-aged White Wine Possible Contribution of These Products to Colour. *South African Journal of Enology and Viticulture*, 29, 98-108.

WatreLOT, A. A., Heymann, H., & Waterhouse, A. L. (2020). Red Wine Dryness Perception Related to Physicochemistry. *Journal of Agricultural and Food Chemistry*, 68(10), 2964-2972. <https://doi.org/https://doi.org/10.1021/acs.jafc.9b01480>

White, S. A. C. (1999). Gasket composition for crown caps. In: Google Patents.

Part A.

Extraction and Phenolic Characterization

Synopses:

Chapter 1- Characterization of the cork polyphenolic fraction from different regions of the Iberian Peninsula able to migrate to wine model solutions

Adapted from:

Joana Azevedo, Joana Oliveira, Samantha Prat- García, Paulo Lopes, Miguel Cabral, Nuno Mateus and Victor Freitas; *not published*

All the work described in this part was carried out by the author

Chapter 2- Optimization of the ultrasound-assisted extraction for the maximized recovery of phenolic compounds from cork industry waste

Adapted from:

Joana Azevedo, Lucia Cassani, Joana Oliveira, Franklim Chamorro, Jesus Simal-Gandara, Paulo Lopes, Nuno Mateus, Victor de Freitas, Miguel Prieto, and Rosa Perez-Gregorio, *Submitted*

All the laboratorial work described in this part was carried out by the author, Lucia Cassani and Miguel Prieto as responsible for statistical treatments and factorial design.

Chapter 3- Sustainable valorization of cork waste through an efficient microwave-assisted extraction of phenolic compounds

Adapted from:

Joana Azevedo, Joana Oliveira, Franklim Chamorro, Paulo Lopes, Nuno Mateus, Rosa Perez-Gregorio, Victor de Freitas, Jesus Simal-Gandara, Miguel Prieto and Lucia Cassani, *In Preparation*

All the laboratorial work described in this part was carried out by the author, Lucia Cassani and Miguel Prieto as responsible for statistical treatments and factorial design.

Chapter 1- Characterization of the cork polyphenolic fraction from different regions of the Iberian Peninsula able to migrate to wine model solutions

Abstract

The phenolic composition of cork from different geographical locations was studied, and a correlation between these compounds and the cork geographical origin was made. For that, the polyphenolic compounds present in eleven cork samples from different geographical regions of the Iberian Peninsula (six Spanish and five Portuguese regions) were extracted with wine model solutions for 45 days. Nineteen compounds previously identified in cork using LC-MS were quantified by HPLC in the different extracts. The absence or presence of each compound and its concentration have shown to be dependent on the origin of the cork used. These preliminary results show that the southernmost regions of the Iberian Peninsula (Algarve and Cádiz) are those that stand out in all the properties measured. This knowledge is very important for the wine industry since it provides the possibility to select natural cork stoppers based on the concentration of phenolic compounds, despite the lack of knowledge about the real influence of phenolic cork on the chemical composition of wine during aging.

Keywords: Cork, Geographical origin, Phenolic compounds, Folin-Ciocalteu, antioxidant properties DPPH, FRAP.

Introduction

Mediterranean Countries are the leading world producers of cork. According to the literature, in Spain, Portugal and Morocco, the total of cork forest, altogether, is approximately 2139942 ha, which corresponds to the production of 201428 tons per year of this natural product. The cork industry is one of the most important industries in Portugal, being Portugal the world's largest cork producer, with 60% of the total cork tree area providing about 80% of the cork produced in the World (APCOR, 2018).

The cork's chemical composition can reflect its quality, geographical origin, and morphological location from the tree. Studies have shown that the composition of Portuguese (Pereira, 1988) and Spanish (Conde, Cadahía, García-Vallejo, & González-Adrados, 1998) cork, and in particular the content of extractives and polyphenols, varies

between samples of different origins. Nonetheless, the ratio of cork's structural constituents, which are suberin, lignin, and hemicellulose (hemicellulose and cellulose), was found to remain constant.

No clear relationship was found between geographical proximity and chemical composition. In fact, differences in the chemical composition of samples from the same source, and even from the same tree, were observed. It has been proposed that several factors may influence the number of minor components of cork tree, such as North or South orientation, age, the distance of the sample from the base, and the location of the sample on the stem or branch of the tree (Conde, Cadahía, García-Vallejo, & González-Adrados, 1998).

Phenolic compounds, triterpenes and aliphatic compounds are cork's main extractable compounds (Santos et al., 2010), along with a small number of carbohydrates (Rocha et al., 2005). Several studies have been carried out regarding the phenolic composition of cork (Azevedo et al., 2014; Conde, Cadahía, García-Vallejo, & De Simón, 1998; Conde et al., 1997; Fernandes et al., 2009; Fernandes et al., 2011; Santos et al., 2010; Santos et al., 2013). The phenolic compounds importance for human health has been extensively studied, providing information on their role in protection against cancer, coronary heart disease and aging (by inhibiting oxidative stress) (Christophoridou et al., 2005).

When the cork is in direct contact with an alcoholic solution such as bottled wine, some cork components can migrate into the wine (Azevedo et al., 2014), possibly affecting wine quality (Varea, García-Vallejo, et al., 2001). Volatile and non-volatile compounds soluble in ethanol/water such as hydrocarbons, alcohols, ketones, phenolic compounds and tannins, are of oenological importance due to their contribution to sensory properties – color, flavor, astringency and bitterness (Mazzoleni et al., 1994).

Knowing that phenolic acids do not directly influence the organoleptic features of wines, some of them are precursors of volatile phenols (especially vinyl and ethyl derivatives of phenols), compounds that affect wine aroma (Singleton, 1995).

In addition to phenolic acids, ellagitannins react with oxygen, leading to the hydroperoxidation of wine constituents, thus playing an important role in the oxidation processes of wine (Vivas & Glories, 1996). This family is also responsible for the rate of condensation of proanthocyanidins, as well as their precipitation and also responsible for the destruction of anthocyanins (Vivas & Glories, 1993), and can undergo numerous chemical transformations reacting with flavanols and other species (Saucier et al., 2006). Most importantly, the taste properties of these compounds play a role in the aging of wines (Pocock et al., 1994). Recently, it was demonstrated that ellagitannin compounds

can react with wine components such as (+)-catechin yielding a new family of ellagitannins derivative compounds called corklins (Azevedo et al., 2017).

Bearing all this, the aim of this work was to identify and quantify different phenolic compounds that can migrate from cork samples, from different geographical regions, to the wine model solutions. Furthermore, the impact of those compounds on the antioxidant properties of wine model extract, namely antiradical and reducing properties, was also evaluated.

In the future, the cork suppliers and winemakers are expected to be able to choose corks from different geographic regions, taking into account the impact of the cork in the properties of the wine.

Material and Methods

Reagents

DPPH (2, 2-diphenyl-1-picrilhidrazyl), FeCl₃, Trolox, TPTZ (2,4,6-tripyridyl-s-triazine) was purchased from Fluka (Madrid, Spain), Sodium acetate (Sigma Aldrich), Acetic acid, Methanol (Sigma Aldrich).

Geographical origins and characteristics of cork

The cork samples (*Quercus suber*) were obtained from eleven different regions from the Iberian Peninsula as presented in **Figure 1**. The granulated cork was provided by Amorim e Irmãos S.A. Granulated with 16-35 mesh and was obtained from two hundred and fifty cylindrical cork stoppers milled in a Retsch crossbeater mill SK1 (Haan, Germany). In turn, cylindrical cork stoppers were obtained by random choice of 10 plates from each region that were washed and selected by their appearance, thickness and porosity then subjected to the machine cutting in the form of a cylindrical stopper.



Figure 1: Geographical representation of all of eleven regions studies (Pinto et al. 2019).

Maceration cork with wine like model solution

50 mL bottles were filled with 35 mL of 12 % water-ethanol solution at pH 3.5 and 2 g of granulated cork from each of the different regions, each extraction was performed in triplicates, totaling 33 bottles. A control was prepared by filling a bottle with the wine like model solution. All bottles were stored during 45 days at room temperature, and then analyzed. The extraction was carried out during 45 days (3 times more than described in Mislata et al. 2020) in order to maximize compounds extraction (Mislata, Puxeu et al. 2020). To prevent oxidation phenomena, the bottles were filled to the top and subjected to an argon stream before closing.

The obtained cork extracts were filtered using paper filters and the compounds that migrate from the granulated cork into wine model solution were extracted by liquid-liquid extraction with ethyl acetate. The organic phase was evaporated, re-dissolved in 1 mL of water/methanol (50:50) and then analyzed by HPLC-MS.

HPLC-DAD analysis

The samples were analyzed using the same methodology described in the literature (Fernandes et al, 2011) and results are expressed as gallic acid equivalents, accordingly to the calibration curve: $\text{area} = 329.09 \text{ concentration (mM)} - 0.0831$, $R^2 = 0.9999$ and an injection volume of 20 μL .

Briefly, the samples were analyzed by HPLC (Thermo® Scientific) on a 150 × 4.6 mm i.d. reversed-phase C18 column (LiChroCART®) thermostated at 25° C (Thermo® Dionex Ultimate Column 3000). Detection was carried out at 280 nm using a diode array detector (Thermo® Dionex Ultimate). Solvents were (A) H₂O/CH₃COOH (99:1; v/v) and (B) CH₃COOH/CH₃CN/H₂O (1:20:79; v/v/v) with the gradient 80-20% A over 55 min, 20-10% A for 55 to 70 min and 10-0% A for 70 to 90 min, at a flow rate of 0.3 mL/min. The sample injection volume was 20 μL . The chromatographic column was washed with 100% B for 10 min and then stabilized with the initial conditions for another 10 min.

LC-DAD/ESI-MS analysis

A Finnigan Surveyor series liquid chromatograph, equipped with a Thermo Finnigan (Hypersil Gold®) reversed-phase column (150 mm × 4.6 mm, 5 μm , C18) thermostated at 25° C was used. The samples were analysed using the same solvents, gradients, injection volume, and flow rate referred above for the HPLC analysis. Double-online detection was done by a photodiode spectrophotometer and mass spectrometry. The mass detector was a Finnigan LCQ DECA XP MAX (Finnigan Corp., San Jose, CA) quadrupole ion trap equipped with atmospheric pressure ionization (API) source, using

electrospray ionization (ESI) interface. The vaporizer and the capillary voltages were 5 kV and 4 V, respectively. The capillary temperature was set at 325° C. Nitrogen was used as both sheath and auxiliary gas at flow rates of 80 and 30, respectively (in arbitrary units). Spectra were recorded in the negative ion mode between m/z 120 and 2000. The mass spectrometer was programmed to do a series of three scans: a full mass, a zoom scan of the most intense ion in the first scan, and a MS-MS of the most intense ion using relative collision energies of 30 and 60. The samples were also directly injected into the MS spectrometer with a pump at a flow rate of 0.3 mL/min. The capillary temperature and voltage used were 275 °C and 15 V, respectively, and spectra were obtained in the positive ion mode between m/z 120 and 2000. The mass spectrometer was programmed to do a series of three scans: a full mass, a zoom scan of the most intense ion in the first and a MS-MS of the most intense ion using relative collision energies of 30 and 60 V.

Folin-Ciocalteu Method

The total polyphenol content of the wine like model solutions filtered solution, which was in contact with cork 45 days was determined following the Folin–Ciocalteu method adjusted to a microscale (Arnous, Makris et al. 2001). In an Eppendorf tube, 610 μ L of distilled water, 15 μ L of filtered solution and 75 μ L of Folin–Ciocalteu reagent were mixed. After 30 s, 300 μ L of aqueous 20% Na_2CO_3 and 300 μ L of distilled water were added, and the mixture was mixed (30s) and allowed to stand at room temperature in the dark for 30 min. The absorbance was read at 750 nm, and the total polyphenol concentration was calculated accordingly to the calibration curve: $\square \text{Abs (750 nm)} = 0.9638 \text{ concentration (mM)} - 0.0001$, $R^2 = 0.9999$, using gallic acid as standard.

Spectrophotometric measurement

The filtered solution, which was in contact with cork 45 days, was diluted 5 times and placed in a 1 mm quartz optical path length cuvette and absorbance was measured at 280, 320 and 420 nm using a Thermo Scientific Evolution Array UV-Visible spectrophotometer.

Radical scavenging assay (DPPH)

Procedures followed the method based in Bondet et al. (Bondet, Brand-Williams et al. 1997) and described in the literature (Azevedo, Fernandes et al. 2010). The radical activities were determined using DPPH (2,2-diphenyl-1-picrilhidrazyl) as a free radical. The tested extracted compound reacts with DPPH and induces a decrease of the absorbance measured at 515 nm, which indicates the compound's scavenging potential.

The reaction for scavenging DPPH radicals was performed in a microplate reader of 96 well plates (Biotek Powerwave XS with software KC4). The reaction was carried out on the plate wells with a temperature of 25 °C. A solution of 60 µM DPPH was prepared in methanol, 270 µL of this latter solution was added in each well together with 30 µL of cork extract from different cork regions. The decrease in absorbance was measured at 515 nm, at t=0 and every 5 minutes, during 20 min. For the final results, the 0-20 min reaction time window was used. Antiradical activity was calculated from the equation determined from linear regression after plotting known solutions of Trolox with different concentrations, and it was expressed as µM Trolox equivalents.

Ferric Reducing Antioxidant Power (FRAP)

The FRAP assay developed by Benzie & Strain (Benzie and Strain 1996) was performed as described in (Azevedo, Fernandes et al. 2010). The reaction was performed in a microplate reader of 96 well plates (Biotek Powerwave XS with software KC4), and it was carried out on the plate wells with a temperature of 37 °C. In short, FRAP reagent (10 vol of 300 mM acetate buffer, pH 3.6 + 1 vol of 10 mM TPTZ in 40 mM HCl + 1 vol of 20 mM FeCl₃) was diluted to one-third with acetate buffer, 270 µL of this solution was added in each well together with 30 µL of wine model solution in contact with different types of granulated cork. The blank assay was performed using 270 µL of FRAP reagent and 30 µL of wine model solution. The absorbance at 593 nm was measured in time 0 min and 4 min. The results were expressed as Trolox equivalents.

Statistical results

The results are expressed as the arithmetic means (n = 3) ± standard error (SD). Statistical significance of the difference between various groups was evaluated by two-way analysis of variance ANOVA and PCA, they were performed using the software Statgraphics Centurion XVI statistics software (version XVI; StatPoint Inc., USA).

Results and Discussion

The extraction was performed using granulated cork by maceration for 45 days in order to maximize compounds extraction and to evaluate the potential of extractable phenolics in cork from different regions.

The identification of the phenolic compounds that migrate to the wine model solutions after 45 days of maceration was performed by HPLC-DAD/ESI-MS analysis, and further quantification was done by HPLC-DAD (**Table 1**).

Table 1: Total amounts of phenolic compounds extracted from granulated cork for different regions (Folin-Ciocalteu method and HPLC quantification), measurement of Absorbance at 280 nm, and antioxidant assays (DPPH and FRAP). The results are expressed as the mean of the three replicates \pm SD and the same letter does not differ statistically.

	Folin Ciocalteu (mg/L)	HPLC quantification (mg/L)	Absorbance 280 nm	DPPH method	FRAP method
Algarve	606 \pm 9 a	404 \pm 59	0.84 \pm 0.09 a	22 \pm 2 a	38 \pm 3 a
Badajoz	528 \pm 47 ab	250 \pm 30	0.63 \pm 0.04 a	19 \pm 3 a	31 \pm 4 a
Cádiz	486 \pm 12 cd	263 \pm 39	0.58 \pm 0.03 c	20 \pm 3 a	33 \pm 3 a
Douro	464 \pm 73 ab	259 \pm 20	0.48 \pm 0.05 ab	18 \pm 2 a	31 \pm 2 a
Castelo Branco	456 \pm 21 e	152 \pm 12	0.49 \pm 0.03 d	20 \pm 1 a	32 \pm 2 a
Alcácer do Sal	453 \pm 33 cd	92 \pm 5	0.61 \pm 0.03 b	23 \pm 2 a	35 \pm 1 a
Córdoba II	409 \pm 25 a	210 \pm 20	0.50 \pm 0.03 a	21 \pm 3 a	26 \pm 2 a
Sevilha	366 \pm 30 e	108 \pm 7	0.44 \pm 0.03 c	23 \pm 4 a	27 \pm 3 a
Toledo	354 \pm 32 de	136 \pm 6	0.39 \pm 0.02 c	17 \pm 2 a	25 \pm 1 a
Córdoba_I	341 \pm 11 bc	153 \pm 13	0.38 \pm 0.03 b	22 \pm 2 a	24 \pm 2 a
Évora	329 \pm 30 cd	190 \pm 12	0.39 \pm 0.02 b	24 \pm 5 a	27 \pm 1 a

Nineteen compounds, previously identified in cork using LC/MS, were quantified by HPLC in the cork extracts (**Figure 2**).

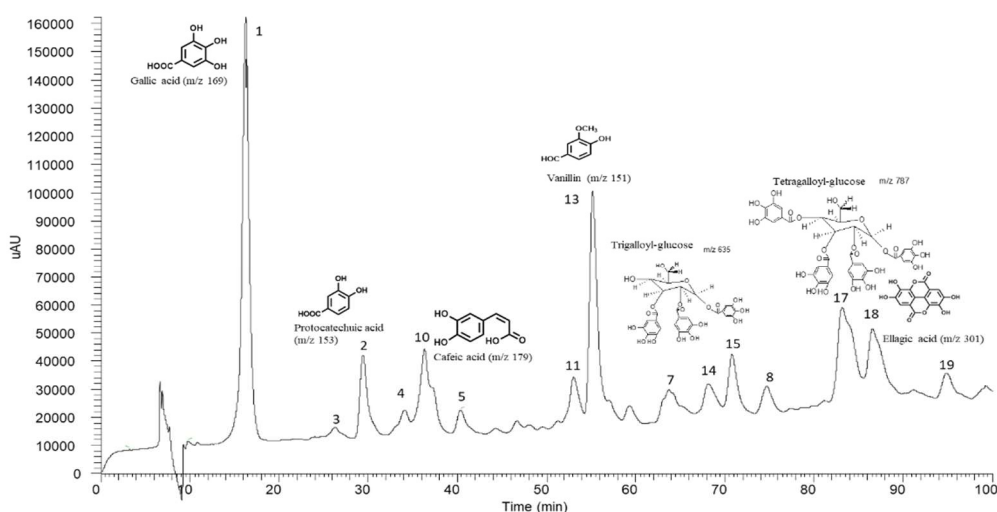


Figure 2: Representative HPLC chromatogram, at 280 nm, showing the identification of the cork migrant compounds for model wine solutions.

The most predominant compounds found in the samples were gallic acid, caffeic acid, vanillin and sinapic acid similarly to what was described elsewhere (Touati et al., 2015; Conde et al., 1997; Santos et al., 2010). With the analysis from the geographical representation of all of eleven regions studies (**Figure 1**), Córdoba I, Córdoba II and Seville (closer geographically) would be expected to have a similar chemical contribution, and possibly different from Douro (north region), Cádiz and Algarve (south regions). Always bearing in mind that there are other factors that are involved, such as soil and/or climate. However, a very recent study developed by Pereira et al. 2020 suggests that the tree genetic information, or its expression, plays a much more important role on the chemical composition of cork than the drought conditions occurring during cork growth (Leite et al., 2020).

Analyzing **Table 1**, it can be seen that Algarve's cork sample presented the highest level of phenolic compounds analyzed by HPLC (404 ± 59 mg/L), Folin Ciocalteu method (606 ± 9 mg/L), absorbance at 280 nm (0.84 ± 0.09) and overall higher antioxidant capacity (DPPH, 22 ± 2 and FRAP, 38 ± 3 assays). This fact results from the contribution of the higher amounts of gallic, sinapic, caffeic acids and vanillin (**Figure 2** and **Table 2**) (Fernandes, Fernandes et al. 2009)

Table 2: List of compounds identified and quantified for the eleven different regions from Iberian Peninsula. The quantities were obtained from HPLC analysis and express in mg/L equivalent Gallic acid. The results are expressed as the mean of the three replicates \pm SD.

Regions (mg/L)	Évora	Badajoz	Cádiz	Castelo Branco	Alcácer do Sal	Toledo	Douro	Algarve	Córdoba II	Córdoba I	Sevilha
Galic acid-1	46 \pm 12	122 \pm 7	156 \pm 14	50 \pm 6	18 \pm 1	25 \pm 2	68 \pm 1	222 \pm 3	87 \pm 30	53 \pm 12	29 \pm 7
Protocatechuic acid-2	16 \pm 2	11 \pm 1	11.6 \pm 0.7	13 \pm 1	1.6 \pm 0.1	3 \pm 2	14 \pm 1	15 \pm 1	16 \pm 1	16 \pm 3	5 \pm 1
Vescalagin-3	0.8 \pm 0.2			0.7 \pm 0.1		3 \pm 2	1.5 \pm 0.3				
Protocatechuic aldehyde-4	2.4 \pm 0.4	3.7 \pm 0.3	4 \pm 3			3 \pm 2	3.1 \pm 0.4			1.2 \pm 0.2	0.8 \pm 0.5
Dehydrated tergallic-C-glucoside-5	1.9 \pm 0.5	14 \pm 9	10 \pm 8	6 \pm 1	9 \pm 3	2 \pm 1	3 \pm 1	14 \pm 1	7 \pm 4	4.8 \pm 0.4	6 \pm 2
Valoneic acid dilactone-6	6.5 \pm 0.7	4.5 \pm 0.3	1.1 \pm 0.8	6.7 \pm 0.8	9 \pm 2	7 \pm 3	9 \pm 1	9.0 \pm 0.6	7 \pm 2	5 \pm 1	1.9 \pm 0.5
m/z 595-7	1.3 \pm 0.1	1.6 \pm 0.1	3 \pm 2	1.4 \pm 0.3	0.9 \pm 0.2	2.0 \pm 0.6	2.0 \pm 0.5		2.2 \pm 0.7	1.4 \pm 0.4	1.1 \pm 0.2
m/z 873-8	3.1 \pm 0.2	3.9 \pm 0.6	7 \pm 3	2.2 \pm 0.8	1.8 \pm 0.2	1.9 \pm 0.5	1.9 \pm 0.3		3 \pm 2	1.9 \pm 0.5	2.9 \pm 0.8
Conyferaldehyde-9	6 \pm 2	10.3 \pm 0.7	19 \pm 13	5.2 \pm 0.3	0.85 \pm 0.2	9 \pm 1	8.2 \pm 0.5	9.1 \pm 0.6	11 \pm 1	11 \pm 2	5 \pm 1
Caffeic acid-10	31 \pm 6	19.8 \pm 0.9	3 \pm 1	18 \pm 1	5.4 \pm 0.6	10 \pm 1	65 \pm 17	50 \pm 5	22 \pm 7	16 \pm 3	8 \pm 1
Ferulic acid-11	4.5 \pm 0.4	3.9 \pm 0.5	3 \pm 2	1.7 \pm 0.6	2.3 \pm 0.8	0.9 \pm 0.2	6.4 \pm 0.5	2.5 \pm 0.4	3 \pm 1	1.5 \pm 0.9	1.5 \pm 0.5
Di-HHDP-Galloylglucose-12	4 \pm 1	2.5 \pm 0.2	5 \pm 3	1.9 \pm 0.6	1.4 \pm 0.2	0.5 \pm 0.3	2 \pm 1	3.2 \pm 0.1	3 \pm 2	10 \pm 2	9 \pm 5
Vanillin-13	19 \pm 2	5.5 \pm 0.6	13 \pm 9	10 \pm 8	5.7 \pm 0.4	11 \pm 4	21 \pm 2	26 \pm 2	8 \pm 5	8 \pm 2	8 \pm 2
Trigalloyl-glucose-14	7 \pm 1	15.5 \pm 2	11 \pm 7	8 \pm 1	2.0 \pm 0.1	9.7 \pm 0.8	11 \pm 1	8 \pm 1	9 \pm 3	13 \pm 2	3.3 \pm 0.8
Tetragalloyl-glucose-15	3 \pm 2		14 \pm 9	0.9 \pm 0.5	1.7 \pm 0.4	3.4 \pm 0.9	1.3 \pm 0.7	3.5 \pm 0.1	3 \pm 1		14 \pm 4
Sinapic acid-16	20 \pm 7	14 \pm 3		12.9 \pm 0.7	1.8 \pm 0.6	8.8 \pm 0.9	25 \pm 4	15 \pm 4	13 \pm 2	7 \pm 4	8 \pm 2
Tetragalloyl- glucose-17	15 \pm 1			12 \pm 1	6.3 \pm 0.6	14 \pm 1	11 \pm 2		14 \pm 9		
Ellagic acid-18	1.5 \pm 0.8	17 \pm 3	3 \pm 2	2 \pm 1	18 \pm 8	17 \pm 4	2.4 \pm 0.2	25 \pm 2	2 \pm 1	3.2 \pm 0.4	3.2 \pm 0.7
Pentagalloyl- glucose -19					2.3 \pm 0.1	3.9 \pm 0.5	2.8 \pm 0.7		1.0 \pm 0.6		3.1 \pm 0.6

On the other hand, Alcácer do Sal presented the lowest concentration of phenolic compounds by HPLC (92 ± 5 mg/L) not supported by Folin-Ciocalteu quantification (453 ± 33 mg/L) neither absorbance 280 nm (0.61 ± 0.03) (**Table 1**). Samples from Córdoba II, Seville, Toledo, Córdoba I and Évora are those that presented lower values in HPLC quantification, total phenolics (Folin-Ciocalteu method) and absorbance at 280 nm (**Table 1**). It should be noted that these regions are geographically close, hence a similar behavior could be expected. However, a previous work described in Guedes de Pinho et al, using unsupervised pattern recognition techniques, unveiled three main clusters of regions according to their chemical similarity but not related to geographical proximity (Pinto et al., 2019). In that work, nineteen compounds were found to be responsible for the clusters, including terpenes, polyphenols (vescalagin, castalagin), among others (pyrogallol, glucosan, sitost-4-en-3-one, o-cymene, quinic acid, five unknowns).

The quantities, and presence or absence of some of them, depend on the origin of the cork used (**Table 2**). The isomers vescalagin and castalagin are hydrolysable tannins known to be extracted from wood to the wine during the maturation and aging process in oak barrels (García-Estévez et al., 2010), and to have an impact in wine taste perception (Bajec & Pickering, 2008). These compounds have also been described as some of the compounds that migrate from cork stopper to model wine solutions (Azevedo et al., 2017). These compounds were found only in the samples from Évora, Castelo Branco, Toledo, and Douro, interestingly in the northernmost regions of the Iberian Peninsula.

As observed in **Table 2**, the compounds detected include valoneic acid dilactone, vescalagin, HHDP-galloyl-glucose, tetragalloyl- glucose, pentagalloyl- glucose. A similar phenolic profile has already been described in the literature after direct extraction of phenolic compounds from triturated cork (Varea, Garcia-Vallejo, et al., 2001). Pentagalloyl-glucose was found only in Douro, Alcácer do Sal, Toledo Cordoba II and Sevilha (**Figure 1** and **Table 2**). Caffeic acid and Vanillin were detected in higher amounts in Évora, Douro and Algarve regions. Caffeic acid and vanillin, alongside vescalagin, are described to be reactive with the major wine components giving rise to more complex compounds (corklins and pyranoanthocyanins) (Azevedo et al., 2017) (**Table 2**).

In the PCA analysis, that includes the studied parameters: Total amounts of phenolic compounds by Folin-Ciocalteu, antioxidant capacity (DPPH and FRAP methods) and Absorbance measurement at 280 nm there is a clear difference in Algarve region and Badajoz due to its phenolic content that is superior to the rest of the regions, on the other hand Évora and Cordoba I appear in the opposite quadrant. (**Figure 3**).

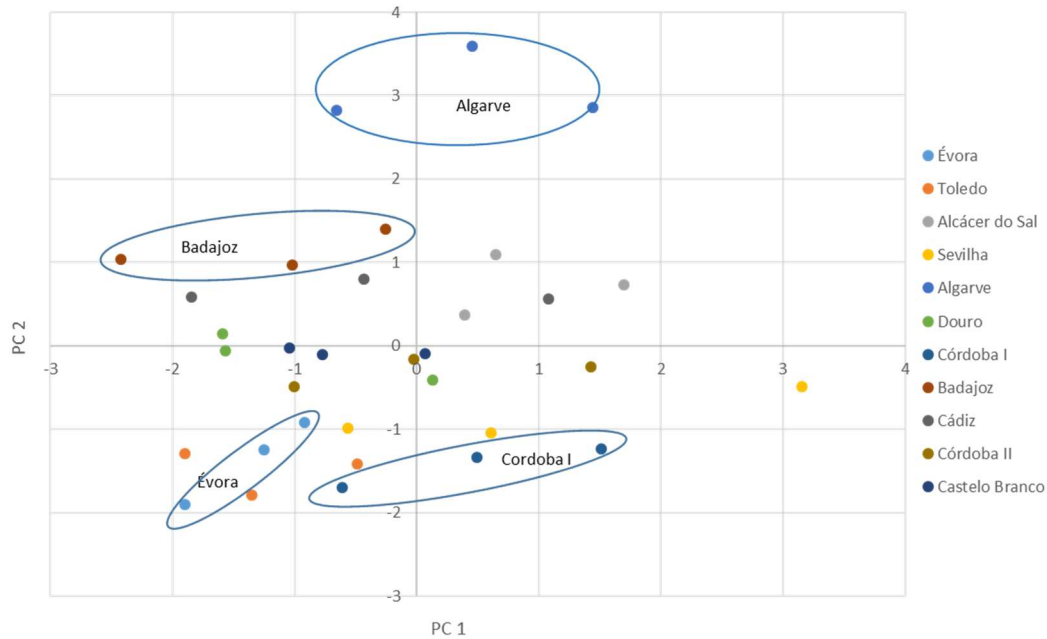


Figure 3: PCA analysis. PCA with trust 98.25%.

Antioxidant features

Two methods were used to estimate the antioxidant potential of each cork region: the reducing power (FRAP) and the ability to scavenge free radicals (DPPH). As it was already reported in literature for other cork extracts (Chirinos et al., 2008; Santos et al., 2010; Touati et al., 2015), the extract from different regions have showed different antioxidant properties.

From the results shown in **Table 1**, it is possible to infer that all wine model solutions presented radical scavenging capacity but no statistical differences were observed.

Furthermore, the reducing capacity of the wine model solutions was assessed using the FRAP method. Generally, the migrating compounds, found in the different wine model solutions, presented reducing capacity (**Table 1**). When comparing the whole group, there are no statistical differences between the different regions. When comparing the samples individually, Algarve and Badajoz stood out. These regions have also higher levels of total phenolic compounds (**Table 1**).

The fact that there are no statistically relevant differences between each of the regions tested may be related to the amount of gallic, protocatechuic, and ellagic acids (Table 2) present in all regions, and which has already been described as the main responsible for the antioxidant activity of cork extracts (Fernandes et al., 2009; Touati et al., 2015). These compounds are known to play an important role as an antioxidant through different mechanisms of action, such as elimination of free radicals, extinction of reactive oxygen species, inhibition of oxidative enzymes, transition metal chelators (Chirinos et al., 2008).

Conclusion

This preliminary study aimed to find cork's geographical markers. Nineteen compounds were identified and quantified as able to migrate from the cork to the wine like model solutions over 45 days at room temperature. All cork samples displayed different amounts of each of the compounds, however, cork harvested in the southern regions of the Iberian Peninsula (Figure 1 and Table 1) showed higher quantities of phenolic compounds. This suggests that the cork originated in the southern regions of Iberian Peninsula has increased ability to scavenge free radicals (DPPH) and higher reducing power (FRAP). The amounts of gallic acid, protocatechuic acid, ellagic acid, protocatechuic aldehyde, and vanillin found in the cork appear to be crucial for the antioxidant activity observed.

It is important to bear in mind that other factors such as different tree ages, climatic conditions may have an influence in the discrimination of samples in addition to geographical regions. The cork stoppers may bring several benefits to wine's physical-chemistry properties, as a result of the new and diverse bioactive compounds that can migrate from cork.

Acknowledgments

This work was developed under the CorkPlus 3310 project – “Contribution of cork stoppers to the chemical and sensory properties of bottled wine” co-financed by the European Regional Development Found (FEDER) through the Operational Competitiveness and Internationalization Program (COMPETE 2020), IF/00225/2015, SFRH/BD/139709/2018 and by UIDB/50006/2020 with funding from FCT/MCTES through national funds.

References

APCOR: Available at:

http://www.apcor.pt/wp-content/uploads/2017/12/Boletim_Estatistico_APCOR_17_18.pdf (2018)

(12-04-2018)

Arnous, A., Makris, D. P., & Kefalas, P. (2001). Effect of principal polyphenolic components in relation to antioxidant characteristics of aged red wines. *J Agric Food Chem*, 49(12), 5736-5742. <https://doi.org/https://doi.org/10.1021/jf010827s>

Azevedo, J., Fernandes, A., Oliveira, J., Brás, N. F., Reis, S., Lopes, P., Roseira, I., Cabral, M., Mateus, N., & de Freitas, V. (2017). Reactivity of Cork Extracts with (+)-Catechin and Malvidin-3-O-glucoside in Wine Model Solutions: Identification of a New Family of Ellagitannin-Derived Compounds (Corklins). *J Agric and Food Chem*, 65(39), 8714-8726. <https://doi.org/https://doi.org/10.1021/acs.jafc.7b02845>

Azevedo, J., Fernandes, I., Faria, A., Oliveira, J., Fernandes, A., Freitas, V., & Mateus, N. (2010). Antioxidant properties of anthocyanidins, anthocyanidin-3-glucosides and respective portisins. *Food Chemistry*, 119(2), 518-523. <https://doi.org/https://doi.org/10.1016/j.foodchem.2009.06.050>

Azevedo, J., Fernandes, I., Lopes, P., Roseira, I., Cabral, M., Mateus, N., & Freitas, V. (2014). Migration of phenolic compounds from different cork stoppers to wine model solutions: antioxidant and biological relevance [journal article]. *Eur Food Res and Techno*, 239(6), 951-960. <https://doi.org/https://doi.org/10.1007/s00217-014-2292-y>

Bajec, M. R., & Pickering, G. J. (2008). Astringency: Mechanisms and Perception. *Critical Reviews in Food Science and Nutrition*, 48(9), 858-875. <https://doi.org/https://doi.org/10.1080/10408390701724223>

Benzie, I. F., & Strain, J. J. (1996). The ferric reducing ability of plasma (FRAP) as a measure of "antioxidant power": the FRAP assay. *Anal Biochem*, 239(1), 70-76. <https://doi.org/https://doi.org/10.1006/abio.1996.0292>

Bondet, V., Brand-Williams, W., & Berset, C. (1997). Kinetics and Mechanisms of Antioxidant Activity using the DPPH.Free Radical Method. *LWT - Food Science and Technology*, 30(6), 609-615. <https://doi.org/https://doi.org/10.1006/fstl.1997.0240>

Chirinos, R., Campos, D., Warnier, M., Pedreschi, R., Rees, J. F., & Larondelle, Y. (2008). Antioxidant properties of mashua (*Tropaeolum tuberosum*) phenolic extracts against oxidative damage using biological in vitro assays [Article]. *Food Chemistry*, 111(1), 98-105. <https://doi.org/https://doi.org/10.1016/j.foodchem.2008.03.038>

Christophoridou, S., Dais, P., Tseng, L. I. H., & Spraul, M. (2005). Separation and identification of phenolic compounds in olive oil by coupling high-performance Liquid Chromatography with Postcolumn Solid-Phase Extraction to Nuclear Magnetic Resonance Spectroscopy (LC-SPE-NMR) [Article]. *Journal of Agricultural and Food Chemistry*, 53(12), 4667-4679. <https://doi.org/https://doi.org/10.1021/jf040466r>

Conde, E., Cadahía, E., García-Vallejo, M. C., & De Simón, B. F. (1998). Polyphenolic Composition of *Quercus suber* Cork from Different Spanish Provenances [Article]. *Journal of Agricultural and Food Chemistry*, 46(8), 3166-3171. <https://doi.org/https://doi.org/10.1021/jf970863k>

Conde, E., Cadahía, E., García-Vallejo, M. C., Fernández De Simón, B., & González Adrados, J. R. (1997). Low Molecular Weight Polyphenols in Cork of *Quercus suber* [Article]. *J of Agric and Food Chem*, 45(7), 2695-2700. <https://doi.org/https://doi.org/10.1021/jf960486w>

Conde, E., Cadahía, E., García-Vallejo, M. C., & González-Adrados, J. R. (1998). Chemical characterization of reproduction cork from spanish *Quercus suber* [Article]. *Journal of Wood Chemistry and Technology*, 18(4), 447-469. <https://doi.org/https://doi.org/10.1080/02773819809349592>

Fernandes, A., Fernandes, I., Cruz, L., Mateus, N., Cabral, M., & De Freitas, V. (2009). Antioxidant and biological properties of bioactive phenolic compounds from *Quercus suber* L [Article]. *J of Agric and Food Chem*, 57(23), 11154-11160. <https://doi.org/https://doi.org/10.1021/jf902093m>

Fernandes, A., Sousa, A., Mateus, N., Cabral, M., & de Freitas, V. (2011). Analysis of phenolic compounds in cork from *Quercus suber* L. by HPLC-DAD/ESI-MS. *Food Chem*, 125(4), 1398-1405. <https://doi.org/https://doi.org/10.1016/j.foodchem.2010.10.016>

- García-Estévez, I., Escribano-Bailón, M. T., Rivas-Gonzalo, J. C., & Alcalde-Eon, C. (2010). Development of a fractionation method for the detection and identification of oak ellagitannins in red wines. *Analytica Chimica Acta*, 660(1), 171-176. <https://doi.org/https://doi.org/10.1016/j.aca.2009.10.020>
- Leite, C., Oliveira, V., Miranda, I., & Pereira, H. (2020). Cork oak and climate change: Disentangling drought effects on cork chemical composition [Article]. *Scientific Reports*, 10(1), Article 7800. <https://doi.org/10.1038/s41598-020-64650-9>
- Mazzoleni, V., Caldentey, P., Careri, M., Mangia, A., & Colagrande, O. (1994). Volatile components of cork used for production of wine stoppers [Article]. *American Journal of Enology and Viticulture*, 45(4), 401-406. <https://www.ajevonline.org/content/45/4/401>
- Mislata, A. M., Puxeu, M., & Ferrer-Gallego, R. (2020). Aromatic Potential and Bioactivity of Cork Stoppers and Cork By-Products. *Foods (Basel, Switzerland)*, 9(2), 133. <https://doi.org/10.3390/foods9020133>
- Pereira, H. (1988). Chemical composition and variability of cork from *Quercus suber* L. *Wood Sci and Techno*, 22(3), 211-218. <https://doi.org/https://doi.org/10.1007/BF00386015>
- Pinto, J., Oliveira, A. S., Lopes, P., Roseira, I., Cabral, M., Bastos, M. L., & Guedes de Pinho, P. (2019). Characterization of chemical compounds susceptible to be extracted from cork by the wine using GC-MS and (1)H NMR metabolomic approaches. *Food Chem*, 271, 639-649. <https://doi.org/https://doi.org/10.1016/j.foodchem.2018.07.222>
- Pocock, K. F., Sefton, M. A., & Williams, P. J. (1994). Taste thresholds of phenolic extracts of french and American oakwood: The influence of oak phenols on wine flavor [Article]. *American Journal of Enology and Viticulture*, 45(4), 429-434. <https://www.ajevonline.org/content/45/4/429>
- Rocha, S. M., Ganito, S., Barros, A., Carapuça, H. M., & Delgado, I. (2005). Study of cork (from *Quercus suber* L.)-wine model interactions based on voltammetric multivariate analysis [Article]. *Analytica Chimica Acta*, 528(2), 147-156. <https://doi.org/https://doi.org/10.1016/j.aca.2004.10.001>
- Santos, S. A. O., Pinto, P. C. R. O., Silvestre, A. J. D., & Neto, C. P. (2010). Chemical composition and antioxidant activity of phenolic extracts of cork from *Quercus suber* L [Article]. *Industrial Crops and Products*, 31(3), 521-526. <https://doi.org/https://doi.org/10.1016/j.indcrop.2010.02.001>
- Santos, S. A. O., Villaverde, J. J., Sousa, A. F., Coelho, J. F. J., Neto, C. P., & Silvestre, A. J. D. (2013). Phenolic composition and antioxidant activity of industrial cork by-products [Article]. *Ind Crops Prod.*, 47, 262-269. <https://doi.org/https://doi.org/10.1016/j.indcrop.2013.03.015>
- Saucier, C., Jourdes, M., Glories, Y., & Quideau, S. (2006). Extraction, detection, and quantification of flavano-ellagitannins and ethylvescalagin in a Bordeaux red wine aged in oak barrels [Article]. *Journal of Agricultural and Food Chemistry*, 54(19), 7349-7354. <https://doi.org/https://doi.org/10.1021/jf061724i>
- Singleton, G. (1995). Accord VII: Collective Bargaining in a Labourist Framework. *Policy, Organisation and Society*, 10, 98-115. <https://doi.org/https://doi.org/10.1080/10349952.1995.11876638>
- Touati, R., Santos, S. A. O., Rocha, S. M., Belhamel, K., & Silvestre, A. J. D. (2015). The potential of cork from *Quercus suber* L. grown in Algeria as a source of bioactive lipophilic and phenolic compounds. *Ind Crops Prod.*, 76, 936-945. <https://doi.org/https://doi.org/10.1016/j.indcrop.2015.07.074>
- Varea, S., Garcia-Vallejo, M. C., Cadahia, E., & de Simon, B. F. (2001). Polyphenols susceptible to migrate from cork stoppers to wine. *European Food Research and Technology*, 213(1), 56-61. <https://doi.org/https://doi.org/10.1007/s002170100327>
- Varea, S., García-Vallejo, M. C., Cadahía, E., & Fernández De Simón, B. (2001). Polyphenols susceptible to migrate from cork stoppers to wine [Article]. *European Food Research and Technology*, 213(1), 56-61. <https://doi.org/https://doi.org/10.1007/s002170100327>
- Vivas, N., & Glories, Y. (1993). Les phénomènes d'oxydoréduction liés à l'élevage en barriques des vins rouges: Aspects technologiques. *Rev. Fr. Oenol.*, 142(142), 33-38.
- Vivas, N., & Glories, Y. (1996). Role of oak wood ellagitannins in the oxidation process of red wines during aging. *Am. J. Enol. Vitic.*, 47(1), 103-107. <https://www.ajevonline.org/content/47/1/103>

Chapter 2- Optimization of the ultrasound-assisted extraction for the maximized recovery of bioactive phenolic compounds from cork industry waste

Abstract

In the present work, the use of trituration and defatting (alone or in combination) as pretreatments to improve the recovery of total phenolic compounds (TPC) from cork-processing wastes prior to ultrasound-assisted extraction (UAE) (20 °C, 70% amplitude, 500 W, 20 kHz) was studied and compared with a control sample (without treatment). The effects of the critical UAE conditions (time and ethanol concentration) on the extraction yield and TPC of different cork samples (pretreated and control) were investigated using RSM with a central composite design (CCD). The results showed that none of the pretreatments improved yield or TPC when compared to the control. On the other hand, the experimental data from the control sample fit well to second-order polynomial models and were thus used to determine the optimal UAE conditions (20 min and 75% ethanol concentration) that resulted in the highest yield (23.74 ± 3.71 mg extract/g dry weight) and TPC (0.69 ± 0.03 mg/g dw). Finally, different UAE cycles were applied to the cork sample obtained at the optimal extraction conditions in order to increase the extraction yield and TPC even further. In light of this, the use of two UAE cycles significantly improved ($p < 0.05$) extraction yield (32.24 ± 0.82 mg extract/ g dw) and TPC (0.98 ± 0.015 mg/g dw) of cork industry waste. These results were comparable to those obtained using the conventional maceration method (35 °C, 7 d), demonstrating the efficacy of UAE in the sustainable and rapid extraction of bioactive compounds from cork processing wastes. To our knowledge, this is the first time that the extraction of phenolic compounds from cork using UAE technique is reported.

Keywords: phenolic compounds, cork industry by-products, UAE, sustainable extraction, response surface methodology.

Introduction

The circular economy is a relatively new concept that emphasizes reducing, reusing, recovering, and upcycling materials, resources, and energy. In general, there is an urgent need to redesign processes, products, and new business models in order to maximize resource utilization (Reike, Vermeulen, & Witjes, 2018). As a result, the search for new solutions to make extraction processes more efficient (using less organic solvents and reducing extraction time and energy consumption) that are industrially applicable and have a lower environmental impact becomes critical.

The recovery of bioactive compounds from food processing wastes is a sustainable strategy (Sharma, Gaur, Sirohi, Varjani, Hyoun Kim, & Wong, 2021). Although the characterization and applications of enological by-products such as grape pomace, press residues, or wine lees have been extensively researched, the valorization of cork-processing wastes (cork that is not used in the production of stoppers) has received little attention. Cork contains phenolic compounds, in particular, phenolic acids (primarily gallic and protocatechuic acids), aldehydes (primarily vanillin and protocatechuic aldehyde), condensed tannins and ellagitannins such as vescalagin and mongolicain (Azevedo et al., 2014; Reis, Teixeira, et al., 2020; Santos, Villaverde, Sousa, Coelho, Neto, & Silvestre, 2013). Furthermore, cork stoppers and cork by-product extracts have high aromatic compounds and antioxidant potential allowing them to be reused in various industries such as agriculture, cosmetics, and pharmaceuticals, thereby expanding their applications. (Azevedo et al., 2014; Carriço, Ribeiro, & Marto, 2018; A. Fernandes, Fernandes, Cruz, Mateus, Cabral, & De Freitas, 2009; Manrique, 2017; Mislata, Puxeu, & Ferrer-Gallego, 2020; Quideau et al., 2005; Reis, Lopes, Roseira, Cabral, Mateus, & Freitas, 2019; Santos, Pinto, Silvestre, & Neto, 2010; Touati, Santos, Rocha, Belhamel, & Silvestre, 2015).

The use of ultrasound-assisted technology to extract cork phenolic compounds is a valuable tool for achieving the stated goals of sustainable “green” chemistry (Chemat, Rombaut, Sicaire, Meullemiestre, Fabiano-Tixier, & Abert-Vian, 2017). In ultrasound-assisted extraction (UAE), high-intensity ultrasonic waves induce cavitation around cells breaking the cell wall and facilitating solute solubilization, diffusion and heat transfer resulting in improved extraction efficiency (Carreira-Casais et al., 2021; Chemat et al., 2017). The most important advantages are the reduced extraction temperature and time, as well as the reduced energy consumption and solvent (Medina-Torres, Ayora-Talavera, Espinosa-Andrews, Sánchez-Contreras, & Pacheco, 2017; Zhang, Lin, & Ye, 2018). As a result, this technique is suitable for extracting heat-sensitive bioactive and

food components at lower processing temperatures (Vilkhu, Mawson, Simons, & Bates, 2008), such as phenolic compounds from plants and food by-products (Sun et al., 2022). Among the extraction solvents, ethanol has been classified as GRAS (generally recognized as safe) (Rodrigues, Fernandes, de Brito, Sousa, & Narain, 2015) and it is both an affordable and renewable source (sugar cane). Furthermore, ethanol has been described as having the highest affinity for phenolic compounds in various systems, making it the primary option for phenolic compound extraction from fruit and vegetable wastes (Osorio-Tobón, 2020; Ramić, Vidović, Zeković, Vladić, Cvejic, & Pavlić, 2015). One of the most important factors influencing UAE yield is the percentage of ethanol in hydroalcoholic solvent, which should be optimized using powerful mathematical tools (Kumar, Srivastav, & Sharanagat, 2021).

In this context, proper optimization of ultrasound extraction conditions such as solvents, temperature, time, particle size, and solid-to-solvent ratio is required for maximum recovery of phenolic compounds from cork by-products (Sridhar, Ponnuchamy, Kumar, Kapoor, Vo, & Prabhakar, 2021). Pretreatments for cork samples, such as trituration and defatting, are two strategies for increasing extraction yield by increasing the contact surface area and removing impurities, respectively. To obtain tannins, Reis et al. defatted granulated cork and cork powder in chloroform for 8 h using a Soxhlet system (Reis et al., 2019). Similarly, Santos et al. extracted the lipidic fraction from cork using Soxhlet extraction with dichloromethane for 6 h (Santos et al., 2013).

Given the lack of studies dealing with the optimization of extraction procedures and the effects of pretreatments on cork by-products to improve the recovery of phenolic compounds, the main goal of this work was to compare the application of trituration and defatting pretreatments (alone or combined) on the ultrasound-assisted extraction of phenolic compounds from cork-processing wastes using response surface methodology (RSM). For this purpose, the UAE critical conditions (time, and % ethanol concentration) were optimized using central composite design (13 experimental runs) in order to simultaneously maximize yield and total phenolic content (TPC) from cork-processing wastes subjected to the aforementioned pretreatments. Based on these findings, the best pretreatment was selected, taking into account the highest yield and TPC, as well as the ability of developed models to explain variation in experimental data. Finally, different UAE cycles were applied to the sample obtained at the optimal extraction conditions in order to increase the extraction yield and TPC even further. The obtained results were compared to those obtained using the traditional maceration method.

Materials and Methods

Reagents

Gallic acid ($\geq 98\%$), Acetic acid ($\geq 99\%$), Acetonitrile ($\geq 99.5\%$) and Caffeic acid were obtained from Sigma-Aldrich, Madrid, Spain. Ellagic acid ($\geq 96\%$, HPCE) was obtained from Fluka Biochemical College Park, MD, USA. Ethanol (99.5%) was purchased from AGA®, Prior Velho, Portugal.

Cork material

Granulated cork, with 1-2 mm particle size was obtained from the equivalent of three hundred natural cork stoppers by grinding and sieving cork (*Q. suber L*) stoppers, supplied by Amorim & Irmãos company (Mozelos, Portugal).

Application of different pretreatments to cork-processing waste

Prior to being subjected to UAE, cork samples were subjected to various pretreatments such as trituration and defatting (alone or in combination) to increase the recovery of phenolic compounds. Triturated cork was prepared to increase the contact surface area between the sample and the solvent. For this, 15 g granulated cork sample was triturated to obtain a small particle size using ultra-turrax at 9500 min^{-1} for 15 min (T 25 digital ULTRA-TURRAX® IKA®-Werke GmbH & Co. KG, Germany). The obtained sample was named TRI_CORK and this acronym was used throughout the manuscript.

To separate the lipophilic fraction, defatted cork was obtained. Cork samples (5 g) were defatted by extracting them in 120 mL of chloroform for 4 h using an automatic Soxhlet Büchi Extraction System B-811 (Büchi Labortechnik AG, Flawil, Switzerland). The cork sample was left in the extractor chamber for 24 h to allow the chloroform to evaporate. This defatted cork sample was called DF_CORK and this acronym was used throughout the manuscript.

The trituration and defatted treatments were combined as previously described to evaluate a possible synergetic effect between treatments, and the resulting cork sample was referred to throughout the manuscript as TRI DF CORK. Finally, untreated cork was used as a control (CORK). The different cork samples obtained through the aforementioned pretreatments are summarized in **Table 1**.

Table 1: Pretreatments applied to cork samples

Sample acronym	Pretreatment	
	Trituration	Defatting
CORK	NO	NO
TRI_CORK	YES	NO
DF_CORK	NO	YES
TRI_DF_CORK	YES	YES

UAE

UAE was applied to cork samples that had undergone the three pretreatments described in section 2.3 (TRI_CORK, DF_CORK, and TRI_DF_CORK) and to the control sample (CORK). An ultrasonic system (Optic IVYMEN® system ultrasonic Model CY-500, Barcelona, Spain) equipped with a titanium probe was used to perform UAE. All extractions were performed at 20 kHz, 500 W, and 70% amplitude.

In this case, 1.5 g of the corresponding cork samples (with or without pretreatments) was placed in a graduated test tube with 35 mL of solvent. The temperature probe was also placed in the reaction tube. This system was then immersed in a cold-water bath to prevent the temperature from rising and keep this parameter constant at 20 °C. Experimental runs were carried out in accordance with the experimental design matrix (Table 2), which combined different levels of time (min) and solvent concentration (% ethanol). The ranges for each independent variable (time and % ethanol concentration) were selected based on the literature (Ghiteșcu, Volf, Carausu, Bühlmann, Gilca, & Popa, 2015). In the UAE, ethanol-water mixtures are recommended for phenolic compound extraction. Individual solvents produce poor results, possibly due to the hydroalcoholic mixtures' intermediate polarity, which increases the solubility of the target compounds. Ethanol increases the solubility of phenolic compounds, whereas water increases their desorption from the sample (Osorio-Tobón, 2020). Based on preliminary tests, the solid-to-solvent ratio was kept constant at 42.85 g/L. (**data not shown**). After the extraction, the extracts were filtered through a 0.45 m filter and stored at -80 °C for further analysis.

Response variables evaluated in the UAE optimization

Extraction yield

An aliquot (10 mL) of each extract was placed in an empty, dry, and weighted crucible, which was then put in an oven at 104 °C for 24 h. Following that, crucibles containing the dry extract were weighted, and the extraction yield was determined according to (Silva et al., 2021) using Equation 1, with results expressed as mg extract/ g dry weight.

$$\text{Yield} \left(\frac{mg E}{g dm} \right) = \frac{P_{t=24 h} - P_{t=0}}{\left(\frac{m_{sw} \times V_a}{V_{sv}} \right) \times \left(\frac{100 - MC_{sw}}{100} \right)}$$

Equation 1

Where,

P_{t=0}: mass of empty crucible; **P_{t=24 h}**: mass of crucible with dry extract; **m_{sw}**: mass of granulated cork; **V_a**: volume of extract (10mL); **V_{sv}**: solvents volume (35 mL); **MC_{sw}**: moisture content (%) of granulated cork

Characterization of phenolic compounds

HPLC-DAD and LC-ESI-MS were used to identify phenolic compounds using a Finnigan Surveyor series liquid chromatograph equipped with a Thermo Finnigan (Hypersil Gold®) reversed-phase column C18 (150 mm 4.6 mm i.d., 5 m) at 25 °C and the methodology described previously in (Azevedo et al., 2014).

The total phenolic compounds (TPC) were calculated as the sum of all phenolic compounds individually identified by HPLC using area and curve calibration. Results are expressed as gallic acid equivalents.

Experimental design

RSM with a central composite design (CCD) was used to investigate the effects of critical extraction factors (time and ethanol concentration) on the extraction yield and TPC obtained through UAE of different cork samples (pretreated and control). Time and solvent concentration were evaluated at five levels (-α; -1; 0, 1, + α). The α-value (1.41) was chosen to ensure rotatable prediction variance distribution (Teglia, Gonzalo, Culzoni, & Goicoechea, 2019). This resulted in a total of 13 experiments including five central point replicates. Table 2 depicts the experimental design matrix for the two factors. Following the measurement of extraction yield and TPC for each experimental run, appropriate mathematical models were fitted to each response variable using the least-squares regression method (**Equation 2**).

$$Y_n = \beta_0 + \sum_{i=1}^3 \beta_i X_i + \sum_{i=1}^2 \sum_{j=2, j>i}^3 \beta_{ij} X_i X_j + \sum_{i=1}^3 \beta_{ii} X_i^2$$

Equation 2

Where,

Y_n: the predicted response (Y₁= extraction yield; Y₂= TPC); **β_i**: linear coefficient; **β_{ii}**: quadratic coefficient; **β_{ij}**: coefficient for the interaction effect; **X_i**: the dimensionless coded value of the independent variable, x_i (x₁= time; x₂= ethanol concentration).

Simultaneous optimization, validation, and evaluation of extraction cycles addition

Optimization was performed to find the extraction conditions that maximize extraction yield and TPC individually. On the other hand, the desirability function was used to carry out a simultaneous optimization where all the responses are maximized at the same time (Cassani, Tomadoni, Ponce, Agüero, & Moreira, 2017). For validation purposes, a new set of experiments under optimal extraction conditions was performed to assess the reliability of the simultaneous optimization. To this, cork samples were extracted at optimal factor levels and all response variables were measured to compare predicted results with experimental data. On the other hand, the effect of extraction cycle addition on further improving extraction yield and TPC measured under optimal extraction conditions was also evaluated.

Conventional extraction procedure

Results obtained from the simultaneous optimization studies (UAE section) were compared with those found in samples subjected to traditional maceration previously described (Azevedo et al., 2017). In brief, granulated cork (1.5 g) were placed in 50 mL capacity glass bottles with 35 mL hydroalcoholic solution (50% ethanol) at 35 °C for 7 days. Once the extraction was finished, extracts were filtered with a 0.45 µm filter and stored at -80 °C to further analysis. Extraction yield and TPC were determined as was previously described for the UAE samples.

Statistical analysis

Data analysis regarding RSM, individual and simultaneous optimization, and the corresponding figures were performed using Stat-Ease Design-Expert 11.0 software (Stat-Ease, Inc., Minneapolis, USA). The statistical analysis of regression models was evaluated through analysis of variance test (ANOVA) considering p-value <0.05 and insignificant lack of fit ($p > 0.05$). In this sense, significant factors ($p < 0.05$) were only considered in models for having a significant effect on the responses. The adjusted coefficient of determination (R^2_{adj}) was calculated for all models indicating the percentage of variance explained by them. according to the design proposed by (Teglia et al., 2019), the coefficients of the developed mathematical models were calculated using backward multiple regression and validated using ANOVA tests ($p < 0.05$)

Results and Discussion

Effects of pretreatments on yield and TPC of cork samples subjected to the UAE

Table S1 shows the phenolic compounds LC-MS profile of the CORK sample after UAE by comparing the retention time with standards and the fragmentation pattern to data described elsewhere (Azevedo et al., 2014; Ana Fernandes, Sousa, Mateus, Cabral, & de Freitas, 2011). Gallic, caffeic, protocatechuic and ellagic acids, protocatechuic aldehyde, and vanillin, as well as the isomers castalagin/vescalagin and dehydrated tergallic-C-glucoside, were the main compounds identified (**Figure 1**).

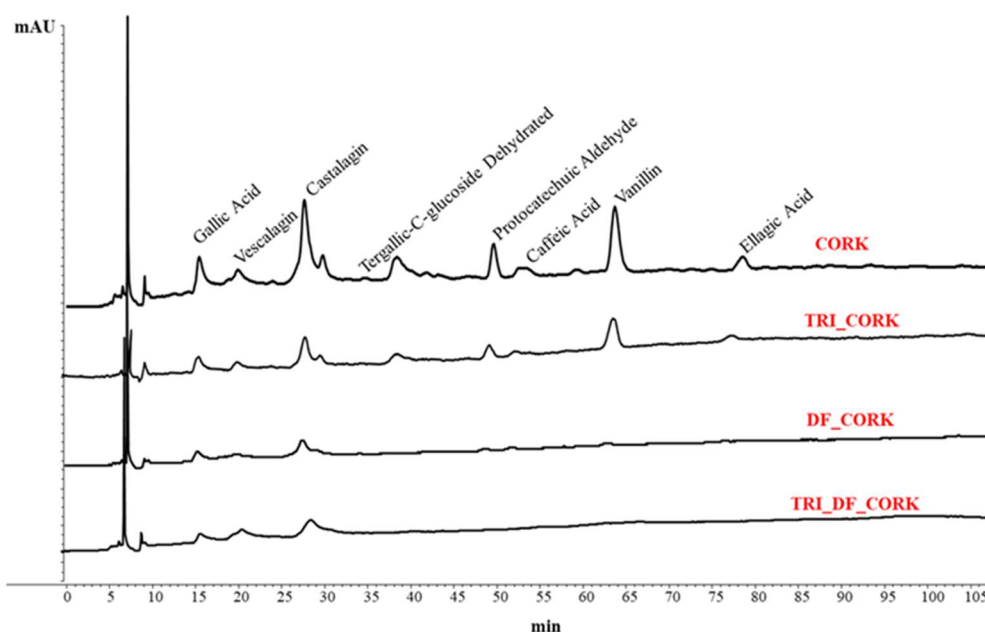


Figure 1: HPLC chromatogram at 280 nm obtained for cork samples subjected to different pretreatments and UAE procedure (under conditions established in run 10, **Table 2**). Triturated cork (TRI_CORK), Defatted cork (DF_CORK), Triturate and Defatted cork (TRI_DF_CORK), and Cork without pretreatment (CORK).

Figure 1 depicts the impact of pre-processing on phenolic profile of cork samples subjected to UAE under the conditions established in run 10 (**Table 2**). These compounds have previously been found in cork (Cantos, Espín, López-Bote, de la Hoz, Ordóñez, & Tomás-Barberán, 2003; Conde, Cadahía, García-Vallejo, Fernández De Simón, & González Adrados, 1997; Ana Fernandes et al., 2011; Varea, Garcia-Vallejo, Cadahia, & de Simon, 2001). In particular, gallic acid, protocatechuic acid, protocatechuic aldehyde and vanillin found in cork as described with antioxidant activity, anti-inflammatory, and antineoplastic properties (Azevedo et al., 2014; Kakkar & Bais, 2014). They as been reported with therapeutic activities in gastrointestinal, neuropsychological, metabolic, and cardiovascular disorders (Kahkeshani et al., 2019; Kakkar et al., 2014). In the same line, castalagin and vescalagin demonstrated biological

properties, specific with greater potential to inhibit the growth of the three cancer cell lines and DNA topoisomerase inhibitor beyond presented bactericidal activity (Araújo et al., 2021; Fernandes et al., 2009; Quideau et al., 2005; Quideau et al., 2003).

Table 2: Thirteen experimental runs involved in the central composite experimental design for the ultrasound-assisted extraction of cork samples.

Run	Factors		
	Space point type	Time (min)	% ethanol
1	Factorial	6.95	21.72
2	Factorial	26.05	21.72
3	Factorial	6.95	78.28
4	Factorial	26.05	78.28
5	Axial	3.00	50.00
6	Axial	30.00	50.00
7	Axial	16.50	10.00
8	Axial	16.50	90.00
9	Center	16.50	50.00
10	Center	16.50	50.00
11	Center	16.50	50.00
12	Center	16.50	50.00
13	Center	16.50	50.00

In addition, **Table 3** shows the phenolic compounds content quantified in each RSM design run for each sample (treated or not), as well as the total phenolic content obtained by the sum of all phenolic compounds identified for each sample. Defatting improved vescalagin extraction in those experiments with 50% ethanol concentration, regardless of extraction time (runs 5, 6, 9, 10, 11, 12, 13), as higher content was observed in comparison to other samples (**Table 3**).

Table 3: Phenolic compounds (mg/g dw) detected in the 13 runs involved in the central composite design for the ultrasound-assisted extraction optimization of treated and non-treated cork samples.

Compound/Run	Sample	Experimental runs (mg/g dw)												
		1	2	3	4	5	6	7	8	9	10	11	12	13
Gallic acid	TRI_CORK	0.0065	0.0079	0.0100	0.0136	0.0073	0.0199	0.0103	0.0165	0.0181	0.0177	0.0161	0.0173	0.0161
	DF_CORK	0.0352	0.0226	0.0186	0.0246	0.0176	0.0297	0.0120	0.0218	0.0410	0.0227	0.0247	0.0372	0.0326
	TRI_DF_CORK	0.0280	0.0321	0.0247	0.0266	0.0112	0.0154	0.0119	0.0123	0.0090	0.0123	0.0127	0.0139	0.0154
	CORK	0.0191	0.0240	0.0244	0.0426	0.0194	0.0472	0.0279	0.0449	0.0448	0.0498	0.0533	0.0363	0.0445
Vescalagin	TRI_CORK	0.0026	0.0027	0.0010	0.0010	0.0058	0.0123	0.0008	0.0002	0.0096	0.0095	0.0091	0.0117	0.0121
	DF_CORK	0.0381	0.0021	0.0044	0.0057	0.0165	0.0205	0.0111	0.0042	0.0358	0.0231	0.0213	0.0289	0.0293
	TRI_DF_CORK	0.0421	0.0418	0.0071	0.0059	0.0046	0.0064	0.0273	0.0051	0.0038	0.0054	0.0066	0.0080	0.0075
	CORK	0.0225	0.0219	0.0068	0.0070	0.0071	0.0143	0.0395	0.0086	0.0158	0.0162	0.0156	0.0148	0.0154
Castalagin	TRI_CORK	0.0180	0.0249	0.0290	0.0354	0.0286	0.0532	0.0177	0.0405	0.0513	0.0444	0.0420	0.0473	0.0472
	DF_CORK	0.0161	0.0113	0.0465	0.0594	0.0440	0.0667	0.0237	0.0524	0.0925	0.0587	0.0606	0.0812	0.0767
	TRI_DF_CORK	0.0799	0.0799	0.0331	0.0390	0.0328	0.0407	0.0422	0.0197	0.0390	0.0376	0.0438	0.0523	0.0564
	CORK	0.0970	0.1052	0.0853	0.1178	0.0839	0.1506	0.1131	0.1086	0.1414	0.1701	0.1680	0.1491	0.1601
Protocatechuic acid	TRI_CORK	0.0033	0.0054	0.0072	0.0094	0.0059	0.0134	0.0036	0.0094	0.0125	0.0128	0.0115	0.0122	0.0125
	DF_CORK	0.0013	0.0004	0.0121	0.0148	0.0089	0.0151	0.0054	0.0095	0.0197	0.0117	0.0122	0.0155	0.0164
	TRI_DF_CORK	0.0184	0.0187	0.0041	0.0081	0.0067	0.0114	0.0115	0.0026	0.0104	0.0140	0.0137	0.0169	0.0257

	CORK	0.0325	0.0361	0.0227	0.0295	0.0231	0.0350	0.0311	0.0273	0.0346	0.0411	0.0379	0.0321	0.0377
Dehydrated tergallic-C-glucoside	TRI_CORK	0.0068	0.0081	0.0098	0.0126	0.0081	0.0142	0.0078	0.0172	0.0158	0.0143	0.0135	0.0138	0.0131
	DF_CORK	0.0010	0.0002	0.0016	0.0020	0.0006	0.0024	0.0007	0.0023	0.0026	0.0014	0.0016	0.0038	0.0038
	TRI_DF_CORK	ND	ND	ND	ND	ND	ND	ND	ND	ND	ND	ND	ND	ND
	CORK	0.0289	0.0349	0.0385	0.0542	0.0258	0.0531	0.0319	0.0512	0.0510	0.0551	0.0580	0.0477	0.0534
Protocatechuic aldehyde	TRI_CORK	0.0052	0.0071	0.0090	0.0107	0.0059	0.0129	0.0067	0.0140	0.0118	0.0108	0.0104	0.0108	0.0096
	DF_CORK	ND	ND	ND	ND	ND	ND	ND	ND	ND	ND	ND	ND	ND
	TRI_DF_CORK	ND	ND	ND	ND	ND	ND	ND	ND	ND	ND	ND	ND	ND
	CORK	0.0293	0.0320	0.0377	0.0457	0.0233	0.0441	0.0272	0.0425	0.0414	0.0448	0.0460	0.0361	0.0409
Caffeic acid	TRI_CORK	0.0000	0.0000	0.0000	0.0069	0.0039	0.0092	0.0000	0.0090	0.0082	0.0078	0.0065	0.0077	0.0074
	DF_CORK	0.0062	0.0048	0.0030	0.0059	0.0012	0.0058	0.0000	0.0045	0.0081	0.0008	0.0013	0.0058	0.0047
	TRI_DF_CORK	0.0026	0.0034	0.0021	0.0024	0.0000	0.0000	0.0000	0.0000	0.0000	0.0000	0.0000	0.0000	0.0000
	CORK	0.0076	0.0096	0.0065	0.0185	0.0042	0.0234	0.0084	0.0242	0.0216	0.0236	0.0246	0.0175	0.0210
Vanillin	TRI_CORK	0.0204	0.0245	0.0287	0.0340	0.0228	0.0407	0.0210	0.0432	0.0389	0.0356	0.0340	0.0347	0.0318
	DF_CORK	0.0005	0.0001	0.0051	0.0058	0.0033	0.0057	0.0030	0.0083	0.0067	0.0038	0.0046	0.0087	0.0098
	TRI_DF_CORK	0.0007	0.0008	0.0002	0.0004	0.0000	0.0000	0.0000	0.0000	0.0000	0.0000	0.0000	0.0000	0.0000
	CORK	0.0668	0.0755	0.0917	0.1185	0.0614	0.1184	0.0706	0.1127	0.1093	0.1185	0.1165	0.1002	0.1139
Ellagic acid	TRI_CORK	0.0023	0.0031	0.0050	0.0065	0.0038	0.0078	0.0030	0.0114	0.0091	0.0067	0.0068	0.0093	0.0068
	DF_CORK	ND	ND	ND	ND	ND	ND	ND	ND	ND	ND	ND	ND	ND
	TRI_DF_CORK	ND	ND	ND	ND	ND	ND	ND	ND	ND	ND	ND	ND	ND

	CORK	0.0049	0.0087	0.0110	0.0211	0.0065	0.0224	0.0064	0.0223	0.0193	0.0238	0.0208	0.0174	0.0205
Total phenolic content* (mg/g dw)	TRI_CORK	0.0651	0.0837	0.0998	0.1301	0.0920	0.1836	0.0708	0.1613	0.1752	0.1595	0.1499	0.1647	0.1566
	DF_CORK	0.0984	0.0414	0.0913	0.1182	0.0920	0.1461	0.0536	0.1030	0.2063	0.1221	0.1264	0.1809	0.1735
	TRI_DF_CORK	0.1718	0.1766	0.0713	0.0825	0.0553	0.0739	0.0929	0.0397	0.0622	0.0692	0.0769	0.0911	0.1051
	CORK	0.3086	0.3478	0.3245	0.4548	0.2548	0.5083	0.3561	0.4423	0.4792	0.5428	0.5407	0.4514	0.5074

TRI_CORK: Triturated cork; **DF_CORK:** Defatted cork; **TRI_DF_CORK:** Triturated and defatted cork; **CORK:** cork without treatment; **ND:** not detected.
 *Total phenolic content was calculated as the sum of all phenolic compounds detected for each sample.

However, defatting was less effective in extracting the remaining phenolic compounds because their content was lower in comparison to the control sample. It was an unexpected result since defatting is a common pretreatment used to remove waxes that may interfere with target compound extraction. In addition, (Pereira, 1988) reported that cork contains a high concentration of extractives, nearly half of which are waxes and other non-polar compounds extractable with dichloromethane. Thus, in our case, phenolic compounds probably remained in the lipidic fraction as they showed similar polarity with chloroform. Moreover, chloroform was already described as a solvent to extract some phenolics from flowers (Taşkın et al, 2018).

Trituration was the least efficient treatment for extracting phenolic compounds from cork samples, yielding lower values when compared to the control sample (**Table 3**). The goal of triturating cork samples prior to extraction was to improve the UAE process by allowing for smaller particle sizes, which increases the superficial area of contact between matrix and solvent and thus improves extraction efficiency but that didn't happen.

In general, defatting plus trituration did not improve phenolic compounds extraction from cork samples, as evidenced by a significant decrease in content when compared to the untreated sample (**Figure 1, Table 3**). In fact, if trituration and defatted already showed a negative effect individually, when conjugating the two procedures were obtained the lowest quantity of phenolic compounds.

Table 4 displays the extraction yield and TPC mean values for all extracts (pre-treated or not) obtained under the experimental design conditions. As can be seen, the values of response variables varied depending on the time and solvent concentration tested.

Table 4: Central composite experimental design matrix* and responses [yield (mg extract/g dw) and total phenolic content (TPC) (mg TP/g)] of treated and non-treated cork samples subjected to ultrasound-assisted extraction.

Run	TRI_CORK		DF_CORK		TRI_DF_CORK		CORK	
	Yield	TPC	Yield	TPC	Yield	TPC	Yield	TPC
1	6.6738	0.0651	2.8971	0.0984	12.0882	0.1718	14.6231	0.3086
2	6.0311	0.0837	4.7770	0.0414	11.3469	0.1766	11.5572	0.3478
3	24.9062	0.0998	19.4452	0.0913	7.7255	0.0713	15.8594	0.3245
4	28.1711	0.1301	21.9764	0.1182	14.2268	0.0825	20.1793	0.4548
5	7.1904	0.0920	3.7366	0.0920	5.7821	0.0553	9.8823	0.2548
6	11.7079	0.0000	8.4855	0.1461	12.7459	0.0739	20.0713	0.5083
7	4.8905	0.0708	2.2917	0.0536	5.2595	0.0929	13.9538	0.3561
8	12.1102	0.1613	5.1686	0.1030	8.6466	0.0397	25.3900	0.4423
9	9.2823	0.1752	11.1972	0.2063	7.9686	0.0622	17.8185	0.4792
10	7.8488	0.1595	5.2251	0.1221	8.6443	0.0692	19.4353	0.5428
11	7.7394	0.1499	6.6972	0.1264	13.2092	0.0769	19.8571	0.5407
12	9.5533	0.1647	8.1007	0.1809	13.7124	0.0911	19.2916	0.4514
13	9.1666	0.1566	9.4321	0.1735	16.0912	0.1051	18.2599	0.5074

* $\alpha=1.41$. TRI_CORK: Triturated cork; DF_CORK: Defatted cork; TRI_DF_CORK: Triturated and defatted cork; CORK: cork without treatment.

Given that the extraction yield was determined gravimetrically, this value includes not only the phenolic compounds under study but also other extractable non-phenolic compounds with similar polarity to the solvent concentration tested. This effect can be seen in TRI_CORK experiments #3 and 4, where the maximum yield value did not lead to the maximum TPC. Experiments #3 and 4 for DF_CORK samples and experiment #8 for CORK samples revealed similar results. Regarding TPC, for TRI_CORK, DF_CORK, and CORK samples, the maximum TPC was obtained in experiments conducted using the middle values of time and solvent concentration (16.5 min, 50% ethanol). However, higher TPC were found for TRI DF CORK when 21.72% ethanol was used regardless of extraction time assayed. In the case of phenolic compounds, the literature suggests using ethanol-water mixtures because ethanol increases their solubility while water increases their desorption from the sample (Osorio-Tobón, 2020).

Table 4 also shows that the extraction yield and TPC of treated samples were significantly reduced, with CORK samples having the highest values. These findings suggest that no pre-treatment is required to improve the recovery of phenolic compounds from cork processing waste, which is advantageous because it reduces the use of reagents, energy, and time, contributing to a more sustainable extraction methodology. On the other hand, **Table 5** displays ANOVA results for each response variable of pretreated and untreated cork samples after fitting **Equation (2)** to the experimental data in **Table 4** using the non-linear square method.

Table 5: Model fitting parameters for each studied response of treated and non-treated cork samples and estimated regression coefficients (when corresponding) obtained from the RSM analysis.

Sample/Response	Terms	ANOVA p-value			Coefficient estimate	Standard error
		Model	Lack of fit	Adjusted R ²		
TRI_CORK						
Yield	B-Ethanol concentration****	< 0.0001	0.0658	0.7755	-	
TPC	A-Time B-Ethanol concentration* A ^{2**}	0.0032	0.0093	0.691	-	
DF_CORK						
Yield	B- Ethanol concentration**	0.0067	0.0818	0.4569	-	
TPC	B- Ethanol concentration B ^{2*}	0.0238	0.5349	0.432	-	
TRI_DF_CORK						
Yield	Data did not fit any model					
TPC	B- Ethanol concentration*	0.012	0.0754	0.4007	-	
CORK						
Yield	A-Time B- Ethanol concentration*** AB* A ^{2**}	0.0001	0.1523	0.923	A=19.23 B=0.5329 AB=3.25 A ² =1.85 Intercept=-3.99	A=0.433 B=0.5304 AB=0.4165 A ² =0.589 Intercept=0.5728
TPC	A-Time** B- Ethanol concentration** A ^{2**} B ^{2**}	0.0015	0.3857	0.797	A=0.066 B=0.0306 A ² =-0.0692 B ² =-0.0604 Intercept=0.5043	A=0.0152 B=0.0152 A ² =0.0163 B ² =0.0163 Intercept=0.0192

* Significant with p<0.05

** Significant p<0.01

*** Significant p<0.001

**** Significant p<0.0001

Although the yield and TPC models for TRI CORK and DF CORK could be considered satisfactory because the regression was significant (p<0.05), these models did not adequately explain the variation in data, as evidenced by the low adjusted R². In addition, the lack of fit in the TPC model for TRI_CORK was statistically significant (p<0.05). In contrast, data from CORK samples fit well to second-order polynomial models in both response variables studied. Furthermore, both responses had an insignificant lack of fit, with adjusted R² of 0.923 and 0.797 for yield and TPC, respectively. These findings

confirmed that developed models for the CORK sample are adequate for prediction purposes.

Given that the control sample produced the best results, this represents a significant advantage, making the process more sustainable by eliminating the need for pre-treatments, reducing extraction time, and reducing solvent consumption. Thus, the untreated cork sample was used in subsequent analyses.

Influence of critical extraction factors on response variables of CORK sample

Concerning yield, the linear effect of ethanol concentration and the quadratic effect of extraction time was found to play a significant (**Table 5**, $p < 0.001$) role. In addition, the interaction between both factors was also statistically significant. **Figure 2A** depicts response surface plots that combine the effect of ethanol concentration and time on CORK sample extraction yield.

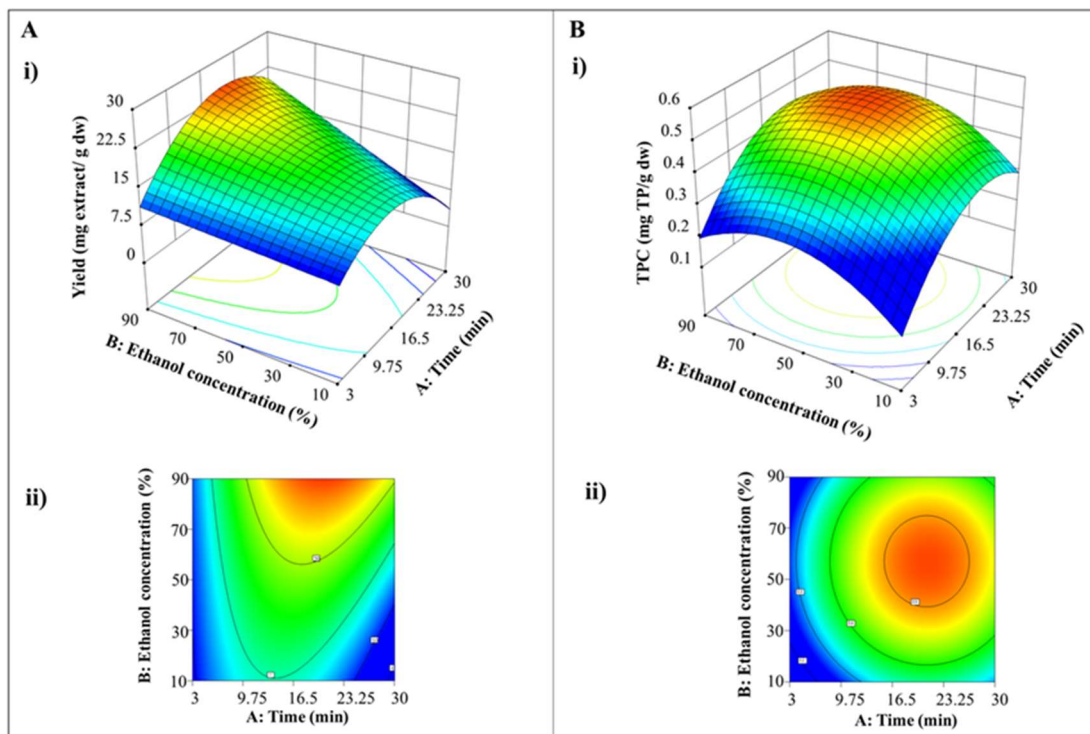


Figure 2: Response surface 3D (i) and contour plots (ii) obtained for extraction yield (A) and total phenolic compounds (B) in untreated cork sample subjected to UAE, demonstrating the combined effect of time and ethanol concentration.

As can be seen, yield increased with time until a certain point was reached (around the middle value). Beyond this point, yield decreased over time due to their non-linear relationship (**Figure 3Ai**). The literature described that inadequate extraction conditions in UAE can lead to their incomplete recovery and with undesired effects such as

degradation of interest compounds, the formation of secondary products that can interfere with extraction (Ameer, Shahbaz, & Kwon, 2017; Babotă et al., 2022) which may be what happens after the optimal extraction point is reached.

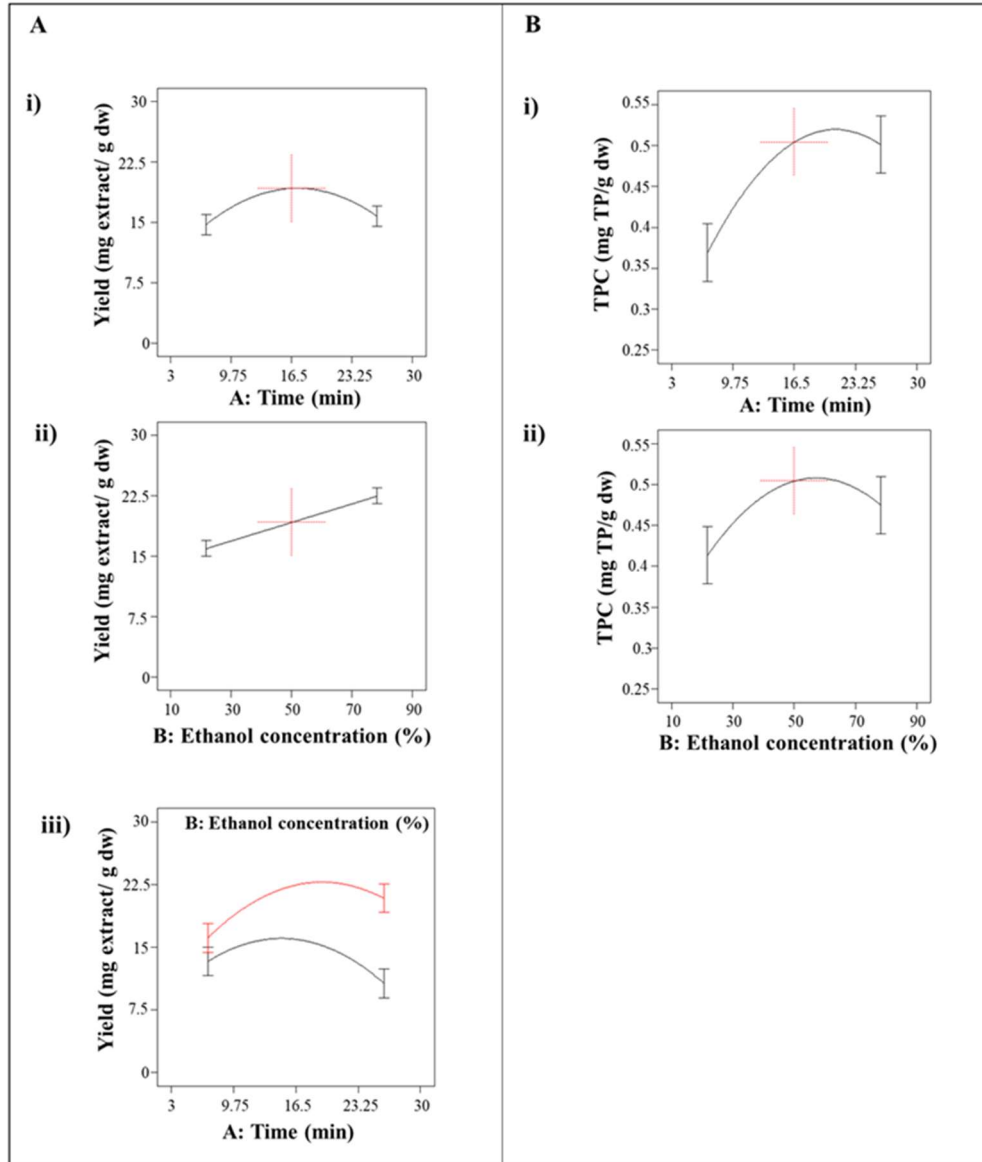


Figure 3: Effect of time (i) and ethanol concentration (ii) on yield (A) and total phenolic compounds (B) and interaction between time and ethanol concentration on yield (iii) in untreated cork sample subjected to UAE. The black and red lines represent ethanol concentrations of 21.71% and 78.28%, respectively.

Extraction yields increased as ethanol concentration increased (**Figure 3Aii**), indicating that the majority of the extractable compounds in the CORK sample have polarity properties similar to aqueous ethanol. This behaviour has already been described in the literature, with increasing ethanol concentration accelerating mass transfer between liquid and solid and improving polar phenolic compound solubility (Ghiteșcu et al., 2015). **Figure 3Aiii** depicts the interaction of time and ethanol concentration on CORK sample

yield. As can be seen, there are significant differences in yield when longer times are used, resulting in higher yield at higher ethanol concentrations employed. In fact, literature described ethanol, a polar solvent, as a solvent able to extract flavonoids including their glycosides, and tannins from raw plant materials (Bazykina, Nikolaevskii, Filippenko, & Kaloerova, 2002). In this context, the optimal UAE conditions for maximizing yield (**Table 6**) were 20.26 min and 90% ethanol. Under these conditions, the predicted values of yield and TPC were 24.45 mg extract/ g dw and 0.44 g/g dw, respectively.

Regarding TPC, the linear and quadratic effects of time and ethanol concentration on the recovery of phenolic compounds from CORK samples were statistically significant ($p < 0.01$) (**Figure 2B**). A curvature indicating a non-linear relationship between extraction factors and TPC was observed in both cases. TPC increased with time and ethanol concentration up to a certain extent (around middle values). TPC then decreased as both factors were increased. Other works using UAE, already described better results in TPC extraction for intermediate % ethanol (50%), but with different sources, male chestnut flowers and wild thyme (Alaya et al., 2021; Babotă et al., 2022).

One explanation for this behavior was the mixtures containing intermediate ethanolic concentrations are more able to interact with phenolic compounds from cork with intermediate polarity (**Table 3**) (Babotă et al., 2022). Moreover, was described that applying UAE for 20 min prevents the degradation of some phenolics, despite being a different natural source (rom oat) the compounds are the same (Chen et al., 2018). The optimal extraction conditions for TPC were 21.05 min and 57.15% ethanol (**Table 6**). The models predict that UAE performed under these conditions will result in TPC and yield of 0.52 mg/g dw and 19.63 mg extract/g dw, respectively. To our knowledge, there is no description in the literature, of the optimization of the extraction of phenolic compounds from cork using the UAE.

Table 6: Independent and simultaneous optimization of UAE factors for each response and their predicted and experimental values obtained under these conditions.

Optimization	Optimal conditions		Predicted responses		Experimental values	
	Time (min)	Solvent concentration (% ethanol)	Yield	TPC	Yield	TPC
Independent						
yield	20.26	90.00	24.45	0.44		
TPC	21.05	57.15	19.63	0.52		
Simultaneous	20.02	75.15	22.39 [19.26; 25.50]	0.50 [0.39; 0.61]	23.74 ± 3.71	0.69 ± 0.03

Simultaneous optimization and validation of the UAE procedure

The results of the individually optimized response variables show that the optimal conditions for maximizing yield were similar to those found for TPC, with a few exceptions, most notably in ethanol concentration. As previously stated, the yield was determined gravimetrically, including not only phenolics but also other extractable non-phenolic compounds present in the CORK sample. However, when only yield was optimized, models predicted higher yield and lower TPC values than those found when extraction was carried out under optimal TPC conditions (**Table 6**). These findings suggest that simultaneous optimization is required to maximize both responses simultaneously.

The results of the simultaneous optimization with the Desirability function are shown in **Figure 4**. The optimal UAE conditions resulted in 20.02 min and 75.15% ethanol (**Table 6**). The predicted values for each response under these conditions were: 22.39 mg extract/g dw for yield and 0.50 mg/g dw for TPC. This result confirms the advantage of applying simultaneous optimization to find good values for yield and TPC, reaching a compromise solution.

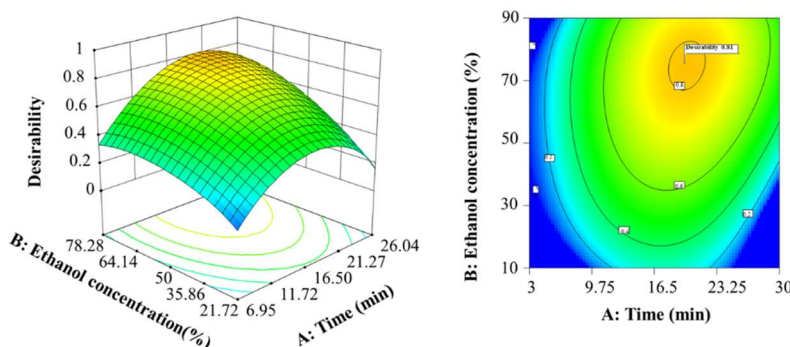


Figure 4: Desirability 3D surface (i) and contour plots (ii) as a function of time and ethanol concentration.

To our knowledge, there is no work using UAE for the extraction of phenolic compounds from cork samples and by this it is not possible to compare our results with the literature. The literature describes amounts from different classes of phenolics and different ways to obtain them, mostly applied previously to soxhlet extraction to defatted cork sample using dichloromethane, followed by extraction using different solvents like methanol, methanol/water, acetone (Reis, Coelho, et al., 2020; Reis et al., 2019; Santos et al., 2013). From the natural cork stoppers, compounds that are able to pass to model wine solution was described 31 ± 10 mg/cork stopper with 30% of ellagitannins, 10 % condensed tannins and the remaining material (60%) probably attributed to phenolic acids, aldehydes, and other low molecular weight compounds, (Reis, Coelho, et al., 2020). In case of granulated cork, a total amount of 30-52 mg/g cork granulate, with 15–

32 mg/g cork granulate of ellagitannin, 6–13 mg/g cork granulate of phenolic acids and the phenolic derivatives were described (Reis, Teixeira, et al., 2020). In natural cork, Santos et al described an extraction yield of 6% and TPC 336.34 ± 1.15 mg GAE g⁻¹ of extract and 19.94 ± 0.07 g GAE kg⁻¹ of dry starting material (Santos et al., 2013).

A new set of experiments was performed under optimal extraction conditions to assess the reliability of the simultaneous optimization. The experimental values for extraction yield did not differ significantly from the predicted values, whereas the experimental data for TPC was slightly higher than the predicted values (**Table 6**). The values obtained by simultaneous optimization agree with the experimental data, confirming the robustness of the models. Recent work has also had good results when comparing experimental results with predicted ones, using a simultaneous optimization, in UAE extraction of compounds from Carob Pods (Nieto & Akkal, 2022).

Following that, the addition of extraction cycles under optimal conditions was evaluated in order to increase yield and TPC even further. **Figure 5** shows that running a second UAE cycle under conditions obtained through simultaneous optimization increased the yield and TPC values of cork samples significantly ($p < 0.05$). Indeed, some studies have suggested that successive short periods of cork granulate extraction may result in a more efficient extraction of ellagitannins (Reis et al., 2019).

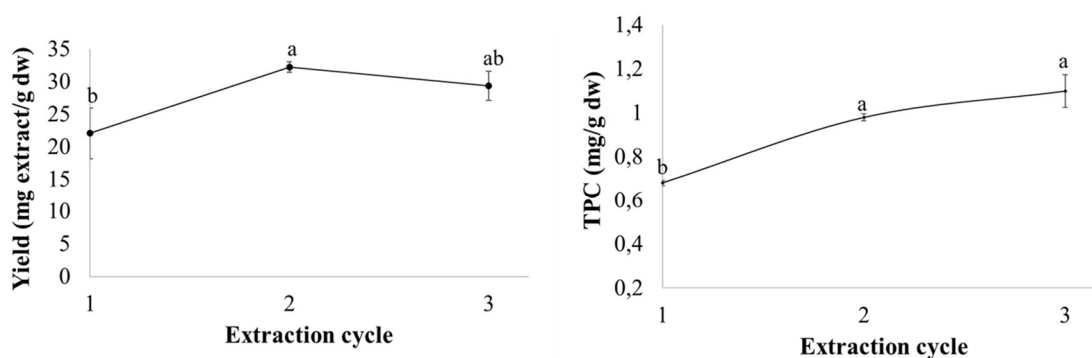


Figure 5: Effect of UAE cycles on extraction yield (i) and total phenolic compounds (ii) under optimal conditions (20.02 min and 75.15% ethanol). Significant differences ($p < 0.05$) between cycles are indicated by values with different letters.

Based on these findings, two consecutive UAE cycles (for a total of 40 min of extraction) yielded 32.24 ± 0.82 mg extract/g dw for yield and 0.98 ± 0.015 mg/g dw for TPC. When these results are compared to those obtained by the conventional maceration method (50.31 mg/g extract for yield and 1.36 mg/g dw for TPC), it is possible to conclude that two consecutive UAE cycles under optimal conditions achieved similar TPC values to conventional extraction while consuming significantly less time and energy. Similar result

was already described in literature, but for the other matrix (grapes), that UAE produced similar or higher phenolics recoveries than reference methodology however in a much shorter extraction time (6 min instead of 60 min) (Carrera et al, 2012).

Conclusion

The valorization of cork processing wastes by extracting bioactive compounds is a smart approach for contributing to sustainability while also adding value to underutilized food-related products. Extraction conditions must be optimized to ensure a successful extraction of phenolic compounds with biological activity. In this study, the UAE conditions (time and ethanol concentration) were optimized using response surface methodology (RSM) and central composite design to maximize yield and total phenolic compounds from previously treated cork samples (trituration, defatting, or by a combination of both). According to the findings, the pretreatments had a negative effect on the yield and total phenolic content of cork samples, as their values were significantly lower than the control sample. Furthermore, experimental data from pretreated samples did not adequately explain variation in data. ANOVA results for the control sample (cork without pretreatment) revealed that extraction time and ethanol concentration were significant factors in both responses. When both responses were optimized individually, the optimal conditions for obtaining the maximum extraction yield (20.26 min and 90% ethanol) differed from those found when optimizing only TPC (21.05 min and 57.15% ethanol). In this case, simultaneous optimization enabled the finding of a compromise solution between factors maximizing extraction yield and TPC. As a result, the optimal UAE conditions were 20.02 min and 75.15% ethanol, resulting in cork processing waste extracts with predicted extraction yield and TPC of 22.39 mg/ g dw and 0.50 mg/ g dw, respectively. Validation assays revealed that experimental values obtained under optimal conditions were in close agreement with predicted values, confirming the models' robustness. Finally, using two consecutive UAE cycles of extraction under optimal conditions increased yield (32.24 ± 0.82 mg extract/g dw) and TPC (0.98 ± 0.015 mg/g dw). These results were comparable to those obtained by the traditional maceration method, with the added benefit of saving time and lowering solvent and energy consumption. In this regard, the findings of this study promote the recovery of bioactive compounds from cork processing waste.

Acknowledgements

The authors thank the Science and Technology Foundation (FCT) for financial the scholarships SFRH/BD/139709/2018, UIDB/50006/2020 and UIDBP/50006/2020. And also thanks the *IACOBUS program* (based on the priorities defined in the Galicia - Northern Portugal Joint Investment Plan (PIC 21-27) and on the strategic areas established by the Galicia - Northern Portugal Cross-border Intelligent Specialization Strategy (RIS3-T)) and has support from the European Union, through funding for the INTERREG V-A Spain-Portugal Program (POCTEP) 2014-2020. And also supported by MICINN supporting the Ramón y Cajal grant for M.A. Prieto (RYC-2017-22891), the María Zambrano grant for R. Perez-Gregorio (CO34991493-20220101ALE481), and the Xunta de Galicia supporting the post-doctoral grant for L. Cassani (ED481B-2021/152). The authors are also grateful to Ibero-American Program on Science and Technology (CYTED-AQUA-CIBUS, P317RT0003). This work has received funding from the Argentinean Agency for the Scientific and Technological Promotion (ANPCyT, Argentina) under the project PICT (2020)/1602

References

- Alaya, I. b., Pereira, E., Dias, M. I., Pinela, J., Calhella, R. C., Soković, M., . . . Barros, L. (2021). Development of a Natural Preservative from Chestnut Flowers: Ultrasound-Assisted Extraction Optimization and Functionality Assessment. *Chemosensors*, 9(6), 141. <https://doi.org/https://doi:10.3390/chemosensors9060141>.
- Ameer, K., Shahbaz, H. M., & Kwon, J. H. (2017). Green extraction methods for polyphenols from plant matrices and their byproducts: A review. *Comprehensive Reviews in Food Science and Food Safety*, 16(2), 295-315.
- Azevedo, J., Fernandes, A., Oliveira, J., Brás, N. F., Reis, S., Lopes, P., . . . de Freitas, V. (2017). Reactivity of Cork Extracts with (+)-Catechin and Malvidin-3-O-glucoside in Wine Model Solutions: Identification of a New Family of Ellagitannin-Derived Compounds (Corklins). *Journal of Agriculture and Food Chemistry*, 65(39), 8714-8726. <https://doi.org/https://doi.org/10.1021/acs.jafc.7b02845>.
- Azevedo, J., Fernandes, I., Lopes, P., Roseira, I., Cabral, M., Mateus, N., & Freitas, V. (2014). Migration of phenolic compounds from different cork stoppers to wine model solutions: antioxidant and biological relevance. *European Food Research and Technology*, 239(6), 951-960. <https://doi.org/https://doi.org/10.1007/s00217-014-2292-y>.
- Babotă, M., Frumuzachi, O., Găvan, A., Iacoviță, C., Pinela, J., Barros, L., . . . Mocan, A. (2022). Optimized ultrasound-assisted extraction of phenolic compounds from *Thymus comosus* Heuff. ex Griseb. et Schenk (wild thyme) and their bioactive potential. *Ultras Sonochem*, 84, 105954. <https://doi.org/https://doi.org/10.1016/j.ultsonch.2022.105954>.
- Bazykina, N., Nikolaevskii, A., Filippenko, T., & Kaloerova, V. (2002). Optimization of conditions for the extraction of natural antioxidants from raw plant materials. *Pharmaceutical Chemistry Journal*, 36, 46-49.
- Cantos, E., Espín, J. C., López-Bote, C., de la Hoz, L., Ordóñez, J. A., & Tomás-Barberán, F. A. (2003). Phenolic Compounds and Fatty Acids from Acorns (*Quercus* spp.), the Main Dietary Constituent of Free-Ranged Iberian Pigs. *Journal of Agriculture and Food Chemistry*, 51(21), 6248-6255. <https://doi.org/https://10.1021/jf030216v>.
- Carreira-Casais, A., Otero, P., Garcia-Perez, P., Garcia-Oliveira, P., Pereira, A. G., Carpena, M., . . . Prieto, M. A. (2021). Benefits and Drawbacks of Ultrasound-Assisted Extraction for the Recovery of Bioactive Compounds from Marine Algae. *International Journal Environ Research Public Health*, 18(17). <https://doi.org/https://10.3390/ijerph18179153>.
- Carrera, C., Ruiz-Rodríguez, A., Palma, M., & Barroso, C. G. (2012). Ultrasound assisted extraction of phenolic compounds from grapes. *Analytica Chimica Acta*, 732, 100-104. <https://doi.org/https://doi.org/10.1016/j.aca.2011.11.032>.
- Carriço, C., Ribeiro, H. M., & Marto, J. (2018). Converting cork by-products to ecofriendly cork bioactive ingredients: Novel pharmaceutical and cosmetics applications. *Industrial Crops and Products*, 125, 72-84. <https://doi.org/https://doi.org/10.1016/j.indcrop.2018.08.092>.
- Cassani, L., Tomadoni, B., Ponce, A., Agüero, M. V., & Moreira, M. R. (2017). Combined Use of Ultrasound and Vanillin to Improve Quality Parameters and Safety of Strawberry Juice Enriched with Prebiotic Fibers. *Food and Bioprocessing Technology*, 10(8), 1454-1465. <https://doi.org/https://10.1007/s11947-017-1914-3>.

- Chemat, F., Rombaut, N., Sicaire, A.-G., Meullemiestre, A., Fabiano-Tixier, A.-S., & Abert-Vian, M. (2017). Ultrasound assisted extraction of food and natural products. Mechanisms, techniques, combinations, protocols and applications. A review. *Ultras Sonochemical*, 34, 540-560. <https://doi.org/https://doi.org/10.1016/j.ultsonch.2016.06.035>.
- Chen, C., Wang, L., Wang, R., Luo, X., Li, Y., Li, J., . . . Chen, Z. (2018). Ultrasound-assisted extraction from defatted oat (*Avena sativa* L.) bran to simultaneously enhance phenolic compounds and β -glucan contents: Compositional and kinetic studies. *Journal of Food Enge*, 222, 1-10. <https://doi.org/https://doi.org/10.1016/j.jfoodeng.2017.11.002>.
- Conde, E., Cadahía, E., García-Vallejo, M. C., Fernández De Simón, B., & González Adrados, J. R. (1997). Low Molecular Weight Polyphenols in Cork of *Quercus suber*. *Journal of Agriculture and Food Chemistry*, 45(7), 2695-2700. <https://doi.org/https://doi.org/10.1021/jf960486w>.
- Fernandes, A., Fernandes, I., Cruz, L., Mateus, N., Cabral, M., & De Freitas, V. (2009). Antioxidant and biological properties of bioactive phenolic compounds from *Quercus suber* L. *Journal of Agriculture and Food Chemistry*, 57(23), 11154-11160. <https://doi.org/https://doi.org/10.1021/jf902093m>.
- Fernandes, A., Sousa, A., Mateus, N., Cabral, M., & de Freitas, V. (2011). Analysis of phenolic compounds in cork from *Quercus suber* L. by HPLC-DAD/ESI-MS. *Food Chemistry*, 125(4), 1398-1405. <https://doi.org/https://doi.org/10.1016/j.foodchem.2010.10.016>.
- Ghitescu, R.-E., Volf, I., Carausu, C., Bühlmann, A.-M., Gilca, I. A., & Popa, V. I. (2015). Optimization of ultrasound-assisted extraction of polyphenols from spruce wood bark. *Ultras Sonochem*, 22, 535-541. <https://doi.org/https://doi.org/10.1016/j.ultsonch.2014.07.013>.
- Kahkeshani, N., Farzaei, F., Fotouhi, M., Alavi, S. S., Bahramsoltani, R., Naseri, R., . . . Bishayee, A. (2019). Pharmacological effects of gallic acid in health and diseases: A mechanistic review. *Iran J Basic Med Sci*, 22(3), 225-237. <https://doi.org/10.22038/ijbms.2019.32806.7897>.
- Kakkar, S., & Bais, S. (2014). A Review on Protocatechuic Acid and Its Pharmacological Potential. *ISRN Pharmacology*, 2014, 952943. <https://doi.org/10.1155/2014/952943>.
- Kumar, K., Srivastav, S., & Sharanagat, V. S. (2021). Ultrasound assisted extraction (UAE) of bioactive compounds from fruit and vegetable processing by-products: A review. *Ultras Sonochem*, 70, 105325. <https://doi.org/https://doi.org/10.1016/j.ultsonch.2020.105325>.
- Manrique, Y. J. A. (2017). Supercritical fluid extraction and fractionation of bioactive natural products from cork.
- Medina-Torres, N., Ayora-Talavera, T., Espinosa-Andrews, H., Sánchez-Contreras, A., & Pacheco, N. (2017). Ultrasound Assisted Extraction for the Recovery of Phenolic Compounds from Vegetable Sources. *Agronomy*, 7(3), 47. <https://doi.org/https://doi:10.3390/agronomy7030047>.
- Mislata, A. M., Puxeu, M., & Ferrer-Gallego, R. (2020). Aromatic Potential and Bioactivity of Cork Stoppers and Cork By-Products. *Foods (Basel, Switzerland)*, 9(2), 133. <https://doi.org/https://10.3390/foods9020133>.
- Nieto, G., & Akkal, S. (2022). Process Optimization of Phytoantioxidant and Photoprotective. *Molecules*, 27. <https://doi.org/10.3390/molecules27248802>.
- Osorio-Tobón, J. F. (2020). Recent advances and comparisons of conventional and alternative extraction techniques of phenolic compounds. *Journal Food Science and Technology*, 57(12), 4299-4315. <https://doi.org/https://10.1007/s13197-020-04433-2>.
- Pereira, H. (1988). Chemical composition and variability of cork from *Quercus suber* L. *Wood Science and Technology*, 22(3), 211-218. <https://doi.org/https://doi.org/10.1007/BF00386015>.
- Quideau, S., Jourdes, M., Lefeuvre, D., Montaudon, D., Saucier, C., Glories, Y., . . . Pourquier, P. (2005). The Chemistry of Wine Polyphenolic C-Glycosidic Ellagitannins Targeting Human Topoisomerase II. *Chemical European Journal* 11(22), 6503-6513. <https://doi.org/https://doi.org/10.1002/chem.200500428>.
- Ramić, M., Vidović, S., Zeković, Z., Vladić, J., Cvejic, A., & Pavlić, B. (2015). Modeling and optimization of ultrasound-assisted extraction of polyphenolic compounds from *Aronia melanocarpa* by-products from filter-tea factory. *Ultras Sonochemical*, 23, 360-368. <https://doi.org/https://doi.org/10.1016/j.ultsonch.2014.10.002>.
- Reike, D., Vermeulen, W. J. V., & Witjes, S. (2018). The circular economy: New or Refurbished as CE 3.0? — Exploring Controversies in the Conceptualization of the Circular Economy through a Focus on History and Resource Value Retention Options. *Resource Conservation and Recycle*, 135, 246-264. <https://doi.org/https://doi.org/10.1016/j.resconrec.2017.08.027>.
- Reis, S. F., Coelho, E., Evtuguin, D. V., Coimbra, M. A., Lopes, P., Cabral, M., . . . Freitas, V. (2020). Migration of Tannins and Pectic Polysaccharides from Natural Cork Stoppers to the Hydroalcoholic Solution. *Journal of Agricultural and Food Chemistry*, 68(48), 14230-14242. <https://doi.org/10.1021/acs.jafc.0c02738>.
- Reis, S. F., Lopes, P., Roseira, I., Cabral, M., Mateus, N., & Freitas, V. (2019). Recovery of added value compounds from cork industry by-products. *Industrial Crops Products*, 140, 111599. <https://doi.org/https://doi.org/10.1016/j.indcrop.2019.111599>.
- Reis, S. F., Teixeira, T., Pinto, J., Oliveira, V., Lopes, P., Cabral, M., . . . de Freitas, V. (2020). Variation in the Phenolic Composition of Cork Stoppers from Different Geographical Origins. *Journal of Agriculture and Food Chemistry*, 68(50), 14970-14977. <https://doi.org/https://10.1021/acs.jafc.0c00586>.

- Rodrigues, S., Fernandes, F. A., de Brito, E. S., Sousa, A. D., & Narain, N. (2015). Ultrasound extraction of phenolics and anthocyanins from jaboticaba peel. *Industrial Crops Products*, 69, 400-407. <https://doi.org/https://doi.org/10.1016/j.indcrop.2015.02.059>.
- Santos, S. A. O., Pinto, P. C. R. O., Silvestre, A. J. D., & Neto, C. P. (2010). Chemical composition and antioxidant activity of phenolic extracts of cork from *Quercus suber* L. *Industrial Crops and Products*, 31(3), 521-526. <https://doi.org/https://doi.org/10.1016/j.indcrop.2010.02.001>.
- Santos, S. A. O., Villaverde, J. J., Sousa, A. F., Coelho, J. F. J., Neto, C. P., & Silvestre, A. J. D. (2013). Phenolic composition and antioxidant activity of industrial cork by-products. *Industrial Crops Products*, 47, 262-269. <https://doi.org/https://doi.org/10.1016/j.indcrop.2013.03.015>.
- Sharma, P., Gaur, V. K., Sirohi, R., Varjani, S., Hyoun Kim, S., & Wong, J. W. C. (2021). Sustainable processing of food waste for production of bio-based products for circular bioeconomy. *Bioresearch and Technology*, 325, 124684. <https://doi.org/https://doi.org/10.1016/j.biortech.2021.124684>.
- Silva, A., Rodrigues, C., Garcia-Oliveira, P., Lourenço-Lopes, C., Silva, S. A., Garcia-Perez, P., . . . Prieto, M. A. (2021). Screening of Bioactive Properties in Brown Algae from the Northwest Iberian Peninsula. *Foods (Basel, Switzerland)*, 10(8). <https://doi.org/https://10.3390/foods10081915>.
- Sridhar, A., Ponnuchamy, M., Kumar, P. S., Kapoor, A., Vo, D.-V. N., & Prabhakar, S. (2021). Techniques and modeling of polyphenol extraction from food: a review. *Environmental Chemical Letter*, 19(4), 3409-3443. <https://doi.org/https://10.1007/s10311-021-01217-8>.
- Sun, S., Zhao, Y., Wang, L., Tan, Y., Shi, Y., Sedjoah, R.-C. A.-A., . . . Xin, Z. (2022). Ultrasound-assisted extraction of bound phenolic compounds from the residue of *Apocynum venetum* tea and their antioxidant activities. *Food Bioscience*, 47, 101646. <https://doi.org/https://doi.org/10.1016/j.fbio.2022.101646>.
- Taşkın, T., Taşkın, D., Rayaman, E., Dikpinar, T., Süzgeç-Selçuk, S., & Arabacı, T. (2018). Characterization of the Biological Activity and Phenolics in *Achillea lycanica*. *Analytical Letters*, 51(1-2), 33-48. <https://doi.org/10.1080/00032719.2017.1318140>.
- Teglia, C. M., Gonzalo, L., Culzoni, M. J., & Goicoechea, H. C. (2019). Determination of six veterinary pharmaceuticals in egg by liquid chromatography: Chemometric optimization of a novel air assisted-dispersive liquid-liquid microextraction by solid floating organic drop. *Food Chemistry*, 273, 194-202. <https://doi.org/https://doi.org/10.1016/j.foodchem.2017.08.034>.
- Touati, R., Santos, S. A. O., Rocha, S. M., Belhamel, K., & Silvestre, A. J. D. (2015). The potential of cork from *Quercus suber* L. grown in Algeria as a source of bioactive lipophilic and phenolic compounds. *Industrial Crops Products*, 76, 936-945. <https://doi.org/https://doi.org/10.1016/j.indcrop.2015.07.074>.
- Varea, S., Garcia-Vallejo, M. C., Cadahia, E., & de Simon, B. F. (2001). Polyphenols susceptible to migrate from cork stoppers to wine. *European Food Research and Technology*, 213(1), 56-61. <https://doi.org/https://doi.org/10.1007/s002170100327>.
- Vilkhu, K., Mawson, R., Simons, L., & Bates, D. (2008). Applications and opportunities for ultrasound assisted extraction in the food industry — A review. *Innovation Food Science Emerg Technololy*, 9(2), 161-169. <https://doi.org/https://doi.org/10.1016/j.ifset.2007.04.014>.
- Zhang, Q. W., Lin, L. G., & Ye, W. C. (2018). Techniques for extraction and isolation of natural products: a comprehensive review. *Chinese Medicine*, 13, 20. <https://doi.org/https://10.1186/s13020-018-0177-x>.

Supporting Information

Table S1: Phenolic compounds identified by LC-MS/MS in cork sample (control) subjected to ultrasound-assisted extraction.

Compound	Retention time (min)	[MH] ⁻	[MS] ²
Gallic acid	15	169	125
Vescalagin	20	933	631; 915
Castalagin	27	933	631; 915
Protocatechuic acid	29	153	109
Dehydrated tergallic-C-glucoside	38	613	493;593; 523
Protocatechuic aldehyde	49	137	109
Caffeic acid	52	179	-
Vanillin	63	151	136
Ellagic acid	80	301	257; 229

Chapter 3- Sustainable valorization of cork waste through an efficient microwave-assisted extraction of phenolic compounds

Abstract

The valorization of cork by-products was herein studied through the extraction of bioactive compounds by using microwave-assisted extraction (MAE) and further compared with ultrasound-assisted extraction (UAE) and conventional maceration. The MAE conditions (time, % ethanol, and temperature) to maximize the extraction yield (EY) and the total phenolic content (TPC) of cork extracts through RSM analysis. The factorial design was applied considering the time (5- 25 minutes), % ethanol in solvent (10-90%), and temperature (50-150 °C). Extraction yield (EY) and total phenolic content (TPC) were the response variables considered in the factorial regression. EY was gravimetrically determined and TPC was calculated as the sum of individual phenolic compounds characterized by LC-DAD-MS/MS. The optimal conditions obtained by using MAE were 25 min, 150 °C, and 90% ethanol, and it was possible to obtain an EY of 127 ± 7 mg/g DW and a TPC of 1.85 ± 0.3 mg/g DW. These results were compared to the already optimized conditions for traditional extraction methodology and with UAE technique. Briefly, the MAE optimal conditions (25 minutes) allowed to obtain around 40% increased TPC and a two-fold EY than those obtained in a traditional maceration (7 days). Likewise, MAE almost doubled the amount of TPC and EY achieved from UAE in half of the time. At the end, MAE results in a suitable, short-time, low cost and higher yield alternative to improve the extraction of bioactive compounds from cork by-products in a sustainable circular economy approach.

Keywords: Microwave-assisted extraction (MAE), Ultrasound assisted extraction (UAE); Phenolic compounds, Cork by-products, simultaneous optimization, and Green technology;

Introduction

Cork is a renewable and sustainable resource, currently gaining more interest as a raw material (Bom et al. 2019). The unique physical-chemical properties of cork made it an attractive material for multiple applications. Besides the wide use of cork wastes as fiber-

enhancer bio composite material for plastic substitution (Dairi et al. 2022), it has also been described as a promising sustainable raw material for cosmetic or food industry applications (Mota et al. 2022). Indeed, cork is a source of bioactive compounds widely known by their antioxidant properties such as phenolic acids, terpenoids, and tannins (Carriço, Ribeiro, and Marto 2018), which have been attracted specific attention for upcycling initiatives.

The cork-related industry presents high ecological, economic and social value but cork oak forests and cork waste need to be correctly managed to continue being sustainable (Pereira 2011). Among cork production, approximately 70% is used to produce wine stoppers in oenological industry. The main by-products are cork granulates obtained during the cutting of raw cork, together with the material rejected at the end of the production-chain during the selection stage, which represent approximately 20–30% of the industry's raw cork. Despite the rejected granulate is to some extent reintroduced in the manufacturing process, cork waste remains a by-product of the cork industry with a low commercial value but high potential to be used.

Under this context, the extraction of bioactive compounds from cork industry arises as a powerful tool to obtain high-added value molecules in a circular economy approach. Some conventional methods such as Soxhlet extraction, percolation, hydrodistillation or traditional maceration have been widely used for years. Maceration is a very simple extraction method but with the disadvantage of long extraction time and low-efficiency (Zhang, Lin, and Ye 2018). Thus, searching for new solutions to make extraction processes more efficient, reducing time and solvents and by this, the impact on the environment are the main challenges of nowadays (Priyadarshini, Tiwari, and Rajauria 2022). Indeed, the use of novel extraction technologies such as microwave-assisted extraction (MAE) or ultrasound-assisted extraction (UAE) have arisen as promising sustainable alternatives.

Microwaves used in MAE was described as facilitating the extraction process and improving extraction yield (Paré, Bélanger, and Stafford 1994). Heat is generated by interacting with polar compounds in the plant matrix via ionic conduction and dipole rotation mechanisms (Letellier and Budzinski 1999). Heat and mass transfers will occur in the same direction, resulting in a synergistic effect that accelerates extraction and yields (Zhang, Lin, and Ye 2018). For all these reasons, a green technology approach has been considered (Chemat, Vian, and Cravotto 2012). The matrix, solvent, temperature, pressure, and time are the main factors that affect the extraction process (Hernández, Lobo, and González 2009). Under this context, the main benefits of green

extraction methodologies in general and MAE in particular are the decrease in extraction and processing time, the amount of energy and solvents used, the unit operations, and the reduction in CO₂ emissions (Chemat et al. 2017).

Likewise, joined with MAE, UAE stands out as a sustainable alternative, which requires moderate energy and less solvent. In UAE, acoustic cavitation damage cell walls favoring the release of bioactive compounds from plant sources.

Both, the MAE and UAE technologies were applied, with better results compared with traditional maceration, at the extraction of phenolic compounds from prickly pear (Badawy et al. 2022), elderberry (Terzić et al. 2023), olive pomace (Belghith et al. 2023), peach by-products (Tsiaka et al. 2023), tea (Xia, Shi, and Wan 2006), Chardonnay grape marc (Garrido et al. 2019) or bark extracts (Bouras et al. 2015). However, despite the large use in a wide amount of different plant sources, to our knowledge, this technology has never been applied to cork or its sub-products.

The main objective of this work was to valorize cork wastes through an optimized and sustainable extraction of bioactive phenolic compounds. For this purpose, response surface methodology (RSM) with a central composite design was applied to optimize the extraction conditions (time, temperature, and % ethanol in solvent) affecting the MAE of cork wastes. The optimization criteria were to simultaneously maximize extraction yield and the recovery of total phenolic compounds identified by LC-MS. Results obtained under optimal MAE conditions were compared to those observed using the previously optimized conventional extraction and UAE techniques.

Materials and Methods

Reagents

Gallic acid ($\geq 98\%$), Acetic acid ($\geq 99\%$), Acetonitrile ($\geq 99.5\%$) and Caffeic acid were obtained from Sigma-Aldrich, Madrid, Spain. Ellagic acid ($\geq 96\%$, HPCE) was obtained from Fluka Biochemical College Park, MD, USA. Ethanol (99.5%) was purchased from AGA®, Prior Velho, Portugal.

Cork material

Granulated cork (1-2 mm particle size) was obtained by grinding and sieving cork (Q. suber L) stoppers supplied by Amorim & Irmãos company (Mozelos, Portugal), yielding 1 kg of granulated cork.

Microwave-assisted extraction (MAE)

MAE was carried out using a Microwave Reaction System Anton Paar® - Multiwave 3000 (Microwave Sample Preparation Platform System, Oosterhout, Netherlands), 500 W, and 70% amplitude. The solid-to-solvent ratio was maintained constant at 42.85 g/L based on preliminary tests (data not shown). In this case, 1.5 g of Cork was placed in a microwave vessel with 35 mL of solvent and a magnetic stirrer was also incorporated to ensure a correct homogenization. Experimental runs were carried out according to the experimental design matrix (**Table 1**) where different levels of time (5- 25 min), solvent concentration (10-90% ethanol), and temperature (50- 150 °C) were combined. Once the extraction was finished the extracts were transferred to falcon tubes and then filtered with a 0.45 µm filter and stored at -80 °C to further analysis.

Table 1. Experimental conditions

Factors			
Run	A: Time (min)	B: Temperature (°C)	C: Solvent concentration (% ethanol)
1	9.05 (-1)	70.27 (-1)	26.22 (-1)
2	20.95 (+1)	70.27 (-1)	26.22 (-1)
3	9.05 (-1)	129.73 (+1)	26.22 (-1)
4	20.95 (+1)	129.73 (+1)	26.22 (-1)
5	9.05 (-1)	70.27 (-1)	73.78 (+1)
6	20.95 (+1)	70.27 (-1)	73.78 (+1)
7	9.05 (-1)	129.73 (+1)	73.78 (+1)
8	20.95 (+1)	129.73 (+1)	73.78 (+1)
9	5.00 (-1.68)	100.00 (0)	50.00 (0)
10	25.00 (+1.68)	100.00 (0)	50.00 (0)
11	15.00 (0)	50.00 (-1.68)	50.00 (0)
12	15.00 (0)	150.00 (+1.68)	50.00 (0)
13	15.00 (0)	100.00 (0)	10.00 (-1.68)
14	15.00 (0)	100.00 (0)	90.00 (+1.68)
15	15.00 (0)	100.00 (0)	50.00 (0)
16	15.00 (0)	100.00 (0)	50.00 (0)
17	15.00 (0)	100.00 (0)	50.00 (0)
18	15.00 (0)	100.00 (0)	50.00 (0)
19	15.00 (0)	100.00 (0)	50.00 (0)
20	15.00 (0)	100.00 (0)	50.00 (0)
21	5.00 (-1.68)	50.00 (-1.68)	10.00 (-1.68)
22	5.00 (-1.68)	50.00 (-1.68)	90.00 (+1.68)
23	5.00 (-1.68)	150.00 (+1.68)	10.00 (-1.68)
24	5.00 (-1.68)	150.00 (+1.68)	90.00 (+1.68)
25	25.00 (+1.68)	50.00 (-1.68)	10.00 (-1.68)
26	25.00 (+1.68)	50.00 (-1.68)	90.00 (+1.68)
27	25.00 (+1.68)	150.00 (+1.68)	10.00 (-1.68)
28	25.00 (+1.68)	150.00 (+1.68)	90.00 (+1.68)

Response variables evaluated during the MAE optimization

Extraction yield (EY)

To obtain the EY, 10 mL of each sample, resulting from extraction, were dried using an empty, and weighted crucible using an oven at 104 °C for 24 h. After, crucibles were weighted and the extraction yield was determined according to (Silva et al. 2021) using Equation 1 and results were expressed as mg extract/ g dry weight.

$$EY \left(\frac{mg E}{g dm} \right) = \frac{P_{t=24 h} - P_{t=0}}{\left(\frac{m_{sw} \times V_a}{V_{sv}} \right) \times \left(\frac{100 - MC_{sw}}{100} \right)}$$

Equation 1

Where, Pt=0: mass of empty crucible; Pt=24 h: mass of crucible with dry extract; msw: mass of granulated cork; Va: volume of extract (10mL); Vsv: solvents volume (35 mL); MCsw: moisture content (%) of granulated cork

Identification and quantification of total phenolic compounds (TPC) by High Performance Liquid Chromatography (HPLC) coupled to Diode Array Detector (DAD) and Tandem Mass Spectrometry (MS/MS) Analysis

All samples were analyzed by LC-DAD-MS/MS as described in a previous work (Azevedo et al. 2014) and the results are expressed as gallic acid equivalents, according to the calibration curve:

$$\text{Area} = 1932.4 \text{ Concentration (g/L)} + 0.180, R^2 = 0.9999$$

The TPC was calculated as the sum of all phenolic compounds individually identified.

Experimental design

Response surface methodology (RSM) with a central composite design (CCD) was applied to study the effects of extraction factors (time, temperature and % ethanol in solvent) on extraction yield, and total phenolic content of granulated cork samples.

The critical factors were rated on a five-point scale (-α; -1; 0, 1, + α). The -value (1.68) was chosen to ensure rotatable prediction variance distribution (Teglia et al., 2019). This resulted in a total of 28 experiments, including six central point replicates. **Table 1** depicts the experimental design matrix for the three factors.

Two response variables were evaluated, extraction yield (EY), total phenolic content (TPC), Data were fitted to appropriate mathematical models (**Equation 2**) for each response variable according to the least-squares regression method.

$$Y_n = \beta_0 + \sum_{i=1}^3 \beta_i X_i + \sum_{i=1}^2 \sum_{j=2, j>i}^3 \beta_{ij} X_i X_j + \sum_{i=1}^3 \beta_{ij} X_i X_j + \sum_{i=1}^3 \beta_{ii} X_i^2$$

Equation 2

Where, Y_n : the predicted response (Y_1 = extraction yield; Y_2 = TPC); β_i : linear coefficient; β_{ii} : quadratic coefficient; β_{ij} : coefficient for the interaction effect; X_i : dimensionless coded value of the independent variable, x_i (x_1 = time; x_2 = pressure and x_3 = ethanol concentration).

Simultaneous optimization and validation

The EY and TPC optimization were performed to find the optimum extraction conditions that maximize these two parameters individually. On the other hand, the desirability function was used to perform simultaneous optimization, which maximizes all responses at the same time (Cassani et al. 2017). A new set of experiments was performed under optimal extraction conditions to assess the reliability of the simultaneous optimization. Cork samples were extracted at optimal factor levels, and all response variables were measured in order to compare predicted and experimental results.

The results were compared to those obtained from traditional maceration (7 days at 37°C) and UAE.

Ultrasound-assisted extraction (UAE)

UAE was carried out using an ultrasonic system (Optic IVYMEN® system ultrasonic Model CY-500, Barcelona, Spain) equipped with a titanium probe. All extractions were performed at 20 kHz, 500 W, and 70% amplitude. The use of the ethanol–water mixture in UAE is recommended in case of polyphenols (Osorio-Tobón 2020).

In this case, 1.5 g of granulated cork was placed in a graduated test tube with 35 mL of solvent. The temperature probe was also placed in the reaction tube. This system was then immersed in a cold water bath to avoid increasing temperature and keep this parameter constant at 20 °C. Experimental runs were already optimized being the best conditions for extractions 20 minutes and 75% ethanol (Azevedo et al., 2023).

Conventional Extraction by Maceration

Granulated cork (1.5 g) was placed in 50 mL capacity glass bottles with 35 mL hydroalcoholic solution (50% ethanol) for 7 days at 35 °C following the procedure described in (Azevedo, Fernandes et al. 2017). After the extraction was completed, the extracts were filtered through a 0.45 m filter and stored at -80 °C for further analysis.

Statistical analysis

For RSM optimization and figures were made using Stat-Ease Design-Expert 11.0 software (Stat-Ease, Inc., Minneapolis, USA). ANOVA test was used to statistical analysis of regression models considering p-value <0.05 and insignificant lack of fit ($p>0.05$). The significant factors ($p<0.05$) were only considered in models for having significant effect on the responses. The adjusted coefficient of determination (R^2_{adj}) was calculated for all models indicating the percentage of variance explained by them. As described to (Teglia, Gonzalo et al. 2019) the coefficients of the developed mathematical models were calculated by backward multiple regression and validated through ANOVA tests ($p<0.05$).

Principal Components Analysis and clustering analysis (dendrogram) were performed by using the software Statgraphics centurium 19.0

Results and Discussion

Identification and quantification of phenolic compounds extracted from cork waste by using MAE

The phenolic compounds chromatographic profile of the samples after MAE is presented in **Figure 1**, where the sum of isolated compounds already identified corresponds to TPC value. The identification was made by LC-DAD-MS/MS by comparing the retention time with standards and the fragmentation pattern according to the data described elsewhere (Azevedo et al. 2017). Moreover, **Table 2** shows all the compounds identified and quantified in the 28 runs involved in the central composite design for the microwave-assisted extraction of cork. As shown by **Figure 1** and **Table 2**, the main compounds identified were phenolic acids. Namely gallic, caffeic, protocatechuic and ellagic acids, protocatechuic aldehyde and vanillin, as well as the isomers castalagin/vescalagin and dehydrated tergallic-C-glucoside. These compounds have been previously found in cork (Conde et al. 1997; Cantos et al. 2003; Varea et al. 2001; Fernandes et al. 2011).

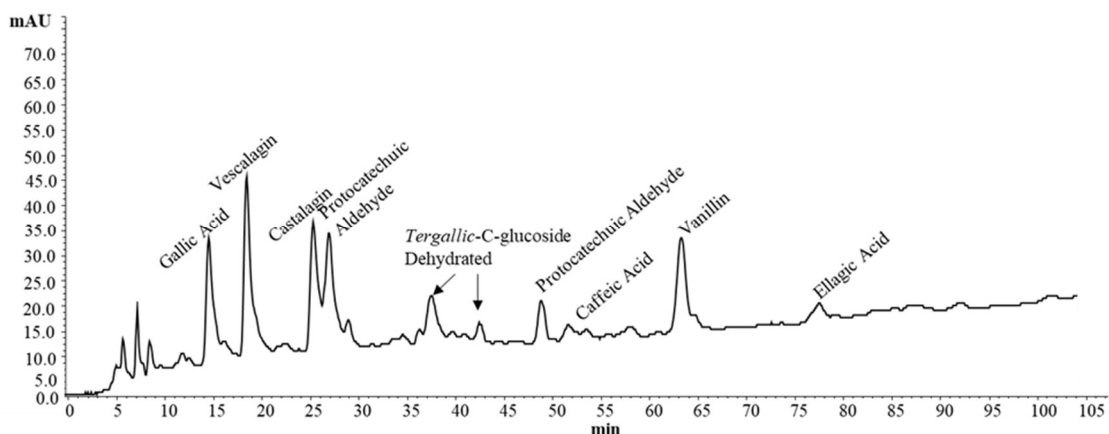


Figure 1: HPLC-DAD chromatogram at 280 nm obtained from MAE process. MAE Extraction -Run 4- Table 3, 21min; 130 °C; 26% ethanol).

Despite the already described phenolic compounds found in cork, it should be noticed the presence of the vescalagin-ethanol derivative ($m/z - 977$), which could be explained by the reactivity of vescalagin present in cork with the ethanol in the MAE extraction process (**Table 2**). It has already been described in the literature that the vescalagin-ethanol derivative is formed by the exposition of vescalagin to ethanol, giving rise to hemiketal derivatives containing an ethoxy group (Puech et al. 1999; Azevedo et al. 2017). In fact, higher amounts of vescalagin-ethanol derivative were found after testing ethanol $\geq 50\%$ and temperature above 100°C . Indeed, the vescalagin-ethanol derivative were mainly found in run 12 (50% EtOH, 15min at 150°C) followed by run 8 (74% EtOH 21min at 129°C), run 7 (74% EtOH 9min at 129°C) and run 24 (90% EtOH 5min at 150°C). Indeed, based on the results presented herein, not only the % ethanol in solvent but also the time of exposition and temperature clearly affect the formation of vescalagin-ethanol derivative.

Table 2: Phenolic compounds (mg/g dw) identified and quantified in the 28 runs involved in the central composite design for the microwave-assisted extraction of cork waste samples.

Run	Gallic acid	Vescalagin	Castalagin	Protocatechuic acid	Dehydrated tergallic-C-glucoside	Non-identified	Protocatechuic aldehyde	Caffeic acid	Vescalagin Ethanol Derivative	Vanillin	Ellagic Acid Pentose	Ellagic acid	Total phenolic content
1	0.0682	0.0702	0.1107	0.0275	0.0295	ND	0.0294	0.0081	0.0041	0.0782	0.0137	ND	0.4397
2	0.0732	0.0738	0.1096	0.0273	0.0264	ND	0.0301	0.0096	0.0038	0.0827	0.0163	ND	0.4529
3	0.1685	0.1842	0.1961	0.0357	0.0720	0.0118	0.0439	0.0164	0.0176	0.1925	0.0271	0.0056	0.9714
4	0.2774	0.3964	0.3079	0.0423	0.0951	0.0255	0.0523	0.0061	0.0227	0.2821	0.0278	0.0184	1.5540
5	0.0522	0.0119	0.0975	0.0085	0.0378	ND	0.0348	0.0169	ND	0.1032	0.0288	ND	0.3915
6	0.0707	0.0321	0.1064	0.0806	0.0473	ND	0.0395	0.0195	ND	0.1186	0.0299	ND	0.5445
7	0.1141	0.2576	0.1517	0.0163	0.1626	0.0241	0.0357	0.0026	0.1732	0.0972	0.0278	0.3798	1.4426
8	0.1673	0.0932	0.2148	0.1322	0.2251	0.0930	0.0384	0.0167	0.2151	0.2104	0.0240	0.3406	1.7710
9	0.1055	0.1252	0.1936	0.1172	0.0520	ND	0.0388	0.0167	ND	0.1236	0.0290	0.0620	0.8637
10	0.1207	0.1077	0.2523	0.1330	0.0618	0.0511	0.0119	0.0402	0.0115	0.1150	0.0638	0.1015	1.0706
11	0.0633	0.0605	0.0857	0.0814	0.0420	ND	ND	0.0305	0.0058	ND	0.0871	0.0174	0.4738
12	0.2414	0.1007	0.1829	0.2930	0.0927	0.0812	0.0546	0.0694	0.2507	0.2204	0.0293	0.4308	2.0470
13	0.1104	0.0091	0.1564	0.1276	0.0288	0.0379	0.0036	0.0359	0.0109	0.0058	0.0921	0.0201	0.6387
14	0.0605	0.0131	0.1315	0.0823	0.0483	0.0270	0.0286	0.0225	0.0077	0.1172	0.0286	0.3785	0.9459
15	0.1089	0.0110	0.2046	0.1206	0.0647	0.0198	0.0327	0.0229	0.0106	0.1348	0.0324	0.0911	0.8540
16	0.0900	0.1102	0.1206	0.0819	0.0531	0.0179	0.0127	0.0294	0.0110	0.1040	0.0244	0.0709	0.7261
17	0.1051	0.0106	0.2003	0.1133	0.0818	0.0060	0.0414	0.0155	0.0071	0.1329	0.0347	0.0358	0.7846
18	0.0887	0.0107	0.1785	0.1278	0.0619	0.0160	0.0361	0.0138	0.0059	0.1077	0.0280	0.0307	0.7057
19	0.1008	0.0121	0.1978	0.1440	0.0742	0.0254	0.0136	0.0334	0.0099	0.1205	0.0130	0.0264	0.7709
20	0.0975	0.0098	0.1828	0.1435	0.0784	0.0113	0.0436	0.0161	0.0021	0.1203	0.0348	0.1231	0.8633
21	0.0654	0.0038	0.0926	0.0788	0.0469	ND	0.0229	0.0005	ND	0.0582	0.0074	ND	0.3764
22	0.0530	0.0030	0.0934	0.1046	0.0656	ND	0.0363	0.0152	ND	0.1034	0.0222	ND	0.4969

23	0.2527	0.1873	0.2247	0.0354	0.0685	0.0193	0.0549	ND	0.0094	0.2074	0.0248	ND	1.0822
24	0.1401	0.2166	0.1828	0.0285	0.1708	0.0325	0.0515	0.0071	0.1871	0.1672	0.0298	0.5366	1.7507
25	0.0541	0.0122	0.0766	0.0676	0.0193	0.0202	0.0145	ND	0.0047	0.0505	0.0059	ND	0.3257
26	0.0458	0.0392	0.0851	0.0971	0.0248	0.0375	0.0314	0.0157	ND	0.0899	0.0273	ND	0.4939
27	0.3411	0.3385	0.0847	0.3544	0.1200	0.0130	0.0265	0.0446	0.0286	0.2755	0.0132	0.0158	1.6558
28	0.2296	0.0382	0.0356	0.1928	0.4207	0.1574	0.0610	0.0596	0.0246	0.2512	0.3929	0.0190	1.8824

TPC: Total phenolic content was calculated as the sum of all phenolic compounds identified and quantified in cork waste extracts by LC-MS/MS.

When looking at gallic acid extracted individually in each run, it is possible to see that higher amounts were obtained in concentrations of ethanol below 50%, which is in line with what is described in the literature, that the use of the ethanol-water mixture was the adequate for the phenolic family and solvents of higher polarity enhance the extraction of phenolic compounds (Osorio-Tobón 2020). Different behaviors were observed in all 28 runs, where runs 1, 2, 5, 21, and 25 were the ones that yielded lower amounts of TPC (TPC < 0.5 mg/g dw), and all these runs used temperatures 70 °C and 50°C. On the other hand, runs 4, 7, 8, 12, and 24 were the ones that obtained higher concentrations of TPC (TPC > 1.4 mg/g dw). In all of these the temperature used was higher than 129 °C, which is in agreement with the literature that described that higher temperatures enhance the release of greater amounts of phenolic compounds in MAE extractions (Osorio-Tobón 2020).

In view of abovementioned, different factors can influence the extraction process in different ways, so the study of the influence of critical extraction factors on response variables was performed for a deeper understanding.

Influence of critical extraction factors on response variables

Table 3 shows the results obtained for EY and TPC in the performed runs with different set factors (time, temperature, and, % ethanol in solvent) to deeper understand the influence and the response variables.

The highest EY were obtained with 150 °C and 90 % ethanol (runs 24 and 28). Since temperature and % ethanol played a pivotal role in the EY, time did not significantly affect the results. Indeed, the general behavior after fixing temperature and % ethanol and considering the time as a dependent variable (first 8 runs) was to slightly increase with time (9 minutes pass to 21 minutes). Likewise, the EY increased depending on temperature, achieving a higher yield as higher was the set temperature, which is in agreement with previous observations, when the extraction temperature was raised from 110 to 150 °C (Alara, Abdurahman et al. 2018). The same occurs with the % ethanol in the solvent, which induce a concomitantly increase of EY, as already reported (Moreira, Barroso et al. 2017).

Table 3: Results obtained for extraction yield (mg extract/ g dw) and total phenolic content (TPC, mg/ g dw) under different experimental conditions defined in the central composite design in actual and (coded) values.

Factors				Response variables	
Run	A: Time (min)	B: Temperature (°C)	C: Solvent concentration (% ethanol)	Yield (mg extract/ g dw)	TPC (mg TP/g dw)
1	9.05 (-1)	70.27 (-1)	26.22 (-1)	21.4529	0.4397
2	20.95 (+1)	70.27 (-1)	26.22 (-1)	19.2213	0.4529
3	9.05 (-1)	129.73 (+1)	26.22 (-1)	39.4756	0.9714
4	20.95 (+1)	129.73 (+1)	26.22 (-1)	52.0008	1.5540
5	9.05 (-1)	70.27 (-1)	73.78 (+1)	32.5962	0.3915
6	20.95 (+1)	70.27 (-1)	73.78 (+1)	35.9858	0.5445
7	9.05 (-1)	129.73 (+1)	73.78 (+1)	66.1527	1.4426
8	20.95 (+1)	129.73 (+1)	73.78 (+1)	82.1751	1.7710
9	5.00 (-1.68)	100.00 (0)	50.00 (0)	35.7528	0.8637
10	25.00 (+1.68)	100.00 (0)	50.00 (0)	43.8111	1.0706
11	15.00 (0)	50.00 (-1.68)	50.00 (0)	21.9208	0.4738
12	15.00 (0)	150.00 (+1.68)	50.00 (0)	69.7745	2.0470
13	15.00 (0)	100.00 (0)	10.00 (-1.68)	21.3357	0.6387
14	15.00 (0)	100.00 (0)	90.00 (+1.68)	54.5874	0.9459
15	15.00 (0)	100.00 (0)	50.00 (0)	40.4633	0.8540
16	15.00 (0)	100.00 (0)	50.00 (0)	33.7294	0.7261
17	15.00 (0)	100.00 (0)	50.00 (0)	42.2845	0.7846
18	15.00 (0)	100.00 (0)	50.00 (0)	30.8939	0.7057
19	15.00 (0)	100.00 (0)	50.00 (0)	37.1487	0.7709
20	15.00 (0)	100.00 (0)	50.00 (0)	34.3662	0.8633
21	5.00 (-1.68)	50.00 (-1.68)	10.00 (-1.68)	11.3773	0.3764
22	5.00 (-1.68)	50.00 (-1.68)	90.00 (+1.68)	25.3440	0.4969
23	5.00 (-1.68)	150.00 (+1.68)	10.00 (-1.68)	40.5139	1.0822
24	5.00 (-1.68)	150.00 (+1.68)	90.00 (+1.68)	103.5783	1.7507
25	25.00 (+1.68)	50.00 (-1.68)	10.00 (-1.68)	14.1657	0.3257
26	25.00 (+1.68)	50.00 (-1.68)	90.00 (+1.68)	40.5522	0.4939
27	25.00 (+1.68)	150.00 (+1.68)	10.00 (-1.68)	71.2851	1.6558
28	25.00 (+1.68)	150.00 (+1.68)	90.00 (+1.68)	98.5677	1.8824

TPC: Total phenolic content was calculated as the sum of all phenolic compounds identified and quantified in cork waste extracts by LC-MS/MS.

To determine the optimum levels of variables for the MAE, three-dimensional surface plots were constructed according to the polynomial models (**Figure 2**). These figures show the effect of extraction time, temperature and % ethanol in solvent on the EY.

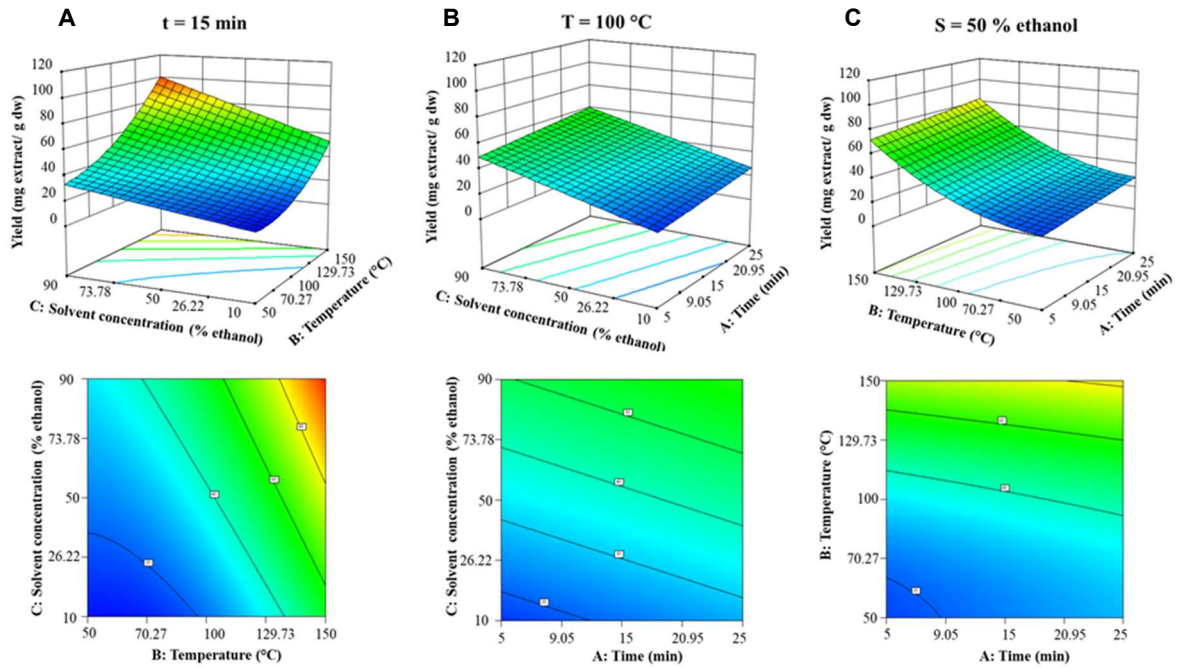


Figure 2: Graphic representations of EY with time, temperature, and % of ethanol in a hydroalcoholic solvent on the extract from cork by MAE. **A)** represent solvent concentration and temperature; **B)** represent solvent concentration and time; **C)** represent temperature and time.

In the surface and contour plot presentations, it is possible to observe that EY mainly increases with % ethanol and extraction temperature (**Figure 2A**). Regarding the impact of time combined with % ethanol (**Figure 2B**), it was possible to observe that EY increased in a lower extent. On the other hand, when representing temperature and time (**Figure 2C**) it is possible to observe that EY increased with both variables. The literature already described temperature as a crucial parameter in MAE, with temperatures between 30 and 180 °C having been used to extract phenolic compounds and EY and TPC increase when the extraction temperature is raised (Osorio-Tobón 2020; Alara and Abdurahman 2019). In fact, TPC values were higher for the highest temperatures (**Table 3**). The same was observed with % ethanol in the solvent, on the other hand, time was the variable that seemed to influence less. But when the data is presented in a surface and contour plot presentation (**Figure 3**) the influence of factors in TPC is clearer.

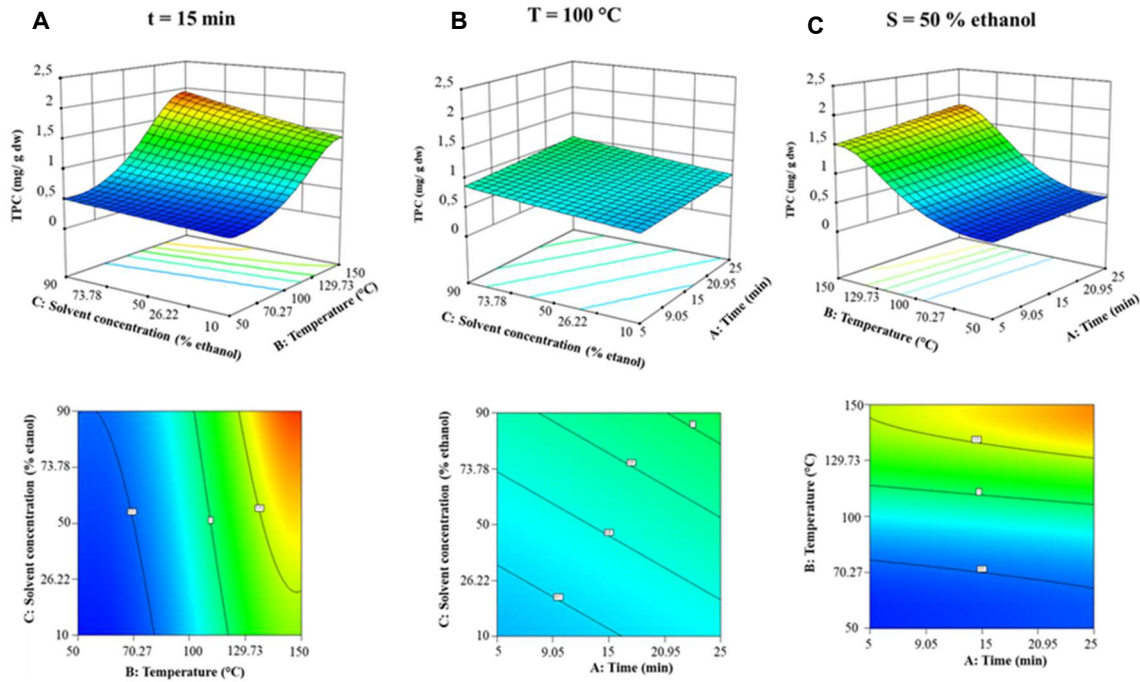


Figure 3: Graphic representations of TPC with time, temperature and % of ethanol in a hydroalcoholic solvent on extract from cork by MAE. **A)** represent solvent concentration and temperature; **B)** represent solvent concentration and time; **C)** represent temperature and time.

For TPC, the influence % ethanol in solvent and temperature (**Figure 3A**) demonstrated that higher quantities of TPC were obtained for higher values of temperature (129-150 °C) and for higher % ethanol in solvent, more than 50%. The same behaviour was observed in surface and contour plot presentation of time with temperature (**Figure 3C**). As for the representation of time with % ethanol in solvent it is clear a lower impact of these factors in final TPC values.

Bearing this, a central composite experimental design matrix allowed to study the interactions between the parameters studied and establish which of these interactions had a major influence. **Table 4** shows the statistical parameters of the adjusted model. Analyzing the table, it is possible to observe a linear effect for three factors studied. On the other hand, only the factor temperature T showed a quadratic effect in EY and TPC.

Table 4: Regression coefficients obtained for each response variable and statistical parameters associated with each fitted model.

Effect	EY	TPC
<i>Intercept</i>	38.1 ± 1.55	-0.0942
<i>Linear effect</i>		
A- Time	5.41 ± 1.56	0.0398 ± 0.0167
B-Temperature	27.12 ± 1.56	0.4762 ± 0.0561
C-Solvent concentration	16.71 ± 1.56	0.0694 ± 0.0167
<i>Quadratic effect</i>		
A ²	NS	NS
B ²	11.97 ± 2.47	0.0152 ± 0.0265
C ²	NS	NS
<i>Cubic effect</i>		
A ³	NS	NS
B ³	NS	-0.1834 ± 0.0625
C ³	NS	NS
<i>Interactive effect</i>		
AB	NS	NS
AC	NS	NS
BC	6.69 ± 1.86	NS
<i>Statistical parameters</i>		
Model significance (p-value)	< 0.0001	< 0.0001
Lack of fit (p-value)	0.2527	0.0927
R ²	0.9549	0.9472
R ² _{adj}	0.9447	0.9352
NS: non-significant (p>0.05)		

When the interactive effect was determined, only temperature and % ethanol interacted obtaining a synergistic effect. As already mentioned, the temperature was the main factor affecting the extraction of phenolic compounds from cork wastes. **Figure 4** shows a principal components analysis in order to understand the weight of each component in the extraction process.

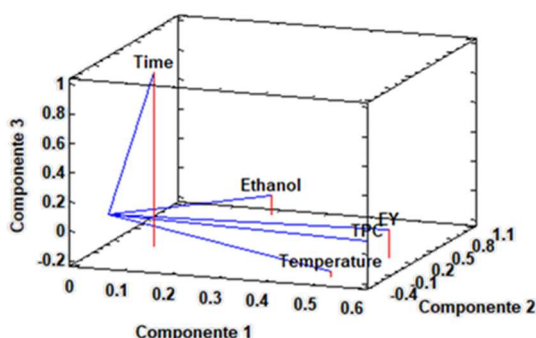


Figure 4: Principal component analysis to understand the impact of multivariate factors on the MAE

As displayed, the time affect in a lower extent to the total amount of bioactive compounds extraction as well as the extraction yield. Firstly, temperature and secondly, time are the main factors affecting the whole process. Indeed, and as displayed in **Figure 5**, the top

five higher phenolic compounds extraction was yielded in runs, 12, 28, 8, 24 and 27, where the temperature was set at 150°C and the %Ethanol varies between 10 and 90%. However, it should be noticed that despite the effect of time was not significant, the run 27 was performed by using 10% ethanol for an extended period of time, which favoured the extraction at the highest temperature. A compromise between the spend of energy (time and temperature) and the use of natural resources (solvent and % of ethanol) must be considered prior to choose the conditions.

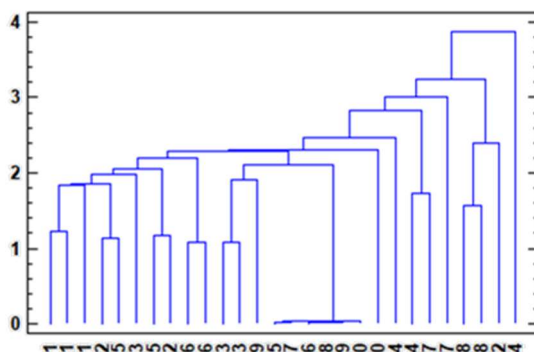


Figure 5: Dendrogram grouping the MAE runs

Simultaneous optimization and validation of the MAE procedure

For the previously results the simultaneous optimization is necessary to maximize both responses at the same time (Cassani et al., 2017). For the optimization, it was used a desirability function of MAE and for each factor the best conditions were obtained. **Figure 6** shows the desirability function and it is possible to find the best conditions in order to maximize the extraction: 25 minutes, 150°C, and 90% ethanol in the solvent. Similar conditions were already described in the literature for apple tree (*Malus domestica*) bark: 60 % ethanol, 20 min, 100 °C (Moreira, Barroso et al. 2017) and for *T. fontanesii* plant extracts was 50% ethanol, 150 °C, and 9.5 min (Nabet, Gilbert-López et al. 2019).

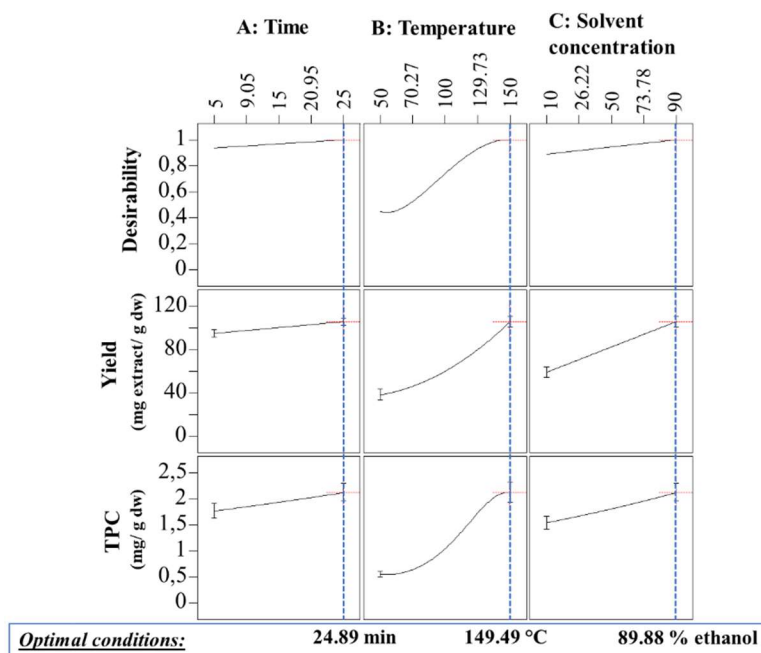


Figure 6: desirability function and it is possible to find the best conditions in order to maximize the extraction: 25 minutes, 150°C, and 90% ethanol in the solvent

In the same way, **Table 5** shows the simultaneous optimization, that is, maximizing the three variables simultaneously, a compromise situation is obtained.

Table 5: Simultaneous optimization using Desirability function of MAE factors for each response and their predicted and experimental values obtained under optimal conditions.

Optimization	Optimal conditions			Predicted responses		Experimental values	
	Time (min)	Temperature (°C)	Solvent concentration (% ethanol)	Yield (mg extract/ g dw)	TPC (mg/ g dw)	Yield (mg extract/ g dw)	TPC (mg/ g dw)
Simultaneous	24.89	149.94	89.88	105.70 [91.83; 119.56]	2.10 [1.51; 2.93]	126.89 ± 6.45	1.85 ± 0.26

For the optimum MAE conditions, it was predicted to obtain 105.70 mg extract/g dw and 2.10 mg/g dw. In this sense, the simultaneous optimization allowed finding good values for both variables, EY and TPC, reaching a compromise solution. With the intention to validate and test the reliability of the optimization, a new set of experiments was made using the best conditions found. For EY it was obtained 126.89 mg extract/g dw, a value that was a little higher than expected but very close to the predicted value. For TPC the values obtained were within the expected range. Globally, it is possible to state, based on the results obtained, the robustness of the models since the values obtained by simultaneous optimization agree with the experimental data. The values obtained were in the same order than another work that described the MAE technique as the one that produces the highest total phenolic content (227.63 mg GAE/g dry basis) when

compared with other techniques such as ultrasound-assisted extraction (Osorio-Tobón 2020). In the same way, when comparing the data obtained with UAE extraction it is possible to see that MAE technique give origin to more 50% of the amount obtained in UAE (Azevedo, Cassani et al. 2022), in half of the time. These results were also compared with those obtained by the conventional maceration method (50.31 mg/g extract for EY and 1.36 mg/g dw for TPC), and it was possible to observe that using MAE during 25 min it can be obtained more than the double of the quantities in case of EY, and more 40% in case of TPC, showing a drastically reduced time, solvents, and energy consumption.

Table 6 summarizes the results obtained after applying different extraction technologies to obtain phenolic compounds from cork waste. As displayed, the best performing conditions include the use of 50 %ethanol in all cases. The main differences were the working temperature ranging from room temperature used in UAE to 37°C set under conventional maceration and 150°C achieving the more efficient bioactive compounds extraction in MAE. MAE yielded the highest phenolic compounds extraction achieving a 10-fold increased extraction when compared with conventional maceration and a 4-fold higher extraction of target compounds when compared with UAE.

Table 6. Comparison between MAE and UAE or conventional maceration

Extraction Technology	Time	Temperature	%Ethanol	TPC
MAE	15 min	150°C	50	2.047
UAE	16.5 min	21°C	50	0.543
Maceration	7days	35°C	50	0.220

At the end, MAE resulted to be a proper extraction technology to obtain a higher phenolic compounds extraction. Previous results observed a similar cell disruption favoring the extraction of phenolic compounds by UAE and MAE (Huma, Jayasena et al. 2018). However, during MAE the diffusion of water into the cells of the matrix is facilitated leading to better heating and while improving the pass of targeted compounds from the cell walls to the solvent at higher mass transfer rates. Furthermore, when conventional maceration is tested, a simple diffusion of solvent is occurring into the cell components promoting the compounds solubilization. In the specific case of cork, and considering the nature and chemistry, the differences in extraction yield is more significant since the wax and resins difficult the process.

Conclusion

For the microwave-assisted extraction, critical conditions (time, temperature, and, % ethanol in solvent) were optimized using response surface methodology (RSM) to simultaneously maximize EY and TPC using a Desirability function as a way to extract the maximum of bioactive compounds from cork. The EY was obtained gravimetrically and TPC was obtained by the sum of HPLC peaks identified. The main compounds found were gallic acid, the isomers castalagin/vescalagin, protocatechuic acid and aldehyde, caffeic acid, ellagic acid and ellagic acid pentose. Beside these, the presence of the vescalagin–ethanol derivative was also detected resulting from the reactivity of vescalagin present in cork with ethanol in MAE extraction process.

The results showed that the increase of temperature, time and % ethanol increases the EY and TPC and an optimization was performed to find the optimum extraction conditions that maximize extraction of compounds for each factor studied. For that a desirability function was used to carried out a simultaneous optimization where all the responses are maximized at the same time. Thus, 25min, 150 °C and 90% ethanol concentration led to the maximized yield (126.89 ± 6.45 mg extract/g dw) and TPC (1.85 ± 0.26 mg/g dw). Finally, when comparing these results with those found by applying the conventional maceration method and with UAE technique, in 25 minutes it was possible to obtain around 40% plus (TPC) and double (EY) than in traditional maceration (7 days) and more 50% for TPC and EY when compare with UAE extraction. These results provide references of green technology applied to MAE technique, since it allows the reduction of time, solvents and energy.

Acknowledgements

The authors thank the Science and Technology Foundation (FCT) for financial the scholarships SFRH/BD/139709/2018, UIDB/50006/2020 and UIDBP/50006/2020. And also thanks the *IACOBUS program* (based on the priorities defined in the Galicia - Northern Portugal Joint Investment Plan (PIC 21-27) and on the strategic areas established by the Galicia - Northern Portugal Cross-border Intelligent Specialization Strategy (RIS3-T)) and has support from the European Union, through funding for the INTERREG V-A Spain-Portugal Program (POCTEP) 2014-2020. And also supported by MICINN supporting the Ramón y Cajal grant for M.A. Prieto (RYC-2017-22891), the María Zambrano grant for R. Perez-Gregorio (CO34991493-20220101ALE481), and the Xunta de Galicia supporting the post-doctoral grant for L. Cassani (ED481B-2021/152). The authors are also grateful to Ibero-American Program on Science and Technology (CYTED-AQUA-CIBUS, P317RT0003).

References

- Alara, O. R., & Abdurahman, N. H. (2019). Microwave-assisted extraction of phenolics from Hibiscus sabdariffa calyces: Kinetic modelling and process intensification. *Industrial Crops and Products*, 137, 528-535. <https://doi.org/https://doi.org/10.1016/j.indcrop.2019.05.053>.
- Alara, O. R., Abdurahman, N. H., Ukaegbu, C. I., & Azhari, N. H. (2018). Vernonia cinerea leaves as the source of phenolic compounds, antioxidants, and anti-diabetic activity using microwave-assisted extraction technique. *Industrial Crops and Products*, 122, 533-544. <https://doi.org/https://doi.org/10.1016/j.indcrop.2018.06.034>.
- Azevedo, J., Cassani, L., Oliveira, J., Chamorro, F., Simal-Gandara, J., Lopes, P., . . . Perez-Gregorio, R. (2022). Optimization of the ultrasound-assisted extraction for the maximized recovery of bioactive phenolic compounds from cork industry waste. *Food and Bioproducts Processing*, submitted.
- Azevedo, J., Fernandes, A., Oliveira, J., Brás, N. F., Reis, S., Lopes, P., . . . de Freitas, V. (2017). Reactivity of Cork Extracts with (+)-Catechin and Malvidin-3-O-glucoside in Wine Model Solutions: Identification of a New Family of Ellagitannin-Derived Compounds (Corklins). *Journal of Agriculture and Food Chemistry* 65(39), 8714-8726. <https://doi.org/https://doi.org/10.1021/acs.jafc.7b02845>.
- Azevedo, J., Fernandes, I., Lopes, P., Roseira, I., Cabral, M., Mateus, N., & Freitas, V. (2014). Migration of phenolic compounds from different cork stoppers to wine model solutions: antioxidant and biological relevance. *European Food Research and Technology*, 239(6), 951-960. <https://doi.org/https://doi.org/10.1007/s00217-014-2292-y>.
- Badawy, E., Vinatoru, M., Calinescu, I., Shams, K., Abel-Azim, N., Fahmi, A., . . . Saleh, I. (2022). The use of ultrasound (UAE) and microwaves (MAE) to improve the extraction of pharmaceutically active materials from the fruit of the prickly pear (*Opuntia ficus-indica*).
- Belghith, Y., Kallel, I., Rosa, M., Stathopoulos, P., Skaltsounis, L. A., Allouche, N., . . . Tomao, V. (2023). Intensification of Biophenols Extraction Yield from Olive Pomace Using Innovative Green Technologies. *Biomolecules*, 13(1), 65. <https://www.mdpi.com/2218-273X/13/1/65>.
- Bom, S., Jorge, J., Ribeiro, H., & Marto, J. (2019). A step forward on sustainability in the cosmetics industry: A review. *Journal of Cleaner Production*, 225, 270-290.
- Bouras, M., Chadni, M., Barba, F. J., Grimi, N., Bals, O., & Vorobiev, E. (2015). Optimization of microwave-assisted extraction of polyphenols from Quercus bark. *Industrial Crops and Products*, 77, 590-601.
- Cantos, E., Espín, J. C., López-Bote, C., de la Hoz, L., Ordóñez, J. A., & Tomás-Barberán, F. A. (2003). Phenolic Compounds and Fatty Acids from Acorns (*Quercus* spp.), the Main Dietary Constituent of Free-Ranged Iberian Pigs. *Journal of Agriculture and Food Chemistry*, 51(21), 6248-6255. <https://doi.org/https://10.1021/jf030216v>.
- Carriço, C., Ribeiro, H. M., & Marto, J. (2018). Converting cork by-products to ecofriendly cork bioactive ingredients: Novel pharmaceutical and cosmetics applications. *Industrial Crops and Products*, 125, 72-84. <https://doi.org/https://doi.org/10.1016/j.indcrop.2018.08.092>.
- Cassani, L., Tomadoni, B., Ponce, A., Agüero, M. V., & Moreira, M. R. (2017). Combined Use of Ultrasound and Vanillin to Improve Quality Parameters and Safety of Strawberry Juice Enriched with Prebiotic Fibers. *Food and Bioprocessing Technology*, 10(8), 1454-1465. <https://doi.org/https://10.1007/s11947-017-1914-3>.
- Chemat, F., Rombaut, N., Sicaire, A.-G., Meullemiestre, A., Fabiano-Tixier, A.-S., & Abert-Vian, M. (2017). Ultrasound assisted extraction of food and natural products. Mechanisms, techniques, combinations, protocols and applications. A review. *Ultras Sonochemical*, 34, 540-560. <https://doi.org/https://doi.org/10.1016/j.ultsonch.2016.06.035>.
- Chemat, F., Vian, M. A., & Cravotto, G. (2012). Green extraction of natural products: Concept and principles. *International journal of molecular sciences*, 13(7), 8615-8627.
- Conde, E., Cadahía, E., García-Vallejo, M. C., Fernández De Simón, B., & González Adrados, J. R. (1997). Low Molecular Weight Polyphenols in Cork of *Quercus suber*. *Journal of Agriculture and Food Chemistry*, 45(7), 2695-2700. <https://doi.org/https://doi.org/10.1021/jf960486w>.
- Dairi, B., Bellili, N., Hamour, N., Boulassel, A., Djidjelli, H., Boukerrou, A., & Bendib, R. (2022). Cork waste valorization as reinforcement in high-density polyethylene matrix. *Materials Today: Proceedings*, 53, 117-122. <https://doi.org/https://doi.org/10.1016/j.matpr.2021.12.420>.
- Fernandes, A., Sousa, A., Mateus, N., Cabral, M., & de Freitas, V. (2011). Analysis of phenolic compounds in cork from *Quercus suber* L. by HPLC-DAD/ESI-MS. *Food Chemistry*, 125(4), 1398-1405. <https://doi.org/https://doi.org/10.1016/j.foodchem.2010.10.016>.

- Garrido, T., Gizdavic-Nikolaidis, M., Leceta, I., Urdanpilleta, M., Guerrero, P., de la Caba, K., & Kilmartin, P. A. (2019). Optimizing the extraction process of natural antioxidants from chardonnay grape marc using microwave-assisted extraction. *Waste Management*, *88*, 110-117. <https://doi.org/https://doi.org/10.1016/j.wasman.2019.03.031>.
- Hernández, Y., Lobo, M. G., & González, M. (2009). Factors affecting sample extraction in the liquid chromatographic determination of organic acids in papaya and pineapple. *Food Chemistry*, *114*(2), 734-741.
- Huma, Z.-E., Jayasena, V., Nasar-Abbas, S. M., Imran, M., & Khan, M. K. (2018). Process optimization of polyphenol extraction from carob (*Ceratonia siliqua*) kibbles using microwave-assisted technique. *Journal of Food Processing and Preservation*, *42*(2), e13450. <https://doi.org/https://doi.org/10.1111/jfpp.13450>.
- Letellier, M., & Budzinski, H. (1999). Microwave assisted extraction of organic compounds. *Analisis*, *27*(3), 259-270.
- Moreira, M. M., Barroso, M. F., Boeykens, A., Withouck, H., Morais, S., & Delerue-Matos, C. (2017). Valorization of apple tree wood residues by polyphenols extraction: Comparison between conventional and microwave-assisted extraction. *Industrial Crops and Products*, *104*, 210-220. <https://doi.org/https://doi.org/10.1016/j.indcrop.2017.04.038>.
- Mota, S., Pinto, C., Cravo, S., Rocha e Silva, J., Afonso, C., Sousa Lobo, J. M., . . . Almeida, I. F. (2022). Quercus suber: A Promising Sustainable Raw Material for Cosmetic Application. *Applied Sciences*, *12*(9), 4604. <https://www.mdpi.com/2076-3417/12/9/4604>.
- Nabet, N., Gilbert-López, B., Madani, K., Herrero, M., Ibáñez, E., & Mendiola, J. A. (2019). Optimization of microwave-assisted extraction recovery of bioactive compounds from *Origanum glandulosum* and *Thymus fontanesii*. *Industrial Crops and Products*, *129*, 395-404. <https://doi.org/https://doi.org/10.1016/j.indcrop.2018.12.032>.
- Osorio-Tobón, J. F. (2020). Recent advances and comparisons of conventional and alternative extraction techniques of phenolic compounds. *Journal Food Science and Technology*, *57*(12), 4299-4315. <https://doi.org/https://10.1007/s13197-020-04433-2>.
- Paré, J. J., Bélanger, J. M., & Stafford, S. S. (1994). Microwave-assisted process (MAP™): a new tool for the analytical laboratory. *TrAC Trends in Analytical Chemistry*, *13*(4), 176-184.
- Pereira, H. (2011). *Cork: biology, production and uses*: Elsevier.
- Priyadarshini, A., Tiwari, B. K., & Rajauria, G. (2022). Assessing the Environmental and Economic Sustainability of Functional Food Ingredient Production Process. *Processes*, *10*(3), 445. <https://www.mdpi.com/2227-9717/10/3/445>.
- Puech, J. L., Mertz, C., Michon, V., Le Guerneve, C., Doco, T., & Herve Du Penhoat, C. (1999). Evolution of castalagin and vescalagin in ethanol solutions. Identification of new derivatives. *J Agric Food Chem*, *47*(5), 2060-2066.
- Silva, A., Rodrigues, C., Garcia-Oliveira, P., Lourenço-Lopes, C., Silva, S. A., Garcia-Perez, P., . . . Prieto, M. A. (2021). Screening of Bioactive Properties in Brown Algae from the Northwest Iberian Peninsula. *Foods (Basel, Switzerland)*, *10*(8). <https://doi.org/https://10.3390/foods10081915>.
- Teglia, C. M., Gonzalo, L., Culzoni, M. J., & Goicoechea, H. C. (2019). Determination of six veterinary pharmaceuticals in egg by liquid chromatography: Chemometric optimization of a novel air assisted-dispersive liquid-liquid microextraction by solid floating organic drop. *Food Chemistry*, *273*, 194-202. <https://doi.org/https://doi.org/10.1016/j.foodchem.2017.08.034>.
- Terzić, M., Majkić, T., Zengin, G., Beara, I., Cespedes-Acuña, C. L., Čavić, D., & Radojković, M. (2023). Could elderberry fruits processed by modern and conventional drying and extraction technology be considered a valuable source of health-promoting compounds? *Food Chem*, *405*(Pt A), 134766. <https://doi.org/10.1016/j.foodchem.2022.134766>.
- Tsiaka, T., Lantzouraki, D. Z., Polychronaki, G., Sotiroudis, G., Kritsi, E., Sinanoglou, V. J., . . . Zoumpoulakis, P. (2023). Optimization of Ultrasound- and Microwave-Assisted Extraction for the Determination of Phenolic Compounds in Peach Byproducts Using Experimental Design and Liquid Chromatography–Tandem Mass Spectrometry. *Molecules*, *28*(2), 518. <https://www.mdpi.com/1420-3049/28/2/518>.
- Varea, S., Garcia-Vallejo, M. C., Cadahia, E., & de Simon, B. F. (2001). Polyphenols susceptible to migrate from cork stoppers to wine. *European Food Research and Technology*, *213*(1), 56-61. <https://doi.org/https://doi.org/10.1007/s002170100327>.

- Xia, T., Shi, S., & Wan, X. (2006). Impact of ultrasonic-assisted extraction on the chemical and sensory quality of tea infusion. *Journal of Food Engineering*, 74(4), 557-560. <https://doi.org/10.1016/j.jfoodeng.2005.03.043>.
- Zhang, Q. W., Lin, L. G., & Ye, W. C. (2018). Techniques for extraction and isolation of natural products: a comprehensive review. *Chinese Medicine*, 13, 20. <https://doi.org/https://10.1186/s13020-018-0177-x>.

Part B.

Sensory Implications: molecular interactions between cork compounds and their impact in astringency and copigmentation phenomena's

Synopses:

Chapter 1- Interaction between salivary proteins and cork phenolic compounds able to migrate to wine model solution

Adapted from:

Joana Azevedo, Mónica Jesus, Elsa Brandão, Susana Soares, Joana Oliveira, Paulo Lopes, Nuno Mateus and Victor de Freitas, Food Chemistry, **2022**, DOI: 10.1016/j.foodchem.2021.130607;

All the work described in this part was carried out by the author, the salivary proteins studies was made by Mónica Jesus.

Chapter 2- On the Limits of Anthocyanins Co-Pigmentation Models and Respective Equations

Adapted from:

Joana Oliveira, Joana Azevedo, Natércia Teixeira, Paula Araújo, Victor de Freitas, Nuno Basílio and Fernando Pina, Journal of Agricultural and Food Chemistry, **2021**, DOI: 10.1021/acs.jafc.0c05954;

All the experimental work described in this part was carried out by the author, mathematical equations and expressions are responsible of Fernando Pina.

Chapter 3- Copigmentation of anthocyanins with copigments possessing an acid-base equilibrium in moderately acidic solution

Adapted from:

Joana Oliveira, Joana Azevedo, André Seco, Johan Mendoza, Nuno Basílio, Victor de Freitas and Fernando Pina, Dyes and Pigments, **2021**, DOI: 10.1016/j.dyepig.2021.109438;

All the experimental work described in this part was carried out by the author, André Seco and Juan Mendoza. Fernando Pina was the main responsible for writing conceptualization and constants determinations.

Chapter 1- Interaction between salivary proteins and cork phenolic compounds able to migrate to wine model solution

Abstract

This work reports the study of the interaction of human salivary proteins (SP) with phenolic compounds that migrate from cork stoppers to wine. This study yields valuable data to understand the influence that these compounds may have on the sensory perception of wine from an astringency perspective. For that, three cork fractions containing the phenolic compounds that migrate in greater amounts from cork to model wine solutions were selected. Fraction M1 contains gallic acid, protocatechuic acid, vanillin and protocatechuic aldehyde; fraction M2 comprises essentially gallic acid and ellagic acid, as well as castalagin and dehydrocastalagin; and fraction M3 contains the two isomeric ellagitannins castalagin and vescalagin. The reactivity of each fraction towards SP was $M3 > M2 > M1$. Within M3 fraction, castalagin showed a higher ability to precipitate SP (mainly aPRPs, statherin and P-B peptide) comparatively to vescalagin. In M1 fraction, caffeic and sinapic acids were the compounds with the highest interaction with SP, mainly cystatins. In addition, there also seems to be a matrix effect (presence of other compounds) that could be affecting these interactions.

Keywords: Phenolic compounds, Salivary Proteins, Ellagic Tannins, Phenolic acids, Aldehydes, Interactions

Introduction

Cork stoppers are among the most widely used closures for common alcoholic beverages, namely wine, spirits, among others. Cork is a suberized cellular tissue produced by the cork oak tree (*Quercus subber* L.) commonly occurring in the Mediterranean region. Cork stoppers are very important since a number of previous sensory studies (Furtado et al., 2021; Gao et al., 2015; Karbowski et al., 2009; Lopes et al., 2009; Reynolds et al., 2018; Tchouakeu Betnga et al., 2020) found that consumers link high quality wines to wines bottled with these stoppers instead of alternative stoppers (Díaz-Maroto et al., 2021; Jung & Hamatscheck, 1992; Kontoudakis et al., 2008).

Although the main function of a closure is to ensure a good seal and to avoid leakage, cork is a semi-permeable material that allows oxygen permeability in small amounts, which is important for a gradual and proper wine aging (Lopes et al., 2007; Lopes et al., 2009). On the other hand, cork is not an inert material, allowing the migration of some compounds to the alcoholic matrices, such as phenolic acids, aldehydes, tannins and pectic polysaccharides (Azevedo et al., 2017; Azevedo et al., 2014; Pinto et al., 2019; Reis, Coelho, et al., 2020; Reis, Teixeira, et al., 2020; Varea et al., 2001). In the case of phenolic compounds, they can affect positively or negatively the sensory properties of beverages, namely colour and taste, particularly bitterness and astringency (Azevedo et al., 2020; Watrelot et al., 2020). These changes can occur directly or indirectly because some of these cork phenolic compounds can undergo numerous chemical transformations such as reaction with anthocyanins or proanthocyanins (Azevedo et al., 2017; He et al., 2012; Puech et al., 1999; Schwarz et al., 2003).

Phenolic compounds are a large family of secondary metabolites produced by plants (Harborne et al., 1993; Randhir et al., 2004). These compounds are commonly divided into non-flavonoids and flavonoids. The non-flavonoids include simple phenolic acids (e.g. caffeic acid, gallic acid), stilbenes and some other miscellaneous compounds such as lignins. Flavonoids are the most abundant phenolic compounds in foods sharing a common structural feature due to the presence of a flavanic core (two aromatic rings linked by a heterocyclic pyranic ring). They are further divided into different classes such as anthocyanins, flavanols, flavonols, flavones, among others, based on the oxidation degree of the pyranic ring and substitution pattern of the aromatic rings. Another common designation to some complex phenolic compounds is tannins. Tannins are a family of phenolic compounds structurally divided in condensed tannins which are polymers of flavan-3-ol units, and hydrolysable tannins described as monosaccharide esters (usually a glucose) with gallic acid (gallotannins) or ellagic acid (ellagitannins). These compounds can be found in plant-based foodstuffs and beverages (Tsao, 2010).

Among the phenolic compounds present in cork, the ones that usually migrate to alcoholic beverages are phenolic acids (mainly gallic and protocatechuic acids), aldehydes (mainly vanillin and protocatechuic aldehyde), condensed tannins and ellagitannins such as vescalagin and mongolicain (Azevedo et al., 2014; Reis, Coelho, et al., 2020). Tannins are well-known to interact with salivary protein (SP) leading to the formation of (in)soluble aggregates which are supposed to be at the origin of the astringency sensation. Astringency is an oral sensation involving dryness, tightening, and shrinking of the oral cavity. Among the different families of SP, proline-rich proteins

(PRPs) are the ones mainly related to astringency perception (Bacon & Rhodes, 2000; Cheynier, 2005; Soares et al., 2012). The major SP that constitute altogether more than 95% of the salivary protein content are commonly grouped into six structurally related major families: amylases, histatins, basic PRPs (bPRPs), acidic PRPs (aPRPs), glycosylated PRPs (gPRPs), statherin, and cystatins (Bennick, 2002; Brandao et al., 2014; Humphrey & Williamson, 2001). The differences between the several families of PRPs depend on their charge and presence or absence of carbohydrates in their structure. All SP have important biological functions in saliva, such as the contribution to the balance of calcium phosphates salts (statherin and PRPs), the lubricant role (gPRPs), antimicrobial properties (histatins), protection of oral tissues against degradation by inhibiting activity of cysteine proteases (cystatins), and playing an additional biologic role in the non-immune defence system (Helmerhorst & Oppenheim, 2007; Huq et al., 2007; Kauffman et al., 1993; Oppenheim et al., 1988; Schlesinger et al., 1989).

Among the different families of SP, the different classes of PRPs have been widely reported to interact with different phenolic compounds and have been related to astringency perception in both in vitro and in vivo studies. This work aims to study the interaction of human salivary proteins with cork phenolic compounds able to migrate into wine model solutions. This will provide more insights about the putative contribution of the migration of these phenolic compounds on taste properties of wine.

Materials and Methods

Reagents

The L-(+)-tartaric acid (99%), ethyl acetate (99.9%), methanol (99.8%), acetonitrile (99.8%), acetic acid (99.7%), Trifluoroacetic acid (99.8%), and sodium bisulfite (Sigma-Aldrich®, Madrid, Spain). Ethanol (AGA® (96%), Prior Velho, Portugal) and HCl 37% (Fluka®, College Park, MD, USA). TSK Toyopearl® gel HW-40 (S) (Tosoh Corporation, Tokyo, Japan).

Cork material extraction

Granulated cork (1-2 mm particle size) was obtained from 300 natural cork stoppers, by grinding and sieving cork (*Q. suber L*) stoppers, supplied by Amorim & Irmãos (Mozelos, Portugal), giving rise to 1 kg of granulated cork. The compounds were extracted by direct contact between granulated cork (200 g) and a hydroalcoholic solution (12% ethanol) in 5 L capacity bottles at 35 °C during 10 days following the procedure described by Azevedo (Azevedo et al., 2017). 5 bottles were prepared with a final volume of 25 L of

hydroalcoholic extracts. The extracts were passed through a 1.2 μm filter and then centrifuged during 5 min at 10 000 rpm and 20 °C. The ethanol solvent was removed by evaporation under vacuum and the resulting aqueous solution was extracted based on the procedure described by Yang (Yang et al., 2017). For that, 10 mL of organic cork extract, 10 mL of ethyl acetate and 5 mL of acetonitrile were added to a falcon and vortexed during 10 s and then the samples were centrifuged during 5 min at 5400 g and 20 °C. Organic and aqueous phases were separated and the same procedure was repeated twice. Organic fractions were combined, and the solvent was removed using a CentriVac Concentrator Labconco system (Kansas City, MO, USA) and resuspended in water. At the end, the organic fraction was freeze-dried (5 g) dissolved in methanol and further applied in a chromatography column to obtain fractions with different compositions. The sample used for each fractionation procedure was prepared by dissolving 200 mg of the organic fraction in 8 mL ethanol.

Column chromatography

Phenolic compounds from the cork extract were fractionated by low-pressure column chromatography according to the method described by Fernandes (Fernandes et al., 2011). Briefly, the previously obtained ethanolic extract was applied into a Toyopearl® (Griesheim, Germany) gel column (300x16 mm, i.d.) using ethanol as the eluent at 0.8 mL.min⁻¹ flow rate. Phenolic compounds were separated based on molecular weight. Fractions were collected upon detection with a Gilson 115 UV (Cambridgeshire, U.K) Detector and a SP4290 integrator from Spectra-Physics at 280 nm. The different fractions (M1, M2, M3) were obtained and characterized by Liquid Chromatography (LC) Electron Spray Ionization (ESI) - Mass Spectrometry (MS) (Finnigan Corp, San Jose, California), as presented in **Table 1**. The average molecular weight of each fraction was estimated based on the relative abundance of each identified compound. This allowed also to estimate the mean molarity of each fraction.

Saliva collection

Human saliva was collected from thirteen healthy non-smoker volunteers (males and females, ages between 23 to 43 years old), and kept on ice for further processing. The saliva from all volunteers was pooled together to obtain a whole representative human saliva. Trifluoroacetic acid (TFA) solution (10% aqueous TFA) was immediately added to saliva (900 μL of saliva to 25 μL of TFA solution). The addition of TFA has two main functions: to preserve sample protein composition and to precipitate several high molecular weight proteins that cannot be analysed directly by HPLC. After this treatment, saliva was centrifuged for 5 min at 13,400 g and 20°C. The supernatant was separated

from the precipitate, aliquoted and kept at -80 °C until use. Several physical-chemical parameters of the isolated saliva were characterized, namely ionic strength, total protein concentration, and profile of the families of salivary proteins. The ionic strength was analysed by a conductometer (WTW Inolab 740, Weilheim in Oberbayern, Germany). The total protein concentration was assessed using the Bradford assay: 5 µL of saliva were added to 250 µL of the Bradford reagent (Coomassie brilliant Blue G-250, Sigma®). The samples were mixed and kept for 10 min at room temperature protected from the light. A calibration curve was made with Bovine Seric Albumin (BSA) (0.0, 0.1, 0.3, 0.5, 0.8, 1.1, 1.4 mg. mL⁻¹) in the same way as described. The total protein concentration was determined to be 663 µg BSA.mL⁻¹ saliva.

Salivary protein profile

The profile of the families of salivary proteins was analysed by a High Performance Liquid Chromatography (HPLC) – Diode Array Detector (DAD) on a JASCO LC-4000 HPLC (Tokyo, Japan) system equipped with a kinesis Telos MDC reversed-phase C-8 column (Altrincham, United Kingdom) (150 × 2.1 mm, 5 µm). The solvents used were solvent A, 0.2% aqueous TFA and solvent B, 0.2% TFA in acetonitrile/water 80/20 (v/v). The elution program was 5% to 90% of B during 76 min at a flow of 0.5 mL.min⁻¹. Detection was carried out at 214 nm and 280 nm. The salivary protein families present in the chromatogram have been previously identified (Messana et al., 2004; Soares et al., 2011). The concentration of the different salivary protein families was determined as acidic Proline-rich Protein (aPRP) equivalents, except for cystatins. For this, calibration curves were made with these protein families. The calibration curves were established for a concentration range of 0.05 to 0.7 mg. mL⁻¹ for both protein families. For aPRPs the calibration curve was $\text{Concentration} = (\text{Area} + 771081)/4 \times 10^7$ ($R^2=0.9991$) and was used to determine the concentration of the bPRP, aPRP, gPRP, statherin and P-B families; for cystatins the calibration curve was $\text{Concentration} = (\text{Area} - 3 \times 10^6)/2 \times 10^7$ ($R^2=0.9834$) and was used to calculate the concentration of this family.

Interaction between each fraction and human saliva

The interaction between three cork fractions (M1, M2 and M3) and human saliva was studied for four different concentrations of each fraction, 0.25, 0.5, 1.0 and 1.5 mg. mL⁻¹. As fractions have different phenolic compositions, the average molecular weight of each one was estimated based on the relative abundance of each compound (**Table 1**). From a freeze-dried fraction powder, a stock solution (4.0 g. L⁻¹) of M1, M2 e M3 were prepared. The fraction was first dissolved in ethanol (final concentration <7%) and then the final volume was adjusted with wine model solution (WMS, 12% ethanol, aqueous

tartaric acid 5 g.L⁻¹, pH=3.5). For the interaction between a fraction and SP, several mixtures were prepared according to the volumes detailed in Table S1, Supplementary Data. Briefly, different volumes of fraction stock solutions (M1, M2 and M3) were added to saliva (96.4 µL) to obtain different concentrations (0.25, 0.50, 1.00 and 1.5 g. L⁻¹). Appropriate volumes of WMS were added to make the final volume to 150 µL. Samples were kept 5 min at room temperature (20-25 °C). For control conditions, a mixture of saliva (96.4 µL) and WMS (53.6 µL) was used as the control for SP profile; a mixture of fraction (M1, M2 and M3) stock solution and WMS was used as the control for the phenolic compounds profile. After this time, the solutions were collected, centrifuged at 8000 g, 5 min, 20 °C and the supernatants were recovered. Supernatants were analysed by HPLC to determine the changes in phenolic compounds and SP profiles. HPLC conditions for protein analysis are the ones described above. For phenolic compounds profile, a HPLC (JASCO LC-4000 system) (Tokyo, Japan) equipped with a Poroshell 120 Agilent C18 column (Little River, Delaware, United States of America) (250 x 4.6 mm, 2.7 µm) was used. The solvents used were A, 1% aqueous formic acid and B, 1% formic acid in acetonitrile. The elution program was 10% to 35% during 45 min to M1 fraction, 10% to 35% during 45 min to M2 fraction and 5% to 20% during 30 min to M3 fraction, at a flow rate of 0.5 mL. min⁻¹. The concentration of each compound was determined in gallic acid equivalents and for this, a calibration curve was established for different concentrations (0.029 to 0.88 mmol. L⁻¹) of gallic acid. The interaction experiments were performed in triplicate.

Statistical analysis

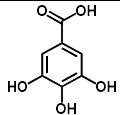
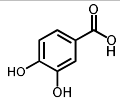
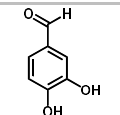
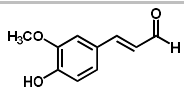
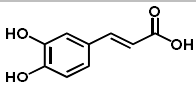
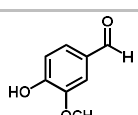
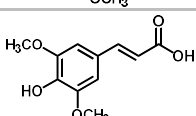
All assays were performed on three independent experiments and the results were expressed as mean values and Standard Error of the Mean (SEM). The statistical data analysis was performed using analysis of variance (ANOVA) followed by Fisher's Least Significant Difference test. All statistical data were processed using GraphPad Prism version 8.0 for Windows (San Diego, California). Values statistically different are indicated (*p<0.05).

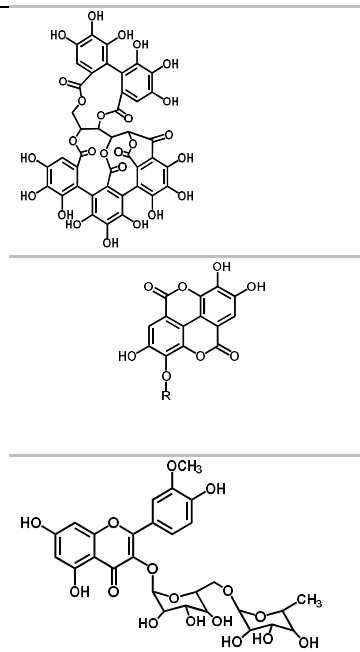
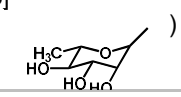
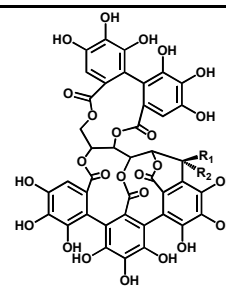
Results and discussion

Phenolic characterization of cork fractions

Three phenolic compounds fractions (M1, M2 and M3) with different phenolic compound profiles were obtained from a cork extract. The phenolic compounds present in each fraction (Table 1, Figure S1) were identified by LC-MS by comparing the retention time with standards and the fragmentation pattern with the literature (Glabasnia & Hofmann, 2007; Nuncio-Jáuregui et al., 2015; Schulze, 2021). Fractions M1 and M2 are representative fractions of phenolic compounds that migrate in greater amounts to wine model solutions (WMS) and include compounds such as gallic acid, protocatechuic acid and protocatechuic aldehyde. A previous study reported that 2 mg. L⁻¹ of each compound present in the M1 fraction can migrate from cork stoppers to WMS after 27 months in bottle (Azevedo et al., 2014). Fraction M3 is representative of ellagitannins present in cork (Table 1) that have already been identified in wines (Rasines-Perea et al., 2019) and reported to contribute to wine astringency (Glabasnia & Hofmann, 2007). All these compounds have already been previously identified in cork (Azevedo et al., 2017; Fernandes et al., 2011; Santos et al., 2013). In addition to the migration from cork stoppers, most of these compounds (e.g., gallic acid, protocatechuic acid) occur naturally in wine (Rothwell et al., 2013). Regarding vescalagin and castalagin, they can also occur in wine due to migration from oak (García-Estévez et al., 2010) during wine ageing in oak barrels. In this case, several factors affect the content of these ellagitannins as well as their migration to wines (e.g., the oak species, the age, the silvicultural treatment of the tree, the processing of wood in cooperage that changes its chemical composition, among others).

Table 1- Phenolic compounds identified in fractions M1, M2 and M3 obtained by fractionation in column chromatography (Toyopearl® gel) of a cork extract.

Fraction	Compound	RT (min)	[MH] ⁻	[MS] ²	Relative Abundance (%)	Average molecular weight (g mol ⁻¹) ^a	Structure
M1	Gallic acid	7.87	169	-	24	164.9	
	Protocatechuic acid	13.47	153	-	22		
	Protocatechuic aldehyde	18.80	137	-	14		
	Coniferaldehyde	23.40	177	-	7		
	Caffeic acid	24.02	179	-	7		
	Vanillin	31.52	151	-	20		
	Sinapic acid	36.23	221	-	7		
M2	Gallic acid	5.76	169	-	20	482.6	-
	Castalagin	6.92	933	-	14		-
	Unknown	9.17	279	-	15		-

	*Dehydrocastalagin [Glabasnia and Hofmann 2007]	11.96	931	-	8	
	*Dehydrocastalagin [Glabasnia and Hofmann 2007]	12.71	931	-	6	
	*Ellagic acid rhamnoside [Nuncio-Jáuregui, Nowicka et al. 2015] (R= )	17.12	447	301, 257	9	
	Ellagic acid (R = H)	30.08	301	257	18	
	*Isorhamnetin-3-O-rutinoside [Schulze 2021]	36.54	461	316	11	
M3	Vescalagin (R ₁ = OH, R ₂ = H)	12.12	933	-	24	
	Castalagin (R ₁ = H, R ₂ = OH)	17.46	933	-	76	

933.0

^a The average molecular weight was calculated based on the relative abundance of each compound identified by LC-MS.

* Compounds were identified based on literature according to the fragmentation pattern.

RT – retention time.

Reactivity of each fraction toward human saliva

The chromatographic profile of human saliva (control saliva) and the different families of SP present are displayed in **Figure 1**. This profile is similar to the ones observed previously and the identification of each family of SP was also based on previous proteomic studies (Soares et al, 2011). The typical human saliva profile is commonly divided into bPRP, gPRP, aPRP, statherin, P-B peptide and cystatins (Soares et al, 2011).

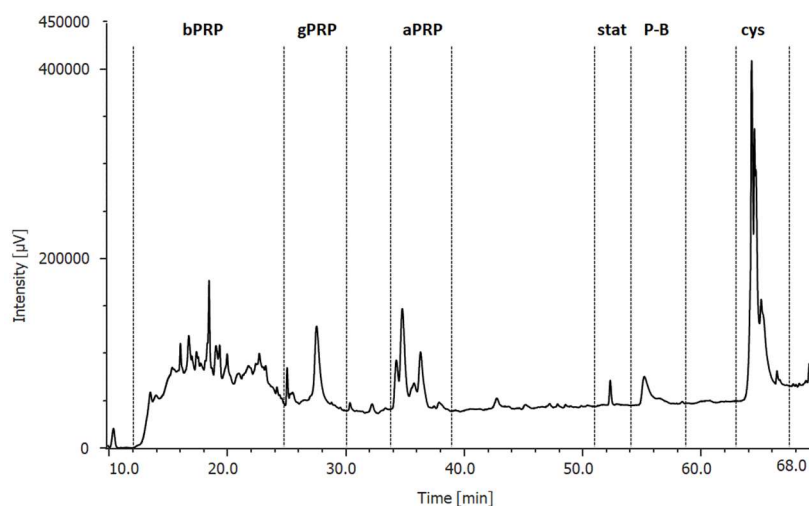
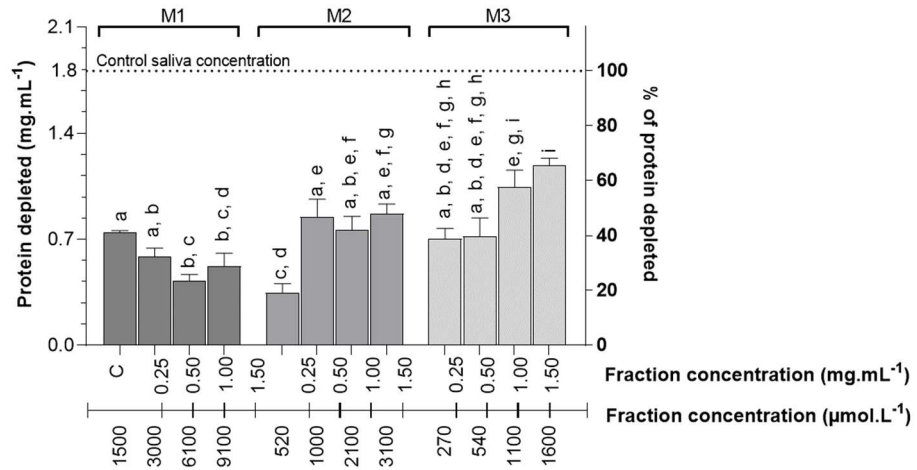


Figure 1. HPLC profile detected at 214 nm of human saliva (control). The major family of SP identified previously is assigned to each eluting region.

After the interaction of human saliva with fractions M1, M2 or M3 at different concentrations, the insoluble aggregates were removed by centrifugation. The three fractions were studied at the same mass concentration ($\text{mg} \cdot \text{mL}^{-1}$). The eventually formed soluble aggregates that remain in the supernatant cannot be detected as they are destroyed and re-dissolved under the acidic HPLC solvent conditions, as already reported elsewhere (Soares et al., 2012). Therefore, this approach only allows to study the protein-phenolic interactions that yield to precipitation.

Then, the supernatant was analysed to quantify the different families of SP that remained in solution after the interaction with the phenolic compounds. This unprecipitated concentration was subtracted to the control condition (maximal concentration of protein in saliva) to determine proteins depletion (**Figure 2**).

A.



B.

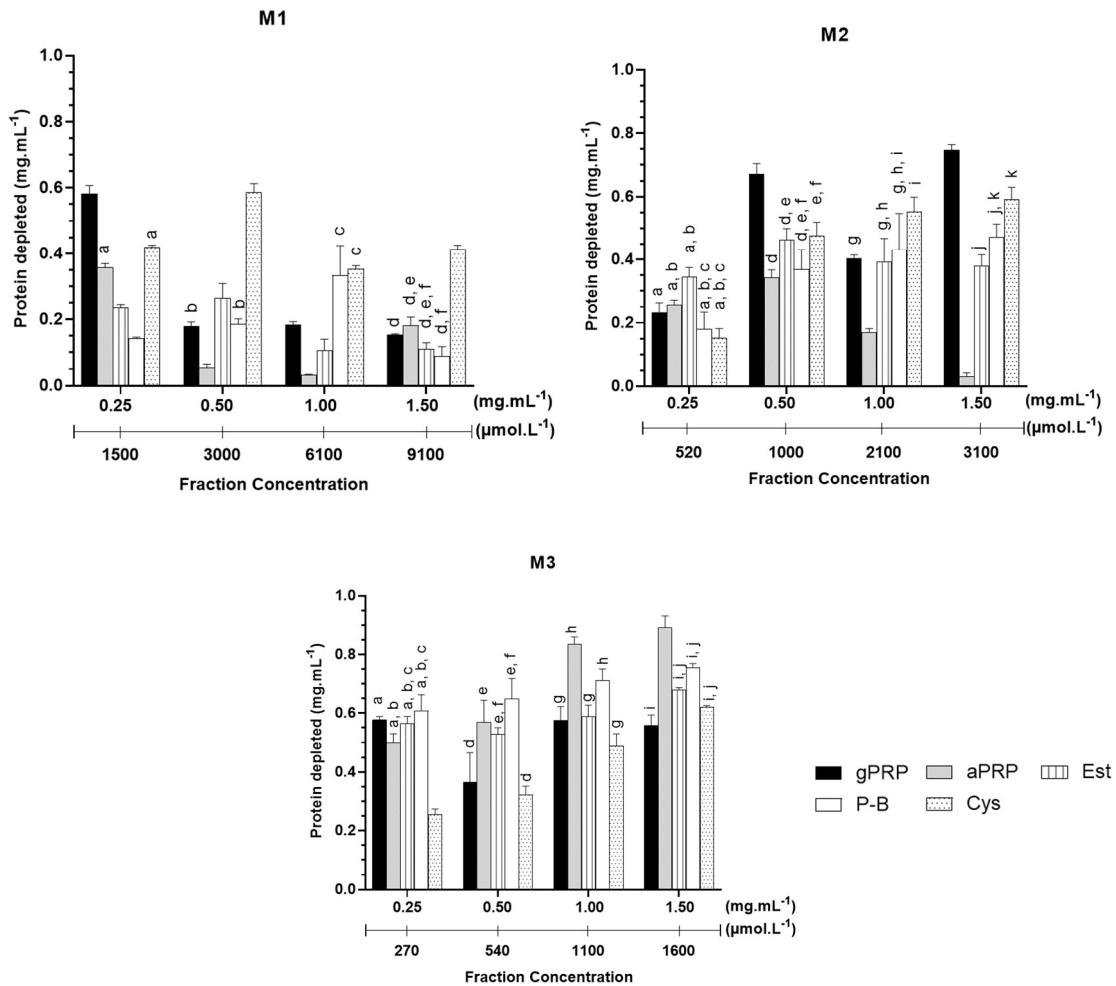


Figure 2. Concentration of salivary proteins depleted upon the interaction with fractions (M1, M2 and M3) at different concentrations (0.25, 0.50, 1.00 and 1.50 mg. mL⁻¹). (A) Concentration of the total SP depleted. The dotted line represents the total SP content (1.8 mg. mL⁻¹, 100%) in control saliva. (B) Concentration (mg. mL⁻¹) of each family of SP depleted. These data are normalized to the concentration in the control condition. Data are presented as mean ± SEM, mean of three independent experiments.

Based on **Figure 2A**, fraction M3 at a concentration of 1600 μM was able to precipitate the highest amount of SP, near 1.3 mg. mL^{-1} (around 70%) (**Figure 2A**). The highest concentrations of M1 and M2 fractions, 9100 and 3100 μM , respectively, were only able to precipitate 30 and 50% of SP, respectively. Moreover, even at the lowest concentration (270 μM), fraction M3 was able to precipitate a significant concentration of total SP (40-45%), while 1500 and 1000 μM of fractions M1 and M2, respectively, were needed to achieve the same degree of SP precipitation. This also means that fraction M2 is more effective in precipitating SP than fraction M1. Therefore, the fractions reactivity toward total SP precipitation seems to be $\text{M3} > \text{M2} > \text{M1}$, at least for the two highest concentrations.

While for fractions M2 and M3 it was observed an increased precipitation of SP with their concentration, the same was not true for fraction M1. Even when the concentration of this fraction increases 3-times, the quantity of precipitated SP remained the same. Some hypotheses can be designed to explain the results obtained for fraction M1: i) low reactivity of the phenolic compounds present in this fraction; ii) formation of soluble complexes, instead of insoluble aggregates; iii) self-aggregation of these phenolic compounds at higher concentration competing with their ability to interact with SP. It is important to highlight that the experimental approach used does not allow to monitor the formation of soluble protein-phenolic complexes as these complexes are destroyed by the HPLC acidic conditions. So, if these complexes increase along with fraction M1 concentration, they are not detectable.

Looking at the precipitation levels for each family of SP (**Figure 2B**) it was only possible to analyze the gPRPs, aPRPs, statherin, P-B peptide and cystatins. For bPRPs family, it was not possible to have reliable data due to their co-elution with phenolic compounds. The results show a different reactivity among fractions toward the individual families of SP. Fractions M1 and M2 had a similar reactivity conversely to fraction M3. Looking at the closest molar concentrations of fractions M1 and M2 (1500 μM and 1000 μM , respectively), the main families of SP precipitated were gPRPs and cystatins, while aPRPs were the ones with the lowest precipitation. On the other hand, for fraction M3 (1100 μM), aPRPs and P-B peptide were the most precipitated SP. At the highest concentration of fraction M3 (1600 μM), 0.89 mg. mL^{-1} of aPRPs and 0.72 mg. mL^{-1} of P-B peptide were precipitated. The phenolic compounds present in fraction M3 are the ellagitannins castalagin and vescalagin, already reported to interact with SP, in particular with aPRPs and P-B peptide (Silva et al., 2017; Susana Soares et al., 2019).

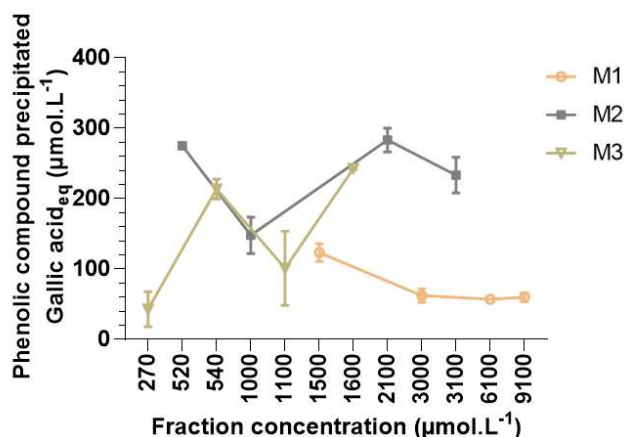
Ultimately, the reactivity of the different fractions toward SP seems to be directly linked to the fraction average molecular weight ($\text{M3} > \text{M2} > \text{M1}$) and to the family of phenolic

compounds present within each fraction. This is in agreement with previous results: higher molecular weight is usually linked to higher interactions and tannins are usually the phenolic compounds with higher interaction with SP (Soares et al., 2007). Moreover, fractions rich in phenolic acids seem to precipitate preferentially gPRPs and cystatins while (ellagi)tannins seem to precipitate mainly aPRPs and P-B peptide.

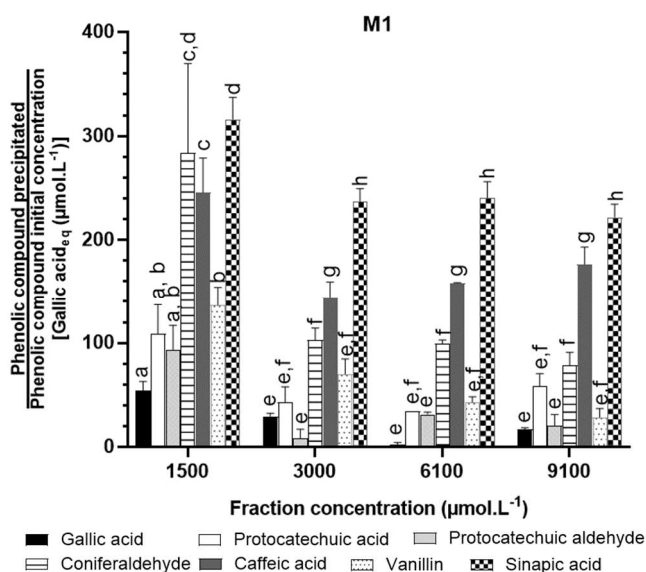
Reactivity of polyphenolic compounds toward SP

After the removal of the formed insoluble aggregates by centrifugation, the supernatant was analysed by HPLC to quantify also the phenolic compounds that were not precipitated by the SP. The unprecipitated concentration was subtracted from the control condition (control fraction) to determine the precipitated concentration (Figure 3). As referred before, the phenolic compounds involved in soluble complexes cannot be quantified by HPLC since the soluble complexes are expected to be destroyed by the acidic HPLC solvents, as described elsewhere (Soares et al., 2012). So, this approach does not provide information about the possible protein-phenolic soluble complexes.

A.



B.



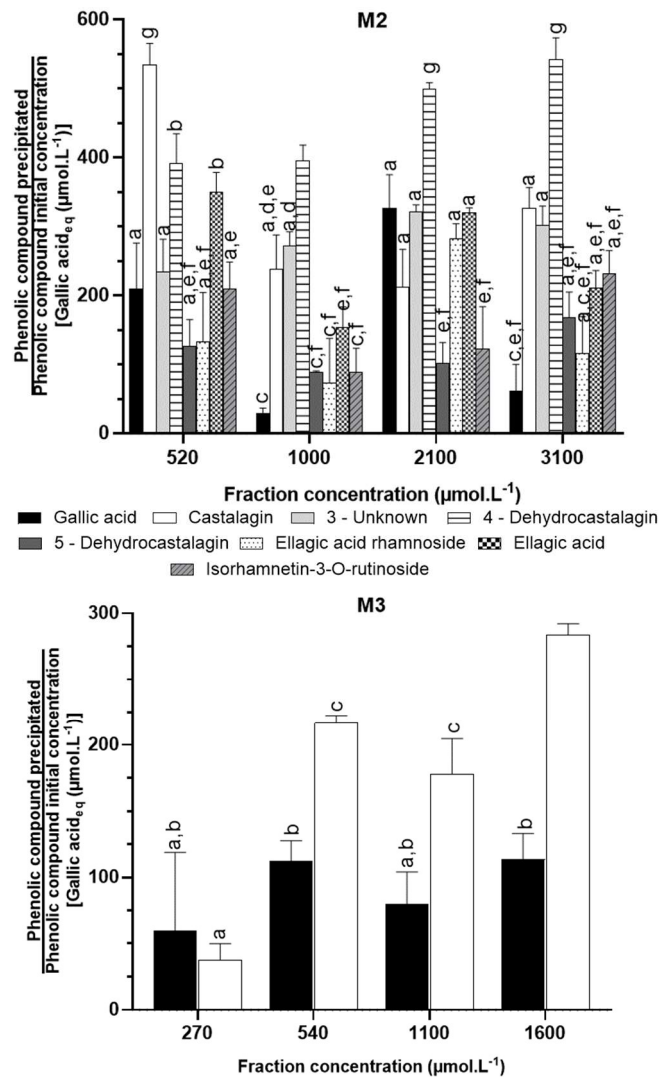


Figure 3. Concentration of precipitated phenolic compounds of fractions M1, M2 and M3 after interaction with human saliva, for the four different initial fractions concentration. The concentrations are presented in equivalents of gallic acid. (A) Total concentration of phenolic compounds precipitated. (B) Precipitated concentration of each phenolic compound within fractions M1, M2 and M3. The values were normalized to the initial concentration of each phenolic compound to compare the phenolic compounds within fractions. Data are presented as the mean of three independent experiments and error bars indicate SEM.

Fractions M2 and M3 were the ones with the highest total concentration of phenolic compounds precipitated with SP (**Figure 3A**). In general, for these fractions, regardless of the initial concentration, the concentration of phenolic compounds precipitated is quite similar. Surprisingly, for each fraction the profile of the precipitated phenolic compounds is not the same along the studied concentrations.

It is interesting that although a similar concentration of phenolic compounds is precipitated at M1 1500 µM, M2 1000 µM and M3 1100 µM (**Figure 3A**), M3 leads to a higher precipitation of total SP, followed by M2 and finally by M1 (**Figure 2A**). One hypothesis for this behaviour lies on the ability of each phenolic compound to act as a multidentate ligand: the same number of molecules of (ellagi)tannins in M3 are able to

establish a more extensive network of SP than the phenolic acids present fractions in M2 and M1, due to a higher number of binding sites (galloyl groups), and leading to a higher precipitation of SP. This ability of ellagitannins has already been reported (Dobrev et al., 2014; Karonen et al., 2019) and is also in agreement with the reactivity presented in the previous section. On the other hand, in general, the increase on the concentration of each fraction does not seem to have a consistent effect on the amount of phenolic compounds that are precipitated (**Figure 3A**) while the amount of SP precipitated is the same (**Figure 2A**). For example, for the two highest concentrations of M2 (2100 μM and 3100 μM), the concentration of phenolic compounds that are precipitated is greater than for the concentration of 1500 μM but the amount of SP precipitated is similar. A possible explanation for this behaviour lies on the hypothesis of the formation of phenolic compound-phenolic compound aggregates by inter-molecular interaction that thereafter interact with salivary proteins.

In **figure 3B** it can be observed the amounts of each phenolic compound within each fraction that were precipitated upon the interaction with SP. These values were normalized to the initial concentration of each phenolic compound to take out the effect of the relative concentration. The phenolic compounds within all fractions were precipitated differently.

In fraction M1, caffeic and sinapic acids were the ones that precipitated more by the interaction with SP. Their precipitation increases along with fraction M1 concentration. These two compounds show more precipitation in relation to the others, resulting in a precipitation of approximately 200 μM of caffeic acid and sinapic acid (for the initial concentration of 9100 μM M1 fraction). This similar precipitation toward SP can be explained by the similar structure of caffeic and sinapic acids. Protocatechuic acid and vanillin interact at the same extent, approximately 60 μM , while gallic acid and protocatechuic aldehyde are the ones with the lowest precipitation. Therefore, it seems that within fraction M1, caffeic and sinapic acids are the major responsible for the observed precipitation of gPRPs and cystatins. In fact, a study carried out with a mixture of polyphenolic compounds rich in caffeoyl groups (caffeic acid) derived from apple cider also showed a specific interaction with cystatins (Castillo-Fraire et al., 2020), as observed herein.

Within the phenolic compounds of fraction M2, the profile of the precipitated compounds is not the same (**Figure 3B**). At M2 520 μM , castalagin is the main precipitated compound whereas at 2000 μM and 3100 μM it is 4-dehydrocastalagin (**Figure 3B**), a castalagin-derivative. This compound seems to be the one with the highest precipitation of SP binding approximately 600 μM at the highest M2 concentration. On the other hand,

its isomer 5-dehydrocastalagin exhibited a significantly low precipitation. Moreover, when comparing the interaction of ellagic acid and its rhamnose derivative, the former presents always a higher precipitation than the latter. All these changes in precipitation ability highlight the important role that the structure of the phenolic compounds has on the interaction with SP (Deaville et al., 2007; Soares et al., 2007). Here, the precipitation of SP seems to be decreased by minor changes in the structure like the ones among the two castalagin-derived compounds. Moreover, major changes in the structure, like the addition of sugar moieties, seems also to decrease the precipitation by the SP.

Finally, at M2 2000 μM , gallic acid is significantly precipitated whereas for the other fraction M2 concentrations it is not. Similarly, isorhamnetin-3-O-rutinoside is precipitated in a significant concentration at M2 3100 μM .

All these changes in the profile of the precipitated phenolic compounds can also arise once again from the phenolic compound-phenolic compound inter-molecular interactions, which can increase the variability of all the possible interactions between phenolic compound-SP and phenolic compound-phenolic compound. However, these phenomena are not possible to be deepened with the used approach.

Fraction M3 is composed by only two isomeric polyphenolic compounds, castalagin and vescalagin. Although both compounds were precipitated by SP, castalagin was always the one with the highest precipitation as already previously observed (Soares et al., 2019). At 1600 μM , 300 μM of castalagin is precipitated. As previously mentioned, this fraction was the one that yielded to the greatest precipitation of total SP (**Figure 4A**).

Matrix effect on the interaction polyphenolic compound-SP

Some of the studied phenolic compounds occur in different fractions, which is the case of gallic acid and castalagin. Gallic acid occurs in fractions M1 and M2, and castalagin occurs in fractions M2 and M3. Their reactivity was compared across the referred fractions to understand if their interaction with SP was affected by the presence of other compounds (matrix effect) (**Table 1**). The cases that were compared were the ones where the initial concentration of these compounds within fractions was similar. For gallic acid this was observed in M1 at 1500 μM and M2 at 3100 μM that have 30 μM and 20 μM , respectively (Supplementary Information, Figure S1). In this case, the amount of phenolic compound precipitated by interaction with SP is similar in both fractions. For castalagin, it occurs at 14 μM and 20 μM in M2 at 3100 μM and M3 at 270 μM , respectively. The concentration of castalagin precipitated by SP is much higher in fraction M2.

Although gallic acid precipitation is not affected by the matrix effect, the results obtained for castalagin evidence that the compound has a different behaviour in the interaction with SP influenced by the presence of other phenolic compounds. This matrix effect was also reported for phenolic acids (Ferrer-Gallego et al., 2017) and flavanols (Ramos-Pineda et al., 2017) in other studies.

Table 2. Amount of phenolic compound present in the initial sample (control – μM) and amount of polyphenolic compound that were precipitated by salivary proteins (interacted – μM). These results represent the average of three independent experiments. Different letters indicate a statistically significant difference between concentration of each compound ($p < 0.05$)

Fraction	Gallic acid		Castalagin	
	Control (μM)	Interacted (μM)	Control (μM)	Interacted (μM)
M1	29.7 \pm 1.0 ^a	1.6 \pm 0.5 ^c (5%)	-	-
M2	19.7 \pm 0.6 ^b	0.5 \pm 0.5 ^c (2.5%)	13.8 \pm 0.9 ^d	4.4 \pm 0.7 ^f (31.9%)
M3	-	-	20.8 \pm 0.9 ^e	0.7 \pm 0.4 ^g (3.4%)

Comparison of phenolic compounds interaction and sensory threshold

It has been previously reported that the studied phenolic compounds are able to migrate from cork stoppers to wine at the studied concentrations (Azevedo et al., 2014). Also, it is widely known that interactions between phenolic compounds and SP are one of the most explored and related mechanisms to the oral sensation of astringency. So, in order to understand if the studied interactions can affect the astringency perception of wine, the bounded concentrations (Supplementary Information, Figure S1) were compared to the reported threshold concentration (TC) of astringency perception for each phenolic compound (**Table 3**) (Glabasnia & Hofmann, 2006, 2007; Hufnagel & Hofmann, 2008). By analysis of **Table 3** it is possible to verify that SP bound 32 to 125 μM of caffeic acid depending on the fraction M1 concentration. The TC of astringency perception reported for caffeic acid is 72 μM , which is within the bounded concentrations. For gallic and protocatechuic acids, the maximum amount of compound that bound to SP are 11 and 37 μM , respectively. For these two compounds none of these values comes close to the TC reported which are 292 and 206 μM , respectively. So, while caffeic acid is expected to contribute to astringency perception of fraction M1 at 6100 and 9100 μM , gallic and protocatechuic acids are not.

Within fraction M2, gallic acid reaches its maximum precipitation (20 μM) at M2 2100 μM . This value is much lower than astringency TC reported. In the case of castalagin and its derivative (4-dehydrocastalagin) the minimum and the maximum of compound

precipitated is 7.8 to 31.9 μM for castalagin and 7.8 to 57.5 μM for 4-dehydrocastalagin. In all concentration of fraction M2 analysed, these compounds are precipitated above the TC reported value which are 1.1 and 4.4 μM , respectively. SP bound 5 to 25 μM of ellagic acid in M2 fraction, only at the concentration of 1000 μM . So, also ellagic acid is precipitated at a higher concentration than the astringency threshold value reported (6.6 μM). Thus, it is expected that all these compounds mentioned above, except for gallic acid, contribute to astringency perception of fraction M2.

In fraction M3, castalagin precipitates between 0.9 to 34.8 μM after interaction with SP. Only for the lowest fraction M3 concentration, the concentration of precipitated castalagin does not reach de TC concentration (1.1 μM). On the other hand, vescalagin exhibit a minimum and a maximum of compound precipitated of 1.7 to 14.9 μM . Both concentrations are higher than TC concentration (1.1 μM). So, it is expected that both compounds can contribute to astringency perception of fraction M3.

However, it is important to refer that the TC values reported in the literature (Glabasnia et al., 2007; Hofmann et al., 2006) were obtained from sensory analysis using individual compounds, oppositely to what is reported in the present study. Therefore, the matrix effect can affect the TC value and consequently the astringency perception of the cork fractions.

Table 3. Taste threshold concentrations (TC) of some phenolic compounds reported on literature and comparison with the compound bounded concentration to the salivary proteins under the studied molarities (μM).

Compound	TC ($\mu\text{mol.L}^{-1}$) [REF]	C compound bonded ($\mu\text{mol.L}^{-1}$)											
		M1				M2				M3			
		1500	3000	6100	9100	520	1000	2100	3100	270	540	1100	1600
Gallic acid	292	7	7	1	11	5	1	20	6	-			
Caffeic acid	72	32	33	76	125	-				-			
Protocatechuic acid	206	14	10	15	37	-				-			
Castalagin	1.1	-				16.7	7.8	13.9	31.9	0.9	9.6	8.8	34.8
Vescalagin	1.1	-								1.7	5.3	4.1	14.9
Ellagic acid	6.6	-				11.2	5.0	25	21.7	-			
Dehydrocastalagin*	4.4	-				8.8	7.8	37.2	57.5	-			

*The compound considered was 4-Dehydrocastalagin, one of the derivatives that have more interaction in this study in the M2 fraction.

As already referred, previous studies had reported that except for dehydrocastalagin, most of these compounds can migrate from cork stoppers to WMS after 9 to 27 months. The reported concentrations depend on the phenolic compound, cork treatment as well as the migration time. The highest reported concentrations due to migration are 35 μM for gallic acid, 11 μM for caffeic acid, 38 μM protocatechuic acid, 0.1 for μM castalagin/vescalagin and 6.6 μM for ellagic acid (Azevedo et al., 2014). Crossing these data with the concentrations in Table 3, concerning the migration, only ellagic acid can actively contribute to astringency. However, it is important to keep in mind that most of these compounds occur already naturally in wines although their concentration is highly dependent on wine-making practices, like barrel aging (Ginjom et al., 2011; Neveu et al., 2010).

Conclusion

This study aimed to determine the interaction of three different fractions of phenolic compounds obtained from cork stoppers (M1, M2 and M3) with human salivary proteins. The experimental approach used allows to understand if these compounds are able to complex and precipitate SP, a mechanism that is described to contribute to the perception of astringency in wine. To attain this, the changes in the chromatographic profiles of the SP families and phenolic compounds were studied upon their interaction and after removal of the insoluble precipitates formed by centrifugation.

Overall, the results of this study suggest that cork fraction M3 is the most reactive toward SP comparing to the other fractions, followed by fraction M2 and by fraction M1. Within M3, castalagin was the compound that most interacted with SP, mainly aPRPs and P-B peptide. Within fraction M2, 4-dehydrocastalagin was the most precipitated compound by all families of SP. In fraction M1, caffeic and sinapic acids were the compounds with the highest binding to SP, mainly cystatins. Within the referred fractions, castalagin, 4-dehydrocastalagin, caffeic and ellagic acids were almost always precipitated above their reported astringency thresholds, so they may contribute to astringency perception. In addition, there seems to be a matrix effect (due to the presence of other compounds) that could affect the binding of a specific compound. Here, this was observed for castalagin that was bound in higher amounts to SP in presence of other phenolic compounds. In the end, the migration of compounds within fractions M2 and M3 into wine may actively contribute to astringency perception.

Acknowledgments

The authors thank the Science and Technology Foundation (FCT) for financial support the researcher contracts IF/00225/2015, CEECIND/01598/2018, CEECIND/01265/2018 and the scholarships SFRH/BD/139709/2018, UIDB/50006/2020 and UIDBP/50006/2020. This research is supported by AgriFood XXI I&D&I project (NORTE-01-0145-FEDER-000041 cofinanced by European Regional Development Fund (ERDF), through the NORTE 2020 (Programa Operacional Regional do Norte 2014/2020).

This research is supported by cLabel+ Project (POCI-01-0247-FEDER-046080) cofinanced by European Regional Development Fund (ERDF), through the COMPETE 2020 - Incentive System to Research and Technological Development, within the Portugal 2020 Competitiveness and Internationalization Operational Program.

References

- Azevedo, J., Brandão, E., Soares, S., Oliveira, J., Lopes, P., Mateus, N., & de Freitas, V. (2020). Polyphenolic Characterization of Nebbiolo Red Wines and Their Interaction with Salivary Proteins. *Foods (Basel, Switzerland)*, 9(12). <https://doi.org/https://10.3390/foods9121867>
- Azevedo, J., Fernandes, A., Oliveira, J., Brás, N. F., Reis, S., Lopes, P., Roseira, I., Cabral, M., Mateus, N., & de Freitas, V. (2017). Reactivity of Cork Extracts with (+)-Catechin and Malvidin-3-O-glucoside in Wine Model Solutions: Identification of a New Family of Ellagitannin-Derived Compounds (Corklins). *Journal of Agricultural and Food Chemistry*, 65(39), 8714-8726. <https://doi.org/10.1021/acs.jafc.7b02845>
- Azevedo, J., Fernandes, I., Lopes, P., Roseira, I., Cabral, M., Mateus, N., & Freitas, V. (2014). Migration of phenolic compounds from different cork stoppers to wine model solutions: antioxidant and biological relevance [journal article]. *European Food Research and Technology*, 239(6), 951-960. <https://doi.org/https://doi.org/10.1007/s00217-014-2292-y>
- Bacon, J. R., & Rhodes, M. J. C. (2000). Binding Affinity of Hydrolyzable Tannins to Parotid Saliva and to Proline-Rich Proteins Derived from It. *Journal of Agricultural and Food Chemistry*, 48(3), 838-843. <https://doi.org/10.1021/jf990820z>
- Bennick, A. (2002). Interaction of plant polyphenols with salivary proteins. *Crit Rev Oral Biol Med*, 13(2), 184-196.
- Brandao, E., Soares, S., Mateus, N., & de Freitas, V. (2014). In vivo interactions between procyanidins and human saliva proteins: effect of repeated exposures to procyanidins solution. *J Agric Food Chem*, 62(39), 9562-9568. <https://doi.org/10.1021/jf502721c>
- Castillo-Fraire, C. M., Brandão, E., Poupard, P., Le Quére, J.-M., Salas, E., de Freitas, V., Guyot, S., & Soares, S. J. F. C. (2020). Interactions between polyphenol oxidation products and salivary proteins: specific affinity of CQA dehydrodimers with cystatins and PB peptide. 128496.
- Cheyrier, V. (2005). Polyphenols in foods are more complex than often thought. *The American journal of clinical nutrition*, 81(1), 223S-229S.
- Deaville, E. R., Green, R. J., Mueller-Harvey, I., Willoughby, I., Frazier, R. A. J. J. o. a., & chemistry, f. (2007). Hydrolyzable tannin structures influence relative globular and random coil protein binding strengths. 55(11), 4554-4561.
- Díaz-Maroto, M. C., López Viñas, M., Marchante, L., Alañón, M. E., Díaz-Maroto, I. J., & Pérez-Coello, M. S. (2021). Evaluation of the Storage Conditions and Type of Cork Stopper on the Quality of Bottled White Wines. *Molecules*, 26(1), 232. <https://doi.org/https://doi.org/10.3390/molecules26010232>
- Dobreva, M. A., Green, R. J., Mueller-Harvey, I., Salminen, J.-P., Howlin, B. J., Frazier, R. A. J. J. o. a., & chemistry, f. (2014). Size and molecular flexibility affect the binding of ellagitannins to bovine serum albumin. 62(37), 9186-9194.
- Fernandes, A., Sousa, A., Mateus, N., Cabral, M., & de Freitas, V. (2011). Analysis of phenolic compounds in cork from *Quercus suber* L. by HPLC–DAD/ESI–MS. *Food Chemistry*, 125(4), 1398-1405. <https://doi.org/https://doi.org/10.1016/j.foodchem.2010.10.016>

- Ferrer-Gallego, R. I., Hernández-Hierro, J. M., Brás, N. r. F., Vale, N., Gomes, P., Mateus, N., de Freitas, V., Heredia, F. J., Escribano-Bailón, M. a. T. J. J. o. a., & chemistry, f. (2017). Interaction between wine phenolic acids and salivary proteins by saturation-transfer difference nuclear magnetic resonance spectroscopy (STD-NMR) and molecular dynamics simulations. *65*(31), 6434-6441.
- Furtado, I., Oliveira, A. S., Amaro, F., Lopes, P., Cabral, M., Bastos, M. d. L., Guedes de Pinho, P., & Pinto, J. (2021). Volatile profile of cork as a tool for classification of natural cork stoppers. *Talanta*, *223*, 121698. <https://doi.org/https://doi.org/10.1016/j.talanta.2020.121698>
- Gao, Y., Tian, Y., Liu, D., Li, Z., Zhang, X.-X., Li, J.-M., Huang, J.-H., Wang, J., & Pan, Q.-H. (2015). Evolution of phenolic compounds and sensory in bottled red wines and their co-development. *Food Chemistry*, *172*, 565-574. <https://doi.org/https://doi.org/10.1016/j.foodchem.2014.09.115>
- García-Estévez, I., Escribano-Bailón, M. T., Rivas-Gonzalo, J. C., & Alcalde-Eon, C. (2010). Development of a fractionation method for the detection and identification of oak ellagitannins in red wines. *Analytica Chimica Acta*, *660*(1), 171-176. <https://doi.org/https://doi.org/10.1016/j.aca.2009.10.020>
- Ginjom, I., D'Arcy, B., Caffin, N., & Gidley, M. (2011). Phenolic compound profiles in selected Queensland red wines at all stages of the wine-making process. *Food Chemistry*, *125*(3), 823-834. <https://doi.org/10.1016/j.foodchem.2010.08.062>
- Glabasnia, A., & Hofmann, T. (2006). Sensory-Directed Identification of Taste-Active Ellagitannins in American (*Quercus alba* L.) and European Oak Wood (*Quercus robur* L.) and Quantitative Analysis in Bourbon Whiskey and Oak-Matured Red Wines. *Journal of Agricultural and Food Chemistry*, *54*(9), 3380-3390. <https://doi.org/10.1021/jf052617b>
- Glabasnia, A., & Hofmann, T. (2007). Identification and Sensory Evaluation of Dehydro- and Deoxy-ellagitannins Formed upon Toasting of Oak Wood (*Quercus alba* L.). *Journal of Agricultural and Food Chemistry*, *55*(10), 4109-4118. <https://doi.org/10.1021/jf070151m>
- Glabasnia, A., Hofmann, T. J. J. o. a., & chemistry, f. (2007). Identification and sensory evaluation of dehydro-and deoxy-ellagitannins formed upon toasting of oak wood (*Quercus alba* L.). *55*(10), 4109-4118.
- Harborne, J., Baxter, H., & Moss, G. (1993). A handbook of bioactive compounds from plants. *Phytochemical dictionary*.
- He, F., Liang, N.-N., Mu, L., Pan, Q.-H., Wang, J., Reeves, M. J., & Duan, C.-Q. (2012). Anthocyanins and their variation in red wines. II. Anthocyanin derived pigments and their color evolution. *Molecules (Basel, Switzerland)*, *17*(2), 1483-1519. <https://doi.org/10.3390/molecules17021483>
- Helmerhorst, E., & Oppenheim, F. J. J. o. d. r. (2007). Saliva: a dynamic proteome. *86*(8), 680-693.
- Hofmann, T., Glabasnia, A., Schwarz, B., Wisman, K. N., Gangwer, K. A., Hagerman, A. E. J. J. o. a., & chemistry, f. (2006). Protein binding and astringent taste of a polymeric procyanidin, 1, 2, 3, 4, 6-penta-O-galloyl- β -D-glucopyranose, castalagin, and grandinin. *54*(25), 9503-9509.
- Hufnagel, J. C., & Hofmann, T. (2008). Orosensory-Directed Identification of Astringent Mouthfeel and Bitter-Tasting Compounds in Red Wine. *Journal of Agricultural and Food Chemistry*, *56*(4), 1376-1386. <https://doi.org/10.1021/jf073031n>
- Humphrey, S. P., & Williamson, R. T. (2001). A review of saliva: normal composition, flow, and function. *The Journal of prosthetic dentistry*, *85*(2), 162-169.
- Huq, N. L., Cross, K. J., Ung, M., Myroforidis, H., Veith, P. D., Chen, D., Stanton, D., He, H., Ward, B. R., Reynolds, E. C. J. I. J. o. P. R., & Therapeutics. (2007). A review of the salivary proteome and peptidome and saliva-derived peptide therapeutics. *13*(4), 547-564.
- Jung, R., & Hamatscheck, J. (1992). Structure and characteristics of natural cork in relation to its use as closure material for bottles. *Wein-Wiss*, *47*, 226-234.
- Karbowiak, T., Gougeon, R. D., Alinc, J.-B., Brachais, L., Debeaufort, F., Voilley, A., & Chassagne, D. (2009). Wine Oxidation and the Role of Cork. *Critical Reviews in Food Science and Nutrition*, *50*(1), 20-52. <https://doi.org/10.1080/10408390802248585>
- Karonen, M., Oraviita, M., Mueller-Harvey, I., Salminen, J.-P., Green, R. J. J. o. A., & Chemistry, F. (2019). Ellagitannins with Glucopyranose Cores Have Higher Affinities to Proteins than Acyclic Ellagitannins by Isothermal Titration Calorimetry. *67*(46), 12730-12740.
- Kauffman, D., Keller, P., Bennick, A., Blum, M. J. C. R. i. O. B., & Medicine. (1993). Alignment of amino acid and DNA sequences of human proline-rich proteins. *4*(3), 287-292.

- Kontoudakis, N., Biosca, P., Canals, R., Fort, F., Canals, J. M., & Zamora, F. (2008). Impact of stopper type on oxygen ingress during wine bottling when using an inert gas cover. *Australian Journal of Grape and Wine Research*, 14(2), 116-122. <https://doi.org/10.1111/j.1755-0238.2008.00013.x>
- Lopes, P., Saucier, C., Teissedre, P.-L., & Glories, Y. (2007). Main Routes of Oxygen Ingress through Different Closures into Wine Bottles. *Journal of Agricultural and Food Chemistry*, 55(13), 5167-5170. <https://doi.org/10.1021/jf0706023>
- Lopes, P., Silva, M. A., Pons, A., Tominaga, T., Lavigne, V., Saucier, C., Darriet, P., Teissedre, P.-L., & Dubourdieu, D. (2009). Impact of Oxygen Dissolved at Bottling and Transmitted through Closures on the Composition and Sensory Properties of a Sauvignon Blanc Wine during Bottle Storage. *Journal of Agricultural and Food Chemistry*, 57(21), 10261-10270. <https://doi.org/10.1021/jf9023257>
- Messana, I., Cabras, T., Inzitari, R., Lupi, A., Zuppi, C., Olmi, C., Fadda, M. B., Cordaro, M., Giardina, B., & Castagnola, M. J. J. o. p. r. (2004). Characterization of the human salivary basic proline-rich protein complex by a proteomic approach. 3(4), 792-800.
- Neveu, V., Perez-Jiménez, J., Vos, F., Crespy, V., du Chaffaut, L., Mennen, L., Knox, C., Eisner, R., Cruz, J., Wishart, D., & Scalbert, A. (2010). Phenol-Explorer: an online comprehensive database on polyphenol contents in foods. *Database*, 2010, bap024-bap024. <https://doi.org/10.1093/database/bap024>
- Nuncio-Jáuregui, N., Nowicka, P., Munera-Picazo, S., Hernández, F., Carbonell-Barrachina, Á. A., & Wojdyło, A. (2015). Identification and quantification of major derivatives of ellagic acid and antioxidant properties of thinning and ripe Spanish pomegranates. *Journal of Functional Foods*, 12, 354-364. <https://doi.org/https://doi.org/10.1016/j.jff.2014.11.007>
- Oppenheim, F., Xu, T., McMillian, F., Levitz, S., Diamond, R., Offner, G., & Troxler, R. J. J. o. B. C. (1988). Histatins, a novel family of histidine-rich proteins in human parotid secretion. Isolation, characterization, primary structure, and fungistatic effects on *Candida albicans*. 263(16), 7472-7477.
- Pinto, J., Oliveira, A. S., Lopes, P., Roseira, I., Cabral, M., Bastos, M. L., & Guedes de Pinho, P. (2019). Characterization of chemical compounds susceptible to be extracted from cork by the wine using GC-MS and (1)H NMR metabolomic approaches. *Food Chem*, 271, 639-649. <https://doi.org/https://doi.org/10.1016/j.foodchem.2018.07.222>
- Puech, J.-L., Mertz, C., Michon, V., Le Guernevé, C., Doco, T., & Hervé du Penhoat, C. (1999). Evolution of Castalagin and Vescalagin in Ethanol Solutions. Identification of New Derivatives. *Journal of Agricultural and Food Chemistry*, 47(5), 2060-2066. <https://doi.org/https://doi.org/10.1021/jf9813586>
- Ramos-Pineda, A. M., García-Estévez, I., Brás, N. r. F., Martín del Valle, E. M., Dueñas, M., Escribano Bailon, M. T. J. J. o. a., & chemistry, f. (2017). Molecular approach to the synergistic effect on astringency elicited by mixtures of flavanols. 65(31), 6425-6433.
- Randhir, R., Lin, Y.-T., & Shetty, K. (2004). Stimulation of phenolics, antioxidant and antimicrobial activities in dark germinated mung bean sprouts in response to peptide and phytochemical elicitors. *Process Biochemistry*, 39(5), 637-646. [https://doi.org/https://doi.org/10.1016/S0032-9592\(03\)00197-3](https://doi.org/https://doi.org/10.1016/S0032-9592(03)00197-3)
- Rasines-Perea, Z., Jacquet, R., Jourdes, M., Quideau, S., & Teissedre, P.-L. (2019). Ellagitannins and Flavano-Ellagitannins: Red Wines Tendency in Different Areas, Barrel Origin and Ageing Time in Barrel and Bottle. 9(8), 316. <https://www.mdpi.com/2218-273X/9/8/316>
- Reis, S. F., Coelho, E., Evtuguin, D. V., Coimbra, M. A., Lopes, P., Cabral, M., Mateus, N., & Freitas, V. (2020). Migration of Tannins and Pectic Polysaccharides from Natural Cork Stoppers to the Hydroalcoholic Solution. *Journal of Agricultural and Food Chemistry*, 68(48), 14230-14242. <https://doi.org/10.1021/acs.jafc.0c02738>
- Reis, S. F., Teixeira, T., Pinto, J., Oliveira, V., Lopes, P., Cabral, M., Mateus, N., Guedes de Pinho, P., Pereira, H., & de Freitas, V. (2020). Variation in the Phenolic Composition of Cork Stoppers from Different Geographical Origins. *Journal of Agricultural and Food Chemistry*, 68(50), 14970-14977. <https://doi.org/10.1021/acs.jafc.0c00586>
- Reynolds, D., Rahman, I., Bernard, S., & Holbrook, A. (2018). What effect does wine bottle closure type have on perceptions of wine attributes? *International Journal of Hospitality Management*, 75, 171-178. <https://doi.org/https://doi.org/10.1016/j.ijhm.2018.05.023>
- Rothwell, J. A., Perez-Jimenez, J., Neveu, V., Medina-Remón, A., M'Hiri, N., García-Lobato, P., Manach, C., Knox, C., Eisner, R., Wishart, D. S., & Scalbert, A. (2013). Phenol-Explorer 3.0: a major update of the Phenol-Explorer database to incorporate data on the effects of food processing on polyphenol content. *Database*, 2013. <https://doi.org/10.1093/database/bat070>

- Santos, S. A. O., Villaverde, J. J., Sousa, A. F., Coelho, J. F. J., Neto, C. P., & Silvestre, A. J. D. (2013). Phenolic composition and antioxidant activity of industrial cork by-products. *Industrial Crops and Products*, 47, 262-269. <https://doi.org/https://doi.org/10.1016/j.indcrop.2013.03.015>
- Schlesinger, D. H., Hay, D. I., & Levine, M. J. (1989). Complete primary structure of statherin, a potent inhibitor of calcium phosphate precipitation, from the saliva of the monkey, *Macaca arctoides*. *Int J Pept Protein Res*, 34(5), 374-380. <https://doi.org/10.1111/j.1399-3011.1989.tb00705.x>
- Schulze, T. (2021). *MassBank Europe* <https://massbank.eu/MassBank/>
- Schwarz, M., Jerz, G., & Winterhalter, P. (2003). Isolation and structure of Pinotin A, a new anthocyanin derivative from Pinotage wine [Article]. *Vitis*, 42(2), 105-106.
- Silva, M. S., Garcia-Estevez, I., Brandão, E., Mateus, N., de Freitas, V., Soares, S. J. J. o. a., & chemistry, f. (2017). Molecular interaction between salivary proteins and food tannins. 65(31), 6415-6424.
- Soares, S., Brandão, E., García-Estevez, I., Fonseca, F., Guerreiro, C., Ferreira-da-Silva, F., Mateus, N., Deffieux, D., Quideau, S., & de Freitas, V. (2019). Interaction between Ellagitannins and Salivary Proline-Rich Proteins. *Journal of Agricultural and Food Chemistry*, 67(34), 9579-9590. <https://doi.org/10.1021/acs.jafc.9b02574>
- Soares, S., Brandão, E., García-Estevez, I., Fonseca, F., Guerreiro, C., Ferreira-da-Silva, F., Mateus, N., Deffieux, D., Quideau, S. p., De Freitas, V. J. J. o. a., & chemistry, f. (2019). Interaction between Ellagitannins and salivary proline-rich proteins. 67(34), 9579-9590.
- Soares, S., Mateus, N., & de Freitas, V. (2012). Interaction of different classes of salivary proteins with food tannins. *Food Research International*, 49(2), 807-813. <https://doi.org/https://doi.org/10.1016/j.foodres.2012.09.008>
- Soares, S., Mateus, N., De Freitas, V. J. J. o. A., & Chemistry, F. (2007). Interaction of different polyphenols with bovine serum albumin (BSA) and human salivary α -amylase (HSA) by fluorescence quenching. 55(16), 6726-6735.
- Soares, S., Vitorino, R., Osorio, H., Fernandes, A., Venancio, A., Mateus, N., Amado, F., & de Freitas, V. (2011). Reactivity of human salivary proteins families toward food polyphenols. *J Agric Food Chem*, 59(10), 5535-5547. <https://doi.org/10.1021/jf104975d>
- Tchouakeu Betnga, P. F., de Matos, A. D., Longo, E., & Boselli, E. (2020). Impact of closure material on the chemical and sensory profiles of grappa during storage in bottle. *LWT*, 110014. <https://doi.org/https://doi.org/10.1016/j.lwt.2020.110014>
- Tsao, R. (2010). Chemistry and biochemistry of dietary polyphenols. *Nutrients*, 2(12), 1231-1246. <https://doi.org/10.3390/nu2121231>
- Varea, S., Garcia-Vallejo, M. C., Cadahia, E., & de Simon, B. F. (2001). Polyphenols susceptible to migrate from cork stoppers to wine. *European Food Research and Technology*, 213(1), 56-61. <https://doi.org/https://doi.org/10.1007/s002170100327>
- WatreLOT, A. A., Heymann, H., & Waterhouse, A. L. (2020). Red Wine Dryness Perception Related to Physicochemistry. *Journal of Agricultural and Food Chemistry*, 68(10), 2964-2972. <https://doi.org/https://doi.org/10.1021/acs.jafc.9b01480>
- Yang, P., Li, H., Wang, H., Han, F., Jing, S., Yuan, C., Guo, A., Zhang, Y., & Xu, Z. (2017). Dispersive Liquid-Liquid Microextraction Method for HPLC Determination of Phenolic Compounds in Wine. *Food analytical methods*, 10(7), 2383-2397. <https://doi.org/https://doi.org/10.1007/s12161-016-0781-2>

Supplementary material

Table S1. Volumes mixed of each solution used for the interaction between a fraction and SP.

Condition	Saliva volume (μL)	Wine Model Solution volume (μL)	Stock fraction volume (μL)
Control saliva	96.4	53.6	0.0
0.25 g.L ⁻¹		45.0	8.6
0.50 g.L ⁻¹		36.4	17.1
1.00 g.L ⁻¹		17.1	36.4
1.50 g.L ⁻¹		0.0	53.6
Control fraction	0.0	96.4	53.6

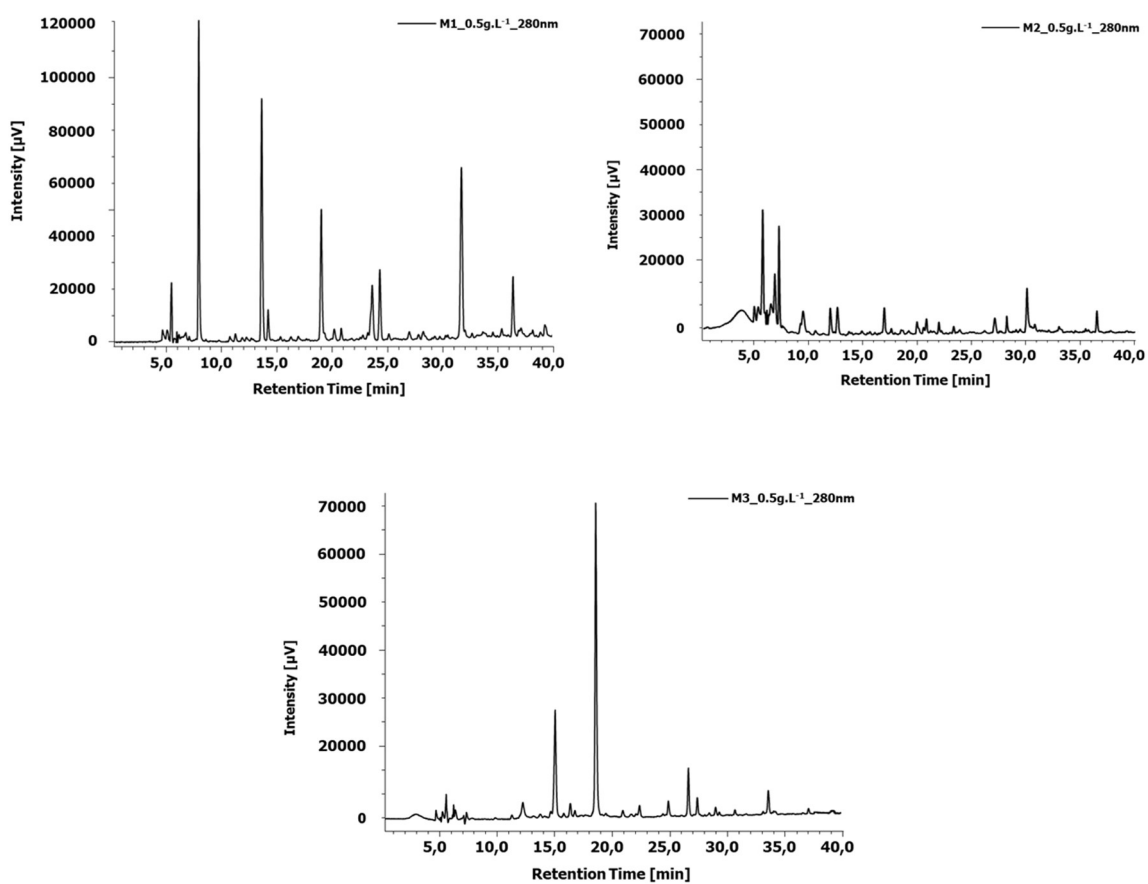


Figure S1. Chromatogram at 280 nm of each fraction at concentration of 0.5 g.L⁻¹ analysed by HPLC (conditions in experimental Section).

Migration of phenolic compounds from cork to wine: reactivity and sensory implications

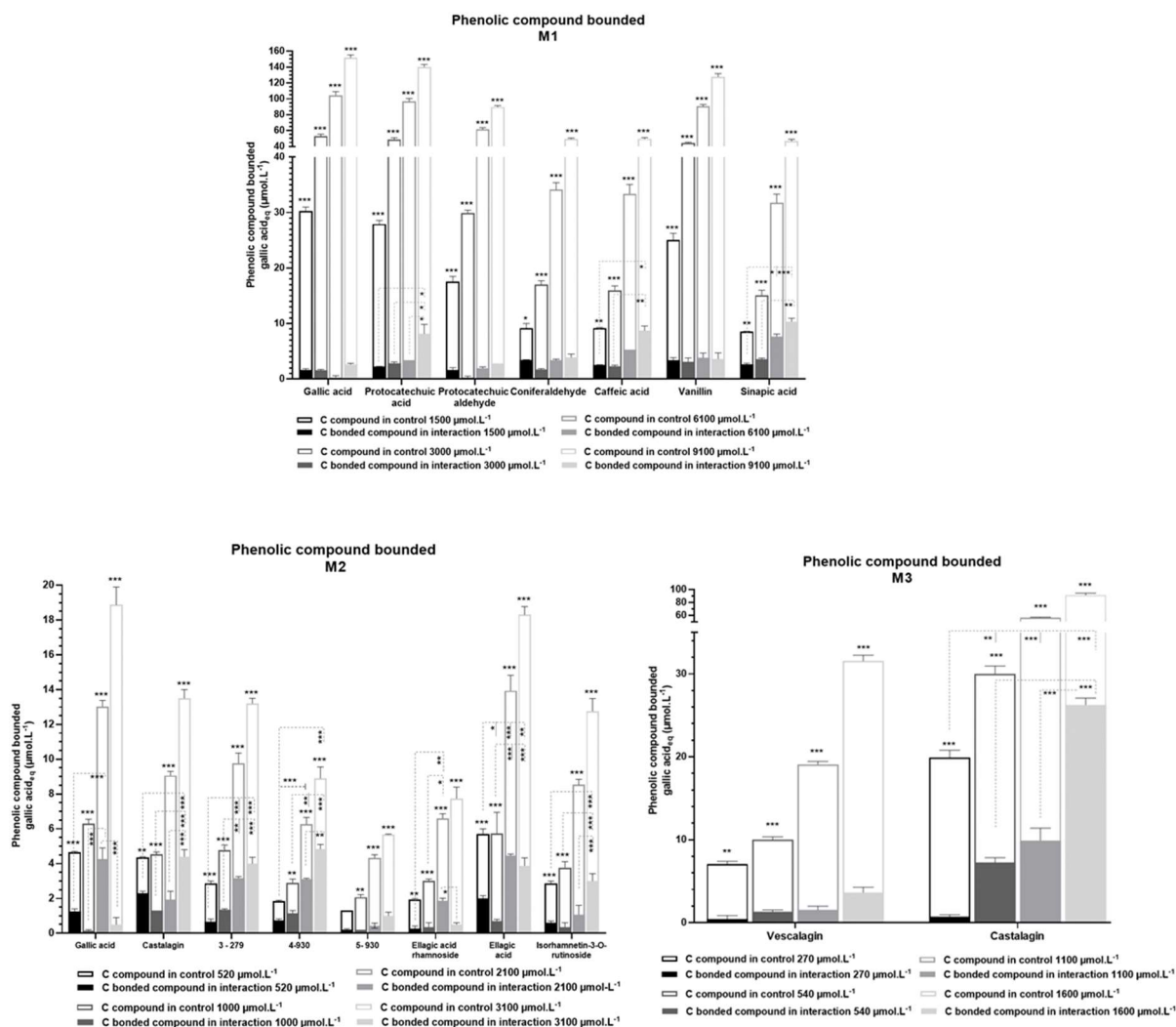


Figure S2. Concentration of each compound in fractions M1, M2 and M3 and concentration that was bounded upon the interaction with SP. It is presented the four different initial fraction molarities evaluated, the bar without filling corresponds to the initial concentration of the compound and the filled bars correspond to the concentration of this compound that is precipitated after interaction with SP.

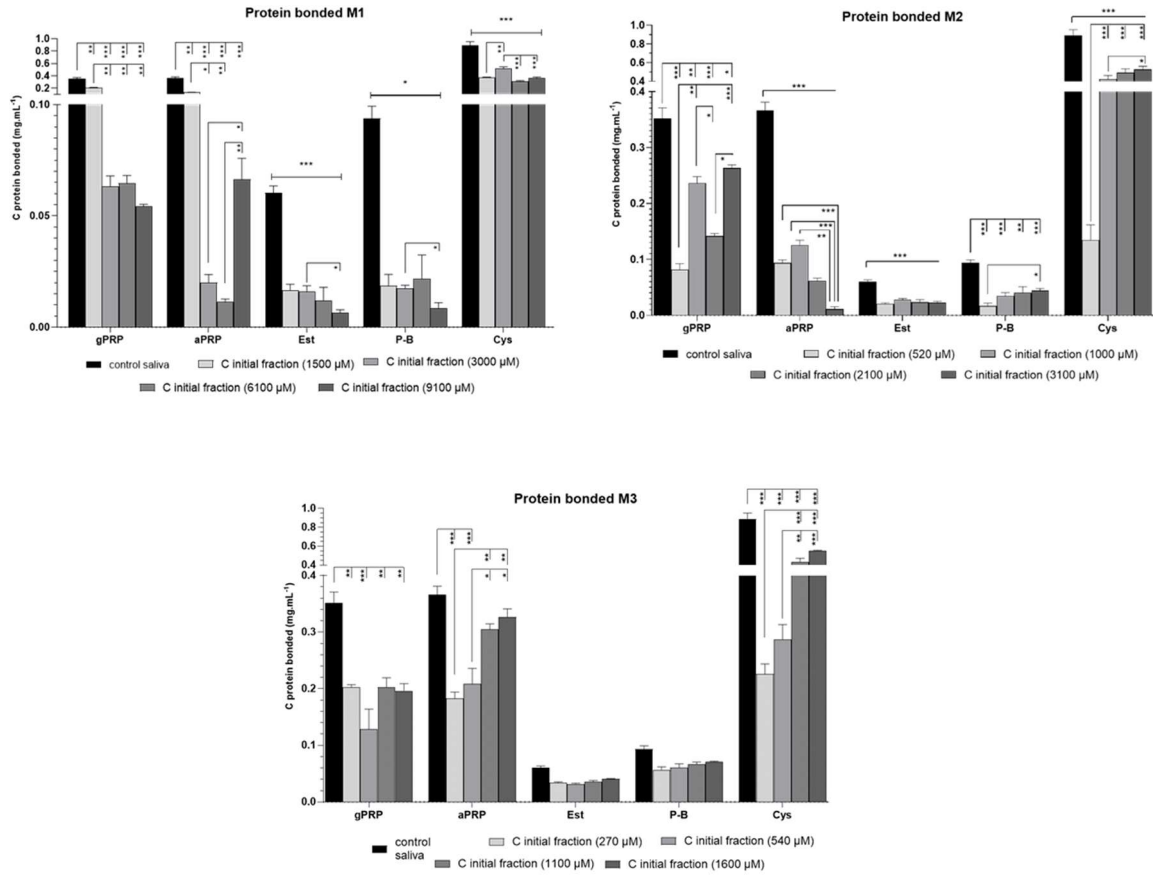


Figure S3. Concentration of precipitated proteins for each family of salivary proteins upon the interaction with each fraction (M1, M2 and M3) at each fraction concentration.

Chapter 2- On the Limits of Anthocyanins Co-Pigmentation Models and Respective Equations

Abstract

Anthocyanins co-pigmentation models with application on 1:1 complexes were revisited, and their limitations were critically commented. The flavylium multistate of species is dramatically simplified to a single acid–base equilibrium between flavylium cation and its conjugated base CB, equal to the sum of quinoidal base, hemiketal, and *cis* and *trans*-chalcones. Bearing this, a new equation that simultaneously allows calculation of the co-pigmentation constant with flavylium cation (K_{AH+CP}) and with its conjugated base CB (K_{CBCP}) was deduced. This equation can be used at a fixed co-pigment concentration with pH as a variable or at fixed pH and co-pigment concentration variable. A global fitting of all data allows us to calculate both association constants with good accuracy. The model was applied to the co-pigmentation of malvidin-3-glucoside with caffeine and pentagalloyl glucose (PGG). Caffeine gives rise to complexes not only with flavylium cation $K_{AH+CP} = 125 \pm 7 \text{ M}^{-1}$ but also with CB with $K_{CBCP} = 23 \pm 3 \text{ M}^{-1}$. PGG complexes exclusively with flavylium cation, $K_{AH+CP} = 914 \pm 10 \text{ M}^{-1}$, and the possible interaction with quinoidal base is lower than the detection limits that the inherent experimental error permits.

Keywords: anthocyanins, co-pigmentation constants, co-pigmentation models, caffeine, pentagalloyl glucose, oenin.

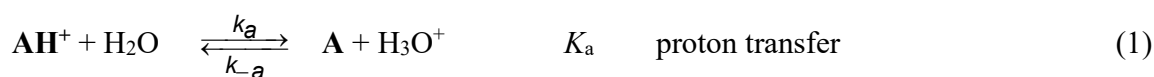
Introduction

Anthocyanins are ubiquitous molecules that confer colour to plants in particular to most flowers and fruits (Andersen 2006, Dangles and Fenger 2018, Silva, Silva et al. 2020). The same anthocyanin could exhibit different colours and hues depending on pH and the presence of other compounds. The term co-pigmentation effect was used by Robinson to define the modifications of the anthocyanins absorption spectrum caused by colorless compounds, such as amino acids, sugars and flavonoids Robinson & Robinson, 1931). A comparable phenomenon due to the increasing of anthocyanins concentration was reported by Asen (Asen et al., 1972). Based on the similarity between these two effects, go to proposed a unified mechanism for co-pigmentation and self-association, which he called the molecular stacking theory. (Goto and Kondo 1991)(Goto

1987),(Yoshida, Mori et al. 2009). Therefore, the chemical driving forces for co-pigmentation and self-association are considered to be the same: the hydrophobic aromatic residues assemble in aqueous solutions (Yoshida et al, 2009). This theory was also extended to polyacylated anthocyanins(Goto and Kondo 1991):(Goto 1987),(Yoshida, Mori et al. 2009). It is known that copigmentation has a high impact on food color, its stability and intensity (Trouillas et al, 2016). For instance, at the wine pH (3.2-3.8), anthocyanins are predominantly present in their non-colored neutral forms, however, the intense red color displayed by young red wines is mainly due to the interaction of the flavylium cation of anthocyanins with other wine components including phenolic acids, flavanols and flavanones (Boulton 2001, He, Liang et al. 2012, Fanzone, Gonzalez-Manzano et al. 2015).

The main question when studying the interaction of anthocyanins with other compounds, in particular co-pigmentation, is the fact that these compounds are a complex system with several species that are reversibly interconnected by external stimuli such as pH, light and temperature. In theory all species could be able to complex with the co-pigment (Pina et al, 2015).

In acidic to moderately acidic medium, anthocyanins equilibrium is given by eq. (1) to eq. (4)



This complex system can be dramatically simplified to a single acid-base equilibrium, eq. (5) (Brouillard et al, 1978; Pina et al, 2015).



With $[\text{CB}] = [\text{A}] + [\text{B}] + [\text{Cc}] + [\text{Ct}]$

In this case, the mole fraction distribution of all multistate species is given by eq. (6) (Pina et al, 2014).

$$\chi_{AH^+} = \frac{[H^+]}{[H^+] + K'_a}; \quad \chi_A = \frac{K_a}{[H^+] + K'_a}; \quad \chi_B = \frac{K_h}{[H^+] + K'_a}; \quad \chi_{Cc} = \frac{K_h K_t}{[H^+] + K'_a}; \quad \chi_{\alpha} = \frac{K_h K_t K_i}{[H^+] + K'_a} \quad (6)$$

When there is a high isomerization barrier, the pseudo-equilibrium can be defined. It is a transient state reached before formation of significant amounts of *trans*-chalcone, with a (pseudo) equilibrium constant given by $K_a^{\wedge} = K_a + K_h + K_h K_t$ and $[CB^{\wedge}] = [A] + [B] + [Cc]$. All mathematical expressions deduced for the equilibrium can be used at the pseudo-equilibrium by substituting K'_a by K_a^{\wedge} .

In this work we are revisiting the equations used in literature to account for the co-pigmentation effect and propose new approaches to deal with these systems.

Materials and methods

Reagents

Sodium citrate dehydrated and citric acid monohydrated were purchase from Sigma-Aldrich, Spain and caffeine was obtained from Fluka. Pentagaloylglucose (PGG) was prepared from tannic acid according to the procedure described in the literature (Chen and Hagerman 2004, Soares, Kohl et al. 2013) and then purified by column chromatography using TSK-Toyopearl HW-40 gel by elution with methanol. Malvidin-3-glucoside (Oenin) was isolated from a young red wine (*Vitis vinifera* L. cv. Touriga Nacional) as described in the literature (Araujo et al, 2017). The Theorell and Stenhagen universal buffer ("Küster FW, Thiel A. Tabelle per le Analisi Chimiche e Chimico- Fische. 12 th ed Milano, Italy: Hoepli; 1982. p. 157–60.") was prepared dissolving 2.25 mL of phosphoric acid 85% (w/w), 7.00 g of monohydrated citric acid, 3.54 g of boric acid and 343 mL of a 1 M NaOH solution in Millipore water until 1 L.

Copigmentation studies

Fixed co-pigment concentration, changing pH.

The pH titration of oenin (4×10^{-5} M) in the presence of two co-pigments (caffeine and pentagalloylglucose) was performed by UV-visible spectroscopy using the pH jump technique from pH = 1 to higher pH values from ~ 2.0 to ~ 5.5. Stock solutions of oenin and co-pigments were prepared in 0.1 M HCl. For caffeine, two fixed concentrations were used 8×10^{-3} and 2.4×10^{-2} M and for pentagalloylglucose, 2.4×10^{-3} M. Moreover, for this later a final concentration of 10% (v/v) ethanol was used due to the low solubility of this co-pigment in water. Then, to plastic 10x10 mm cuvettes 500 μ L of a 0.1 M NaOH

solution, 500 μL of a Theorell and Stenhagen universal buffer solution adjusted to different pH values from 2 to 5.5, 250 μL of the co-pigment stock solution and 250 μL of oenin stock solution (2.4×10^{-4} M) were added. Similar experiments were performed in the absence of co-pigments. The absorption spectra of the different solutions were obtained after equilibration in the dark during one day (equilibrium acidity constant, $\text{p}K'_a$) in a Thermo Scientific Evolution Array UV-Visible spectrophotometer at 25°C. The pH values of all solutions were measured in a WTW pH 320 (Weilheim, Germany) with a CRISON 5209 combined glass electrode of 3 mm diameter (Barcelona, Spain). The pH meter was calibrated with pH 4 and 7 buffer solutions. Fittings for $\text{p}K'_a$ determination were carried out using the Solver program from Microsoft Excel. Similar experiments were performed in the absence of co-pigments.

Fixed pH and co-pigment concentration change.

Oenin copigmentation constants were determined by UV-visible spectroscopy at pH 1 (K_{AH+CP}) and 3.5 (both K_{AH+CP} and K_{CBGP}). For that, a solution of oenin at 4.6×10^{-5} M was prepared in 0.1 M HCl (solution A). A solution containing the same concentration of oenin and each co-pigment at a concentration of 8×10^{-3} M for caffeine and 5×10^{-3} M for pentagalloylglucose was added (Solution B). Then, solutions with different concentration of each co-pigment were obtained by the addition of small volumes of the solution B to the solution A. The visible absorption spectrum of all solutions were recorded in a Thermo Scientific Evolution Array UV-visible spectrophotometer from 350-700 nm in a 10x10 mm quartz cell.

Oenin co-pigmentation constants K_{AH+CP} were determined using Malien-Aubert.(Malien-Aubert et al, 2002) eq.(14) presented below. The r parameter represents the ratio between the molar absorption coefficient of the complex (oenin – co-pigment at the maximum molar ratio) and the free flavylum ion. The fittings for the association constants were carried out using the Solver program from Microsoft Excel.

Similar experiments were performed at pH ~ 3.5 using a 10 mM citrate buffer. For that, a solution of oenin was prepared in citrate buffer (cuvette A). Moreover, a solution containing the same concentration of oenin and the co-pigment at a concentration of 5×10^{-3} M (pentagalloylglucose) or 8×10^{-3} M (caffeine) was prepared in the same buffer (cuvette B). After a period of stabilization during 30 minutes in the absence of light, spectra from 350 to 700 nm of both solutions were recorded in a Thermo Scientific Evolution Array UV-visible spectrophotometer using a 10x10 mm quartz cell. Then, solutions with different concentrations of co-pigment were obtained by addition of small

volumes from cuvette B to cuvette A and recording their UV-visible spectra. The absorbance of each solution at a selected wavelength (where it is observed the higher difference between oenin flavylum cation in the absence and presence of co-pigment) was plotted as a function of co-pigment concentration (M) and the co-pigmentation constants with the neutral species (K_{CBP}) were determined using a model described herein (see below). The fittings for the co-pigmentation constants were carried out using the Solver program from Microsoft Excel.

Results and discussion

Theory

Flavylium cation as the sole species in solution (pH≤1)

When flavylium cation is the sole species in solution, eq. (7) accounts for the co-pigmentation.



The model here described is valid for a 1:1 stoichiometry, does not account for a sequence of complexes of the type 1:1, 1:2, (flavylium cation:co-pigment), etc, and requires an excess of co-pigment in comparison with the anthocyanin concentration to consider [CP], the added co-pigment, in the equilibrium constant of eq. (7).

The mass balance for all species involving the anthocyanin gives eq. (8) with C_0 the total concentration of anthocyanin.

$$C_0 = [AH^+] + [AH^+CP] = [AH^+](1 + K_{AH^+CP}[CP]) \quad (8)$$

From eq. (8), the mole fraction distribution of the two species is achieved, eq. (9)

$$\chi_{AH^+} = \frac{[AH^+]}{C_0} = \frac{1}{1 + K_{AH^+CP}[CP]} \quad \chi_{AH^+CP} = \frac{K_{AH^+CP}[CP]}{1 + K_{AH^+CP}[CP]} \quad (9)$$

On the other hand, the absorbance A_λ is given by eq. (10), a generalization of the Lambert-Beer law.

$$A_\lambda = C_0(\varepsilon_{AH^+}\chi_{AH^+} + \varepsilon_{AH^+CP}\chi_{AH^+CP}) \quad (10)$$

Introducing the parameter eq. (11) r_{AH^+CP} (Brouillard et al, 1989)

$$r_{AH^+CP} = \frac{\varepsilon_{AH^+CP}}{\varepsilon_{AH^+}} \quad (11)$$

With ε_{AH^+} and ε_{AH^+CP} respectively the mole absorption coefficients of the flavylum cation and its complex. Substituting the mole fractions in eq.(10) by their values in eq.(9), the absorbance is given by eq.(12), with . $A_0 = C_0 \varepsilon_{AH^+}$

$$A_\lambda = A_0 \frac{(1+r_{AH^+CP}K_{AH^+CP}[CP])}{(1+K_{AH^+CP}[CP])} \quad (12)$$

This is the expression for the flavylum co-pigmentation with the restrictions above defined.

Or in its linear form after Malien-Aubert *et al* (Malien-Aubert et al, 2002)

$$\frac{A_0}{A_\lambda - A_0} = \frac{1}{(r_{AH^+CP} - 1)} + \frac{1}{(r_{AH^+CP} - 1)K_{AH^+CP}} \frac{1}{[CP]} \quad (13)$$

The parameters r_{AH^+CP} and K_{AH^+CP} are obtained from a non-linear fitting of eq.(12) or from the intercept and slope of eq.(13). In some systems a plateau of A_λ versus $[CP]$ is reached, indicating that all flavylum cation is complexed, which permits the direct calculation of r_{AH^+CP} from the ratio of the absorption at the plateau and the absorbance in the absence of the co-pigment.

Exclusive 1:1 complexation with flavylum cation at higher pH values.

In this case, the other forms of the flavylum multistate have to be considered in spite of not interacting with the co-pigment.

The following expression was reported by Malien-Aubert *et al*. (Malien-Aubert et al, 2002)

$$A_\lambda = A_{0(pH)} \frac{1+r_{AH^+CP}K_{AH^+CP}[CP]}{1+aK_{AH^+CP}[CP]} \quad (\text{C. Malien-Aubert et al}) \quad (14)$$

or in its linear form

$$\frac{A_{0(pH)}}{A_\lambda - A_{0(pH)}} = \frac{a}{r_{AH^+CP} - a} + \frac{1}{(r_{AH^+CP} - a)K_{AH^+CP}[CP]} \quad (15)$$

With $A_{0(pH)}$ the absorption before addition of co-pigment at the working pH and a given by eq. (16)

$$a = \frac{1}{1 + K_h 10^{pH}} \quad (16)$$

At this point a clarification of the meaning of the parameter a is necessary. This parameter is given by eq. (17) (Malien-Aubert et al, 2002).

$$a = \frac{1}{1 + K_h 10^{pH}} = \frac{1}{1 + K_h \frac{1}{10^{-pH}}} = \frac{1}{1 + \frac{K_h}{[H^+]}} = \frac{[H^+]}{[H^+] + K_h} \quad (17)$$

K_h is generally used to account for the equilibrium between flavylum cation and hemiketal, eq. (18), and strictly the parameter a is the mole fraction of AH^+ in its equilibrium with hemiketal B.



However, these authors consider this constant in a broader sense as $K_h = K_h(1 + K_t)$. In common anthocyanins K_a is significantly smaller than $K_h(1 + K_t)$ and the constant K_h defined by Malien-Aubert *et al* is similar to $K'_a = K_a + K_h(1 + K_t)$ used by other authors to define the so called pseudo-equilibrium, as defined above (Pina et al, 2014). (NOTE: The pseudo-equilibrium is a transient state reached before formation of significant amounts of trans-chalcone). Measurements carried out at the equilibrium should use the global equilibrium constant K'_a , see below. In anthocyanins K'_a and K_a are very similar because the mole fraction of *trans*-chalcone at the equilibrium is relatively small. However, in 3-deoxyanthocyanins and many other flavylum based multistate systems they could be very different and the correct expression for a in measurements carried out at the equilibrium should be defined by eq. (20), which is also the experimental parameter, directly obtained from the inflection point of the anthocyanin absorbance versus pH in the absence of co-pigment.

$$a = \frac{[H^+]}{[H^+] + K'_a} \quad (20)$$

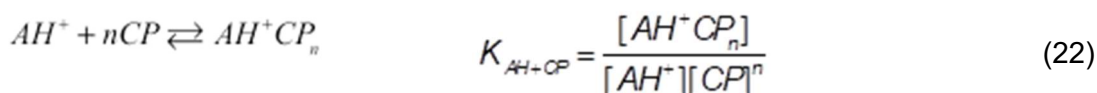
In appendix 1 the following expression was deduced by the usual mass balance and definition of the Lambert-Beer law. This deduction requires the use of the constants K_a if carried out at the equilibrium or K_a^* at the pseudo-equilibrium.

$$A_\lambda = A_0 \left\{ \frac{[H^+](1 + r_{AH^+CP} K_{AH^+CP} [CP])}{(1 + K_{AH^+CP} [CP])[H^+] + K_a^*} \right\} \quad (21)$$

As shown in the same appendix 1, eq.(21) and eq.(14) are exactly the same but in the first, $A_{0(pH)}$ is the absorption of the flavylum cation at the working pH in the absence of co-pigment while in eq.(21) $A_0 = \varepsilon_{AH^+} C_0$ is, the absorption of flavylum cation when it is the sole species (optical path 1cm ε_{AH^+} in $cm^{-1}M^{-1}$).

Some expressions regarding the complexation models previously reported in literature and still used by some authors could lead to misunderstandings (Zhao, Ding et al. 2020),(Zhu, Chen et al.),(Zhang, Wang et al. 2020),(Kanha, Surawang et al. 2019),(Zhang, He et al. 2016),(Fanzone, Gonzalez-Manzano et al. 2015),(Zhang, He et al. 2015), (Zhang, Liu et al. 2015) and for this reason this aspect will be discussed in the next paragraphs.

Based on the possibility of complexation as in eq. (22), Brouillard (Brouillard et al, 1989) deduced eq. (23) that was used at pH=3.65.



$$\frac{A - A_{0(pH)}}{A_{0(pH)}} = r_{AH^+CP} K_{AH^+CP} [CP]^n \quad (23)$$

In its logarithm form eq. (24) would allow calculation of the complex stoichiometry.

$$\ln \frac{A - A_{0(pH)}}{A_{0(pH)}} = \ln(r_{AH^+CP} K_{AH^+CP}) + n \ln [CP] \quad (24)$$

Without loss of generality for n=1 the ratio $\frac{A - A_{0(pH)}}{A_{0(pH)}}$ can be re-calculated from the C. Malien-Aubert *et al* eq.(14).(Malien-Aubert *et al*, 2002)

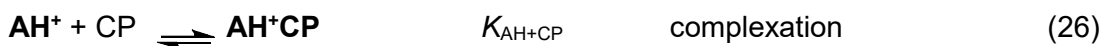
$$\frac{A_\lambda - A_{0(pH)}}{A_{0(pH)}} = \frac{r_{AH^+CP} K_{AH^+CP} [CP] - a K_{AH^+CP} [CP]}{1 + a K_{AH^+CP} [CP]} \quad (25)$$

Eq.(25) gives eq.(23) only if $a=0$ or $aK_{AH+CP}[CP]^n \ll 1$ and $a \ll r_{AH^+CP}$

At pH=3.65 the parameter a is small (0.08 for an anthocyanin with $pK'_a=2.6$) but necessarily different from 0 and the second approximation is dependent on the concentration of [CP] and the value of the association constant. In Brouillard's paper (Brouillard et al, 1989) the values of a , K_{AH+CP} and [CP] permitted to consider eq.(23) as a good approximation but this equation is not as general as the one of Malien-Aubert (Malien-Aubert et al, 2002) *et al*, eq.(14). In appendix 1 a simulation comparing these two equations is reported.

Complexation with flavylum cation and the other forms of the multistate.

The expression deduced by C. Malien-Aubert *et al*. eq. (14) (Malien-Aubert et al, 2002) is restricted to the complexation with flavylum cation. In this work, we deduced and applied one expression that is able to calculate simultaneously the association constant with flavylum cation and a weighted sum of the constant of the co-pigmentation of CB, profiting from the fact that this complex system is equivalent to a single acid base involving flavylum cation and its conjugate base.



As shown in appendix 2, with all mathematical details included, eq.(28) can be straightforwardly deduced by means of mass balance and the generalized Lambert-Beer law.

$$A_\lambda = A_0 \left\{ \frac{(1+r_{AH+CP} K_{AH+CP} [CP])[H^+] + r_{CB} + r_{CB \cdot CP} [CP]}{(1+K_{AH+CP} [CP])[H^+] + (1+K_{CB \cdot CP} [CP]) K'_a} \right\} \quad (28)$$

In eq.(28) K_{AH+CP} and r_{AH+CP} were defined above in eq.(7) and eq.(11). The association constant $K_{CB \cdot CP}$ is the one of eq. (27), see appendix 2.

$$K_{CB \cdot CP} = \frac{(K_{ACP} K'_a + K_{BCP} K_h + K_{CCP} K_h K_i + K_{ClCP} K_h K_i K_j)}{K'_a} \quad (29)$$

The parameter $r_{CB \cdot CP}$ is given by eq. (30)

$$r_{CB} = (r_{ACP} K_a K_{ACP} + r_{BCP} K_h K_{BCP} + r_{CCP} K_h K_t K_{CCP} + r_{CTP} K_h K_t K_j K_{CTP}) \quad (30)$$

The parameter r_{CB} , eq. (31) is calculated from the initial absorbance in the absence of co-pigment, eq. (32).

$$r_{CB} = r_A K_a + r_B K_h + r_C K_h K_t + r_{CT} K_h K_t K_j \quad (31)$$

$$A_{\lambda(CP=0)} = A_0 \left\{ \frac{[H^+] + r_{CB}}{[H^+] + K'_a} \right\} \quad (32)$$

The parameters r_{CB} and r_{CB} are dependent on the wavelength selected to carry out the measurements.

In summary, provided that K'_a is calculated from the pH dependent absorbance of the anthocyanins in the absence of the co-pigment (the standard procedure), eq. (28) needs the fitting of four parameters r_{AH+CP} , K_{AH+CP} defined in eq. (11) and eq.(7) respectively and r_{CB} and K_{CB} respectively eq.(29) and eq.(30). The fact that four parameters need to be fitted requires several sets of experiments and a global fitting. Eq. (28) can be used at a fixed pH as a function of the co-pigment concentration. The parameters r_{AH+CP} , K_{AH+CP} are measured with much more accuracy at pH=1 since eq. (28) are basically function of r_{AH+CP} , K_{AH+CP} , while at pH=3.6 or higher are dependent on r_{CB} and K_{CB} . However, eq. (28) can also be used at a fixed co-pigment concentration changing pH. In this case, we have done the experiments at two co-pigment concentrations and the global fitting is thus carried out in four different independent sets of experiments.

The co-pigmentation constant K_{CB} is the sum of the individual co-pigmentation constants weighted by respective mole fractions of each component of CB (in the absence of co-pigment). It is not possible to access the individual contribution of each of these species. This limitation cannot be overcome by UV-Vis absorption because this technique does not allow a clearly separation of the signal of each CB species. Only reverse pH jumps followed by stopped flow permit to overcome this drawback.² Nevertheless, K_{CB} has an important meaning because accounts for the global co-pigmentation of the species **A**, **B**, **Cc** and **Ct**.

Previous equations

In this section we describe previous equations that paved the way to eq. (28). Brouillard reported eq. (33) and eq. (35) that used together were claimed to permit the calculation

of the copigmentation constants with flavylum cation quinoidal base and anionic quinoidal base (Brouillard et al, 1991).

The first one was defined for the pH range $0.5 < \text{pH} < \text{ca. } 6$ to account for the copigmentation with flavylum cation and quinoidal base

$$\begin{aligned}
 \frac{D - D_0}{D_0} &= \frac{1 + K_S[\text{CP}]}{1 + K_T[\text{CP}]} - 1 \\
 K_S &= \frac{r_1 K_1 [\text{H}^+] + r_3 K_2 K_a}{[\text{H}^+] + r_2 K_a}; \quad K_T = \frac{K_1 [\text{H}^+] + K_2 K_a}{[\text{H}^+] + K_a + K_h}
 \end{aligned} \tag{33}$$

Where $K_1 = K_{\text{AH}^+\text{CP}}$, $K_2 = K_{\text{ACP}}$, $r_1 = \frac{\varepsilon_{\text{AH}^+\text{CP}}}{\varepsilon_{\text{AH}^+}}$, $r_2 = \frac{\varepsilon_A}{\varepsilon_{\text{AH}^+}}$, $r_3 = \frac{\varepsilon_{\text{ACP}}}{\varepsilon_{\text{AH}^+}}$ (34)

D and D_0 the absorbance in the presence and absence of copigment define in our notation by A_λ and $A_{\lambda(\text{pH})}$.

The second one for $\text{ca. } 6 < \text{pH} < 8$ to account for copigmentation with quinoidal base and anionic quinoidal base

$$\begin{aligned}
 \frac{D - D_0}{D_0} &= \frac{1 + K_S[\text{CP}]}{1 + K_T[\text{CP}]} - 1 \\
 K_S &= \frac{r_4 K_2 [\text{H}^+] + r_6 K_3 K_A}{[\text{H}^+] + r_5 K_A}; \quad K_T = \frac{K_2 [\text{H}^+] + K_3 K_A}{K_A + [\text{H}^+] (1 + K_H)}
 \end{aligned} \tag{35}$$

Where $K_3 = K_{\text{ACP}}$, $K_2 = K_{\text{ACP}}$, $r_4 = \frac{\varepsilon_{\text{ACP}}}{\varepsilon_A}$, $r_5 = \frac{\varepsilon_A}{\varepsilon_A}$, $r_6 = \frac{\varepsilon_{\text{ACP}}}{\varepsilon_A}$, $K_H = \frac{K_a}{K_h}$ (36)

And K_A the association constant of the copigment with anionic quinoidal base.

Eq. (33) and eq. (35) were represented at fixed concentration of the co-pigment as a function of pH (Fig.3 of reference (Brouillard et al, 1991)). The fitting requires the optimization of 3 copigmentation constants and 6 r_n parameters. This huge number of adjusting parameters prevents a reliable accuracy of the mathematical solutions. Another limitation of this procedure is the fact that copigmentations with other species of the multistate are neglected. It is firmly established that for example with the copigment caffeine *cis* and *trans* chalcones have significant copigmentation constants (Dangles and Elhajji 1994, Mendoza, Basilio et al. 2019). A minor detail, *trans*-chalcone is neglected in the calculations. In other words, $K_a + K_h$ in these expressions should be substituted by K_a , as already mentioned eq. (20).

Extension of the Malien-Aubert equation to the 1:2 equilibria was reported by Dangles, see appendix 4 (Dangles et al, 1994). This equation is an excellent improving towards a more general equation but only considers the absorbance of flavylum cation and the 1:1 and 1:2 complexes. Nevertheless, this model proved unequivocally the formation of 1:1 together with 1:2 complexes for the copigment chlorogenic acid. It is worth of note that the changes of the anthocyanin model absorbance in the visible upon copigmentation with caffeine, increases up to circa 0.025 M of the copigment and starts to decrease to higher concentrations. The authors justify this behaviour by the formation of complexes with *trans*-chalcone. In fact, the absorbance at 370 nm increases continuously and the *trans*-chalcone copigmentation was corroborated by ¹H-NMR.

Non-adequate mathematical equations

Eq. (37) was recently reported (Zou et al, 2019)

$$\frac{A_{\lambda}}{A_0} = \frac{K_{AH^+CP} (\varepsilon_{AH^+CP} - \varepsilon_{AH^+}) [CP]}{\varepsilon_{AH^+}} \quad (37)$$

As show in appendix 2, eq. (37) has a conceptual error and it is not valid.

Other authors as some of those above cited, use Brouillard's eq. (24) in the form of eq. (38)

$$\ln \frac{A_{\lambda} - A_0}{A_{\lambda}} = \ln K + n \ln [CP]_0 \quad (38)$$

They consider K the association constant. This approximation implies $K = r_{AH^+CP} K_{AH^+CP}$ with $r_{AH^+CP} = \varepsilon_{AH^+CP} / \varepsilon_{AH^+} = 1$. At a wavelength where $r_{AH^+CP} = 1$ no changes in the absorbance upon addition of co-pigment would take place, since corresponds to an isosbestic point. The constants reported by these authors are overestimated by r_{AH^+CP} .

Another incorrect expression (but not the value of the respective constants, K_{AH^+CP}) was reported by some of the present authors (Mendoza et al, 2019)

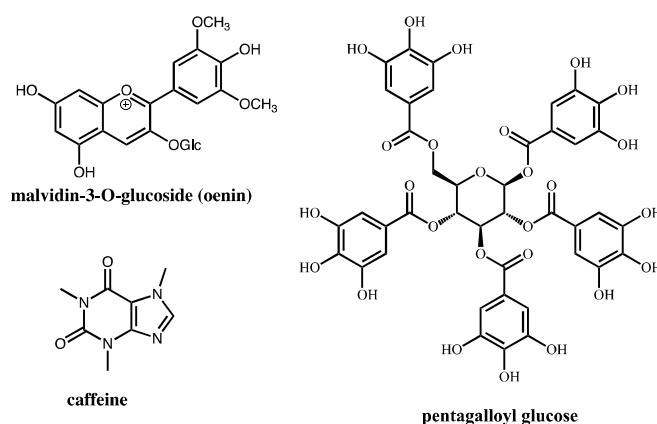
$$A_{\lambda} = \frac{A_0 + A_f (1 + K_{AH^+CP} [CP])}{1 + K_{AH^+CP} [CP]} \quad A_0 = \varepsilon_{AH^+} C_0 \quad A_f = \varepsilon_{AH^+CP} C_0 \quad (39)$$

We used eq. (40) for the calculations. Eq. (39) was included by mistake and was not corrected during the proof's correction (Corrigendum: <https://dx.doi.org/10.1021/acsomega.0c04304>).

$$A_{\lambda} = \frac{A_0 + A_f K_{AH^+CP} [CP]}{1 + K_{AH^+CP} [CP]} \quad \text{correct equation} \quad (40)$$

Application of the present model

The present model was applied to the co-pigmentation of malvidin-3-O-glucoside (oenin) with caffeine and pentagalloyl glucose (PGG), **Scheme 1**.



Scheme 1. Structure of malvidin-3-O-glucoside (oenin) and co-pigments caffeine and pentagalloyl glucose.

Oenin–Caffeine

Fixed pH and co-pigment concentration change.

The experiments have been done at two pH values, pH=1.2 (Fig. 1a and 1b) and pH=3.4 (Fig. 1c and 1d).

The spectral variations occurring by addition of caffeine to a solution of oenin, 4×10^{-5} M, at pH=1.2 are shown in **Fig. 1a**. At this pH the spectral variations reflect the formation of the complex with flavylium cation. Essentially, flavylium cation complex with caffeine giving rise to a red shift in the absorption but no significant hyperchromic effect. The variation of the absorbance at 540 nm, **Fig. 1b**, was one of the experiments used to carry out the global fitting.

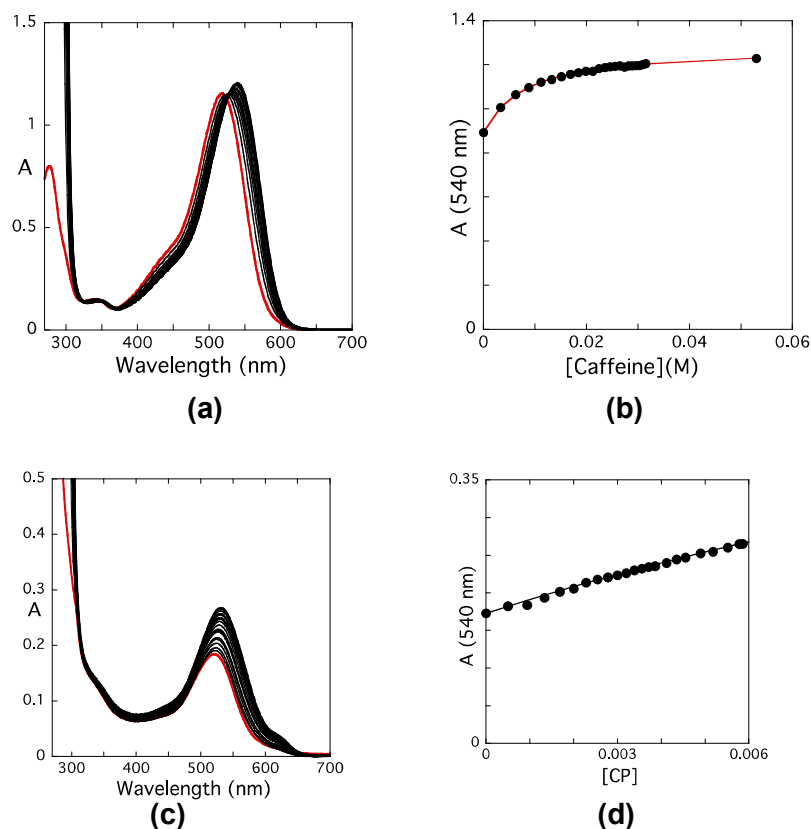


Figure 1. (a) Spectral variations upon addition of caffeine to an aqueous solution of oenin 4×10^{-5} M at pH=1.2; (b) representation of the absorbance at 540 nm versus caffeine concentration; (c) spectral variations upon addition of caffeine to oenin 4×10^{-5} M at pH=3.4; (d) representation of the absorbance at 540 nm used for the global fitting.

In **Fig. 1c** and **1d**, an identical experiment at pH=3.4 is shown. Differently from the spectral variations at pH=1.2, there is a raising of the absorbance and it is clear the formation of an absorption band at higher wavelengths, which cannot be attributed to the flavylum cation or its complex. The raising of the absorbance is in part explained by the formation of more complex with flavylum cation that shifts the equilibrium at the expenses of the other neutral species, for example decreasing the mole fraction of hemiketal. From the shoulder at higher wavelengths, it is also clear that the quinoidal base interacts with caffeine. The data of **Fig. 1d** was used to the global fitting.

Fixed co-pigmentation concentration and pH change

The pH dependent absorption spectra of Oenin is shown in the absence of co-pigment and in the presence of caffeine (**Fig. 2**).

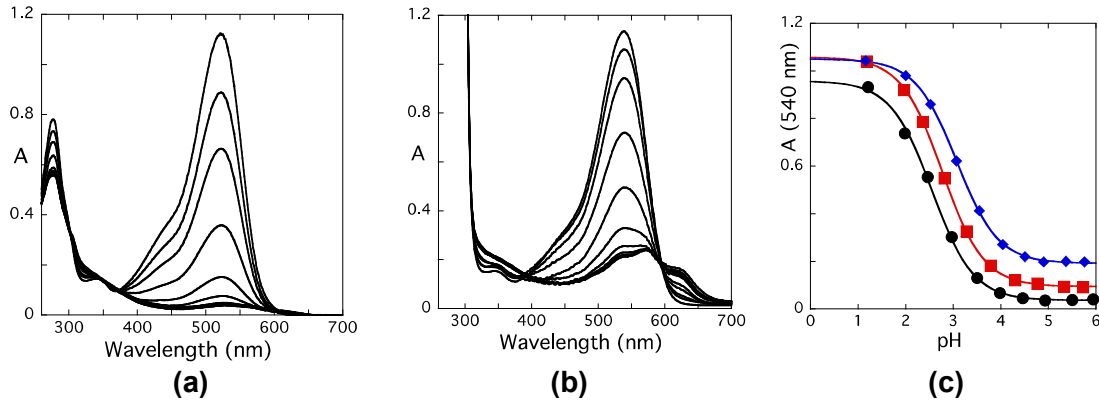


Figure 2. Absorption spectra of equilibrated solutions of malvidin-3-glucoside, 4×10^{-5} M as a function of pH: **(a)** in the absence of co-pigment; **(b)** in the presence of caffeine 0.024 M; **(c)** Representation of the absorbance at 540 nm in the absence of caffeine (black curve) and in the presence of caffeine 8.5×10^{-3} M (red curve) and 2.4×10^{-2} M (blue curve). The black curve permits to calculate $pK'_a=2.6$. The other two curves were used to the global fitting.

Comparison between **Fig. 2a** and **Fig. 2b** indicates that there is a significant raising in the wavelength region where quinoidal base and its complex absorb, confirming the observation made in Fig. 1c. The black curve inflects for $pH=pK'_a=2.6$. The other two curves were used to carry out the fitting of eq. (28). The fittings of the four set of experiments are those shown in the respective figures, for $r_{AH+CP}=1.38$, (540 nm); $K_{AH+CP}=125 \text{ M}^{-1}$; $r_{CBCP}=2.8 \times 10^{-2}$; $K_{CBCP}=22 \text{ M}^{-1}$.

The constant K_{CBCP} is the sum of the association constants of the species quinoidal base, hemiketal, *cis* and *trans* chalcones weighted by the respective mole fractions in the absence of co-pigment, eq. (29). As mentioned above, it is not possible to have the complexation constants of the individual species, based on absorption measurements, since there is no clear separation of the spectra of each species including the respective complexes. This is only achieved by means of a series of reverse pH jumps followed by stopped flow, (Mendoza et al, 2019) see the respective data for the system oenin-caffeine in **Table 1**.

Table 1. Equilibrium constants of Oenin and its complexes with caffeine and pentagalloyl glucose (PGC).

No co-pigment	pK_a	pK_a	$K_h M^{-1}$	K_t	
	2.6	3.8	1.7×10^{-3}	0.4	
Caffeine	$K_{AH^+CP}^{(1)}$	$K_{ACP}^{(1)}$	$K_{BCP}^{(1)}$	$K_{CCCP}^{(1)}$	$K_{CBCP}^{(1)}$
	$125 \pm 7^{(3)}$ $(134)^{(1)}$	303	≈ 0	17	$23 \pm 3^{(3)}$ $(19)^{(2)}$
PGG	$K_{AH^+CP}^{(1)}$				
	$914 \pm 10^{(3)}$				

⁽¹⁾ Reference (Mendoza et al, 2019)

⁽²⁾ At the pseudo-equilibrium (Mendoza et al, 2019);

⁽³⁾ This work.

Calculation of the constant K_{CBCP} of reference (Mendoza et al, 2019) can be done from the data reported in **Table 1**. The value in reference [28] ($19 M^{-1}$) was calculated at the pseudo-equilibrium and is slightly lower than the one of the present work carried out at the equilibrium. The relatively small contribution of C_t , explains the difference. In conclusion, there is a good agreement between the data of the present work and the one in reference (Mendoza et al, 2019), validating in this way the model here presented.

Oenin–pentagalloyl glucose

The model was also tested for oenin in the presence of the co-pigment pentagalloyl glucose (PGG) (**Scheme 1**).

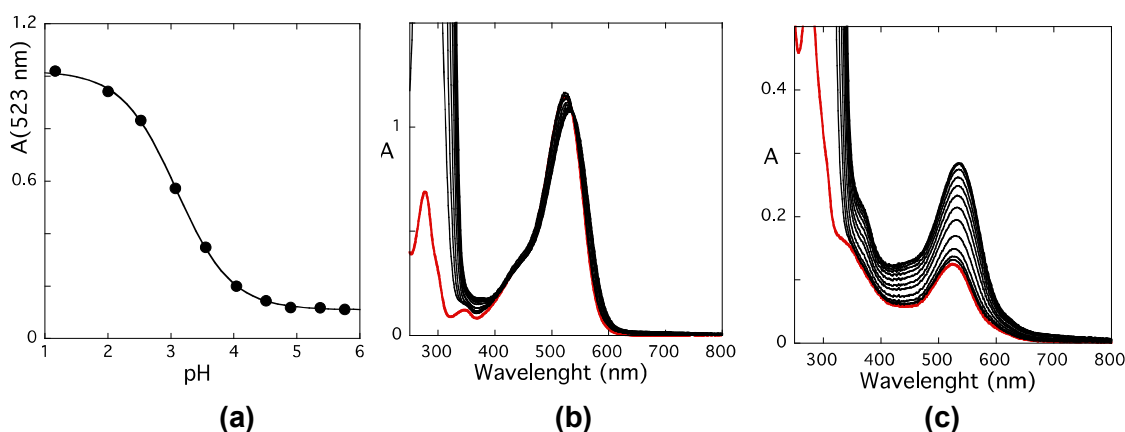


Figure 3. (a) pH dependent spectral variations at 523 nm in water (10% ethanol) of Oenin, 4.6×10^{-5} M in the presence of pentagalloyl glucose, 2.4×10^{-3} M. Fitting was achieved for $pK_{obs} = 3.09$; (b) spectral variations of oenin, 4.6×10^{-5} M upon addition of PGG up to 5×10^{-3} M at pH=0, (c) the same of (b) at pH=3.5. This experiment was made with 10% ethanol and we verified that pK_a of oenin in the same conditions was 2.55 (the same of pure water within experimental error).

The absorption at 523 nm for oenin, 4.6×10^{-5} M and pentagalloyl glucose, 2.4×10^{-3} M was represented as a function of pH. The system behaves as a single acid-base and $pK_{obs}=3.09$ was obtained. The spectral variations of oenin upon addition of PGG are represented at pH=0, Fig. 3b and pH=3.5 Fig. 3c. In contrast with the co-pigmentation with caffeine, the spectral modifications seem to indicate that there is no co-pigmentation with quinoidal base. However, the model goes further and predicts that no significant co-pigmentation takes place with all neutral species component of CB. This is shown in **Fig. 4.**

4.

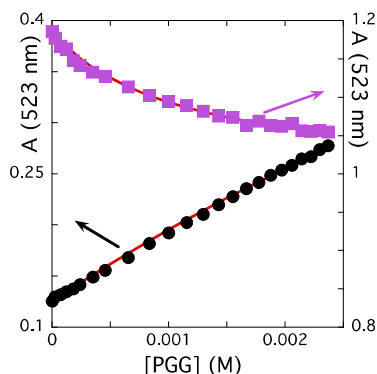


Figure 4. Representation of the oenin absorption in water (10% ethanol) at 523 nm as a function of PGG concentration at pH=0 (purple squares) and pH=3.5 (black circles). A global fitting was made respectively with Malien-Aubert eq.(14) and eq.(28) for the parameters $r_{AH+CP}=0.835$ (523 nm), $K_{AH+CP}=914 \text{ M}^{-1}$, $r_{CBP}=0$ and $K_{CBP}=0$.

In **Fig. 4**, the representation of the oenin absorption at 523 nm as a function of PGG concentration at pH=0 (purple squares) and pH=3.5 (black circles) is shown. The fitting at pH=0 was carried out with the Malien-Aubert eq. (14). This equation has two parameters to fit r_{AH+CP} and K_{AH+CP} . The fitting of the data at pH=3.5 was performed by means of eq. (28) deduced in this work. In this equation, besides r_{AH+CP} and K_{AH+CP} there are two more parameters to fit, r_{CBP} and K_{CBP} . Since two parameters are common, we made a global fitting of these two using the two set of experimental data for r_{AH+CP} and K_{AH+CP} and adjust the other, two from eq.(28). Fitting was achieved for $r_{AH+CP}=0.84$ (523 nm), $K_{AH+CP}=914 \text{ M}^{-1}$, $r_{CBP}=0$ and $K_{CBP}=0$.

Besides the use of eq. (28), when the co-pigment is fixed and the experiments are performed as a function of pH, there is another alternative based on the observed pK in the absence and presence of co-pigment. As shown in appendix 2, the mole fraction of the free and complexed acidic species is given by eq. (41)

$$\chi_{AH} + \chi_{AH+CP} = \frac{(1 + K_{AH+CP}[CP])[H^+]}{(1 + K_{AH+CP}[CP])[H^+] + (1 + K_{CBP}[CP])K'_3} = \frac{[H^+]}{[H^+] + \frac{(1 + K_{CBP}[CP])K'_3}{(1 + K_{AH+CP}[CP])}} \quad (41)$$

Which is equivalent to eq. (42)

$$\chi_{AH^+} + \chi_{AH^+CP} = \frac{[H^+]}{[H^+] + K_{obs}} \quad \text{with} \quad K_{obs} = \frac{(1 + K_{CBCP}[CP])}{(1 + K_{AH^+CP}[CP])} K'_a \quad (42)$$

In the same way for CB species

$$\chi_{CB} + \chi_{CBCP} = \frac{K_{obs}}{[H^+] + K_{obs}} \quad (43)$$

This means that the absorbance versus pH plot is given by a sigmoid curve inflecting for $pH=pK_{obs}$ as shown in Fig. 2c and Fig. 3a. These curves can also be simply fitted according to eq.(44), see in appendix 3 the respective prove.

$$A_\lambda = c_a \frac{[H^+]}{[H^+] + K_{obs}} + c_b \frac{K_{obs}}{[H^+] + K_{obs}} \quad (44)$$

Where c_a and c_b define the acid and basic plateaus (45)

Eq. (44) was calculated in the absence and presence of PGG, giving respectively ($pK'_a=2.55$)

(which compares with $pK'_a=2.6$ in pure water) and $pK_{obs}=3.09$ for the co-pigment concentration 2.4×10^{-3} M gives $K_{AH+CP}= 1004 \text{ M}^{-1}$ in very good agreement with $K_{AH+CP}=914 \text{ M}^{-1}$ previously determined in Fig. 4.

Conclusions

The mathematical expressions used to account for the co-pigmentation with anthocyanins have been critically revisited and their application limits emphasize. The experimental procedure reported in this work have shown that it is possible to distinguish between exclusive co-pigmentation with flavylium cation and co-pigmentation involving flavylium cation and the neutral species of the respective multistate. Besides the association constant with flavylium cation K_{AH+CP} it is possible to calculate the constant K_{CBCP} which reflects the interaction of all neutral species with the co-pigment weighted by their mole fraction in the absence e of the co-pigment. The UV-Vis absorption spectra of anthocyanins do not permit to separate with accuracy the absorption spectra of each of the neutral species and this intrinsic limitation does not allow the determination of the individual association constants with quinoidal base, hemiketal and the *cis* and *trans*

chalcones. This is only possible with another approach based on a series of reverse pH jumps recently reported (Mendoza et al, 2019). The present model is in very good agreement with the constants achieved through this last procedure for the same system oenin–caffeine. The present procedure is a general method to account for any 1:1 type of interaction, including host-guest chemistry involving anthocyanins and related compounds.

Acknowledgements

This work was supported by the Associated Laboratory for Sustainable Chemistry, Clean Processes and Technologies LAQV through the national funds from UIDB/50006/2020 and UIDP/50006/2020. It was also supported by the project PTDC/QUI-OUT/29013/2017 funded by FCT and FEDER. J.A. and P.A. gratefully acknowledge their doctoral grants from FCT (SFRH/BD/139709/2018 and SFRH/BD/143309/2019, respectively). J.O. would like to thank FCT for her IF contract (IF/00225/2015) and N.T. and N.B. acknowledge FCT for their research contract (CEECIND/00025/2018 and CEECIND/00466/2017, respectively).

References

- Andersen, O. M. M., K. R. (2006). *Flavonoids: Chemistry, Biochemistry and Applications*. USA: Taylor & Francis.
- Araujo, P., Fernandes, A., de Freitas, V., & Oliveira, J. (2017). A New Chemical Pathway Yielding A-Type Vitisins in Red Wines. *Int. J. Mol. Sci.*, 18(4), 762. <https://doi.org/10.3390/ijms18040762>.
- Asen, S., Stewart, R. N., & Norris, K. H. (1972). Copigmentation of anthocyanins in plant-tissues and its effect on color. *Phytochemistry*, 11(3), 1139-8. [https://doi.org/10.1016/s0031-9422\(00\)88467-8](https://doi.org/10.1016/s0031-9422(00)88467-8).
- Boulton, R. (2001). The copigmentation of anthocyanins and its role in the color of red wine: A critical review. *American Journal of Enology and Viticulture*, 52(2), 67-87. <Go to ISI>://WOS:000170693800001.
- Brouillard, R., Delaporte, B., & Dubois, J. E. (1978). Chemistry of Anthocyanins Pigments.3. Relaxation Amplitudes in pH-Jump Experiments. *J. Am. Chem. Soc.*, 100(19), 6202-6205. <https://doi.org/10.1021/ja00487a041>.
- Brouillard, R., Mazza, G., Saad, Z., Albrechtgary, A. M., & Cheminat, A. (1989). The copigmentation reaction of anthocyanins-a microprobe for the structural study of aqueous solutions. *Journal of the American Chemical Society*, 111(7), 2604-2610. <https://doi.org/10.1021/ja00189a039>.
- Brouillard, R., Wigand, M. C., Dangles, O., & Cheminat, A. (1991). pH and Solvent effects on the copigmentation reaction of malvin with Polyphenols, purine and pyrimidine-derivatives. *Journal of the Chemical Society-Perkin Transactions* 2(8), 1235-1241. <https://doi.org/10.1039/p29910001235>.
- Chen, Y., & Hagerman, A. E. (2004). Characterization of Soluble Non-covalent Complexes between Bovine Serum Albumin and β -1,2,3,4,6-Penta-O-galloyl-d-glucopyranose by MALDI-TOF MS. *Journal of Agricultural and Food Chemistry*, 52(12), 4008-4011. <https://doi.org/10.1021/jf035536t>.
- Dangles, O., & Elhajji, H. (1994). Synthesis of 3-methoxy-flavylium and 3-(beta-D-glucopyranosyloxy)flavylium ions- Influence of the flavylium substitution pattern on the reactivity of anthocyanins in aqueous solutions. *Helvetica Chimica Acta*, 77(6), 1595-1610. <https://doi.org/10.1002/hlca.19940770616>.
- Dangles, O., & Fenger, J. A. (2018). The Chemical Reactivity of Anthocyanins and Its Consequences in Food Science and Nutrition. *Molecules*, 23(8), 23. <https://doi.org/10.3390/molecules23081970>.
- Fanzone, M., Gonzalez-Manzano, S., Perez-Alonso, J., Escribano-Bailon, M. T., Jofre, V., Assof, M., & Santos-Buelga, C. (2015a). Evaluation of dihydroquercetin-3-O-glucoside from Malbec grapes as

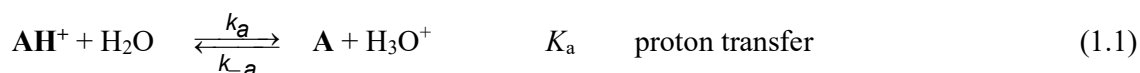
- copigment of malvidin-3-O-glucoside. *Food Chem*, 175, 166-173. <https://doi.org/10.1016/j.foodchem.2014.11.123>.
- Fanzone, M., Gonzalez-Manzano, S., Perez-Alonso, J., Escribano-Bailon, M. T., Jofre, V., Assof, M., & Santos-Buelga, C. (2015b). Evaluation of dihydroquercetin-3-O-glucoside from Malbec grapes as copigment of malvidin-3-O-glucoside. *Food Chemistry*, 175, 166-173. <https://doi.org/10.1016/j.foodchem.2014.11.123>.
- Goto, T. (1987). Structure, stability and color variation of natural anthocyanins. *Progress in the Chemistry of Organic Natural Products* 52, 113-158.
- Goto, T., & Kondo, T. (1991). Structure and molecular stacking of anthocyanins - flower color variation. *Angewandte Chemie, International Edition in English*, 30(1), 17-33. <Go to ISI>://A1991EX12800002
- He, F., Liang, N. N., Mu, L., Pan, Q. H., Wang, J., Reeves, M. J., & Duan, C. Q. (2012). Anthocyanins and their variation in red wines I. Monomeric anthocyanins and their color expression. *Molecules*, 17(2), 1571-1601. <https://doi.org/10.3390/molecules17021571>.
- Kanha, N., Surawang, S., Pitchakarn, P., Regenstein, J. M., & Laokuldilok, T. (2019). Copigmentation of cyanidin 3-O-glucoside with phenolics: Thermodynamic data and thermal stability. *Food Bioscience*, 30, 9. <https://doi.org/10.1016/j.fbio.2019.100419>.
- Küster FW, Thiel A. *Tabelle per le Analisi Chimiche e Chimico- Fisiche*. 12 th ed Milano, Italy: Hoepli; 1982. p. 157–60.
- Malien-Aubert, C., Dangles, O., & Amiot, M. J. (2002). Influence of procyanidins on the color stability of oenion solutions. *Journal of Agricultural and Food Chemistry*, 50(11), 3299-3305. <https://doi.org/10.1021/jf011392b>.
- Mendoza, J., Basilio, N., de Freitas, V., & Pina, F. (2019). New Procedure To Calculate All Equilibrium Constants in Flavylium Compounds: Application to the Copigmentation of Anthocyanins. *ACS Omega*, 4(7), 12058-12070. <https://doi.org/10.1021/acsomega.9b01066>.
- Pina, F. (2014). Chemical Applications of Anthocyanins and Related Compounds. A Source of Bioinspiration. *J. Agric. Food Chem.*, 62(29), 6885-6897. <https://doi.org/10.1021/jf404869m>.
- Pina, F., Oliveira, J., & de Freitas, V. (2015). Anthocyanins and derivatives are more than flavylium cations. *Tetrahedron*, 71(20), 3107-3114. <https://doi.org/10.1016/j.tet.2014.09.051>.
- Robinson, G. M., & Robinson, R. (1931). A survey of anthocyanins. I. *Biochemical Journal*, 25(5), 1687-1705. <https://doi.org/10.1042/bj0251687>.
- Silva, C. P., Silva, G. T. M., Costa, T. D., Carneiro, V. M. T., Siddique, F., Aquino, A. J. A., . . . Quina, F. H. (2020). Chromophores inspired by the colors of fruit, flowers and wine. *Pure and Applied Chemistry*, 92(2), 255-263. <https://doi.org/10.1515/pac-2019-0226>.
- Soares, S., Kohl, S., Thalmann, S., Mateus, N., Meyerhof, W., & De Freitas, V. (2013). Different Phenolic Compounds Activate Distinct Human Bitter Taste Receptors. *Journal of Agricultural and Food Chemistry*, 61(7), 1525-1533. <https://doi.org/10.1021/jf304198k>.
- Trouillas, P., Sancho-García, J. C., De Freitas, V., Gierschner, J., Otyepka, M., & Dangles, O. (2016). Stabilizing and modulating color by copigmentation: insights from theory and experiment. *Chem. Rev.*, 116(9), 4937-4982. <https://doi.org/10.1021/acs.chemrev.5b00507>.
- Yoshida, K., Mori, M., & Kondo, T. (2009). Blue flower color development by anthocyanins: from chemical structure to cell physiology. *Natural Product Reports*, 26(7), 884-915. <https://doi.org/10.1039/b800165k>.
- Zhang, B., He, F., Zhou, P. P., Liu, Y., & Duan, C. Q. (2015). Copigmentation between malvidin-3-O-glucoside and hydroxycinnamic acids in red wine model solutions: Investigations with experimental and theoretical methods. *Food Research International*, 78, 313-320. <https://doi.org/10.1016/j.foodres.2015.09.026>.
- Zhang, B., He, F., Zhou, P. P., Liu, Y., & Duan, C. Q. (2016). The color expression of copigmentation between malvidin-3-O-glucoside and three phenolic aldehydes in model solutions: The effects of pH and molar ratio. *Food Chemistry*, 199, 220-228. <https://doi.org/10.1016/j.foodchem.2015.12.008>.
- Zhang, B., Liu, R., He, F., Zhou, P. P., & Duan, C. Q. (2015). Copigmentation of malvidin-3-O-glucoside with five hydroxybenzoic acids in red wine model solutions: Experimental and theoretical investigations. *Food Chemistry*, 170, 226-233. <https://doi.org/10.1016/j.foodchem.2014.08.026>.

- Zhang, B., Wang, Q., Zhou, P. P., Li, N. N., & Han, S. Y. (2020). Copigmentation evidence of oenin with phenolic compounds: A comparative study of spectrographic, thermodynamic and theoretical data. *Food Chemistry*, 313, 7. <https://doi.org/10.1016/j.foodchem.2020.126163>.
- Zhao, X., Ding, B. W., Qin, J. W., He, F., & Duan, C. Q. (2020). Intermolecular copigmentation between five common 3-O-monoglucosidic anthocyanins and three phenolics in red wine model solutions: The influence of substituent pattern of anthocyanin B ring. *Food Chemistry*, 326, 8. <https://doi.org/10.1016/j.foodchem.2020.126960>.
- Zhu, Y. Y., Chen, H. J., Lou, L. Y., Chen, Y. X., Ye, X. Q., & Chen, J. C. Copigmentation effect of three phenolic acids on color and thermal stability of Chinese bayberry anthocyanins. *Food Science & Nutrition*, 9. <https://doi.org/10.1002/fsn3.1583>.
- Zou, H., Ma, Y., Liao, X. J., & Wang, Y. T. (2019). Effects of high pressure processing on the copigmentation reaction of pelargonidin-3-glucoside and catechin. *Lwt-Food Science and Technology*, 108, 240-246. <https://doi.org/10.1016/j.lwt.2019.03.080>.

Supplementary Material

Appendix 1

Considering exclusive complexation with flavylum cation at moderately acidic pH values.



The mass balance gives

$$C_0 = [AH^+] + [AH^+CP] + [A] + [B] + [Cc] + [Ct] \quad (1.6)$$

Using eq.(1.1) to eq.(1.5)

$$\begin{aligned} C_0 &= [AH^+] \left(1 + K_{AH^+CP}[CP] + \frac{K_a}{[H^+]} + \frac{K_h}{[H^+]} + \frac{K_h K_t}{[H^+]} + \frac{K_h K_t K_i}{[H^+]} \right) = \\ &= [AH^+] \left(1 + K_{AH^+CP}[CP] + \frac{K'_a}{[H^+]} \right) \end{aligned} \quad (1.7)$$

From eq.(1.7) the mole fraction distribution of flavylum cation is obtained

$$\chi_{AH^+} = \frac{[AH^+]}{C_0} = \frac{1}{1 + K_{AH^+CP}[CP] + \frac{K'_a}{[H^+]}} = \frac{[H^+]}{(1 + K_{AH^+CP}[CP])[H^+] + K'_a} = \frac{[H^+]}{D} \quad (1.8)$$

$$D = (1 + K_{AH^+CP}[CP])[H^+] + K'_a$$

As well as of the other species

$$\chi_{AH^+CP} = \frac{K_{AH^+CP}[CP][H^+]}{D}; \chi_A = \frac{K_a}{D}; \chi_B = \frac{K_h}{D}; \chi_{Cc} = \frac{K_h K_t}{D}; \chi_{Ct} = \frac{K_h K_t K_i}{D} \quad (1.9)$$

Working at a wavelength where only flavylum cation and its complex absorb in particular neglecting the contribution of the quinoidal base, which in common anthocyanins is a minor species, as well as the fact that exclusive complexation with flavylum reduces its concentration.

$$A_{\lambda} = \varepsilon_{AH^+} C_0 \chi_{AH^+} + \varepsilon_{AH^+CP} C_0 \chi_{AH^+CP} \quad (1.10)$$

Introducing $r_{AH^+CP} = \frac{\varepsilon_{AH^+CP}}{\varepsilon_{AH^+}}$ and substituting the mole fractions in eq.(1.10)

$$A_{\lambda} = A_0 \frac{[H^+](1+r_{AH^+CP}K_{AH^+CP}[CP])}{(1+K_{AH^+CP}[CP])[H^+]+K'_a} \text{ with } A_0 = \varepsilon_{AH^+} C_0 \quad (1.11)$$

This is the expression that accounts for the exclusive complexation with flavylum cation with the following limitations: *i)* no other species of the multistate interact with the co-pigment, *ii)* the complex is 1:1, *iii)* at the selected wavelength there is no significant absorption of the other species except flavylum cation and its complex.

Comparison of eq.(1.11) with the one of Malien-Aubert at a^1

In this section we prove that the Malien-Auber eq.(1.12) and eq.(1.11) are the same

$$A_{\lambda} = A_{0(pH)} \frac{1+r_{AH^+CP}K_{AH^+CP}[CP]}{1+aK_{AH^+CP}[CP]} \quad (1.12)$$

Substituting the parameter a in its generalized form

$$a = \frac{[H^+]}{[H^+]+K'_a} \quad (1.13)$$

$$A_{\lambda} = A_{0(pH)} \frac{1+r_{AH^+CP}K_{AH^+CP}[CP]}{1+\frac{[H^+]}{[H^+]+K'_a}K_{AH^+CP}[CP]} \quad (1.14)$$

$$\text{Considering that } A_{0(pH)} = \varepsilon_{AH^+} C_0 \frac{[H^+]}{[H^+]+K'_a} \quad (1.15)$$

$$A_{\lambda} = \varepsilon_{AH^+} C_0 \frac{[H^+]}{[H^+]+K'_a} \frac{1+r_{AH^+CP}K_{AH^+CP}[CP]}{1+\frac{[H^+]}{[H^+]+K'_a}K_{AH^+CP}[CP]} \quad (1.6)$$

$$A_{\lambda} = \varepsilon_{AH^+} C_0 \frac{[H^+](1+r_{AH^+CP}K_{AH^+CP}[CP])}{([H^+]+K'_a)(1+\frac{[H^+]}{[H^+]+K'_a}K_{AH^+CP}[CP])} \quad (1.17)$$

$$A_{\lambda} = A_0 \frac{[H^+](1+r_{AH^+CP}K_{AH^+CP}[CP])}{(1+K_{AH^+CP}[CP])[H^+]+K'_a} \quad (1.18)$$

Quod erat demonstrandum

Other expressions that are the same of the one of Malien-Aubert *et al*

The following expression was used in a co-pigmentation study of Malvin with sinapic acid.² The authors refer that took this expression from a Ph.D. Thesis (E.S. Sadlowski, Ph.D. Thesis, Colorado State University, Fort Collins, 1985).

$$K = \frac{A_\lambda - A_0}{C_0 \left\{ rA_0 - \frac{A_\lambda}{(1 + K_h 10^{pH})} \right\}} = \frac{A_\lambda - A_0}{C_0 \left\{ rA_0 - \frac{A_\lambda}{(1 + K_h \frac{1}{[H^+]})} \right\}} = \frac{A_\lambda - A_0}{C_0 \left\{ rA_0 - \frac{A_\lambda [H^+]}{([H^+] + K_h)} \right\}} \quad (1.19)$$

rearranging

$$A_\lambda = KC_0 \left\{ rA_0 - \frac{A_\lambda [H^+]}{([H^+] + K_h)} \right\} + A_0 \quad (1.20)$$

or

$$A_\lambda + \frac{A_\lambda [H^+]}{([H^+] + K_h)} KC_0 = rA_0 KC_0 + A_0 \quad (1.21)$$

$$A_\lambda \left(1 + \frac{[H^+] KC_0}{([H^+] + K_h)} \right) = A_0 (1 + rKC_0) \quad (1.22)$$

$$A_\lambda = \frac{A_0 (1 + rKC_0)}{\left(1 + \frac{[H^+] KC_0}{([H^+] + K_h)} \right)} = A_0 \frac{(1 + rKC_0)}{(1 + aKC_0)} \quad A_\lambda = A_{0(pH)} \frac{1 + r_{AH^+CP} K_{AH^+CP} [CP]}{1 + aK_{AH^+CP} [CP]} \quad (1.23)$$

Comparing the two equations it can be verified that they are the same.

Simulation of Brouillard's approximation³ and Malien-Aubert *et al* expression

Based on the possibility of complexation as in eq.(1.24), Brouillard³ deduced eq.(1.25) that was used at pH=3.65.



$$\frac{A - A_{0(pH)}}{A_{0(pH)}} = r_{AH^+CP} K_{AH^+CP} [CP]^n \quad (1.25)$$

Without loss of generality for n=1 the ratio $\frac{A - A_{0(pH)}}{A_{0(pH)}}$ can be re-calculated from the C. Malien-

Aubert *et al* eq.(14).¹

$$\frac{A_{\lambda} - A_{0(\text{pH})}}{A_{0(\text{pH})}} = \frac{r_{AH^+CP} K_{AH^+CP} [CP] - a K_{AH^+CP} [CP]}{1 + a K_{AH^+CP} [CP]} \quad (1.26)$$

Eq.(1.26) gives eq.(1.25) only if $a=0$ or $aK_{AH^+CP}[CP]^n \ll 1$ and $a \ll r_{AH^+CP}$

In Fig. A1.1a the simulation for a 1:1 complex with $K_{AH^+CP}=134 \text{ M}^{-1}$, $\text{p}K_a= 2.6$, $r_{AH^+CP}=1.43$ at $\text{pH}=3.65$ for both expressions are presented and in the same conditions at $\text{pH}=3.2$ in Fig. A1.1b.

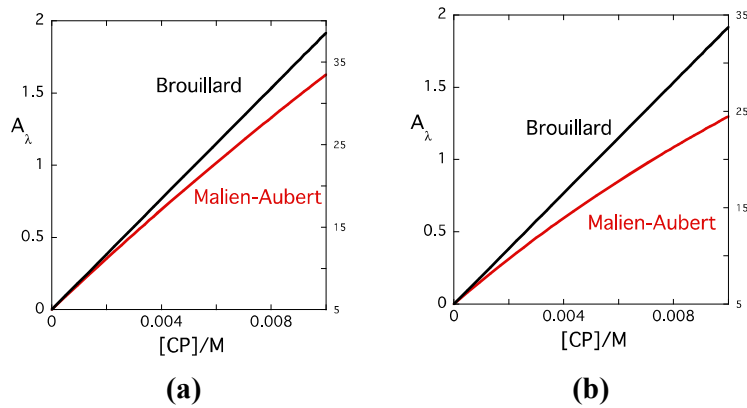


Figure A1.1. (a) Simulation of the ratio $\frac{A_{\lambda} - A_{0(\text{pH})}}{A_{0(\text{pH})}}$ from the Malien-Aubert *et al* equation, eq.(1.12) , and Brouillard

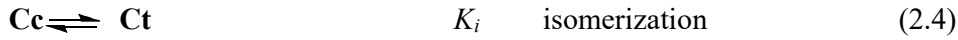
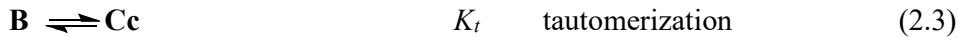
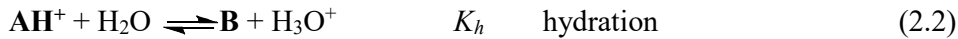
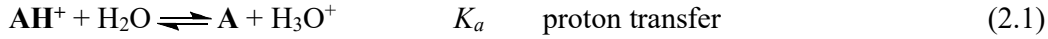
expression, eq.(1.21), $n=1$, for a system having $K_{AH^+CP}=134 \text{ M}^{-1}$, $\text{p}K_a= 2.6$, $r_{AH^+CP}=1.43$ at $\text{pH}=3.65$ and $[\text{anthocyanins}]=5 \times 10^{-5} \text{ M}$; (b) the same for $\text{pH}=3.2$.

Inspection of Fig. A1 shows the limitations of eq.(1.25). It needs a working pH sufficiently higher than $\text{p}K_a$ to have a low value of the parameter a . Moreover, only the product $r_{AH^+CP} K_{AH^+CP}$ is obtained and r_{AH^+CP} should be calculated at $\text{pH} \approx 1$ in the absence and presence of high concentrations of the co-pigment.³ In Brouillard's paper these limit conditions were attained (co-pigment concentration not higher than circa 10^{-3} M and relatively low association constant) but this is not a general equation as the one of Malien-Aubert *et al*.

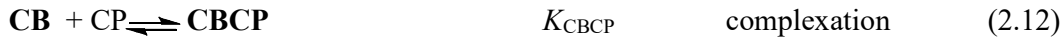
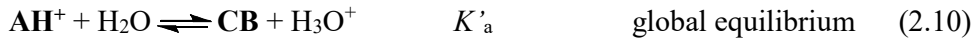
Appendix 2

The General Model

Considering the complete set of equations and restricting the model to the moderately acidic region (to avoid the formation of the anionic species) and assuming complexes having 1:1 stoichiometry, the following set of equations accounts for the system



It is firmly established that the flavylum multistate in moderately acidic medium behaves as a single acid base equilibrium,^{4,5} and the system can be dramatically simplified through eq.(2.10) to eq.(2.12).



With

$$[\text{CB}] = [\text{A}] + [\text{B}] + [\text{Cc}] + [\text{Ct}] \quad \text{and} \quad [\text{CBCP}] = [\text{ACP}] + [\text{BCP}] + [\text{CcCP}] + [\text{CtCP}]$$

Physical meaning of K_{CBCP}

While $K_{\text{AH}^+\text{CP}}$ is the 1:1 association constant of the co-pigment with flavylum cation the meaning of K_{CBCP} needs a clarification.

By definition of the equilibrium constant K_{CBCP} is given by eq.(2.13)

$$K_{\text{CBCP}} = \frac{[\text{CBCP}]}{[\text{CB}][\text{CP}]} = \frac{[\text{ACP}] + [\text{BCP}] + [\text{CcCP}] + [\text{CtCP}]}{([\text{A}] + [\text{B}] + [\text{Cc}] + [\text{Ct}])[\text{CP}]} \quad (2.13)$$

Using eq.(2.6) to eq.(2.9)

$$K_{\text{CBCP}} = \frac{(K_{\text{ACP}}[\text{A}] + K_{\text{BCP}}[\text{B}] + K_{\text{CcCP}}[\text{Cc}] + K_{\text{CtCP}}[\text{Ct}])}{([\text{A}] + [\text{B}] + [\text{Cc}] + [\text{Ct}])} \quad (2.14)$$

From the equilibrium constants eq.(2.1) to eq.(2.4)

$$K_{\text{CBCP}} = \frac{(K_{\text{ACP}}K_a + K_{\text{BCP}}K_h + K_{\text{CcCP}}K_hK_t + K_{\text{CtCP}}K_hK_tK_i)}{K'_a} = \frac{\alpha_{\text{CBCP}}}{K'_a} \quad (2.15)$$

$$\text{With } \alpha_{CBCP} = K_{ACP}K_a + K_{BCP}K_h + K_{CcCP}K_hK_t + K_{CtCP}K_hK_tK_i \quad (2.16)$$

The mole fractions of the CB componentes in the absence of co-pigment are given by eq.(2.17)

$$\chi_A = \frac{K_a}{[H^+] + K'_a}; \chi_B = \frac{K_h}{[H^+] + K'_a}; \chi_{Cc} = \frac{K_hK_t}{[H^+] + K'_a}; \chi_{Ct} = \frac{K_hK_tK_i}{[H^+] + K'_a} \quad (2.17)$$

The limit of the mole fractions of eq.(2.17) when $[H^+] \ll K'_a$ (basic plateau) are K_a/K'_a , K_h/K'_a , K_hK_t/K'_a , $K_hK_tK_i/K'_a$, the coeficients that weight K_{CBCP} . **In conclusion, K_{CBCP} is the sum of the association constants with all neutral species weighed by the contribution each of them have in CB.**

The treatment of this complex system is done as usually from the mass balance and the definition of the Lambert-Beer law.

$$C_0 = [AH^+] + [A] + [B] + [Cc] + [Ct] + [AH^+CP] + [ACP] + [BCP] + [CcCP] + [CtCP] \quad (2.18)$$

Using eq.(2.1) to eq.(2.9)

$$C_0 = [AH^+] \left(1 + K_{AH^+CP}[CP] + \frac{K_a}{[H^+]} + \frac{K_h}{[H^+]} + \frac{K_hK_t}{[H^+]} + \frac{K_hK_tK_i}{[H^+]} + \frac{(K_{ACP}K_a + K_{BCP}K_h + K_{CcCP}K_hK_t + K_{CtCP}K_hK_tK_i)[CP]}{[H^+]} \right) \quad (2.19)$$

$$\text{Introducing } K'_a = K_a + K_h + K_hK_t + K_hK_tK_i \quad (2.20)$$

and α_{CBCP} defined in eq.(2.16), eq.(2.21) can be rewritten

$$C_0 = [AH^+] \left(1 + K_{AH^+CP}[CP] + \frac{K'_a + \alpha_{CBCP}[CP]}{[H^+]} \right) \quad (2.21)$$

from eq.(2.15)

$$C_0 = [AH^+] \left\{ 1 + K_{AH^+CP}[CP] + \frac{(1 + K_{CBCP}[CP])K'_a}{[H^+]} \right\} \quad (2.22)$$

From eq.(2.22) the mole fraction of AH^+ is calculated, as well as those of the other species.

$$\chi_{AH^+} = \frac{[H^+]}{(1 + K_{AH^+CP}[CP])[H^+] + (1 + K_{CBCP}[CP])K'_a} = \frac{[H^+]}{D} \quad (2.23)$$

$$D = (1 + K_{AH^+CP}[CP])[H^+] + (1 + K_{CBCP}[CP])K'_a$$

$$\chi_{AH^+CP} = \frac{K_{AH^+CP}[CP][H^+]}{D}; \chi_A = \frac{K_a}{D}; \chi_B = \frac{K_h}{D}; \chi_{Cc} = \frac{K_hK_t}{D}; \chi_{Ct} = \frac{K_hK_tK_i}{D} \quad (2.24)$$

$$\chi_{ACP} = \frac{K_{ACP}K_a[CP]}{D}; \chi_{BCP} = \frac{K_{BCP}K_h[CP]}{D}; \chi_{CcCP} = \frac{K_{CcCP}K_hK_t[CP]}{D}; \chi_{CtCP} = \frac{K_{CtCP}K_hK_tK_i[CP]}{D} \quad (2.25)$$

The absorbance is given by the generalization of the Lambert-Beer law

$$A_\lambda = \varepsilon_{AH^+}C_0\chi_{AH^+} + \varepsilon_{AH^+CP}C_0\chi_{AH^+CP} + \varepsilon_A C_0\chi_A + \varepsilon_B C_0\chi_B + \varepsilon_{Cc} C_0\chi_{Cc} + \varepsilon_{Ct} C_0\chi_{Ct} + \varepsilon_{ACP} C_0\chi_{ACP} + \varepsilon_{BCP} C_0\chi_{BCP} + \varepsilon_{CcCP} C_0\chi_{CcCP} + \varepsilon_{CtCP} C_0\chi_{CtCP} \quad (2.26)$$

Introducing the mole absorption coefficients ratios gives eq.(2.29)

$$r_{AH^+CP} = \frac{\varepsilon_{AH^+CP}}{\varepsilon_{AH^+}} \quad (2.27)$$

$$r_A = \frac{\varepsilon_A}{\varepsilon_{AH^+}}; \quad r_B = \frac{\varepsilon_B}{\varepsilon_{AH^+}}; \quad r_{Cc} = \frac{\varepsilon_{Cc}}{\varepsilon_{AH^+}} \quad r_{Ct} = \frac{\varepsilon_{Ct}}{\varepsilon_{AH^+}}; \quad (2.28)$$

$$r_{ACP} = \frac{\varepsilon_{ACP}}{\varepsilon_{AH^+}}; \quad r_{BCP} = \frac{\varepsilon_{BCP}}{\varepsilon_{AH^+}}; \quad r_{CcCP} = \frac{\varepsilon_{CcCP}}{\varepsilon_{AH^+}} \quad r_{CtCP} = \frac{\varepsilon_{CtCP}}{\varepsilon_{AH^+}}$$

$$A_\lambda = A_0 \left\{ \begin{array}{l} \chi_{AH^+} + r_{AH^+CP} \chi_{AH^+CP} + r_A \chi_A + r_B \chi_B + r_{Cc} \chi_{Cc} + r_{Ct} \chi_{Ct} + \\ + r_{ACP} \chi_{ACP} + r_{BCP} \chi_{BCP} + r_{CcCP} \chi_{CcCP} + r_{CtCP} \chi_{CtCP} \end{array} \right\} \quad (2.29)$$

With $A_0 = \varepsilon_{AH^+} C_0$

Substituting the mole fractions in eq.(2.29)

$$A_\lambda = A_0 \left\{ \begin{array}{l} \frac{[H^+] + r_{AH^+CP} K_{AH^+CP} [CP] [H^+] + r_A K_a + r_B K_h + r_{Cc} K_h K_t + r_{Ct} K_h K_t K_i}{D} + \\ \frac{(r_{ACP} K_{ACP} K_a + r_{BCP} K_{BCP} K_h + r_{CcCP} K_{CcCP} K_h K_t + r_{CtCP} K_{CtCP} K_h K_t K_i) [CP]}{D} \end{array} \right\} \quad (2.30)$$

Introducing

$$r_{CP} = r_{ACP} K_{ACP} K_a + r_{BCP} K_{BCP} K_h + r_{CcCP} K_{CcCP} K_h K_t + r_{CtCP} K_{CtCP} K_h K_t K_i \quad (2.31)$$

$$r_{CB} = r_A K_a + r_B K_h + r_{Cc} K_h K_t + r_{Ct} K_h K_t K_i \quad (2.32)$$

$$A_\lambda = A_0 \left\{ \frac{[H^+] + r_{AH^+CP} K_{AH^+CP} [CP] [H^+] + r_{CB} + r_{CP} [CP]}{(1 + K_{AH^+CP} [CP]) [H^+] + (1 + K_{CBCP} [CP]) K'_a} \right\} \quad (2.32)$$

The parameter r_{CB} can be calculated from the initial absorbance when $[CP]=0$, eq.(2.33)

$$A_{\lambda(CP=0)} = A_0 \left\{ \frac{[H^+] + r_{CB}}{[H^+] + K'_a} \right\} \quad (2.33)$$

Eq.(2.32) is the general expression that accounts for the 1:1 co-pigmentation considering the possibility of complexation with any species of the multistate.

Eq.(2.32) can be used in two different sets of experiments: *i*) fixed pH and the absorption is function of the co-pigment concentration, or *ii*) fixed co-pigment concentration and the absorption is function of the pH. There are four parameters to fit r_{AH^+CP} , K_{AH^+CP} , r_{CP} and K_{CBCP} . The best procedure is to carry out measurements at pH=1 and at higher pH values for example pH=3.5. A global fitting of all data permits to obtain a good accuracy.

Incorrect expressions reported in the literature^{6,7}

These authors in reference [6] define the possibility of two 1:1 co-pigmentations with flavylum cation and hemiketal. (we are using our notation to facilitate the comparisons)

$$K_{AH^+CP} = \frac{[AH^+CP]}{[AH^+][CP]} \quad K_{BCP} = \frac{[BCP]}{[B][CP]} \quad (2.34)$$

$$A_\lambda = \varepsilon_{AH^+}[AH^+] + \varepsilon_{AH^+CP}[AH^+CP] + \varepsilon_B[B] + \varepsilon_{BCP}[BCP] \quad (2.35)$$

Considering that the hemiketal and its complex do not absorb at the selected wavelength

$$A_\lambda = \varepsilon_{AH^+}[AH^+] + \varepsilon_{AH^+CP}[AH^+CP] \quad (2.36)$$

Eq.(2.36) is correct if $[AH^+]$ and $[AH^+CP]$ are the concentrations of the flavylum cation and its complex, which are variables that change by addition of co-pigment.

In the next step the authors consider the following ratio

$$\frac{A_\lambda}{A_0} = \frac{\varepsilon_{AH^+}[AH^+] + \varepsilon_{AH^+CP}[AH^+CP]}{\varepsilon_{AH^+}[AH^+]_0} \quad (2.37)$$

With A_0 defined as the absorbance before processing a constant value. The authors do not distinguish between $\varepsilon_{AH^+}[AH^+]$ (variable) in the numerator from $\varepsilon_{AH^+}[AH^+]_0$ (constant) in the denominator.

$$\text{Considering that } [AH^+]_0 = [AH^+] + [AH^+CP] \quad (2.38)$$

$$\frac{A_\lambda}{A_0} = \frac{\varepsilon_{AH^+}([AH^+]_0 - [AH^+CP]) + \varepsilon_{AH^+CP}[AH^+CP]}{\varepsilon_{AH^+}[AH^+]_0} = \frac{\varepsilon_{AH^+}[AH^+]_0 + (\varepsilon_{AH^+CP} - \varepsilon_{AH^+})[AH^+CP]}{\varepsilon_{AH^+}[AH^+]_0} \quad (2.39)$$

Giving

$$\frac{A_\lambda}{A_0} = 1 + \frac{(\varepsilon_{AH^+CP} - \varepsilon_{AH^+})[AH^+CP]}{\varepsilon_{AH^+}[AH^+]_0} \quad (2.40)$$

This is the same intermediate equation reported by the authors. From the definition of the equilibrium constant eq.(2.34) can be written as in eq.(2.49)

$$\frac{A_\lambda}{A_0} = 1 + \frac{(\varepsilon_{AH^+CP} - \varepsilon_{AH^+})K_{AH^+CP}[AH^+][CP]}{\varepsilon_{AH^+}[AH^+]_0} \quad (2.49)$$

But not as in eq.(2.50) as reported by the authors.

$$\frac{A_\lambda}{A_0} = 1 + \frac{(\varepsilon_{AH^+CP} - \varepsilon_{AH^+})K_{AH^+CP}[CP]}{\varepsilon_{AH^+}} \quad (2.50)$$

Another incorrect expression (but not the value of the respective constants) was reported by some of the present authors⁷

(Corrigendum: <https://dx.doi.org/10.1021/acsomega.0c04304>)

$$A_\lambda = \frac{A_0 + A_f(1 + K_{AH^+CP}[CP])}{1 + K_{AH^+CP}[CP]} \quad A_0 = \varepsilon_{AH^+}C_0 \quad A_f = \varepsilon_{AH^+CP}C_0$$

Considering the equilibrium and $pH \leq 1$



$$C_0 = [\text{AH}^+] + [\text{AH}^+\text{CP}] = [\text{AH}^+](1 + K_{\text{AH}^+\text{CP}}[\text{CP}]) \quad (2.52)$$

$$\chi_{\text{AH}^+} = \frac{1}{(1 + K_{\text{AH}^+\text{CP}}[\text{CP}])} \quad \text{and} \quad \chi_{\text{AH}^+\text{CP}} = \frac{K_{\text{AH}^+\text{CP}}[\text{CP}]}{(1 + K_{\text{AH}^+\text{CP}}[\text{CP}])}$$

$$A_\lambda = \varepsilon_{\text{AH}^+} \chi_{\text{AH}^+} C_0 + \varepsilon_{\text{AH}^+\text{CP}} \chi_{\text{AH}^+\text{CP}} C_0 \quad (2.53)$$

$$A_\lambda = \frac{\varepsilon_{\text{AH}^+} C_0 + \varepsilon_{\text{AH}^+\text{CP}} C_0 K_{\text{AH}^+\text{CP}}[\text{CP}]}{1 + K_{\text{AH}^+\text{CP}}[\text{CP}]} \quad (2.54)$$

$$A_\lambda = \frac{A_0 + A_f K_{\text{AH}^+\text{CP}}[\text{CP}]}{1 + K_{\text{AH}^+\text{CP}}[\text{CP}]} \quad \text{correct equation} \quad (2.55)$$

The values of the constants in Table 3 and Table 5 of mentioned work⁷ were calculated with the right equation.

Appendix 3

Absorbance versus pH at [CP] Constant

In the general equation, eq.(3.1), the term containing [H⁺] can be separate and both divided by (1 + K_{AH+CP}[CP]) giving eq.(3.2)

$$A_\lambda = A_0 \left\{ \frac{(1 + r_{\text{AH}^+\text{CP}} K_{\text{AH}^+\text{CP}}[\text{CP}])[H^+] + r_{\text{CB}} + r_{\text{CP}}[\text{CP}]}{(1 + K_{\text{AH}^+\text{CP}}[\text{CP}])[H^+] + (1 + K_{\text{CBCP}}[\text{CP}])K'_a} \right\} \quad (3.1)$$

$$A_\lambda = A_0 \frac{\frac{(1 + r_{\text{AH}^+\text{CP}} K_{\text{AH}^+\text{CP}}[\text{CP}])[H^+]}{(1 + K_{\text{AH}^+\text{CP}}[\text{CP}])} + A_0 \frac{r_{\text{CB}} + r_{\text{CP}}[\text{CP}]}{(1 + K_{\text{AH}^+\text{CP}}[\text{CP}])}}{[H^+] + \frac{(1 + K_{\text{CBCP}}[\text{CP}])K'_a}{(1 + K_{\text{AH}^+\text{CP}}[\text{CP}])}} \quad (3.2)$$

With K_{obs} defined previously by eq.(3.3), eq.(3.4) is obtained

$$K_{\text{obs}} = \frac{(1 + K_{\text{CBCP}}[\text{CP}])}{(1 + K_{\text{AH}^+\text{CP}}[\text{CP}])} K'_a \quad (3.3)$$

$$A_\lambda = A_0 \frac{\frac{(1 + r_{\text{AH}^+\text{CP}} K_{\text{AH}^+\text{CP}}[\text{CP}])[H^+]}{(1 + K_{\text{AH}^+\text{CP}}[\text{CP}])} + A_0 \frac{r_{\text{CB}} + r_{\text{CP}}[\text{CP}]}{(1 + K_{\text{AH}^+\text{CP}}[\text{CP}])}}{[H^+] + K_{\text{obs}}} \quad (3.4)$$

Defining c_a

$$c_a = A_0 \frac{(1 + r_{AH+CP} K_{AH+CP} [CP])}{(1 + K_{AH+CP} [CP])} \quad (3.5)$$

And c_b ,

$$A_0 \frac{r_{CB} + r_{CP} [CP]}{(1 + K_{AH+CP} [CP])} = c_b \frac{(1 + K_{CBCP} [CP])}{(1 + K_{AH+CP} [CP])} K'_a \quad (3.6)$$

$$c_b = A_0 \frac{r_{CB} + r_{CP} [CP]}{(1 + K_{CBCP} [CP]) K'_a} \quad (3.7)$$

The absorbance at fixed concentration of co-pigment versus $[H^+]$ is given by eq.(3.8)

$$A_\lambda = c_a \frac{[H^+]}{[H^+] + K_{obs}} + c_b \frac{K_{obs}}{[H^+] + K_{obs}} \quad (3.8)$$

Eq.(3.8) is equivalent to a single acid-base system with acidity constant K_{obs} with c_a defining the acidic plateau and c_b the basic plateau. In Fig. A3.1 a simulation for $pK_{obs}=3$, $c_a=1.2$ and $c_b=0.5$ is shown as a function of pH.

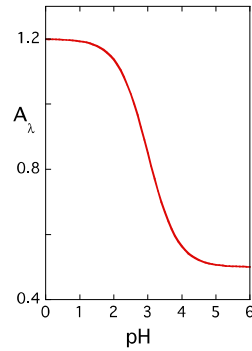
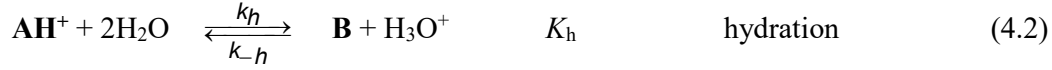
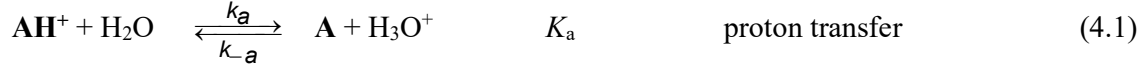


Figure A3.1. Simulation of eq.(3.8) for $pK_{obs}=3$, $c_a=1.2$ and $c_b=0.5$ as a function of pH.

Appendix 4

Generalization of the Malien-Aubert equation to 1:1 and 1:2 equilibria⁸

When flavylum cation forms 1:1 and 1:2 complexes the Malien-Aubert equation could be generalized



The mass balance gives

$$C_0 = [AH^+] + [AH^+CP] + [AH^+CP_2] + [A] + [B] + [Cc] + [Ct] \quad (4.7)$$

Using eq.(4.1) to eq.(4.6)

$$C_0 = [AH^+] \left(1 + K_{AH^+CP(1)} [CP] + K_{AH^+CP(1)} K_{AH^+CP(2)} [CP]^2 + \frac{K_a}{[H^+]} + \frac{K_h}{[H^+]} + \frac{K_h K_t}{[H^+]} + \frac{K_h K_t K_i}{[H^+]} \right) \quad (4.8)$$

$$C_0 = [AH^+] \left(1 + K_{AH^+CP(1)} [CP] + K_{AH^+CP(1)} K_{AH^+CP(2)} [CP]^2 + \frac{K'_a}{[H^+]} \right) \quad (4.9)$$

From eq.(4.9) the mole fraction distribution of the flavylum cation is obtained

$$\begin{aligned} C_0 &= [AH^+] \left(1 + K_{AH^+CP(1)} [CP] + K_{AH^+CP(1)} K_{AH^+CP(2)} [CP]^2 + \frac{K'_a}{[H^+]} \right) \\ \chi_{AH^+} &= \frac{[AH^+]}{C_0} = \frac{1}{1 + K_{AH^+CP(1)} [CP] + K_{AH^+CP(1)} K_{AH^+CP(2)} [CP]^2 + \frac{K'_a}{[H^+]}} = \\ &= \frac{[H^+]}{1 + K_{AH^+CP(1)} [CP] + K_{AH^+CP(1)} K_{AH^+CP(2)} [CP]^2 + K'_a} \end{aligned}$$

$$\chi_{AH^+} = \frac{[AH^+]}{C_0} = \frac{1}{1 + K_{AH^+CP(1)}[CP] + K_{AH^+CP(1)}K_{AH^+CP(2)}[CP]^2 + \frac{K'_a}{[H^+]}} =$$

$$= \frac{[H^+]}{1 + K_{AH^+CP(1)}[CP] + K_{AH^+CP(1)}K_{AH^+CP(2)}[CP]^2[H^+] + K'_a}$$

$$\chi_{AH^+} = \frac{[H^+]}{D}; \chi_{AH^+CP} = \frac{K_{AH^+CP(1)}[CP][H^+]}{D}; \chi_{AH^+CP_2} = \frac{K_{AH^+CP(1)}K_{AH^+CP(2)}[CP]^2[H^+]}{D}$$

$$\chi_A = \frac{K_a}{D}; \chi_B = \frac{K_h}{D}; \chi_{Cc} = \frac{K_h K_t}{D}; \chi_{Ct} = \frac{K_h K_t K_i}{D}$$

$$D = (1 + K_{AH^+CP(1)} + K_{AH^+CP(1)}K_{AH^+CP(2)}[CP]^2)[H^+] + K'_a$$

$$A_\lambda = \varepsilon_{AH^+} C_0 \chi_{AH^+} + \varepsilon_{AH^+CP} C_0 \chi_{AH^+CP} + \varepsilon_{AH^+CP_2} C_0 \chi_{AH^+CP_2}$$

$$A_\lambda = \varepsilon_{AH^+} C_0 \frac{[H^+]}{D} + \varepsilon_{AH^+CP} C_0 \frac{K_{AH^+CP(1)}[H^+][CP]}{D} + \varepsilon_{AH^+CP_2} \frac{C_0 K_{AH^+CP(1)}K_{AH^+CP(2)}[H^+][CP]^2}{D}$$

$$A_\lambda = \frac{\varepsilon_{AH^+} C_0 [H^+] + \varepsilon_{AH^+CP} C_0 K_{AH^+CP(1)} [H^+][CP] + \varepsilon_{AH^+CP_2} C_0 K_{AH^+CP(1)} K_{AH^+CP(2)} [H^+][CP]^2}{(1 + K_{AH^+CP(1)}[CP] + K_{AH^+CP(1)}K_{AH^+CP(2)}[CP]^2)[H^+] + K'_a}$$

In terms of Dangles nomenclature⁸

$$A_\lambda = \frac{A_0[H^+] + A_1 K_1 [H^+] L_t + A_2 \beta_{12} [H^+] L_t^2}{(1 + K_1 + \beta_{12} L_t^2)[H^+] + K'_a}$$

Dividing by $[H^+]$

$$A_\lambda = \frac{A_0 + A_1 K_1 L_t + A_2 \beta_{12} L_t^2}{(1 + K_1 L_t + \beta_{12} L_t^2) + \frac{K'_a}{[H^+]}} \quad A_\lambda = \frac{A_0 + A_1 K_1 L_t + A_2 \beta_{12} L_t^2}{(1 + K_1 + \beta_{12} L_t^2) + \frac{K'_a}{[H^+]}}$$

For a 1:1 equilibrium

$$A_\lambda = \frac{\varepsilon_{AH^+} C_0 [H^+] + \varepsilon_{AH^+CP} C_0 K_{AH^+CP} [H^+][CP]}{(1 + K_{AH^+CP} [CP])[H^+] + K'_a}$$

$$A_\lambda = \frac{\varepsilon_{AH^+} C_0 [H^+] + \varepsilon_{AH^+CP} C_0 K_{AH^+CP} [H^+][CP]}{(1 + K_{AH^+CP} [CP])[H^+] + K'_a}$$

Introducing $r_{AH^+CP} = \frac{\varepsilon_{AH^+CP}}{\varepsilon_{AH^+}}$

$$A_{\lambda} = \frac{\varepsilon_{AH^+} C_0 [H^+] + \varepsilon_{AH^+CP} C_0 K_{AH^+CP} [H^+] [CP]}{(1 + K_{AH^+CP} [CP]) [H^+] + K'_a}$$

Which is one of the forms of the Malien-Aubert expression deduced in appendix 1.

$$A_{\lambda} = A_0 \frac{[H^+] (1 + r_{AH^+CP} K_{AH^+CP} [CP])}{(1 + K_{AH^+CP} [CP]) [H^+] + K'_a}$$

As discussed in the main text K_n should be viewed as K'_a the global equilibrium constant at the equilibrium.

References

- (1) Malien-Aubert, C.; Dangles, O.; Amiot, M. J. Influence of procyanidins on the color stability of oenin solutions. *Journal of Agricultural and Food Chemistry* **2002**, *50* (11), 3299.
- (2) Markovic, J. M. D.; Petranovic, N. A.; Baranac, J. M. The copigmentation effect of sinapic acid on malvin: a spectroscopic investigation on colour enhancement. *J. Photochem. Photobiol. B-Biol.* **2005**, *78* (3), 223.
- (3) Brouillard, R.; Mazza, G.; Saad, Z.; Albrechtgary, A. M.; Cheminat, A. The copigmentation reaction of anthocyanins-a microprobe for the structural study of aqueous solutions. *J. Am. Chem. Soc.* **1989**, *111* (7), 2604.
- (4) Brouillard, R.; Delaporte, B.; Dubois, J. E. Chemistry of Anthocyanins Pigments.3. Relaxation Amplitudes in pH-Jump Experiments. *J. Am. Chem. Soc.* **1978**, *100* (19), 6202.
- (5) Pina, F.; Melo, M. J.; Laia, C. A. T.; Parola, A. J.; Lima, J. C. Chemistry and Applications of Flavylium Compounds: a Handful of Colours. *Chem. Soc. Rev.* **2012**, *41* (2), 869.
- (6) Zou, H.; Ma, Y.; Liao, X. J.; Wang, Y. T. Effects of high pressure processing on the copigmentation reaction of pelargonidin-3-glucoside and catechin. *LWT-Food Sci. Technol.* **2019**, *108*, 240.
- (7) Mendoza, J.; Basilio, N.; de Freitas, V.; Pina, F. New Procedure To Calculate All Equilibrium Constants in Flavylium Compounds: Application to the Copigmentation of Anthocyanins. *ACS Omega* **2019**, *4* (7), 12058.
- (8) Dangles, O.; Elhajji, H. Synthesis of 3-methoxy-flavylium and 3-(beta-D-glucopyranosyloxy)flavylium ions- Influence of the flavylium substitution pattern on the reactivity of anthocyanins in aqueous solutions. *Helvetica Chimica Acta* **1994**, *77* (6), 1595.

Chapter 3- Copigmentation of Anthocyanins with Copigments Possessing an Acid-Base Equilibrium in Moderately Acidic Solutions.

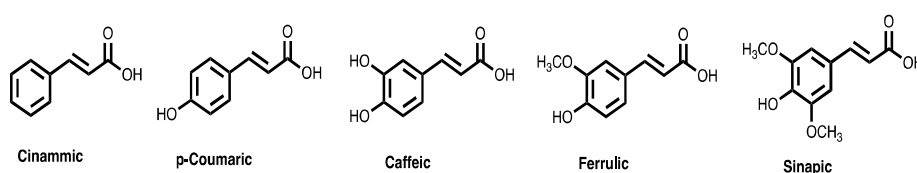
Abstract

The fact that many copigments such as cinnamic acids exhibit an acid-base equilibrium at moderately acidic pH values have not been taken in consideration in the copigmentation models and respective equations. In this work, the copigmentation constants of malvidin-3-O-glucoside and sinapic acid ($pK_a=4.5$) is reported. The flavylium cation (**AH⁺**) in moderately acid medium ($pH \leq 6$) can be considered a monoprotic acid in equilibrium with its conjugated base (**CB**) equal to the sum of the concentrations of quinoidal base (**A**), hemiketal (**B**), *cis* and *trans* chalcones (**Cc** and **Ct**), with equilibrium constant K'_a . Based on this behavior a new mathematical expression to account for the copigmentation of **AH⁺** and **CB** was deduced. The system was also studied by a series of reverse pH jumps monitored by stopped flow and a previously reported procedure was extended to consider the acid-base equilibrium of the copigment. The copigmentation constant of flavylium cation with the acidic form of the copigment, *CP*, is 243 M^{-1} , and no copigmentation with the basic form of the copigment, *CP* (-), was observed. This was explained by the very small superposition of these two species in the pH domain. The copigmentation constants of **CB** with the acidic and basic forms of the copigment, calculated from the UV-Vis measurements are respectively $K_{CB\text{CP}}=53 \text{ M}^{-1}$ and $K_{CB\text{CP}(-)}=78 \text{ M}^{-1}$. The reverse pH jumps monitored by stopped flow allowed the calculation of the copigmentation constants of the acidic form of the copigment (*CP*) with quinoidal base (A), hemiketal (B) and *cis*-chalcone (Cc), respectively $K_{ACP}=531 \text{ M}^{-1}$, $K_{BCP}=17$, $K_{CcCP}=41 \text{ M}^{-1}$ as well as with the basic form of the copigment $K_{ACP(-)}=196 \text{ M}^{-1}$, $K_{BCP(-)}=79$, $K_{CcCP(-)}=94 \text{ M}^{-1}$. The reverse pH jumps followed by a standard spectrophotometer allows for $K_{CtCP}=55 \text{ M}^{-1}$ and $K_{CcCP(-)}=80 \text{ M}^{-1}$ and $K_{CB\text{CP}}=54 \text{ M}^{-1}$ and $K_{CB\text{CP}(-)}=89 \text{ M}^{-1}$. The estimated error for all copigmentation constants is *circa* 10%.

Keywords: Anthocyanins, copigmentation, cinammic acids, sinapic acid, quinoidal base copigmentation, chalcones copigmentation, reverse pH jumps, stopped flow.

Introduction

It is firmly established that in general copigmentation takes place not only with the flavylum cation but also with the quinoidal base, as well as with *cis* and *trans* chalcones (Mistry, Cai et al. 1991),(Brouillard, Wigand et al. 1991, Dangles and Elhajji 1994),(Mendoza, Basilio et al. 2019). This fact implies that interactions involving these equilibrium forms should be taken into account in the copigmentation models and respective mathematical equations (Oliveira, 2021).



Scheme 1. Cinnamic acid derivatives that are able to copigment with anthocyanins.

Table 1. Acidity constants of cinnamic acid and some derivatives

Acid	Cinnamic	p-coumaric	Caffeic	Ferrulic	Sinapic
pK_a	4.44¹	4.7 (Benvidi et al, 2019)	3.95 (Romero et al, 2018) 3.0 (Manoel & Moya, 2015)	4.58 (Serjeant EP, 1979) 3.6 (Manoel & Moya, 2015)	3.61 (Markovic et al, 2005) 4.58 (Manoel & Moya, 2015) 4.5*

*This work: error ± 0.05 .

Some of the most common copigments of anthocyanins are molecules presenting an acid-base equilibrium with acidity constants (pK_a) at moderately pH values, Scheme 1 and Table 1. This is a severe limitation when copigmentation studies with anthocyanins are extended to higher pH values in order to access the complexation of quinoidal base, hemiketal *cis* and *trans* chalcones. Despite the differences on the reported pK_a values, Table 1, cinnamic acids derivatives are an example of these type of copigments. In this work, we report on a model and respective mathematical expression to account for both of these requirements.

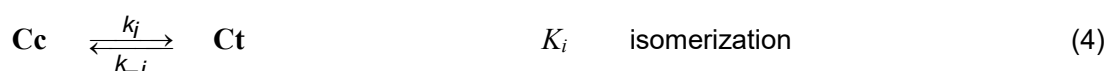
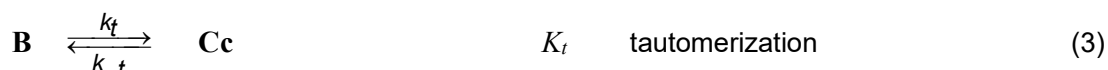
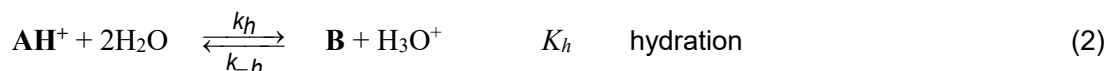
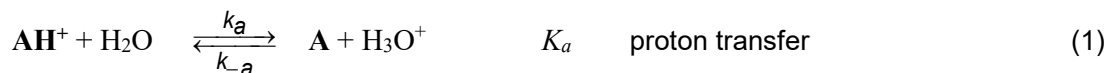
In a recent paper, we described the limits of the copigmentation models and respective equations and deduced an expression that is able to account for the copigmentation constants not only with flavylum cation but also with its conjugate base CB equal to the sum of the concentrations of quinoidal base, hemiketal, *cis* and *trans*-chalcones (Oliveira, 2021). This model is based on an interesting property of the flavylum based

¹ Source FoodDB

¹ Smith, R.M.; Martell, A.E. Critically Selected Stability Constants of Metal Complexes. NIST Standard Reference Database 46. 2004, 8.

multistate of species: the flavylum cation can be considered a polyprotic acid in equilibrium with its conjugated bases $CB=[A]+[B]+[Cc]+[Ct]$ and $CB^-=[A^-]+[B^-]+[Cc^-]+[Ct^-]$, etc.

In acidic to neutral medium the anthocyanins equilibrium is given by eq. (1) to eq. (8)



This complex system can be dramatically simplified considering flavylum cation a diprotic acid in equilibrium with the conjugated bases CB, eq. (5) (Brouillard, Delaporte et al. 1978),(Pina, Oliveira et al. 2015).



With $[CB]=[A]+[B]+[Cc]+[Ct]$

Considering now the possibility of copigmentation with AH^+ and CB, eq. (6) and eq. (7) should be added to the system



with CP, the concentration of the copigment, used in excess relatively to the anthocyanin.

The system can be extended to the anionic species, but the calculation of the respective equilibrium constants presents more uncertainty, due to the errors propagation and the instability of anthocyanins at these pH values. Consequently, in this work our data is limited to pH values not higher than $pH \approx 6$.

Based on this limitations (in particular pH not higher than ≈ 6), eq. (8) was deduced (Oliveira, 2021).

$$A_\lambda = A_0 \left\{ \frac{(1+r_{AH^+CP}K_{AH^+CP}[CP])[H^+] + r_{CB} + r_{CBCP}[CP]}{(1+K_{AH^+CP}[CP])[H^+] + (1+K_{CBCP}[CP])K'_a} \right\} \quad (8)$$

Where A_λ is the absorbance at the selected wavelength λ , and $A_0 = \varepsilon_{AH^+} C_0$ with ε_{AH^+} and C_0 respectively the mole absorption coefficient at the wavelength λ , and total concentration of the anthocyanin. In eq.(8) K_{AH+CP} is defined by eq.(6) and K_{CBP} by eq.(7)

From the definition of the equilibrium constant of eq.(7), it is straightforward to express the global constants K_{CBP} in terms of the contributions of the species **A**, **B**, **Cc** and **Ct**, eq.(9)

$$K_{CBP} = \frac{(K_{ACP}K_a + K_{BCP}K_h + K_{CCP}K_hK_t + K_{CTP}K_hK_tK_i)}{K'_a} \quad (9)$$

K_{XCP} (X=A, B, Cc, Ct) are the copigmentation constants with the species X, and r_{AH+CP} , r_{CB} and r_{CBP} are three parameters that are constant for a fixed wavelength.

$$r_{AH+CP} = \frac{\varepsilon_{AH+CP}}{\varepsilon_{AH^+}} \quad \text{and} \quad r_X = \frac{\varepsilon_{XCP}}{\varepsilon_{AH^+}} \quad (X=A, B, Cc, Ct) \quad (10)$$

$$r_{CB} = r_A K_a + r_B K_h + r_{Cc} K_h K_t + r_{Ct} K_h K_t K_i \quad (11)$$

$$r_{CBP} = r_{ACP} K_a K_{ACP} + r_{BCP} K_h K_{BCP} + r_{CCP} K_h K_t K_{CCP} + r_{CTP} K_h K_t K_i K_{CTP} \quad (12)$$

The parameter r_{CB} can be calculated from the absorbance in the absence of the copigment, eq.(13)

$$A_{\lambda(CP=0)} = A_0 \left\{ \frac{[H^+] + r_{CB}}{[H^+] + K'_a} \right\} \quad (13)$$

Summarizing, in eq.(8) four parameters have to be fitted, K_{AH+CP} , K_{CBP} , r_{AH+CP} and r_{CBP} . In order to reduce the intrinsic uncertainty of the fittings, K_{AH+CP} and r_{AH+CP} should be calculated at $\text{pH} \approx 1$ when the flavylium cation is the sole species. In this case eq.(8) is reduced to eq.(14),

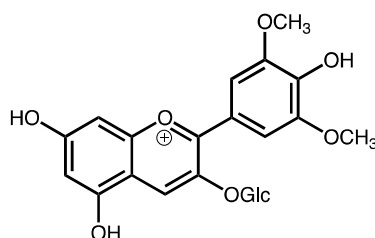
$$A_\lambda = A_0 \left\{ \frac{(1 + r_{AH+CP} K_{AH+CP} [CP])}{(1 + K_{AH+CP} [CP])} \right\} \quad (14)$$

Fitting of A_λ as a function of the copigmentation concentration in eq. (14) allows for the calculation of the parameters r_{AH+CP} and K_{AH+CP} . In other experiments, for example

pH=2.6 and pH=3.5, representation of A_{\square} versus CP , eq. (8), should be used to fit the parameters r_{CP} and K_{CBCP} .

Eq. (8) can also be applied at a fixed concentration of the copigment, A_{\square} versus pH, leading to a sigmoid curve. A global fitting of all these allows for the calculation of the four parameters r_{AH+CP} , K_{AH+CP} , r_{CP} and K_{CBCP} with good accuracy. Eq. (8) has however a limitation, because does not permit the calculation of the individual K_{XCP} (X=A, B, Cc, Ct) constants. Nevertheless K_{CBCP} has a relevant meaning because it is the sum of the copigmentation constants with **A**, **B**, **Cc**, **Ct** weighted by the mole fraction of each of these species in the absence of the copigment. Eq. (8) was successfully applied to the copigmentation of malvidin-3-glucoside (oenin) with caffeine and pentagalloyl glucose, two copigments that do not have any acid-base reaction in acidic to moderately acidic pH values (Oliveira, 2021).

In this work we are introducing an extension of the model by considering a copigment, sinapic acid, possessing a $pK_a=4.5$. Differently from caffeine or pentagalloyl glucose previously reported, (Oliveira, 2021) the copigment changes from the acidic form to the basic one in the working pH range where eq. (8) is applied. This duplicates the number of the fitting parameters from four to eight and needs a concomitant increasing of the number of experiments to get reliable constants. Malvidin-3-O-glucoside (Oenin) was chosen as a representative anthocyanin, **Scheme 2**.



Scheme 2. Malvidin-3-O-glucoside (oenin)

Theory

Equilibrium followed by UV-Vis absorption (excluding anionic species).

Since the copigment with total concentration $[CP]_0$ is distributed between its acidic and basic forms

$$[CP]_0 = [CP] + [CP(-)] \tag{15}$$

The respective mole fractions are given by eq. (16)

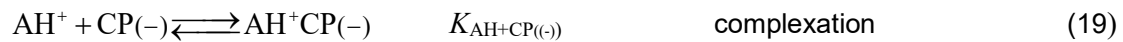
$$\chi_{CP} = \frac{[CP]}{[CP]_0} = \frac{[H^+]}{[H^+] + K_{CP/CP(-)}}; \quad \chi_{CP(-)} = \frac{[CP^-]}{[CP]_0} = \frac{K_{CP/CP(-)}}{[H^+] + K_{CP/CP(-)}} \quad (16)$$

$$[CP] = \chi_{CP}[CP]_0; \quad [CP(-)] = \chi_{CP(-)}[CP]_0 \quad (17)$$

The concentration of $[CP]$ and $[CP(-)]$, eq. (17), changes with pH but the respective mole fractions can be obtained provided that the pK_a of the copigment is previously measured. In this situation the four parameters of eq. (8) should be duplicated, because a priori the basic form of the copigment could interact differently from the acidic one.

$$A_\lambda = A_0 \left\{ \frac{[H^+](1 + r_{AH^+CP} K_{AH^+CP} \chi_{CP} [CP]_0 + r_{AH^+CP(-)} K_{AH^+CP(-)} \chi_{CP(-)} [CP]_0) + r_{CB} + r_{CB/CP} \chi_{CP} [CP]_0 + r_{CB/CP(-)} \chi_{CP(-)} [CP]_0}{(1 + K_{AH^+CP} \chi_{CP} [CP]_0 + K_{AH^+CP(-)} \chi_{CP(-)} [CP]_0)[H^+] + K'_a(1 + K_{CB/CP} \chi_{CP} [CP]_0 + K_{CB/CP(-)} \chi_{CP(-)} [CP]_0)} \right\} \quad (18)$$

Beside the parameters r_{AH^+CP} , K_{AH^+CP} , $r_{CB/CP}$ and $K_{CB/CP}$ resulting from the interaction of the acidic form of the copigment, the equivalent parameters for the interaction with the basic form of the copigment are defined, $r_{AH^+CP(-)}$, $K_{AH^+CP(-)}$, $r_{CB/CP(-)}$ and $K_{CB/CP(-)}$.



$$r_{AH^+CP(-)} = \frac{\varepsilon_{AH^+CP(-)}}{\varepsilon_{AH^+}} \quad (20)$$



$$r_{CB/CP(-)} = r_{ACP(-)} K_a K_{ACP(-)} + r_{BCP(-)} K_h K_{BCP(-)} + r_{CCP(-)} K_h K_t K_{CCP(-)} + r_{CICP(-)} K_h K_t K_i K_{CICP(-)} \quad (22)$$

$$K_{CB/CP(-)} = \frac{(K_{ACP(-)} K_a + K_{BCP(-)} K_h + K_{CCP(-)} K_h K_t + K_{CICP(-)} K_h K_t K_i)}{K'_a} \quad (23)$$

The main question for this kind of measurements is the accuracy of the parameters to be achieved by fitting. At $pH \approx 1$ χ_{CP} is basically equal to 1 and eq. (8) is reduced to eq. (14), with two fitting parameters, r_{AH^+CP} and K_{AH^+CP} .

By the other side at $pH > 5$ the mole fraction of AH^+ can be neglected and for $pH > pK_a(\text{copigment}) + 1$, eq. (24) is a good approximation.

$$A_\lambda = A_0 \left\{ \frac{[H^+] + r_{CB} + r_{CB/CP(-)} [CP]_0}{[H^+] + K'_a \left\{ 1 + K_{CB/CP(-)} [CP]_0 \right\}} \right\} \quad (24)$$

In principle r_{AH^+CP} and K_{AH^+CP} can be calculated from eq. (14) and from eq. (24) $r_{CB/CP(-)}$ and $K_{CB/CP(-)}$.

However, there is still four more parameters to account for, $r_{AH+CP(-)}$, $K_{AH+CP(-)}$, r_{CBCP} and K_{CBCP} . These parameters should be calculated by means of the use of eq. (18) from the absorbance at several pH values between $2 < \text{pH} < 6$ as well as in another experiment where the absorbance is calculated at a fixed copigment concentration as a function of pH. In order to get enough accuracy, we performed five independent experiments and the equilibrium constants were obtained through a global fitting of all data, see results and discussion.

Reverse pH Jumps a powerful tool

Reverse pH jumps are defined by addition of acid back to $\text{pH} \approx 1$ to equilibrated solutions at higher pH values. As shown above, the measurements carried out by a standard UV-Vis absorption spectroscopy have an intrinsic limitation. The constant K_{CBCP} can be determined but it is not possible to obtain the individual constants K_{XCP} ($X=A, B, Cc$ and Ct). However, this can be achieved by means of a series of reverse pH jumps monitored by stopped flow from equilibrated solutions at moderately acidic pH values back to $\text{pH} \leq 1$ (Mendoza et al, 2019). The *cis-trans* isomerization is much slower than the other kinetic processes and the absorbance traces versus time in the stopped flow experiments are constituted by three amplitudes: *i*) the initial one for $t=0$ that corresponds to the quinoidal bases and respective complexes (and some remaining flavylum cation and its complex if the initial pH is more acid) (Pina, 2014); *ii*) the amplitude of a faster kinetic process is due to the conversion of hemiketal and its complex into flavylum cation (at this pH hydration is faster than tautomerization, change of regime); *iii*) the amplitude of the conversion of *cis*-chalcone and its complex into flavylum cation and its complex via hemiketal and its complex, see Fig. 4b. The normalization of the amplitudes (sum=1) gives directly the mole fractions of flavylum cation, quinoidal base, *cis*-chalcone, and the respective complexes. This is a powerful tool to calculate the copigmentation constants with these species (Mendoza et al, 2019). It was applied to obtain the copigmentation constants of 4-hydroxyflavylum and mavidin-3-O-glucoside with caffeine (Mendoza et al, 2019). Moreover, contrary to eq. (8), reverse pH jumps followed by stopped flow can be extended to the anionic species at the pseudo equilibrium, while in this study we restrained the study to $\text{pH} \leq 6$, because the simpler anthocyanins are unstable at higher pH values and there is an increasing error in the case of the anionic species due to the error propagation.

Calculation of the equilibrium and copigmentation constants for a copigment lacking the acidity constant.

Considering a copigment that does not change its form in acidic to moderately basic pHs, the mole fractions of the three amplitudes of the reverse pH jumps experiments monitored by stopped flow are given by eq. (25) to eq. (28), see appendix.

$$\chi_{AH^+} + \chi_{AH^+CP} + \chi_A + \chi_{ACP} = \frac{[H^+] + a_0 K_{a(CP)}^\wedge}{D_{CP}^\wedge} \quad (25)$$

$$\chi_B + \chi_{BCP} = \frac{b_0 K_{a(CP)}^\wedge}{D_{CP}^\wedge} \quad (26)$$

$$\chi_{Cc} + \chi_{CcCP} = \frac{c_0 K_{a(CP)}^\wedge}{D_{CP}^\wedge} \quad (27)$$

$$D_{CP}^\wedge = [H^+] + K_{a(CP)}^\wedge \quad (28)$$

The fitting allows for the determination of the parameters a_0 , b_0 and c_0 ($a_0 + b_0 + c_0 = 1$) for the global equilibrium constant $K_{a(CP)}^\wedge$.

$$K_{a(CP)}^\wedge = \frac{K_a^\wedge (1 + K_{CBCP} [CP])}{1 + K_{AH^+CP} [CP]} \quad (K_a^\wedge = K_a + K_h + K_h K_t \quad \text{and} \quad K_{CBCP} = \frac{K_{ACP} K_a + K_{BCP} K_h + K_{CcCP} K_h K_t}{K_a^\wedge}) \quad (29)$$

The constants $K_{a(CP)}^\wedge$ is calculated by these fittings and within experimental error should be the same of the one calculated from the inflection point of the absorbance at the pseudo-equilibrium versus pH.

As shown in appendix the same mole fractions can be written in terms of the equilibrium and copigmentation constants, eq.30 to eq.31.

$$\chi_{AH^+} + \chi_{AH^+CP} + \chi_A + \chi_{ACP} = \frac{[H^+] + \left(\frac{K_a + K_{ACP} K_a [CP]}{1 + K_{AH^+CP} [CP]} \right)}{D_{CP}^\wedge} \quad (30)$$

$$\chi_B + \chi_{BCP} = \frac{\left(\frac{K_h + K_{BCP} K_h [CP]}{1 + K_{AH^+CP} [CP]} \right)}{D_{CP}^\wedge} \quad (31)$$

$$\chi_{Cc} + \chi_{CcCP} = \frac{\left(\frac{K_h + K_{CcCP} K_h K_t [CP]}{1 + K_{AH^+CP} [CP]} \right)}{D_{CP}^\wedge} \quad (32)$$

Comparing eq. (25) to eq. (27) with eq. (30) to eq. (32) the following relations can be found

$$a_o K_{a(CP)}^{\wedge} = \frac{K_a(1 + K_{ACP}[CP])}{1 + K_{AH^+CP}[CP]}; \quad (33)$$

$$b_o K_{a(CP)}^{\wedge} = \frac{K_h(1 + K_{BCP}[CP])}{1 + K_{AH^+CP}[CP]}; \quad (34)$$

$$c_o K_{a(CP)}^{\wedge} = \frac{K_h K_t(1 + K_{CCP}[CP])}{1 + K_{AH^+CP}[CP]}; \quad (35)$$

The equilibrium constants K_a , K_h , K_t are calculated from the reverse pH jumps in the absence of copigment. The copigmentation constant K_{AH+CP} should be obtained at pH=1, where no other species are present. At this point all the other copigmentation constants can be calculated.

Calculation of the equilibrium and copigmentation constants for a copigment possessing an acidity constant at the working pH range

The reverse pH jumps can be used to account for the copigmentation with a copigment possessing an acid-base equilibrium in the working pH range. In this case, it is considered the possibility of a different interaction of the anthocyanin species with the acidic and basic forms of the copigment.

$$K_{a(CP/CP(-))}^{\wedge} = \frac{K_a^{\wedge} + K_{CB CP} K_a^{\wedge} \chi_{CP} [CP]_0 + K_{CB CP(-)} K_a^{\wedge} \chi_{CP(-)} [CP]_0}{1 + K_{AH^+CP} \chi_{CP} [CP]_0 + K_{AH^+CP(-)} \chi_{CP(-)} [CP]_0} \quad (36)$$

While in eq.29 $K_{a(CP)}$ is constant (is pH independent) in this case there is a pH dependence. Nevertheless, the behaviour of the system is similar to a single acid base equilibrium where it is possible to define the mole fractions of the two forms as in eq.37.

$$\chi_{all AH^+} = \frac{[H^+]}{[H^+] + K_{a(CP/CP(-))}}; \text{ and } \chi_{all CB} = \frac{K_{a(CP/CP(-))}}{[H^+] + K_{a(CP/CP(-))}} \quad (37)$$

When the copigment possesses a relatively high difference between its pK_a and pK_a (and pK_a) the pH superposition between AH^+ and $CP(-)$ is very small and the constant $K_{AH^+CP(-)}$ can be neglected.²

² The fitting can also be done considering this constant. We have done it but when the value of K_{AH+CP} calculated at pH=1 is fixed, the fitting gives $K_{AH+CP(-)}=0$

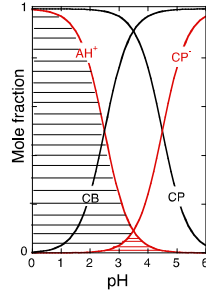


Figure 1. pH superposition between AH⁺ and CP (-) (red); the same for AH⁺ and CP (black).

In order to get more accuracy to the system, eq. (36) was divided in three terms.

$$K_{a(CP/CP(-))}^{\wedge} = \frac{K_a^{\wedge}}{1 + K_{AH^+CP} \chi_{CP}[CP]_0} + \frac{K_{CBCP^-}}{1 + K_{AH^+CP} \chi_{CP}[CP]_0} \chi_{CP}[CP]_0 + \frac{K_{CBCP(-)^-}}{1 + K_{AH^+CP} \chi_{CP}[CP]_0} \chi_{CP(-)}[CP]_0 \quad (38)$$

The first regards the contribution of the free species, the second the complexes with the acidic form of the copigment and the third those with the basic form of the copigment.

The term $1 + K_{AH^+CP} \chi_{CP}[CP]_0$ can be known provided that the constant K_{AH^+CP} is calculated at pH=1.0. At this point the mole fractions can be written.

$$\chi_{AH^+} + \chi_{AH^+CP} + \chi_A + \chi_{ACP} + \chi_{ACP(-)} = \frac{[H^+] + \frac{K_a + K_{ACP} K_a \chi_{CP}[CP]_0 + K_{ACP(-)} K_a \chi_{CP(-)}[CP]_0}{1 + K_{AH^+CP} \chi_{CP}[CP]_0}}{D_{CP/CP(-)}^{\wedge}} \quad (39)$$

$$\chi_B + \chi_{BCP} + \chi_{BCP(-)} = \frac{\frac{K_h + K_{BCP} K_h \chi_{CP}[CP]_0 + K_{BCP(-)} K_h \chi_{CP(-)}[CP]_0}{1 + K_{AH^+CP} \chi_{CP}[CP]_0}}{D_{CP/CP(-)}^{\wedge}} \quad (40)$$

$$\chi_{Cc} + \chi_{CcCP} + \chi_{CcCP(-)} = \frac{\frac{K_h + K_{CcCP} K_h K_t \chi_{CP}[CP]_0 + K_{CcCP} K_h K_t \chi_{CP(-)}[CP]_0}{1 + K_{AH^+CP} \chi_{CP}[CP]_0}}{D_{CP/CP(-)}^{\wedge}} \quad (41)$$

Or

$$\begin{aligned} & \chi_{AH^+} + \chi_{AH^+CP} + \chi_A + \chi_{ACP} = \\ & = a_0 \frac{K_a^{\wedge}}{1 + K_{AH^+CP} \chi_{CP}[CP]_0} + a_{0(CP)} \frac{K_a^{\wedge} K_{CBCP^-}}{1 + K_{AH^+CP} \chi_{CP}[CP]_0} \chi_{CP}[CP]_0 + a_{0(CP(-))} \frac{K_a^{\wedge} K_{CBCP(-)^-}}{1 + K_{AH^+CP} \chi_{CP}[CP]_0} \chi_{CP(-)}[CP]_0 \end{aligned} \quad (42)$$

$$\begin{aligned} & \chi_B + \chi_{BCP} = \\ & = b_0 \frac{K_a^{\wedge}}{1 + K_{AH^+CP} \chi_{CP}[CP]_0} + b_{0(CP)} \frac{K_a^{\wedge} K_{CBCP^-}}{1 + K_{AH^+CP} \chi_{CP}[CP]_0} \chi_{CP}[CP]_0 + b_{0(CP(-))} \frac{K_a^{\wedge} K_{CBCP(-)^-}}{1 + K_{AH^+CP} \chi_{CP}[CP]_0} \chi_{CP(-)}[CP]_0 \end{aligned} \quad (43)$$

$$\begin{aligned} \chi_{Cc} + \chi_{CcCP} &= \\ &= c_0 \frac{K_a^\wedge}{1 + K_{AH^+CP} \chi_{CP}[CP]_0} + c_{0(CP)} \frac{K_a^\wedge K_{CBCP^\wedge}}{1 + K_{AH^+CP} \chi_{CP}[CP]_0} \chi_{CP}[CP]_0 + c_{0(CP(-))} \frac{K_a^\wedge K_{CBCP(-)^\wedge}}{1 + K_{AH^+CP} \chi_{CP}[CP]_0} \chi_{CP(-)}[CP]_0 \end{aligned} \quad (44)$$

And $a_0 + b_0 + c_0 = 1$, $a_{0CP} + b_{0CP} + c_{0CP} = 1$ and $a_{0CP(-)} + b_{0CP(-)} + c_{0CP(-)} = 1$

with $a_0 = K_a/K_a^\wedge$; $b_0 = K_h/K_a^\wedge$; $c_0 = K_h K_t/K_a^\wedge$

Comparing eq.39, eq.40 and eq.41 with eq.42, eq.43 and eq.44, the following relations are obtained

$$\begin{aligned} a_{0CP} K_a^\wedge K_{CB^\wedge CP} &= K_a K_{ACP}; & b_{0CP} K_a^\wedge K_{CB^\wedge CP} &= K_h K_{BCP}; & c_{0CP} K_a^\wedge K_{CB^\wedge CP} &= K_h K_t K_{CcCP} \\ a_{0CP(-)} K_a^\wedge K_{CB^\wedge CP(-)} &= K_a K_{ACP(-)}; & b_{0CP(-)} K_a^\wedge K_{CB^\wedge CP(-)} &= K_h K_{BCP(-)}; & c_{0CP(-)} K_a^\wedge K_{CB^\wedge CP(-)} &= K_h K_t K_{CcCP(-)} \end{aligned} \quad (45)$$

From eq. (45) all copigmentation with the CB species can be obtained.

Trans-chalcone contribution

Reverse pH jumps monitored by stopped flow do not access the mole fractions of the *trans*-chalcone. In this case the measurements should be carried out by means of a standard spectrophotometer and the equilibrium should be considered.

$$K'_{a(CP/CP')} = \frac{K'_a}{(1 + K_{AH^+CP} \chi_{CP}[CP]_0)} + \frac{K_{CBCP} K'_a \chi_{CP}[CP]_0}{(1 + K_{AH^+CP} \chi_{CP}[CP]_0)} + \frac{K_{CBCP(-)} K'_a \chi_{CP(-)}[CP]_0}{(1 + K_{AH^+CP} \chi_{CP}[CP]_0)} \quad (46)$$

After a direct pH jump the absorption is monitored as a function of the time during several hours up to arrive to the equilibrium, see an example in **Fig.7a**. The initial value corresponds to the fraction of the **CB[^]** species and the amplitude of the trace to the amount of **Ct** at the equilibrium. This allows to obtain the mole fraction distribution of the *trans*-chalcone as a function of pH, by representing the ratio between the amplitude of the trace and the final absorbance. In other words, $\chi_{Ct} + \chi_{CtCP} + \chi_{CtCP(-)}$ are obtained directly from these experiments. Considering the overall mole fraction distribution of CB species, eq. (47)

$$\chi_{all\ CB\ species} = \frac{\frac{K'_a}{(1 + K_{AH^+CP}[CP])} + \frac{K_{CBCP} K'_a \chi_{CP}[CP]_0}{(1 + K_{AH^+CP}[CP])} + \frac{K_{CBCP(-)} K'_a \chi_{CP(-)}[CP]_0}{(1 + K_{AH^+CP}[CP])}}{[H^+] + K'_{a(CP)}} \quad (47)$$

The fraction that corresponds to **Ct** is given by q. (48)

$$\chi_{Ct} + \chi_{CtCP} + \chi_{CtCP(-)} = \frac{d_0 \frac{K'_a}{(1 + K_{AH^+CP}[CP])} + \frac{d_{0(CP)} K_{CBCP} K'_a \chi_{CP}[CP]_0}{(1 + K_{AH^+CP}[CP])} + \frac{d_{0(CP(-))} K_{CBCP(-)} K'_a \chi_{CP(-)}[CP]_0}{(1 + K_{AH^+CP}[CP])}}{[H^+] + K'_{a(CP)}} \quad (48)$$

The mole fraction of all Ct species can also be expressed by eq.(49)

$$\chi_{Ct} + \chi_{CtCP} + \chi_{CtCP(-)} = \frac{\frac{K_h K_t K_i}{1 + K_{AH^+CP} \chi_{CP}[CP]_0} + \frac{K_h K_t K_i K_{CtCP} \chi_{CP}[CP]_0}{1 + K_{AH^+CP} \chi_{CP}[CP]_0} + \frac{K_h K_t K_i K_{CtCP(-)} \chi_{CP(-)}[CP]_0}{1 + K_{AH^+CP} \chi_{CP}[CP]_0}}{[H^+] + K'_{a(CP)}} \quad (49)$$

Comparing eq.(48) with eq.(49)

$$d_{0(CP)} K_{CBCP} K'_a = K_h K_t K_i K_{CtCP}; \quad d_{0(CP(-))} K_{CBCP(-)} K'_a = K_h K_t K_i K_{CtCP(-)} \quad (50)$$

The fitting of eq. (48) needs to adjust the parameters $d_{0(CP)}$ and $d_{0(CP(-))}$ as well as K_{CBCP} and $K_{CBCP(-)}$. There is a significant error in the simultaneously determination of the four parameters and consequently the obtained constants K_{CtCP} and $K_{CtCP(-)}$. Nevertheless, the UV-Vis experiments give also the parameters K_{CBCP} and $K_{CBCP(-)}$, that can be used to fit d_0 and $d_{0(CP(-))}$. At the end all constants should be coherent for all experiments performed.

Material and methods

Reagents

Sinapic acid was obtained from Fluka. Malvidin-3-O-glucoside (oenin) was isolated from a young red wine as described previously (Araujo et al, 2017). Theorell and Stenhagen universal buffer was prepared according to the literature ("Küster FW, Thiel A. Tabelle per le Analisi Chimiche e Chimico- Fische. 12 th ed Milano, Italy: Hoepli; 1982. p. 157–60"). Briefly, the universal buffer was prepared by dissolving 2.25 mL of phosphoric acid 85% (w/w), 7.00 g of monohydrated citric acid, 3.54 g of boric acid and 343 mL of a 1 M NaOH solution. A final volume of 1 L was achieved by the addition of Millipore water.

Copigmentation studies

Fixed co-pigment concentration, changing pH.

The titration of oenin (4.2×10^{-5} M) in the presence of sinapic acid was performed by UV-visible spectroscopy by pH jump from pH = 1 to higher pH values from pH ~ 2.0 to ~ 5.5. A stock solution of oenin (3.2×10^{-4} M) was prepared in 0.25 M HCl. The sinapic acid stock solution (5×10^{-2} M) was prepared in ethanol (the concentration of ethanol in the final

solution is 10%, v/v) and a fixed concentration of 5×10^{-3} M of sinapic acid was used. Then, to plastic 10x10 mm cuvettes 500 μ L of a 0.1 M NaOH solution, 500 μ L of a Theorell and Stenhagen universal buffer solution adjusted to different pH values from 2 to 5.5, 150 μ L of the co-pigment stock solution, 150 μ L of Millipore water and 200 μ L of oenin stock solution (3.2×10^{-4} M) were added. Similar experiments were performed in the absence of sinapic acid. The absorption spectra of the solutions were obtained after one day of equilibration in the dark (equilibrium acidity constant, pK'_a) in a Thermo Scientific Evolution Array UV-Visible spectrophotometer at 25°C. The pH values of all solutions were measured in a WTW pH 320 (Weilheim, Germany) with a CRISON 5209 combined glass electrode of 3 mm diameter (Barcelona, Spain). The pH meter was calibrated with pH 4 and 7 buffer solutions. Fittings for pK'_a determination were carried out using the Solver program from Microsoft Excel. Similar experiments were performed in the absence of co-pigments.

Fixed pH and co-pigment concentration change.

Oenin copigmentation constants (K_{AH^+CP} , $K_{AH^+CP^-}$, K_{CBCP} and K_{CBCP^-}) were determined by UV-visible spectroscopy by the titration of oenin with different concentrations of sinapic acid at pH 1.06, 2.89, 3.6, 4.64 and 5.75.

For that, a solution of oenin at 4.2×10^{-5} M was prepared at each pH value (solution A). A solution at the same pH value containing the same concentration of oenin and sinapic acid at a concentration of 5×10^{-3} M was prepared (Solution B). Then, solutions with different concentration of sinapic acid were obtained by the addition of small volumes of the solution B to the solution A. The visible absorption spectrum of all solutions was recorded in a Thermo Scientific Evolution Array UV-visible spectrophotometer from 350-700 nm in a 10x10 mm quartz cell.

The reverse pH jumps from the pseudo-equilibrium were monitored on an SX20 (Applied Photophysics; Surrey, UK) spectrometer equipped with a PDA.1/UV photodiode array detector. A filter of 435 nm was used to prevent the photochemical reactions that could take place from Cc or B.

Results

The spectral variations of oenin versus sinapic acid concentration at five different pH values at the pseudo-equilibrium is shown in **Fig. 3**.

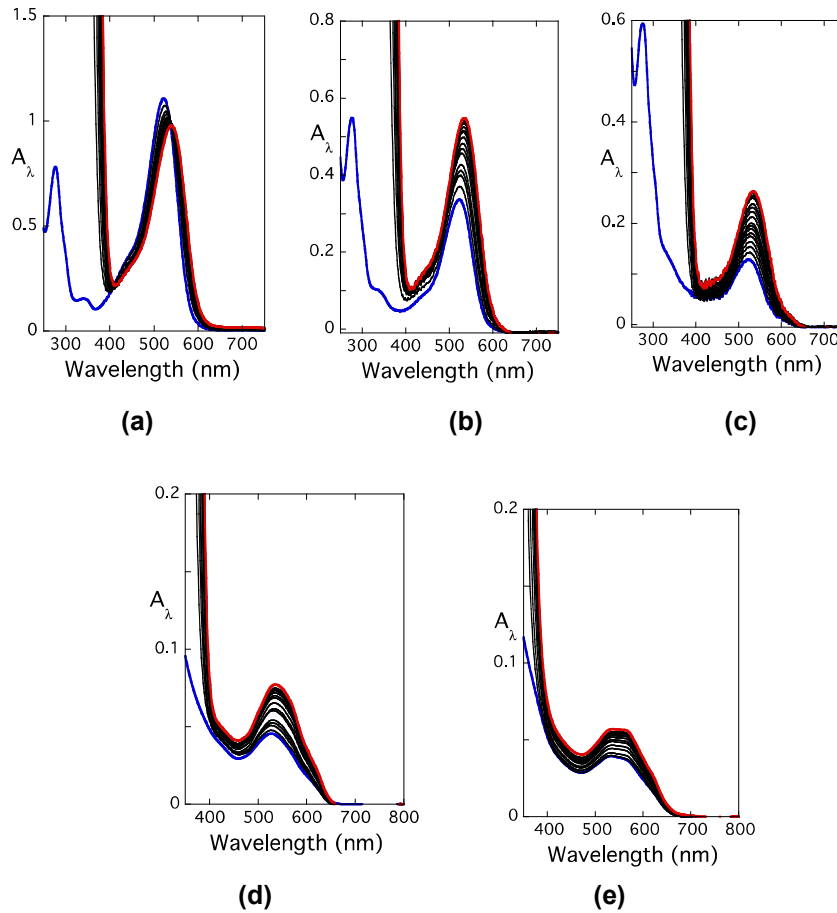


Figure 3. Spectral variation of oenin [4.2×10^{-5} M] as a function of sinapic acid [5×10^{-3} M] addition at different pH values: (a) pH=1.06; (b) pH=2.89; (c) pH=3.6; (d) pH=4.64; ; (e) pH=5.75; Blue color the absorption spectrum in the absence of copigment.

It is worth of note that in Fig. 3d and Fig. 3e the absorption band in the visible (signalled in blue) increases and is slightly red shifted (signalled in red). Considering that at pH=5.75 the sinapic acid is 95% in its basic form, this is a clear evidence for the copigmentation of quinoidal base to give the complex **ACP(-)**.

In Fig.4a the absorbance at 548 nm for pH=1.06, 2.89, 3.6, 4.64 and 5.75 are shown. Fitting was achieved with eq. (14), pH=1.06, (r_{AH^+CP} and K_{AH^+CP}), and eq. (24), pH=5.75 (r_{CBP} and K_{CBP}). A global fitting for the four remaining parameters was carried out with eq. (18) for pH=2.89, 3.6, 4.64 and another independent experiment where eq. (18) was used at a fixed concentration of the copigment versus pH. All the fittings at constant pH versus copigment concentration are presented in **Fig.4a** and versus pH at fixed concentration of the copigment in **Fig. 4c**.

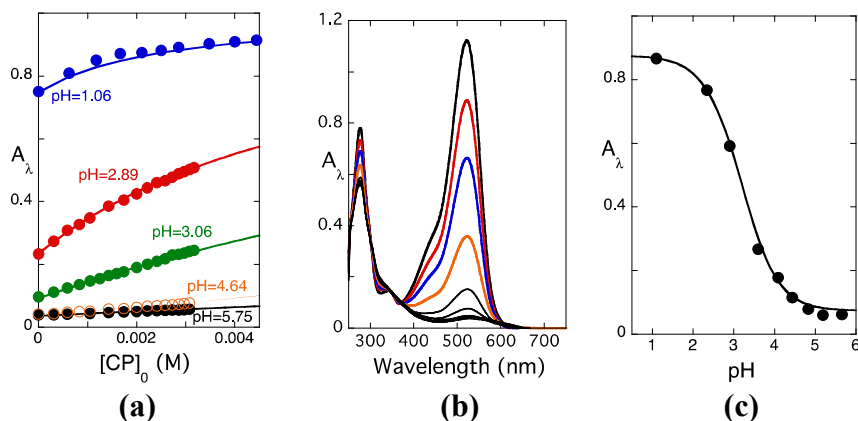


Figure 4. (a) Absorbance of oenin (4.2×10^{-5} M) as a function of sinapic acid addition at different pH values, $A_\lambda = 548$ nm: (a) pH=1.06; 2.89; 3.6; 5.75; (b) spectral variations of oenin 4.2×10^{-5} M in the presence of sinapic acid 5.3×10^{-3} M; (c) the use of eq. (18) at constant concentration of copigment versus pH.

In **Table 2** the parameters resulting from the global fitting of the data reported in **Fig. 3** and **Fig. 4** are reported.

Table 2. Fitting parameters from the global fitting of Fig.3 and Fig.4 data. Estimated error 10%.

K_{AH^+CP}	$K_{AH^+CP(-)}$	K_{CBCP}	$K_{CBCP(-)}$
243 M ⁻¹	≈0	53 M ⁻¹	78 M ⁻¹
$r_{AH^+CP}^{(1)}$	$r_{CBCP}^{(1)}$	$r_{CBCP(-)}^{(1)}$	$r_{CB}^{(1)}$
1.5	0.24	0.03	1.3×10^{-4}

⁽¹⁾ 548 nm

Reverse pH jumps

The spectral variations after a reverse pH jump from pH=5.75 back to flavylum cation monitored by stopped flow are presented in **Fig. 5**. At pH=5.75 the copigment is in its basic form, there is no flavylum cation and the species in solution are A, B, Cc and the respective complexes with the basic form of the copigment, **Fig. 5**.

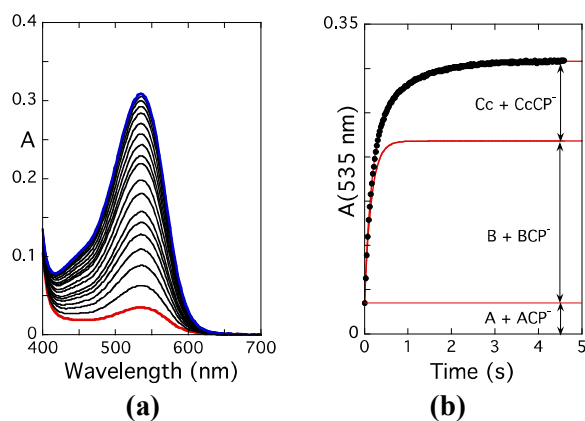


Figure 5. (a) Spectral variations after a reverse pH jump from pH=5.8 back to flavylum cation monitored by stopped flow; (b) traces of the absorbance monitored at 535 nm. Fitting was achieved with a bi-exponential with rate constants of 6.4 s^{-1} and 1.2 s^{-1} . The mole fraction distribution of the species at pH=5.75 can be obtained from the three amplitudes, $t=0$, faster kinetic process and slower kinetic process, upon normalization.

From a series of pH jumps like the one shown in **Fig.5**, the three normalized amplitudes, corresponding to the mole fractions of flavylum cation and its complexes, quinoidal base and hemiketal and its complexes and *cis*-chalcone and its complexes are obtained experimentally and represented in **Fig. 6**.

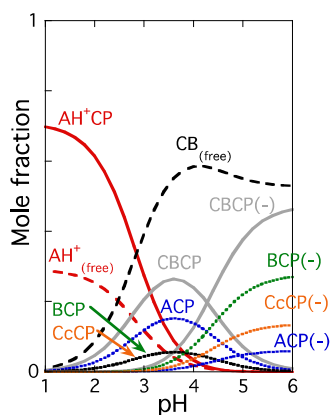


Figure 6. Mole fractions distribution of the normalized amplitudes of Oenin in the presence of sinapic acid 0.01 M obtained from reverse pH jumps monitored by stopped flow: Fitting was achieved for $a_{0(CP)}=0.58$; $b_{0(CP)}=0.21$; $c_{0(CP)}=0.21$; $a_{0(CP-)}=0.13$; $b_{0(CP-)}=0.58$; $c_{0(CP-)}=0.29$.

The fitting of the data presented in **Fig. 6** was achieved by means of eq. (42), eq. (43) and eq. (44), permitting to represent the mole fractions distributions of all species at the pseudo equilibrium.

In **Table 3** the results from the fittings of **Fig. 6** as well as the calculated values of the copigmentation constants are represented.

Table 3. Data from the reverse pH jumps monitored by stopped flow.

Estimated error 10%.

$a_{0(CP)}$	$a_{0(CP(-))}$	$b_{0(CP)}$	$b_{0(CP(-))}$	$c_{0(CP)}$	$c_{0(CP(-))}$
0.58	0.13	0.21	0.58	0.21	0.29

K_{AH+CP}	K_{ACP}	$K_{ACP(-)}$	K_{BCP}	$K_{BCP(-)}$	K_{CcCP}	$K_{CcCP(-)}$
243 M^{-1}	531 M^{-1}	196 M^{-1}	17	79	41 M^{-1}	94 M^{-1}

From the data of **Table 3** a value of $K_{CB^{\wedge}CP}=54\pm 5 \text{ M}^{-1}$ and $K_{CB^{\wedge}CP(-)} = 90\pm 9 \text{ M}^{-1}$ are obtained.

Trans-chalcone contribution

The trace of the absorbance at a fixed wavelength from the pseudo-equilibrium towards the equilibrium is shown in **Fig. 7a**.

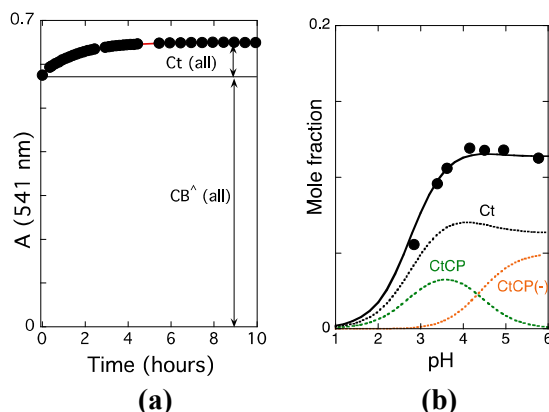


Figure 7. (a) Trace of the reverse pH jump of an equilibrated solution of Oenin in the presence of sinapic acid at pH=5.77; (b) Estimation of the mole fraction distribution of all *trans*-chalcone species. Fitting was achieved by means of eq. (38) for $d_{0(CP)}=0.12$; $d_{0(CP(-))}=0.11$; $K_{CBCP}=54 \text{ M}^{-1}$; $K_{CBCP(-)}=89 \text{ M}^{-1}$ from which $K_{CiCP}=55 \text{ M}^{-1}$ and $K_{CiCP(-)}=80 \text{ M}^{-1}$ were calculated.

Table 4. Contribution of the *trans*-chalcone. Estimated error 10%.

K_{CiCP}	$K_{CiCP(-)}$	K_{CBCP}	$K_{CBCP(-)}$
55 M^{-1}	80 M^{-1}	54 M^{-1}	89 M^{-1}

The ratio between the amplitude of the trace divided by the sum of CB^{\wedge} (all) and Ct (all) gives the mole fraction of Ct at pH=5.77. This experiment extended to other pH values permits to get the mole fraction distribution of the Ct mole fractions. The fitting of these data was carried out by means of eq. (38), for the parameters $d_0=0.12$; $d_0^- = 0.11$; $K_{CBCP}=54 \text{ M}^{-1}$; $K_{CBCP(-)}=89 \text{ M}^{-1}$ and $K_{CiCP}=55 \text{ M}^{-1}$ and $K_{CiCP(-)}=80 \text{ M}^{-1}$, **Table 4**.

Comparing the values of the K_{CBCP} and $K_{CBCP(-)}$ obtained by stopped flow, **Table 4**, with those calculated by the UV-Vis measurements there is an excellent agreement.

Discussion

By means of the UV-Vis absorption measurements it is only possible to calculate the global constants K_{CBCP} and $K_{CBCP(-)}$. These constants are apparently small. However, complexation with CB is the result of a weighted average complexation involving the species **A**, **B**, **Cc** and **Ct**. The mole fraction of each complex depends not only on the respective constant but also on the fraction available to complex. For example, the

contribution of **ACP** for the constant K_{CBCP} is $\frac{K_a}{K'_a} K_{ACP}$, see eq.(9). In other words,

difficultly the mole fraction of the quinoidal base complexes (with CP and CP(-)) will be dominant, because the ratio K_a/K'_a in oenin is $10^{-3.8}/10^{-2.55} = 0.056$ (Mendoza et al, 2019). Only in the case of hemiketal the respective complexes would have some expression since K_h/K'_a is equal to 0.6 (Mendoza et al, 2019). However, previous results (Mendoza et al, 2019) (corroborated by the present work) indicate, that hemiketal is the species exhibiting lower copigmentation constants, an expected behaviour due to the break of $\pi-\pi$ conjugation by the sp^3 carbon atom in position 2, preventing a more efficient $\pi-\pi$ stacking with the pigment.

It is worth of note that the approximations that considers quinoidal base as the only species showing copigmentation in less acidic medium is a limited approximation, because the other species have a significant contribution.

One useful representation to determine the best pH to carry out copigmentation studies with higher spectral changes is to represent $(A-A_0)/A_0$ (in our notation $A=A_{\square}$ and $A_0=A_{\square(CP=0)}$) as a function of pH .(Brouillard, Mazza et al. 1989, Mazza and Brouillard 1990, Brouillard, Wigand et al. 1991, Mistry, Cai et al. 1991, Davies and Mazza 1993, Markovic, Petranovic et al. 2005)(Zhu, Chen et al.). It is possible to have a real fitting of this ratio considering the two forms of the copigment, by using eq. (18) and eq.(13), as shown in Fig.8.

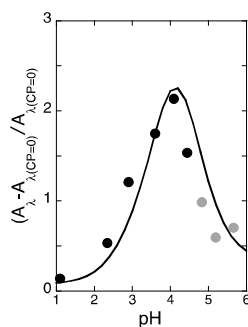


Figure 8. Representation of the ratio $(A_\lambda - A_{\lambda(CP=0)}) / A_{\lambda(CP=0)}$ as a function of pH. This type of representation is not very accurate in particular at higher pH values.

This representation is not accurate in particular at higher pH values. As shown in **Fig. 4c**, the values of A_λ (as well $A_{\lambda(CP=0)}$ for $pH > 4$) are small and its difference has higher uncertainty.

The representation reported in **Fig. 8** has been claimed to account for the magnitude of the copigmentation effect. In fact, it allows to determine the pH where there is more visual contrast by addition of the copigment. It is function not only of the copigmentation constants but also of the difference between the mole absorption coefficients of the anthocyanin species in the absence of copigment and the respective complexes, in the visible concerning flavylum cation and quinoidal base.

Complexation with sinapic acid and malvidin-3,5-diglucoside (malvin) was previously reported by Markovic *et al*, and eq. (51) used (Markovic et al, 2005).

$$K = \frac{A_2 - A_0}{C_0 \left\{ rA_0 - \frac{A_2}{(1 + K_h 10^{pH})} \right\}} \quad (51)$$

This expression was deduced considering the exclusive copigmentation with flavylum cation and is coincident with eq. (14), see appendix 1 in supplementary material of reference (Oliveira, 2021). Markovic *et al*. observed two different copigmentation constants at $pH=2.5$ (21.8 M^{-1}) and $pH=3.6$ (69 M^{-1}) and a maximum value for $(A-A_0)/A_0$ at $pH=3.6$. From the point of view of the used model (deduced on the basis of exclusive copigmentation with flavylum cation) there is no motive to have different constants. The reason for this apparent incoherence is the fact that, similarly to oenin, in malvin there is most probably copigmentation with the CB species. An indication for the copigmentation with quinoidal base can be observed in **Fig. 3** of the mentioned paper (the formation of a new absorption band *c.a.* 630 nm by increasing copigment concentration). In Markovic *et al* paper the basic form of sinapic acid was not considered.

The copigmentation of the Chinese bayberry with phenolic acids, ferulic, sinapic and syringic was reported at pH=3.4 (Zhu et al). The acid-basic equilibrium forms of the copigment was not considered, and at this pH there is a significant fraction of copigment in their anionic form.

In another work the copigmentation of cyanidin 3-glucoside and cyanidin 3-sophoroside from red raspberry fruits with sinapic acid, ferulic acid, caffeic acid, coumaric acid and gallic acid, was studied. The experiments have been extended up to pH=6 and the acidity constants of the copigments was not taken into account (Sun et al, 2010).

Conclusions

The fact that copigmentation occurs not only with flavylum cation but also with quinoidal base *cis* and *trans*-chalcones and in less extent with hemiketal, implies that copigmentation studies should be extended to moderately pH values, typically up to pH=6. Consequently, two requirements are needed for a copigmentation model and respective mathematical expression: *i*) having the possibility of calculating the copigmentation constants with all CB species *ii*) take into account that most of the copigments possess an acid base equilibrium in the pH domain of the CB species. The appropriate copigmentation models and the respective mathematical expression here reported accounts for these two requirements.

Due to the high number of variables in this complex system, special attention should be paid to the accuracy of the data. In this work, we calculated global copigmentation constants from the UV-Vis measurements using an appropriate equation at five different pH values as a function of the copigment concentration as well as a function of pH for a constant copigment concentration. A global fitting was carried out. In addition, a series of reverse pH jumps monitored by stopped flow and a standard spectrophotometer was performed to get the individual copigmentation constants and certify the coherence of the data. Determination of the copigmentation constants is not a simple task requires the appropriate theoretical corpus and an extensive number of experimental works to minimize the inherent errors. In particular reverse pH jumps monitored by stopped flow are an indispensable tool.

Credit authorship contribution statement: **Joana Oliveira:** Conceptualization, Methodology, Project administration, Funding acquisition, experimental work; **Joana Azevedo:** experimental work. **André Seco:** experimental work; **Johan Mendoza:** experimental work; **Nuno Basílio:** Conceptualization, Methodology, Project administration, Funding acquisition; **Victor de Freitas:** Conceptualization, Methodology, Project administration, Funding acquisition; **Fernando Pina:** Conceptualization, Methodology, Supervision. All authors have read and agreed to the published version of the manuscript.

Declaration of competing interest: The authors declare that they have no known competing financial interests or personal relationships that could have appeared to influence the work reported in this paper.

Acknowledgements

This work was supported by the Associated Laboratory for Sustainable Chemistry, Clean Processes and Technologies LAQV through the national funds from UIDB/50006/2020 and UIDP/50006/2020 and by AgriFood XXI I&D&I project (NORTE-01-0145-FEDER-000041) cofinanced by European Regional Development Fund (ERDF), through the NORTE 2020 (Programa Operacional Regional do Norte 2014/2020).

It was also supported by the project PTDC/QUI-OUT/29013/2017 funded by FCT and FEDER. J.A. and A.S. and J.M. gratefully acknowledge their doctoral grants from FCT: SFRH/BD/139709/2018 and 2020.07313.BD, respectively and J.M. CONACyT (MEX/Ref. 288188). J.O. and N.B. would like to thank FCT respectively for contract (IF/00225/2015) and CEECIND/00466/2017.

References

- Araujo, P., Fernandes, A., de Freitas, V., & Oliveira, J. (2017). A New Chemical Pathway Yielding A-Type Vitisins in Red Wines. *Int. J. Mol. Sci.*, 18(4), 762. <https://doi.org/10.3390/ijms18040762>
- Benvidi, A., Dadras, A., Abbasi, S., Tezerjani, M. D., Rezaeinasab, M., Tabaraki, R., & Namazian, M. (2019). Experimental and computational study of the pK(a) of coumaric acid derivatives [Article]. *Journal of the Chinese Chemical Society*, 66(6), 589-593. <https://doi.org/10.1002/jccs.201800265>
- Brouillard, R., Delaporte, B., & Dubois, J. E. (1978). Chemistry of Anthocyanins Pigments.3. Relaxation Amplitudes in pH-Jump Experiments [Article]. *J. Am. Chem. Soc.*, 100(19), 6202-6205. <https://doi.org/10.1021/ja00487a041>
- Brouillard, R., Mazza, G., Saad, Z., Albrechtgary, A. M., & Cheminat, A. (1989). The copigmentation reaction of anthocyanins-a microprobe for the structural study of aqueous solutions. [Article]. *Journal of the American Chemical Society*, 111(7), 2604-2610. <https://doi.org/10.1021/ja00189a039>
- Brouillard, R., Wigand, M. C., Dangles, O., & Cheminat, A. (1991). pH and Solvent effects on the copigmentation reaction of malvin with Polyphenols, purine and pyrimidine-derivatives. [Article]. *Journal of the Chemical Society-Perkin Transactions* 2(8), 1235-1241. <https://doi.org/10.1039/p29910001235>
- Dangles, O., & Elhaji, H. (1994). Synthesis of 3-methoxy-flavylium and 3-(beta-D-glucopyranosyloxy)flavylium ions- Influence of the flavylium substitution pattern on the reactivity of anthocyanins in aqueous solutions. [Article]. *Helvetica Chimica Acta*, 77(6), 1595-1610. <https://doi.org/10.1002/hlca.19940770616>

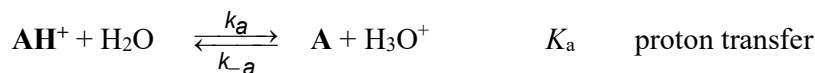
- Davies, A. J., & Mazza, G. (1993). Copigmentation of simple and acylated anthocyanins with colorless phenolic -compounds [Article]. *Journal of Agricultural and Food Chemistry*, 41(5), 716-720. <https://doi.org/10.1021/jf00029a007>
- Küster FW, Thiel A. *Tabelle per le Analisi Chimiche e Chimico- Fisiche*. 12 th ed Milano, Italy: Hoepli; 1982. p. 157–60.
- Manoel, H. R., & Moya, H. D. (2015). A Comprehensive Study of the Use of Cu(I)/4,4 '-Dicarboxy-2,2 '-biquinoline Complexes to Measure the Total Reducing Capacity: Application in Herbal Extracts [Article]. *Molecules*, 20(12), 22411-22421. <https://doi.org/10.3390/molecules201219855>
- Markovic, J. M. D., Petranovic, N. A., & Baranac, J. M. (2005). The copigmentation effect of sinapic acid on malvin: a spectroscopic investigation on colour enhancement [Article]. *Journal of Photochemistry and Photobiology B-Biology*, 78(3), 223-228. <https://doi.org/10.1016/j.jphotobiol.2004.11.009>
- Mazza, G., & Brouillard, R. (1990). The mechanism of copigmentation of anthocyanins in aqueous solutions [Article]. *Phytochemistry*, 29(4), 1097-1102. [https://doi.org/10.1016/0031-9422\(90\)85411-8](https://doi.org/10.1016/0031-9422(90)85411-8)
- Mendoza, J., Basilio, N., de Freitas, V., & Pina, F. (2019). New Procedure To Calculate All Equilibrium Constants in Flavylium Compounds: Application to the Copigmentation of Anthocyanins [Article]. *ACS Omega*, 4(7), 12058-12070. <https://doi.org/10.1021/acsomega.9b01066>
- Mistry, T. V., Cai, Y., Lilley, T. H., & Haslam, E. (1991). Polyphenol interactions.5. Anthocyanin copigmentation. [Article]. *Journal of the Chemical Society-Perkin Transactions 2*(8), 1287-1296. <https://doi.org/10.1039/p29910001287>
- Oliveira, J. A., J.; Teixeira, N.; Araujo, P.; De Freitas, V.; Basilio, N.; Pina, F. . (2021). On the Limits of Anthocyanins Co-Pigmentation Models and Respective Equations. *Journal of Agricultural and Food Chemistry*, <http://dx.doi.org/10.1021/acs.jafc.0c05954>
- Pina, F. (2014). Anthocyanins and Related Compounds. Detecting the Change of Regime Between Rate Control by Hydration or by Tautomerization [Article]. *Dyes and Pigm.*, 102, 308-314. <https://doi.org/10.1016/j.dyepig.2013.10.033>
- Pina, F., Oliveira, J., & de Freitas, V. (2015). Anthocyanins and derivatives are more than flavylium cations [Article]. *Tetrahedron*, 71(20), 3107-3114. <https://doi.org/10.1016/j.tet.2014.09.051>
- Romero, R., Salgado, P. R., Soto, C., Contreras, D., & Melin, V. (2018). An Experimental Validated Computational Method for pKa Determination of Substituted 1,2-Dihydroxybenzenes [Article]. *Frontiers in Chemistry*, 6, 11, Article 208. <https://doi.org/10.3389/fchem.2018.00208>
- Serjeant EP, D. B. (1979). Ionisation constants of organic acids in aqueous solution. *IUPAC Chem Data Ser No.23*. NY,NY: Pergamon pp. 989
- Sun, J. X., Cao, X. M., Bai, W. B., Liao, X. J., & Hu, X. S. (2010). Comparative analyses of copigmentation of cyanidin 3-glucoside and cyanidin 3-sophoroside from red raspberry fruits [Article]. *Food Chemistry*, 120(4), 1131-1137. <https://doi.org/10.1016/j.foodchem.2009.11.031>
- Zhu, Y. Y., Chen, H. J., Lou, L. Y., Chen, Y. X., Ye, X. Q., & Chen, J. C. Copigmentation effect of three phenolic acids on color and thermal stability of Chinese bayberry anthocyanins [Article; Early Access]. *Food Science & Nutrition*, 9. <https://doi.org/10.1002/fsn3.1583>

Supplementary Material

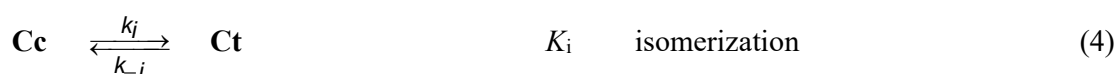
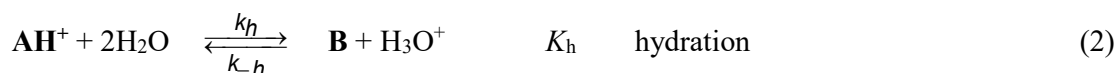
Appendix 1

1. Mole fractions in the absence of copigment

In acidic to neutral medium the anthocyanins equilibrium is given by eq.(1) to eq.(8)



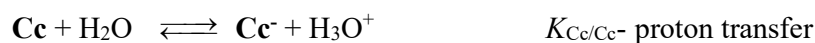
(1)



(5)



(6)

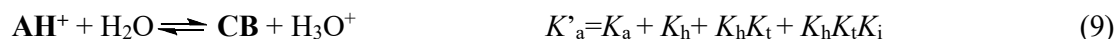


(7)

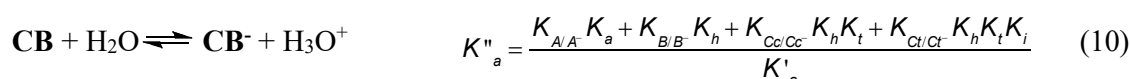


(8)

This complex system can be dramatically simplified¹ considering flavylum cation a diprotic acid in equilibrium with the conjugated bases CB and CB⁻, eq.(9) and eq.(10)^{1,2}



With $[\text{CB}] = [\text{A}] + [\text{B}] + [\text{Cc}] + [\text{Ct}]$



With $[\text{CB}^-] = [\text{A}^-] + [\text{B}^-] + [\text{Cc}^-] + [\text{Ct}^-]$

In the case of anthocyanins the isomerization is much slower than the other kinetic process and a transient state is attained between all species with the exception of Ct,

¹ The model can be extended to more deprotonated species. In the case of anthocyanins they are not stable at these pH values.

1.2. Separation of the mole fractions by reverse pH jumps monitored by stopped flow

Reverse pH jumps monitored by stopped flow can separate the contributions of **AH⁺** and **A** amplitude at $t=0$, from those of the **B**, amplitude of the faster kinetic process and **Cc**, amplitude of the slower process. It refers to the pseudo-equilibrium, because during the time of the stopped flow (few seconds), only the kinetics between the conversion of **CB⁺** and **AH⁺** can be monitored. There is not enough time to follow the isomerization process.

The fact that the system is equivalent to a diprotic acid with constants K'_a and K''_a , allows for representing the mole fraction distribution of **AH⁺**, **CB⁺** and **CB⁻** as in eq.(11)

$$\chi_{AH^+} = \frac{[H^+]^2}{D^{\wedge}}; \chi_{CB^+} = \frac{K_a^{\wedge}[H^+]}{D^{\wedge}}; \chi_{CB^-} = \frac{K_a^{\wedge}K_a^{\wedge\wedge}}{D^{\wedge}}; D^{\wedge} = [H^+]^2 + K_a^{\wedge}[H^+] + K_a^{\wedge}K_a^{\wedge\wedge} \quad (11)$$

The mole fraction of **CB⁺** as well as **CB⁻** can be separated in their components that are given directly from the reverse pH jumps experiments

$$\chi_{AH^+} + \chi_A + \chi_{A^-} = \frac{[H^+]^2 + a_0K_a^{\wedge}[H^+] + a_1K_a^{\wedge}K_a^{\wedge\wedge}}{D^{\wedge}} \quad (12)$$

$$\chi_B + \chi_{B^-} = \frac{b_0K_a^{\wedge}[H^+] + b_1K_a^{\wedge}K_a^{\wedge\wedge}}{D^{\wedge}} \quad (13)$$

$$\chi_{Cc} + \chi_{Cc^-} = \frac{c_0K_a^{\wedge}[H^+] + c_1K_a^{\wedge}K_a^{\wedge\wedge}}{D^{\wedge}} \quad (14)$$

$$a_0 + b_0 + c_0 = 1; a_1 + b_1 + c_1 = 1$$

On the other hand, the mole fractions of **AH⁺**, **CB⁺** and **CB⁻** can be written as in eq.(19)

From the mass balance

$$C_0 = [AH^+] + [A] + [B] + [Cc] + [A^-] + [B^-] + [Cc^-] \quad (15)$$

And using the equilibrium constants above

$$\begin{aligned} C_0 &= [AH^+] \left(1 + \frac{K_a + K_h + K_h K_t}{[H^+]} + \frac{K_{A/A^-} K_a + K_{B/B^-} K_h + K_{Cc/Cc^-} K_h K_t}{[H^+]^2} \right) = \\ &= [AH^+] \left(1 + \frac{K_a^{\wedge}}{[H^+]} + \frac{K_a^{\wedge} K_a^{\wedge\wedge}}{[H^+]^2} \right) \end{aligned} \quad (16)$$

$$\text{With } K_a^{\wedge} = K_a + K_h + K_h K_t \text{ and } K_a^{\wedge} K_a^{\wedge\wedge} = K_{A/A^-} K_a + K_{B/B^-} K_h + K_{Cc/Cc^-} K_h K_t \quad (17)$$

$$\chi_{AH^+} = \frac{[AH^+]}{C_0} = \frac{[H^+]^2}{[H^+]^2 + K_a^{\wedge}[H^+] + K_a^{\wedge}K_a^{\wedge\wedge}} \quad (18)$$

The mole fractions of each species can be calculated :

$$\chi_{AH^+} + \chi_A + \chi_{A^-} = \frac{[H^+]^2 + K_a[H^+] + K_{A/A^-}K_a}{D} \quad (19)$$

$$\chi_B + \chi_{B^-} = \frac{K_h[H^+] + K_{B/B^-}K_h}{D} \quad (20)$$

$$\chi_{Cc} + \chi_{Cc^-} = \frac{K_hK_t[H^+] + K_{Cc/Cc^-}K_hK_t}{D} \quad (21)$$

Comparing eq. (19) to eq. (21) with eq.(11)

for the neutral species:

$$K_a = a_0 K_a^{\wedge}; K_h = b_0 K_a^{\wedge}; K_hK_t = c_0 K_a^{\wedge} \quad (22)$$

for the anionic species:

$$K_{A/A^-}K_a = a_1 K_a^{\wedge}K_a^{\wedge}; K_{B/B^-}K_h = b_1 K_a^{\wedge}K_a^{\wedge}; K_{Cc/Cc^-}K_hK_t = c_1 K_a^{\wedge}K_a^{\wedge} \quad (23)$$

In conclusion, all equilibrium constants of the anthocyanins up to the anionic species can be obtained from reverse pH jumps monitored by stopped flow with good accuracy.³

2. Mole fractions in the presence of copigment (1:1) interactions

Considering the possibility of copigmentation of all species of this multistate



Eq.(23) to eq.(27) can be simplified to eq.(28)



with **CB** defined above in eq.(9) and **CBCP** in eq.(30) and eq.(31)

$$CBCP = [ACP] + [BCP] + [CcCP] + [CtCP] \quad (29)$$

$$K_{CBCP} = \frac{[ACP] + [BCP] + [CcCP] + [CtCP]}{([A] + [B] + [Cc] + [Ct])[CP]} = \frac{K_{ACP}[A] + K_{BCP}[B] + K_{CcCP}[Cc] + K_{CtCP}[Ct]}{[A] + [B] + [Cc] + [Ct]} \quad (30)$$

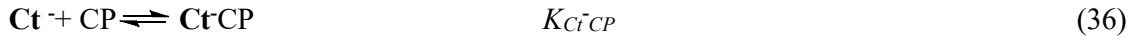
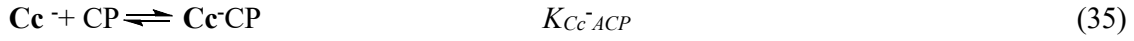
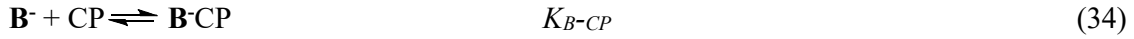
Expressing A, B, Cc and Ct in terms of AH⁺

$$K_{CBCP} = \frac{K_{ACP}K_a + K_{BCP}K_h + K_{CcCP}K_hK_t + K_{CtCP}K_hK_tK_i}{K_a'} \quad (31)$$

The anionic species can be accounted for by two different sets of equations which are not linearly independent, eq.(32) or eq.(33) to eq.(36). The last set was used to be coherent with eq.(17)



Or in alternative



Eq.(33) to eq.(36) can be simplified, eq.(37)



$$\mathbf{CB^{\cdot-}CP} = [\mathbf{A^{\cdot-}CP}] + [\mathbf{B^{\cdot-}CP}] + [\mathbf{Cc^{\cdot-}CP}] + [\mathbf{Ct^{\cdot-}CP}]$$

(38)

By definition of eq.(37)

$$K_{CB^{\cdot-}CP} = \frac{([\mathbf{A^{\cdot-}CP}] + [\mathbf{B^{\cdot-}CP}] + [\mathbf{Cc^{\cdot-}CP}] + [\mathbf{Ct^{\cdot-}CP}])}{([\mathbf{A^{\cdot-}}] + [\mathbf{B^{\cdot-}}] + [\mathbf{Cc^{\cdot-}}] + [\mathbf{Ct^{\cdot-}}])[\mathbf{CP}]} \quad (39)$$

$$K_{CB^{\cdot-}CP} = \frac{K_{A^{\cdot-}CP}[\mathbf{A^{\cdot-}}] + K_{B^{\cdot-}CP}[\mathbf{B^{\cdot-}}] + K_{Cc^{\cdot-}CP}[\mathbf{Cc^{\cdot-}}] + K_{Ct^{\cdot-}CP}[\mathbf{Ct^{\cdot-}}]}{[\mathbf{A^{\cdot-}}] + [\mathbf{B^{\cdot-}}] + [\mathbf{Cc^{\cdot-}}] + [\mathbf{Ct^{\cdot-}}]}$$

(40)

$K_{CB^{\cdot-}CP}$ can be written in terms of the species acid base and copigmentation constants, eq.(41)

$$K_{CB^{\cdot-}CP} = \frac{K_{A^{\cdot-}CP} K_{A/A^{\cdot-}} K_a + K_{B^{\cdot-}CP} K_{B/B^{\cdot-}} K_h + K_{Cc^{\cdot-}CP} K_{Cc/Cc^{\cdot-}} K_h K_t + K_{Ct^{\cdot-}CP} K_{Ct/Ct^{\cdot-}} K_h K_t K_i}{K_{A/A^{\cdot-}} K_a + K_{B/B^{\cdot-}} K_h + K_{Cc/Cc^{\cdot-}} K_h K_t + K_{Ct/Ct^{\cdot-}} K_h K_t K_i} \quad (41)$$

From eq.(10)

$$K_{CB^{\cdot-}CP} = \frac{K_{A^{\cdot-}CP} K_{A/A^{\cdot-}} K_a + K_{B^{\cdot-}CP} K_{B/B^{\cdot-}} K_h + K_{Cc^{\cdot-}CP} K_{Cc/Cc^{\cdot-}} K_h K_t + K_{Ct^{\cdot-}CP} K_{Ct/Ct^{\cdot-}} K_h K_t K_i}{K'_a K''_a} \quad (42)$$

Eq.(43) presents the relations between the four sets of equations, justifying that they are not linearly independent.

$$K_{X^{\cdot-}CP} = \frac{[\mathbf{X^{\cdot-}CP}]}{[\mathbf{X^{\cdot-}}][\mathbf{CP}]} = \frac{K_{XCP} K_{XCP/X^{\cdot-}CP}}{K_{X/X^{\cdot-}}} \quad (\mathbf{X=A, B, Cc \text{ and } Ct}) \quad (43)$$

The mole fraction distributions of each species are straightforwardly achieved from a mass balance and the use of the equilibrium constants above defined.

2. Copigment without acid base equilibrium

A mass balance is given by eq.(44)

$$C_0 = [\mathbf{AH^+}] + [\mathbf{AH^+CP}] + [\mathbf{A}] + [\mathbf{B}] + [\mathbf{Cc}] + [\mathbf{Ct}] + [\mathbf{ACP}] + [\mathbf{BCP}] + [\mathbf{CcCP}] + [\mathbf{CtCP}] +$$

$$+ [\mathbf{A^{\cdot-}}] + [\mathbf{B^{\cdot-}}] + [\mathbf{Cc^{\cdot-}}] + [\mathbf{Ct^{\cdot-}}] + [\mathbf{A^{\cdot-}CP}] + [\mathbf{B^{\cdot-}CP}] + [\mathbf{Cc^{\cdot-}CP}] + [\mathbf{Ct^{\cdot-}CP}]$$

(44)

$$\begin{aligned}
 C_0 = & [AH^+](1 + K_{AH+CP}[CP] + \frac{K'_a}{[H^+]} + K_{ACP} \frac{K_a}{[H^+]}[CP] + K_{BCP} \frac{K_h}{[H^+]}[CP] + K_{CCCP} \frac{K_h K_t}{[H^+]}[CP] + K_{ClCP} \frac{K_h K_t K_l}{[H^+]}[CP] + \\
 & + K_{A/A} \frac{K_a}{[H^+]^2} + K_{B/B} \frac{K_h}{[H^+]^2} + K_{C/Cc} \frac{K_h K_t}{[H^+]^2} + K_{Cl/Cl'} \frac{K_h K_t K_l}{[H^+]^2} + \\
 & + K_{A/CP} K_{A/A} \frac{K_a}{[H^+]^2}[CP] + K_{B/CP} K_{B/B} \frac{K_h}{[H^+]^2}[CP] + K_{C/CP} K_{C/Cc} \frac{K_h K_t}{[H^+]^2}[CP] + K_{Cl/CP} K_{Cl/Cl'} \frac{K_h K_t K_l}{[H^+]^2}[CP])
 \end{aligned} \tag{45}$$

simplifying

$$\begin{aligned}
 C_0 = & [AH^+](1 + K_{AH+CP}[CP] + \frac{K'_a + (K_{ACP}K_a + K_{BCP}K_h + K_{CCCP}K_h K_t + K_{ClCP}K_h K_t K_l)[CP]}{[H^+]}) + \\
 & + \frac{K_{A/A}K_a + K_{B/B}K_h + K_{C/Cc}K_h K_t + K_{Cl/Cl'}K_h K_t K_l + (K_{A/CP}K_{A/A}K_a + K_{B/CP}K_{B/B}K_h + K_{C/CP}K_{C/Cc}K_h K_t + K_{Cl/CP}K_{Cl/Cl'}K_h K_t K_l)[CP]}{[H^+]^2}
 \end{aligned} \tag{46}$$

Using eq.(9), eq.(10), eq.(31) and eq.(42) the mass balance is given by eq.(47)

$$C_0 = [AH^+](1 + K_{AH+CP}[CP] + \frac{K'_a(1 + K_{CBCP}[CP])}{[H^+]} + \frac{K'_a K''_a(1 + K_{CB'CP}[CP])}{[H^+]^2}) \tag{47}$$

From eq.(47) the mole fraction of AH⁺ can be calculated

$$\chi_{AH^+} = \frac{\frac{1}{1 + K_{AH^+CP}[CP]}[H^+]^2}{[H^+]^2 + \frac{K'_a(1 + K_{CBCP}[CP])}{1 + K_{AH^+CP}[CP]}[H^+] + \frac{K'_a K''_a(1 + K_{CB'CP}[CP])}{1 + K_{AH^+CP}[CP]}} \tag{48}$$

The division by $1 + K_{AH+CP}[CP]$, the coefficient of the acid species in eq.(48) is necessary to have mole fraction distributions of all acidic and all basic species (changing from 1 to 0).

Identically the mole fraction distribution of the copigmentation with AH⁺ is given by eq.(49)

$$\chi_{AH^+CP} = \frac{\frac{K_{AH^+CP}[CP]}{1 + K_{AH^+CP}[CP]}[H^+]^2}{[H^+]^2 + \frac{K'_a(1 + K_{CBCP}[CP])}{1 + K_{AH^+CP}[CP]}[H^+] + \frac{K'_a K''_a(1 + K_{CB'CP}[CP])}{1 + K_{AH^+CP}[CP]}} \tag{49}$$

And the sum of all acidic species by eq.(50)

$$\chi_{AH^+} + \chi_{AH^+CP} = \frac{[H^+]^2}{[H^+]^2 + \frac{K'_a(1 + K_{CBCP}[CP])}{1 + K_{AH^+CP}[CP]}[H^+] + \frac{K'_a K''_a(1 + K_{CB'CP}[CP])}{1 + K_{AH^+CP}[CP]}} \tag{50}$$

This is equivalent to a diprotic acid base equilibrium with acidity constants given by eq.(51) and eq.(52)

$$K'_{a(CP)} = \frac{K'_a(1 + K_{CB/CP}[CP])}{1 + K_{AH^+CP}[CP]} \quad (51)$$

$$K''_{a(CP)} = \frac{K''_a(1 + K_{CB/CP}[CP])}{1 + K_{CB/CP}[CP]} \quad (52)$$

Eq.(50) can thus be written as in eq.(53)

$$\chi_{AH^+} + \chi_{AH^+CP} = \frac{[H^+]^2}{[H^+]^2 + K'_{a(CP)}[H^+] + K'_{a(CP)}K''_{a(CP)}} = \frac{[H^+]^2}{D_{CP}} \quad (53)$$

$$D_{CP} = [H^+]^2 + K'_{a(CP)}[H^+] + K'_{a(CP)}K''_{a(CP)} \quad (54)$$

The mole fraction of the other species is now straightforwardly obtained from the equilibrium constants above

For the free neutral anthocyanins species

$$\chi_A = \frac{K_a}{[H^+]} \chi_{AH^+} = \frac{\frac{K_a}{1 + K_{AH^+CP}[CP]}[H^+]}{D_{CP}}; \chi_B = \frac{\frac{K_h}{1 + K_{AH^+CP}[CP]}[H^+]}{D_{CP}}; \chi_{C_c} = \frac{\frac{K_h K_t}{1 + K_{AH^+CP}[CP]}[H^+]}{D_{CP}};$$

$$\chi_{C_t} = \frac{\frac{K_h K_t K_i}{1 + K_{AH^+CP}[CP]}[H^+]}{D_{CP}} \quad (55)$$

For the complexes with neutral species

$$\chi_{ACP} = K_{ACP} \chi_A [CP] = \frac{\frac{K_{ACP} K_a}{1 + K_{AH^+CP}[CP]}[CP][H^+]}{D_{CP}}; \chi_{BCP} = \frac{\frac{K_{BCP} K_h}{1 + K_{AH^+CP}[CP]}[CP][H^+]}{D_{CP}}; \chi_{C_c CP} = \frac{\frac{K_{C_c CP} K_h K_t}{1 + K_{AH^+CP}[CP]}[CP][H^+]}{D_{CP}};$$

$$\chi_{C_t CP} = \frac{\frac{K_{C_t CP} K_h K_t K_i}{1 + K_{AH^+CP}[CP]}[CP][H^+]}{D_{CP}} \quad (56)$$

For the free anionic species

$$\chi_{A^-} = \frac{K_{A/A^-}}{[H^+]} \chi_A = \frac{\frac{K_{A/A^-} K_a}{1 + K_{AH^+CP}[CP]}}{D_{CP}}; \chi_{B^-} = \frac{\frac{K_{B/B^-} K_h}{1 + K_{AH^+CP}[CP]}}{D_{CP}}; \chi_{C_c^-} = \frac{\frac{K_{C_c/C_c^-} K_h K_t}{1 + K_{AH^+CP}[CP]}}{D_{CP}}; \chi_{C_t^-} = \frac{\frac{K_{C_t/C_t^-} K_h K_t K_i}{1 + K_{AH^+CP}[CP]}}{D_{CP}} \quad (57)$$

And for the complexed anionic species

$$\chi_{A^- CP} = K_{A^- CP} \chi_{A^-} [CP] = \frac{\frac{K_{A^- CP} K_{A/A^-} K_a [CP]}{1 + K_{AH^+CP}[CP]}}{D_{CP}}; \chi_{B^- CP} = \frac{\frac{K_{B^- CP} K_{B/B^-} K_h [CP]}{1 + K_{AH^+CP}[CP]}}{D_{CP}}; \chi_{C_c^- CP} = \frac{\frac{K_{C_c^- CP} K_{C_c/C_c^-} K_h K_t [CP]}{1 + K_{AH^+CP}[CP]}}{D_{CP}}$$

$$\chi_{Ct^-CP} = \frac{\frac{K_{Ct^-CP} K_{Ct/Ct} K_h K_t K_l [CP]}{1 + K_{AH^+CP} [CP]}}{D_{CP}} \quad (58)$$

Summarizing, the global system is equivalent to a pseudo diprotic acid with all species involving flavylum cation in equilibrium with all neutral species (including the respective complexes) and the anionic species (including the respective complexes) with constants

$$K'_{a(CP)} = \frac{K'_a (1 + K_{CBCP} [CP])}{1 + K_{AH^+CP} [CP]} \text{ and } K'_{a(CP)} K''_{a(CP)} = \frac{K'_a K''_a (1 + K_{CB^-CP} [CP])}{1 + K_{AH^+CP} [CP]} \quad (59)$$

$$K''_{a(CP)} = \frac{K''_a (1 + K_{CB^-CP} [CP])}{1 + K_{CBCP} [CP]} \quad (60)$$

The mole fractions of global AH⁺ species, global neutral species and global anionic species are given by

$$\chi_{AH^+ global} = \frac{[H^+]^2}{D_{(CP)}}; \chi_{CB global} = \frac{K'_{a(CP)} [H^+]}{D_{(CP)}}; \chi_{C^- global} = \frac{K'_{a(CP)} K''_{a(CP)}}{D_{(CP)}} \quad (61)$$

$$D_{(CP)} = [H^+]^2 + \left(\frac{K'_a + K_{CBCP} K'_a [CP]}{1 + K_{AH^+CP} [CP]} \right) [H^+] + \frac{K'_a K''_a + K_{CB^-CP} K'_a K''_a [CP]}{1 + K_{AH^+CP} [CP]} \quad (62)$$

3. Reverse pH jumps in the presence of copigment monitored by stopped flow

The reverse pH jumps in the presence of the copigment are also very useful to calculate the 1:1 copigmentation constants.³

Above it was proved that in the presence of the copigment the system continues to behave as a diprotic acid involving all flavylum species, all neutral species and all anionic species. In this case the measurements regard the pseudo equilibrium and the global constants are given by

$$K^{\wedge}_{a(CP)} = \frac{K^{\wedge}_a (1 + K_{CB^{\wedge}CP} [CP])}{1 + K_{AH^+CP} [CP]}; \quad K^{\wedge\wedge}_{a(CP)} = \frac{K^{\wedge\wedge}_a (1 + K_{CB^{\wedge}CP} [CP])}{1 + K_{CB^{\wedge}CP} [CP]} \quad (63)$$

with

$$K_{CB^{\wedge}CP} = \frac{K_{ACP} K_a + K_{BCP} K_h + K_{CCP} K_h K_t}{K^{\wedge}_a} \quad (64)$$

$$K_{CB^{\wedge\wedge}CP} = \frac{K_{A^{\wedge}CP} K_{A/A^{\wedge}} K_a + K_{B^{\wedge}CP} K_{B/B^{\wedge}} K_h + K_{C^{\wedge}CP} K_{C/C^{\wedge}} K_h K_t}{K^{\wedge}_a K^{\wedge\wedge}_a} \quad (65)$$

$$K^{\wedge}_a = K_a + K_h + K_h K_t \quad (66)$$

$$K_a^{\wedge\wedge} = \frac{K_{A/A^-} K_a + K_{B/B^-} K_h + K_{Cc/Cc^-} K_h K_t}{K_a^{\wedge}} \quad (67)$$

The mole fractions of all species are obtained as in eq.(44) by removing the terms related to *trans*-chalcone and using $D_{(CP)}^{\wedge}$ instead of $D_{(CP)}$

$$D_{CP}^{\wedge} = [H^+]^2 + K_{a(CP)}^{\wedge} [H^+] + K_{a(CP)}^{\wedge} K_{a(CP)}^{\wedge\wedge} \quad (68)$$

The mole fractions at the pseudo equilibrium in terms of the equilibrium constants are given by eq.(69) to eq.(71)

$$\chi_{AH^+} + \chi_{AH^+CP} + \chi_A + \chi_{ACP} + \chi_{A^-} + \chi_{A^-CP} = \frac{[H^+]^2 + \left(\frac{K_a + K_{ACP} K_a [CP]}{1 + K_{AH^+CP} [CP]}\right) [H^+] + \frac{K_{A/A^-} K_a + K_{A^-CP} K_{A/A^-} K_a [CP]}{1 + K_{AH^+CP} [CP]}}{D_{cp}^{\wedge}} \quad (69)$$

$$\chi_B + \chi_{BCP} + \chi_{B^-} + \chi_{B^-CP} = \frac{\left(\frac{K_h + K_{BCP} K_h [CP]}{1 + K_{AH^+CP} [CP]}\right) [H^+] + \frac{K_{B/B^-} K_h + K_{B^-CP} K_{B/B^-} K_h [CP]}{1 + K_{AH^+CP} [CP]}}{D_{cp}^{\wedge}} \quad (70)$$

$$\chi_{Cc} + \chi_{CcCP} + \chi_{Cc^-} + \chi_{Cc^-CP} = \frac{\left(\frac{K_h K_t + K_{CcCP} K_h K_t [CP]}{1 + K_{AH^+CP} [CP]}\right) [H^+] + \frac{K_{Cc/Cc^-} K_h K_t + K_{Cc^-CP} K_{Cc/Cc^-} K_h K_t [CP]}{1 + K_{AH^+CP} [CP]}}{D_{cp}^{\wedge}} \quad (71)$$

On the other hand, the same mole fractions can be accounted for by eq.(72) to eq.(74).³

$$\chi_{AH^+} + \chi_{AH^+CP} + \chi_A + \chi_{ACP} + \chi_{A^-} + \chi_{A^-CP} = \frac{[H^+]^2 + a_{o(CP)} K_{a(CP)}^{\wedge} [H^+] + a_{i(CP)} K_{a(CP)}^{\wedge} K_{a(CP)}^{\wedge\wedge}}{D_{cp}^{\wedge}} \quad (72)$$

$$\chi_B + \chi_{BCP} + \chi_{B^-} + \chi_{B^-CP} = \frac{b_{o(CP)} K_{a(CP)}^{\wedge} [H^+] + b_{i(CP)} K_{a(CP)}^{\wedge} K_{a(CP)}^{\wedge\wedge}}{D_{cp}^{\wedge}} \quad (73)$$

$$\chi_{Cc} + \chi_{CcCP} + \chi_{Cc^-} + \chi_{Cc^-CP} = \frac{c_{o(CP)} K_{a(CP)}^{\wedge} [H^+] + c_{i(CP)} K_{a(CP)}^{\wedge} K_{a(CP)}^{\wedge\wedge}}{D_{cp}^{\wedge}} \quad (74)$$

Comparing eq.(69) to (71) with eq.(72) to eq.(74)

$$a_{o(CP)} K_{a(CP)}^{\wedge} = \frac{K_a (1 + K_{ACP} [CP])}{1 + K_{AH^+CP} [CP]}; \quad a_{i(CP)} K_{a(CP)}^{\wedge} K_{a(CP)}^{\wedge\wedge} = \frac{K_{A/A^-} K_a (1 + K_{A^-CP} [CP])}{1 + K_{AH^+CP} [CP]} \quad (75)$$

$$b_{\alpha(CP)} K^{\wedge}_{a(CP)} = \frac{K_h(1 + K_{BCP}[CP])}{1 + K_{AH^+CP}[CP]}; \quad b_{1(CP)} K^{\wedge}_{a(CP)} K^{\wedge\wedge}_{a(CP)} = \frac{K_{B/B} K_h(1 + K_{B/CP}[CP])}{1 + K_{AH^+CP}[CP]} \quad (76)$$

$$c_{\alpha(CP)} K^{\wedge}_{a(CP)} = \frac{K_h K_t(1 + K_{CcCP}[CP])}{1 + K_{AH^+CP}[CP]}; \quad c_{1(CP)} K^{\wedge}_{a(CP)} K^{\wedge\wedge}_{a(CP)} = \frac{K_{Cc/Cc} K_h K_t(1 + K_{CcCP}[CP])}{1 + K_{AH^+CP}[CP]} \quad (77)$$

The equilibrium constants K_a , K_h , K_t and K_{A/A^-} , K_{B/B^-} and K_{Cc/Cc^-} are calculated from the reverse pH jumps in the absence of copigment, as above. The copigmentation constant K_{AH^+CP} should be calculated at pH=1, where no other species are present. At this point all the other copigmentation constants can be calculated. It should be stressed that the equilibrium constants of the anionic species are dependent on the values of those of the neutral species and in principle have higher uncertainty due to the propagation of the errors.

4. Extension to a copigment exhibiting acid base equilibrium

The reverse pH jumps can be used to account for the copigmentation with a copigment possessing acid-base equilibrium in the working pH range, including the anionic species.

The total concentration of the copigment now identified by $[CP]_0$ is distributed between its acidic and basic forms according to eq.(78). The interaction of CB^- with the acidic form of the copigment with the anionic species was neglected because the pK_a of cinnamic acids is lower than ca. 4.5 and pK'_a is higher than ca. 6.5.

$$[CP]_0 = \frac{[H^+]}{[H^+] + K_{a(copigment)}} [CP]_0 + \frac{K_{a(copigment)}}{[H^+] + K_{a(copigment)}} [CP]_0 = \chi_{CP} [CP]_0 + \chi_{CP(-)} [CP]_0 \quad (78)$$

Considering eq.(78) in eq.(59) and in eq.(60)

$$K'_{a(CP/CP(-))} = \frac{K'_a(1 + K_{CBCP}\chi_{CP}[CP]_0 + K_{CBCP(-)}\chi_{CP(-)}[CP]_0)}{1 + K_{AH^+CP}\chi_{CP}[CP]_0 + K_{AH^+CP(-)}\chi_{CP(-)}[CP]_0} \quad (79)$$

$$K''_{a(CP/CP(-))} = \frac{K''_a(1 + K_{CB^-CP(-)}\chi_{CP(-)}[CP]_0)}{(1 + K_{CBCP}\chi_{CP}[CP]_0 + K_{CBCP(-)}\chi_{CP(-)}[CP]_0)} \quad (80)$$

$$K_{CBCP} = \frac{K_{ACP}K_a + K_{BCP}K_h + K_{CcCP}K_hK_t + K_{ClCP}K_hK_tK_i}{K^{\wedge}_a} \quad (81)$$

$$K_{CBCP(-)} = \frac{K_{ACP(-)}K_a + K_{BCP(-)}K_h + K_{CcCP(-)}K_hK_t + K_{ClCP(-)}K_hK_tK_i}{K^{\wedge}_a} \quad (82)$$

$$K_{CB^-CP(-)} = \frac{K_{A^-(CP(-))}K_{A/A^-}K_a + K_{B^-(CP(-))}K_{B/B^-}K_h + K_{Cc^-(CP(-))}K_{Cc/Cc^-}K_hK_t + K_{Cl^-(CP(-))}K_{Cl/Cl^-}K_hK_tK_i}{K'_a K''_a} \quad (83)$$



As reported above, the constant $K_{\text{CB-CP}}$ ($K_{\text{A-CP}}$, $K_{\text{B-CP}}$, $K_{\text{Cc-CP}}$ and $K_{\text{Ct-CP}} \approx 0$) was not considered because at the pH domain of the anthocyanins anionic species there is no pH superposition with the acidic forms of cinnamic acids and related copigments. The same for the copigmentation of the anionic species with the basic form of the copigment, because they are both negatively charge. Moreover, the common anthocyanins are not stable at higher pH values and these data have an high uncertainty. Nevertheless, if the measurements are carried out at $\text{pH} \leq 6$ no significant interference of the anionic species takes place. Moreover, at the pseudo equilibrium all copigmentation constants except those involving **Ct** and **Ct⁻**, can be calculated with, without interference of the decomposition process.

While in the previous case the constants $K_{\text{a(CP)}}$ and $K_{\text{a(CP)}}$ were independent on the pH, now are function of the acid base constant of the copigment. Considering the two approximations above the mole fraction of all **AH⁺** and **A** species can be written

$$\begin{aligned} & \chi_{\text{AH}^+} + \chi_{\text{AH}^+\text{CP}} + \chi_{\text{AH}^+\text{CP}(-)} + \chi_{\text{A}} + \chi_{\text{ACP}} + \chi_{\text{ACP}(-)} + \chi_{\text{A}^-} = \\ & \frac{[\text{H}^+]^2 + \left(\frac{K_{\text{a}}(1 + K_{\text{ACP}}\chi_{\text{CP}}[\text{CP}]_0 + K_{\text{ACP}(-)}\chi_{\text{CP}(-)}[\text{CP}]_0)}{1 + K_{\text{AH}^+\text{CP}}\chi_{\text{CP}}[\text{CP}]_0 + K_{\text{AH}^+\text{CP}(-)}\chi_{\text{CP}(-)}[\text{CP}]_0} \right) [\text{H}^+] + \frac{K_{\text{A/A}^-} K_{\text{a}}}{1 + K_{\text{AH}^+\text{CP}}[\text{CP}] + K_{\text{AH}^+\text{CP}(-)}[\text{CP}]_0}}{D_{\text{a(CP/CP}(-))}} \quad (86) \end{aligned}$$

Identically for the hemiketal, *cis*-chalcone and *trans*-chalcone.

$$\begin{aligned} & \chi_{\text{B}} + \chi_{\text{BCP}} + \chi_{\text{BCP}(-)} + \chi_{\text{B}^-} = \\ & \frac{\left(\frac{K_{\text{h}}(1 + K_{\text{BCP}}\chi_{\text{BP}}[\text{CP}]_0 + K_{\text{BCP}(-)}\chi_{\text{CP}(-)}[\text{CP}]_0)}{1 + K_{\text{AH}^+\text{CP}}\chi_{\text{CP}}[\text{CP}]_0 + K_{\text{AH}^+\text{CP}(-)}\chi_{\text{CP}(-)}[\text{CP}]_0} \right) [\text{H}^+] + \frac{K_{\text{B/B}^-} K_{\text{h}}}{1 + K_{\text{AH}^+\text{CP}}[\text{CP}] + K_{\text{AH}^+\text{CP}(-)}[\text{CP}]_0}}{D_{\text{a(CP/CP}(-))}} \quad (87) \end{aligned}$$

$$\begin{aligned} & \chi_{\text{Cc}} + \chi_{\text{CcCP}} + \chi_{\text{CcCP}(-)} + \chi_{\text{Cc}^-} + \chi_{\text{Cc}^-\text{CP}(-)} = \\ & \frac{\left(\frac{K_{\text{h}}K_{\text{t}}(1 + K_{\text{CcCP}}\chi_{\text{BP}}[\text{CP}]_0 + K_{\text{CcCP}(-)}\chi_{\text{CP}(-)}[\text{CP}]_0)}{1 + K_{\text{AH}^+\text{CP}}\chi_{\text{CP}}[\text{CP}]_0 + K_{\text{AH}^+\text{CP}(-)}\chi_{\text{CP}(-)}[\text{CP}]_0} \right) [\text{H}^+] + \frac{K_{\text{Cc/Cc}^-} K_{\text{h}}K_{\text{t}}}{1 + K_{\text{AH}^+\text{CP}}[\text{CP}] + K_{\text{AH}^+\text{CP}(-)}\chi_{\text{CP}(-)}[\text{CP}]_0}}{D_{\text{a(CP/CP}(-))}} \quad (88) \end{aligned}$$

$$\begin{aligned} & \chi_{\text{Ct}} + \chi_{\text{CtCP}} + \chi_{\text{CtCP}(-)} + \chi_{\text{Ct}^-} + \chi_{\text{Ct}^-\text{CP}(-)} = \\ & \frac{\left(\frac{K_{\text{h}}K_{\text{t}}K_{\text{i}}(1 + K_{\text{CtCP}}\chi_{\text{CP}}[\text{CP}]_0 + K_{\text{CtCP}(-)}\chi_{\text{CP}(-)}[\text{CP}]_0)}{1 + K_{\text{AH}^+\text{CP}}\chi_{\text{CP}}[\text{CP}]_0 + K_{\text{AH}^+\text{CP}(-)}\chi_{\text{CP}(-)}[\text{CP}]_0} \right) [\text{H}^+] + \frac{K_{\text{Ct/Ct}^-} K_{\text{h}}K_{\text{t}}K_{\text{i}}}{1 + K_{\text{AH}^+\text{CP}}[\text{CP}] + K_{\text{AH}^+\text{CP}(-)}\chi_{\text{CP}(-)}[\text{CP}]_0}}{D_{\text{a(CP/CP}(-))}} \quad (89) \end{aligned}$$

In spite of the global constants exhibit a pH dependence on the acidity constant of the copigment, the system is similar to a diprotic acid with constants given by eq.(80) and eq.(81).

These mole fractions can be used at the pseudo equilibrium by removing the terms regarding **Ct**.

In this case it can be considered a system where all **AH⁺** species including those not interacting, interacting with the acidic form of the copigment and with the basic form of the copigment are in equilibrium with **CB** and **CB⁻** species in the same conditions

$$\chi_{all\ AH^+} = \frac{[H^+]^2}{D_{(CP/CP(-))}}; \chi_{all\ CB} = \frac{K'_{a(CP/CP(-))}[H^+]}{D_{(CP/CP(-))}}; \chi_{all\ CB^-} = \frac{K'_{a(CP/CP(-))} K''_{a(CP/CP(-))}}{D_{(CP/CP(-))}} \quad (90)$$

$$D_{(CP/CP(-))} = [H^+]^2 + K'_{a(CP/CP(-))}[H^+] + K'_{a(CP/CP(-))} K''_{a(CP/CP(-))} \quad (91)$$

4.1 Reverse pH jumps monitored by stopped flow with a copigment with an acidity constant

As we are dealing with the pseudo equilibrium eq.(59) and eq.(60) become eq.(92) and eq.(93)

$$K_{a(CP/CP(-))}^{\wedge} = \frac{K_a^{\wedge}(1 + K_{CB^{\wedge}CP} \chi_{CP}[CP]_0 + K_{CB^{\wedge}CP(-)} \chi_{CP(-)}[CP]_0)}{1 + K_{AH^+CP} \chi_{CP}[CP]_0 + K_{AH^+CP(-)} \chi_{CP(-)}[CP]_0} \quad (92)$$

$$K_{a(CP/CP(-))}^{\wedge\wedge} = \frac{K_a^{\wedge\wedge}}{(1 + K_{CB^{\wedge}CP} \chi_{CP}[CP]_0 + K_{CB^{\wedge}CP(-)} \chi_{CP(-)}[CP]_0)} \quad (93)$$

In this case it can be considered a system where all **AH⁺** species and all **CB** and **CB⁻** species including their complexes with the two forms of the copigment, behave as a diprotic acid, eq.(94)

$$\chi_{all\ AH^+} = \frac{[H^+]^2}{D_{CP/CP(-)}^{\wedge}}; \chi_{all\ CB} = \frac{K_{a(CP/CP(-))}^{\wedge}[H^+]}{D_{CP/CP(-)}^{\wedge}}; \chi_{all\ CB^-} = \frac{K_{a(CP/CP(-))}^{\wedge} K_{a(CP/CP(-))}^{\wedge\wedge}}{D_{CP/CP(-)}^{\wedge}} \quad (94)$$

$$\text{With } D_{CP/CP(-)}^{\wedge} = [H^+]^2 + K_{a(CP/CP(-))}^{\wedge}[H^+] + K_{a(CP/CP(-))}^{\wedge\wedge} K_{a(CP/CP(-))}^{\wedge}$$

In this case the parameters $K_{a(CP/CP(-))}^{\wedge}$ and $K_{a(CP/CP(-))}^{\wedge\wedge}$ are not constants and the approximation used in eq.(72) to (74) cannot be done.

Inspection of eq.(94) indicates that the contribution of the neutral species can be separated in three parts. The first one is only dependent on the fraction of anthocyanins not complexed, the second is dependent on the interaction with the acidic form of the copigment and the third on the interaction with the basic form of the copigment. All three parcels are divided by $1 + K_{AH^+CP} \chi_{CP}[CP]_0$.

The mole fractions of all species can now be calculated

$$\chi_{AH^+} + \chi_{AH^+CP} + \chi_{AH^+CP(-)} + \chi_A + \chi_{ACP} + \chi_{A^-} = \frac{[H^+]^2 + (a_0 \frac{K_a^{\wedge}}{1 + K_{AH^+CP} \chi_{CP}[CP]_0} + a_{0CP} \frac{K_a^{\wedge} K_{CB^{\wedge}CP} \chi_{CP}[CP]_0}{1 + K_{AH^+CP} \chi_{CP}[CP]_0} + a_{0CP(-)} \frac{K_a^{\wedge} K_{CB^{\wedge}CP(-)} \chi_{CP(-)}[CP]_0}{1 + K_{AH^+CP} \chi_{CP}[CP]_0}) [H^+] + a_1 K_{a(CP/CP(-))}^{\wedge} K_{a(CP/CP(-))}^{\wedge\wedge}}{D_{a(CP/CP(-))}^{\wedge}} \quad (95)$$

$$\begin{aligned} \chi_B + \chi_{BCP} + \chi_{BCP(-)} + \chi_{B^-} = \\ \frac{(b_0 \frac{K_a}{1 + K_{AH^+CP} \chi_{CP} [CP]_0} + b_{0CP} \frac{K_a K_{CB^*CP} \chi_{CP} [CP]_0}{1 + K_{AH^+CP} \chi_{CP} [CP]_0} + b_{0CP(-)} \frac{K_a K_{CB^*CP(-)} \chi_{CP(-)} [CP]_0}{1 + K_{AH^+CP} \chi_{CP} [CP]_0}) [H^+] + b_1 K_{a(CP/CP(-))} K_{a(CP/CP(-))}^{\wedge}}{D_{a(CP/CP(-))}^{\wedge}} \end{aligned} \quad (96)$$

$$\begin{aligned} \chi_{Cc} + \chi_{CCCP} + \chi_{CCCP(-)} + \chi_{Cc^-} = \\ \frac{(c_0 \frac{K_a}{1 + K_{AH^+CP} \chi_{CP} [CP]_0} + c_{0CP} \frac{K_a K_{CB^*CP} \chi_{CP} [CP]_0}{1 + K_{AH^+CP} \chi_{CP} [CP]_0} + c_{0CP(-)} \frac{K_a K_{CB^*CP(-)} \chi_{CP(-)} [CP]_0}{1 + K_{AH^+CP} \chi_{CP} [CP]_0}) [H^+] + c_1 K_{a(CP/CP(-))} K_{a(CP/CP(-))}^{\wedge}}{D_{a(CP/CP(-))}^{\wedge}} \end{aligned} \quad (97)$$

And $a_0 + b_0 + c_0 = 1$, $a_{0CP} + b_{0CP} + c_{0CP} = 1$ and $a_{0CP(-)} + b_{0CP(-)} + c_{0CP(-)} = 1$

with $a_0 = K_a / K_a^{\wedge}$; $b_0 = K_h / K_a^{\wedge}$; $c_0 = K_h K_t / K_a^{\wedge}$

Comparing the mole fractions written in terms of the equilibrium constants with those of eq.(98) with eq.(100)

$$a_{0CP} K_a^{\wedge} K_{CB^*CP} = K_a K_{ACP}; \quad b_{0CP} K_a^{\wedge} K_{CB^*CP} = K_h K_{BCP}; \quad c_{0CP} K_a^{\wedge} K_{CB^*CP} = K_h K_t K_{CCCP} \quad (98)$$

$$a_{0CP(-)} K_a^{\wedge} K_{CB^*CP(-)} = K_a K_{ACP(-)}; \quad b_{0CP(-)} K_a^{\wedge} K_{CB^*CP(-)} = K_h K_{BCP(-)}; \quad c_{0CP(-)} K_a^{\wedge} K_{CB^*CP(-)} = K_h K_t K_{CCCP(-)} \quad (99)$$

From eq.(98) and eq.(99) it is possible to distinguish the interaction of A, B and Cc with the acidic and basic forms of the copigment, provided that K_{AH+CP} and $K_{AH+CP(-)}$ are available.

References

- (1) Brouillard, R.; Delaporte, B.; Dubois, J. E. Chemistry of Anthocyanins Pigments.3. Relaxation Amplitudes in pH-Jump Experiments. *J. Am. Chem. Soc.* **1978**, *100* (19), 6202.
- (2) Pina, F.; Oliveira, J.; de Freitas, V. Anthocyanins and derivatives are more than flavylum cations. *Tetrahedron* **2015**, *71* (20), 3107.
- (3) Mendoza, J.; Basilio, N.; de Freitas, V.; Pina, F. New Procedure To Calculate All Equilibrium Constants in Flavylum Compounds: Application to the Copigmentation of Anthocyanins. *ACS Omega* **2019**, *4* (7), 12058.

Part C.

Wine Impact

Synopses:

Chapter 1- The Impact of Storage Conditions and Bottle Orientation on the Evolution of Phenolic and Volatile Compounds of Vintage Port Wine

Adapted from:

Joana Azevedo, Joana Pinto; Natércia Teixeira; Joana Oliveira; Miguel Cabral; Paula Guedes de Pinho; Paulo Lopes; Nuno Mateus; Victor de Freitas, *Foods*, 2022, DOI: 10.3390/foods11182770;

All the work described in this part was carried out by the author for the chemical characterization, the volatile characterization was carried out by Joana Pinto.

Chapter 2- Identification and structural characterization of a novel (+)-catechin-caffeic acid adduct present in wines

Adapted from:

Joana Azevedo, Joana Oliveira, Luís Cruz, Paulo Lopes, Nuno Mateus and Victor de Freitas, *in preparation*.

All the work described in this part was carried out by the author.

Chapter 3- Polyphenolic Characterization of Nebbiolo Red Wines and Their Interaction with Salivary Proteins

Adapted from:

Joana Azevedo, Elsa Brandão, Susana Soares, Joana Oliveira, Paulo Lopes, Nuno Mateus and Victor de Freitas., *Foods*, 2020, DOI: 10.3390/foods9121867;

The chemical characterization was carried out by the author, the interactions studies with salivary proteins were made by Elsa Brandão.

Chapter 1- The Impact of Storage Conditions and Bottle Orientation on the Evolution of Phenolic and Volatile Compounds of Vintage Port Wine

Abstract: This work evaluates the influence of the cellar conditions and bottle orientation, on the phenolic and volatile composition of a Vintage Port wine, sealed with natural cork stoppers, for 44 months post-bottling. The storage was performed in two different cellars, namely a cellar A with controlled temperature and humidity, and a cellar B, representing a traditional cellar, with uncontrolled temperature and humidity. The impact of bottle orientation was studied in cellar A, where the bottles were stored in horizontal and vertical positions. The phenolic and volatile composition of the bottled Vintage Port wine were analyzed after 6, 15 and 44 months. The results unveiled that the cellar conditions and bottle orientation had an impact in Port wine composition which was higher at 44 months post-bottling. The samples stored in the traditional cellar unveiled significantly higher yellow tones, lower tannin specific activity, and higher levels of furfural and 5-methylfurfural. Furthermore, the samples stored in the horizontal position revealed significant higher levels of total proanthocyanidins and higher tannin specific activity than the samples stored in the vertical position. Interestingly, for the first time to our knowledge, an ellagitannin-derived compound (Corklin) was detected in Vintage Port wines stored in the horizontal position, which results from the reaction of cork constituents with phenolic compounds present in wines.

Keywords: Vintage Port Wine; phenolic compounds; volatile compounds; cellar conditions; bottle orientation; cork

Introduction

Port wine is a fortified wine produced in the Douro region of Portugal (Moreira & Guedes de Pinho, 2011). There are several special categories of Port wine according to the winemaking processes (e.g., Vintage, Ruby, Tawny, among others). The term Vintage is only attributed to Port wine with superior quality and structure that is made from grapes of a single vintage. This type of Port wine is matured in wood for 2-3 years followed by bottle ageing for 10 to 50 years or more before consumption. During bottle ageing, the

polyphenolic and volatile profiles of Port wine undergo important transformations having an impact in the commercial value of aged Vintage Port wine. Thus, the storage conditions, namely temperature and oxygen (O₂) exposure, are critical for color and aroma characteristics of these wines as they directly influence oxidative transformations during wine ageing (Furtado et al., 2021; Scrimgeour et al., 2015). Indeed, some studies have investigated the influence of dissolved O₂ and free SO₂ levels, pH, and time/temperature on the volatile profile of Port wine. Among these effects, temperature and pH had the largest impact leading to the formation of several volatiles such as 5-methylfurfural, furfural, sotolon, acetaldehyde, heterocyclic acetals (Castro et al., 2014; da Silva Ferreira et al., 2002), glyoxal and methylglyoxal (Moreira et al., 2019). Moreover, the aldehydes present in Port wine can be involved in the condensation processes of anthocyanins with proanthocyanidins having an impact in the color stability and evolution (He et al., 2012; Mateus & de Freitas, 2001). In line with this, the decrease on polyphenols during wine ageing has been reported in the literature and can be due to the chemical transformation, polymerization, complexation, and degradation phenomena's (Bakker & Timberlake, 1986; de Freitas et al., 2017; Edwin, 1980; Lopes et al., 2006; Muche et al., 2018; Oliveira et al., 2013; Oliveira et al., 2007; Saucier et al., 1997). Furthermore, it has been reported that when cork is in contact with an aqueous solution of ethanol, such as the case of Port wine, phenolic and volatile compounds can be extracted from cork (Azevedo et al., 2014; Pinto et al., 2019) and can participate in the same interactions.

Considering the importance of storage conditions for the quality of bottle-aged Vintage Port wine, the aim of this work was to evaluate the influence of cellar conditions (controlled and uncontrolled temperature and humidity) and bottle orientation (horizontal and vertical) on the phenolic and volatile composition of a Port wine sealed with a natural cork stopper, over a period of 44 months. This work also had the purpose to detect and identify compounds that could arise from the interaction of cork with wine in the horizontal position. A better understanding of the impact of cellar conditions and bottle orientation on the physical-chemical properties of Vintage Port is of extreme importance for the Port wine industry to select the most appropriate storage conditions to produce high quality wines.

Materials and Methods

Reagents

The L-(+)-tartaric acid (99%), ethyl acetate (99.9%), methanol (99.8%), acetonitrile (99.8%), acetic acid (99.7%), Folin–Ciocalteu reagent, and sodium bisulfite were obtained from Sigma-Aldrich, Madrid, Spain. Ethanol was purchased from AGA® (96%), Prior Velho, Portugal and HCl 37% from Fluka®, College Park, MD, USA. All standard compounds used in the quantification of volatiles presented high purity ($\geq 95\%$) as described elsewhere [19] and were purchased from Sigma-Aldrich, Inc. (Steinheim, Germany).

Port Wine Samples

The Port wine used in this study was a Vintage Port Wine 2014 produced with a blend from several varieties from Douro region (*Touriga Franca*, *Touriga Nacional*, *Tinta Barroca*, *Tinta Roriz* and *Tinto Cão*) using the traditional method for Vintage Port wine. The wine presented the following chemical characteristics: alcohol % vol. (20 °C): 19.73; density (g/L): 1022.0; baume: 3.37; color 420 nm (1 mm PL): 0.888; color 520 nm (1 mm PL): 1.521; total SO₂: 90.0 mg/L. Forty-six bottles (Vintage model 1790 of a single batch of manufacture) were filled with the Port wine obtained from the same tank and sealed with natural cork stoppers of grade A 49×24 mm from the same origin (provided by Amorim® Cork S.A.). The study was designed to maintain the homogeneity of wine samples, with the physical-chemical features being only affected by the two factors under study, namely the cellar conditions and bottle orientation. The characteristics of the cellars used in this study are presented in **Table 1**. Cellar A had air conditioning and consequently minor variations of temperature and humidity, while Cellar B represents a traditional cellar without any humidity and temperature control, allowing the wine to suffer temperature fluctuations according to the season of year. All bottles were protected from light in both cellars. In cellar A, half of the total bottles were stored in vertical position and the other half in the horizontal position, whereas in Cellar B all bottles were stored in horizontal position. At each analysis time (0, 6, 15, 44 months), five bottles from each condition were analyzed: Cellar A vertical, Cellar A horizontal, and Cellar B horizontal.

Table 1. Average, maximum, minimum and amplitude of temperature and humidity recorded in the Cellars A and B during the period under study (44 months).

Local	Temperature (°C)/Humidity (%)			
	Average	Maximum	Minimum	Amplitude ^a
Cellar A	18/60	22/81	14/40	1/5
Cellar B	23/58	33/85	13/34	3/8

^a The amplitude indicates the difference between the average highest temperature/humidity and the average lowest temperature/humidity in the studied time period.

Color Index (CIELAB, Color Index and Hue)

The color characteristics were evaluated by the chromatic intensity (CI), color hue and CIELAB color coordinates (L^* , C^* , H^*), where L^* is the lightness, C^* the chromaticity and H^* the hue, measured by direct absorption and determined by Color Win-MSCV[®] Coordinates software. For that, the absorbance (Abs) at 450, 520, 570 and 630 nm were determined for all samples using a 2 mm optical path cuvette (Guerreiro, Teixeira et al. 2017). For the color index determination, the Abs at 420, 520 and 620 nm of all wine samples were determined using a 1 mm cell. The hue was determined by the ratio between the Abs at 420 and 520 nm. All determinations were performed on a UV–vis spectrophotometer Thermo[®] Scientific Evolution Array UV–vis spectrophotometer (ThermoFisher Scientific, Waltham, MA USA).

Total Phenolics Index

The relative amount of total phenolic compounds between samples was estimated by recording the Abs at 280 nm of diluted wine samples (10 times with wine model solution, 12% ethanol, 5 g/L tartaric acid, pH 3.5) using a quartz cell of 1 mm (Flanzy and Poux 1958, Boulet, Ducasse et al. 2017).

Total Proanthocyanidins

The total proanthocyanidins (condensed tannins) were determined based on the Bate-Smith reaction, (Gonçalves, Mateus et al. 2011). This method consists on the acidic decomposition of condensed tannins in the presence of heat (100 °C) in strongly acidic conditions yielding to anthocyanidins that can be determined at 520 nm (Ribéreau-Gayon and Stonestreet 1966). As Port wines contain a high concentration of sugar and to avoid caramelization reactions that will have an impact on the Abs at 520 nm, samples were pre-treated to remove sugars. This operation consisted in the application of 1 mL of Port wine in a C18 gel cartridge[®] which was washed with distilled water, and then the wine fraction without sugar was recovered with 4 mL of methanol. Methanol was evaporated and the sample resuspended in 1 mL of distilled water. Then, each wine

sample was diluted 50 times with a wine model solution (tartaric acid 5 g/L, 12% ethanol, pH 3.5) and 4.0 mL of these diluted wine plus 2.0 mL of water and 6.0 mL of HCl (37%) were placed into a hydrolysis tube and heated to 100 °C for 30 minutes. The tubes were cooled in water, protected from light for 10 minutes and then, 1.0 mL of ethanol was added and mixed. The procedure was performed in triplicate for each sample and reference was obtained using the same procedure but in the absence of heat. The Abs at 520 nm of all samples was recorded using a 1 cm glass cell in a Thermo® Evolution Array spectrophotometer (ThermoFisher, Waltham, MA USA). The change in Abs is calculated by the difference between the Abs of the sample and the Abs of the reference tube, according to the equation:

$$\Delta \text{ Abs} = \text{ Abs (520nm) }_{\text{sample}} - \text{ Abs (520 nm) }_{\text{reference}}$$

The concentration of condensed tannins in wines was determined through a calibration curve ($R^2 = 0.9911$) obtained using different concentrations of procyanidins ranging from 0.264–5.92 mg/mL. Procyanidin standards were comprised by a fraction of dimeric and trimeric procyanidins purified from grape seeds (Gonçalves, Mateus et al. 2011, Azevedo, Brandão et al. 2020).

Total Free Anthocyanins

The concentration of free anthocyanins was determined using the procedure described in the literature (Mateus et al., 2001), by adaptation of the Sommers & Evans method (Somers & Evans, 1977). Briefly, 40.0 mL of HCl 2%, 2.0 mL of ethanol and 2.0 mL of wine were added to a glass flask. Then, 10.0 mL of the mixture was added to four glass tubes and then 4.0 mL of sodium bisulfite 20% (w/v) was added to three of them. To the fourth tube (reference), 4.0 mL of water was added. The samples were vortexed and left in the dark during 20 minutes. The Abs at 520 nm was recorded for all the samples using a 1 cm glass cell in a Thermo® UV-VIS Evolution Array Spectrophotometer (Thermo Fisher Scientific, Waltham, MA USA). The concentration of the free anthocyanins in wine corresponds to the difference between the Abs of the samples and the reference using the calibration curve prepared with malvidin-3-O-glucoside, according to the equations:

$$\Delta \text{ Abs} = \text{ Abs (520nm) }_{\text{reference}} - \text{ Abs (520 nm) }_{\text{sample}}$$

$$[\text{Anthocyanins}_{\text{Wine}}]_{\text{mg/L}} = (\Delta \text{ abs} - 0.00024) / 0.0015$$

Dialysis Index

This assay was performed according to the procedure described in the literature (Glories, 1984; Mateus et al., 2001). Briefly, 5.0 mL of wine was introduced into a dialysis tubing

(cellulose; 6 mm i.d. nominal molecular weight cut-off 12.000-16.000; average porous radius of 25 Å) and then submerged in a glass bottle with 50.0 mL of 12 % aqueous ethanol solution (5 g/L tartaric acid, pH 3.5). In a second bottle, 5.00 mL of wine was diluted directly with the same hydroalcoholic solution up to 50.0 mL (reference). Both glass bottles were closed and stored at room temperature during 24 h. Then, the Abs at 280 nm was determined in a 1 mm quartz cell. The difference between the Abs at 280 nm of the reference and the sample correspond to the fraction of more polymerized phenolic compounds that were retained inside the dialysis membrane.

Tannin Specific Activity

The Tannin Specific Activity (TSA) determines the capacity of phenolic compounds to precipitate a protein (bovine serum albumin, BSA) and it is measured by turbidimetry as described elsewhere (De Freitas and Mateus 2001, Azevedo, Brandão et al. 2020). Red wines were diluted to 1:50 with a filtered (0.45 µm) wine model solution (12% ethanol, 5.0 g/L tartaric acid, pH 3.50). Then, 4.0 mL of this solution were transferred to a turbidimetry tube and the turbidimetry values were recorded in Turbidimeter HACH 2100 N (HACH, Lisbon, Portugal) adapted for cells of 100x12 mm. Then, 150 µL of BSA (0.8 mg/mL) was added to each tube and vortexed. The tubes were kept in the dark during 30 min, and then, the maximum turbidity was determined. The TSA was expressed in turbidity units NTU/mL of wine and determined by the following expression, where 0.08 corresponds to the dilution factor of wine: $\text{Turbidity (NTU/mL of wine)} = (\text{Turbidity}_{\text{after BSA}} - \text{Turbidity}_{t_0})/0.08$

Volatile Composition

The concentration of 36 volatile compounds in Porto Wine was determined by headspace solid-phase microextraction (HS-SPME) coupled to gas chromatography– mass spectrometry (GC–MS) using a method adapted from Barros *et al.* (Paula Barros, Moreira et al. 2012). The volatile compounds included several alcohols, aldehydes, ethyl esters, ketones, and isoprenoids. Briefly, 250 µL of each wine were placed in a 20 mL glass vial and the HS-SPME procedure was carried out using a Combi-PAL autosampler (Varian Pal Autosampler, Switzerland). The GC-MS analysis was performed in a 436-GC model coupled to a SCION single quadrupole (SQ) mass spectrometer (Bruker Daltonics, Bremen, Germany) and a Bruker Daltonics MS workstation (version 8.2.1, Bruker Daltonics, Bremen, Germany). The HS-SPME and GC-MS conditions considered for analysis of Porto Wine are described in detail in our previous studies (Oliveira, Furtado et al. 2020, Amaro, Almeida et al. 2022). The calibration curves determined for quantification of volatile compounds were achieved by analysis, under the same

analytical conditions, of standard compounds dissolved in a wine model solution (12% ethanol, 5 g/L of tartaric acid, pH 3.2) in a range of known concentrations.

Identification of Cork Phenolic Compounds extracted to Port Wines

Wine Treatment

The first step was the elimination of ethanol from the Port wine, under vacuum using rotary evaporator. After that, 100 mL of Port Wine were applied into a C18 gel (using a G3 funnel with Buchner and vacuum system) and the aqueous phase was collected (1 L). This fraction was then evaporated under vacuum to about 200 mL of the final volume. The aqueous fraction was extracted with ethyl acetate three times (80 mL) and then all organic fractions were combined and the organic solvent evaporated. The solid phase was resuspended in 5 mL methanol/water (1:1) and then analyzed by LC-ESI-MS.

Detection of Corklin by Liquid Chromatography-DAD/Electron Spray Ionization (ESI)-Mass Spectrometry (MS) Analysis

A Finnigan Surveyor series liquid chromatograph (Thermo Fisher Scientific, Waltham, MA USA), equipped with a Thermo Finnigan (Hypersil Gold®) reversed-phase column (150 mm × 4.6 mm, 5 µm, C18) thermostated at 25 °C was used. The samples were analyzed using the same solvents, gradient, injection volume, and flow rate referred above for the HPLC analysis. Double-online detection was done by a photodiode spectrophotometer and mass spectrometer (Thermo Fisher Scientific, Waltham, MA USA). The mass detector was a Finnigan LCQ DECA XP MAX (Finnigan Corp., San Jose, CA) quadrupole ion trap equipped with atmospheric pressure ionization (API) source, using electrospray ionization (ESI) interface. The vaporizer and the capillary voltages were 5 kV and 4 V, respectively. The capillary temperature was set at 325° C. Nitrogen was used as both sheath and auxiliary gas at flow rates of 80 and 30, respectively (in arbitrary units). Spectra were recorded in the negative ion mode between m/z 120 and 2000. The mass spectrometer was programmed to perform a series of three scans: a full mass, a zoom scan of the most intense ion in the first scan, and a MS-MS of the most intense ion using relative collision energies of 30 and 60 V.

Statistical Analysis

All determinations were performed in triplicated, except for volatile composition. Values are expressed as the arithmetic means ± standard deviation. Statistical significance of the difference between the wines was evaluated by ANOVA followed by Tukey test for

multiple testing correction, using GraphPad Prism 9 software (version 9.3.0, San Diego, CA, USA).

Results and Discussion

Effect of the Cellar Conditions

The effect of the cellar conditions (temperature and humidity) on the phenolic and volatile composition of Vintage Port wine was studied over a period of 44 months. As shown in **Table 1**, the cellar A presented a lower thermic amplitude and a higher medium humidity due to the presence of air conditioner. On the other hand, the cellar B was under a higher thermic amplitude, with a much higher maximum temperature when compared with cellar A, namely 33 °C versus 22 °C, respectively (**Table 1**). **Table 2** presents the statistically significant alterations occurring in color, phenolic and volatile composition of Porto wine induced by cellar conditions. These results showed that the main differences in color and phenolic composition between both cellars were in the wines b* CIELAB coordinate, hue, and tannin specific activity. Wines stored at cellar B displayed higher hues and b* values after 44 months of storage, indicating more yellow tones than the wines stored at cellar A. This result is in agreement with a recent study showing that “Verdejo” white wines stored under commercial conditions (diffuse white LEDs and temperature of 24 ± 2 °C) revealed higher levels of brown-yellowish hues when compared with wines stored in the dark at 12 °C (Díaz-Maroto, López Viñas et al. 2021). The comparison of the phenolic profile of red wines under different storage conditions (controlled cellar and typical domestic conditions) (Tzachristas et al. 2021) also revealed that the controlled cellar (15–17 °C, ~70% humidity) preserved better the chemical and organoleptic characteristics of the wines even after 2 years of storage, while the wines stored in typical domestic conditions (20–27 °C, uncontrolled humidity) aged approximately four times faster.

Furthermore, the tannin specific activity data showed that the wines stored at cellar A presented a higher ability to interact with proteins which may indicate a higher astringency.

Table 2. Color, phenolic parameters and volatile composition of Vintage Port wine stored under different cellar conditions and bottle orientation for 44 months in bottle (*n*=5).

	months	Cellar A		Cellar B	Statistical differences	Descriptor (olfactory threshold)
		vertical	horizontal	horizontal		
b*	T= 0	28	28	28	-	
	6	16.0 (6.6)	19.7 (3.1)	21.1 (3.7)	n.s.	
	15	26.4 (2.6)	26.6 (0.9)	26.4 (1.3)	n.s.	-
	44	19.1 (0.7)	18.2 (2.1) a	25.1 (13.7) a	*	
Hue (Abs 420 nm/ Abs 520 nm)	T= 0	0.58	0.58	0.58	-	
	6	0.74 (0.08)	0.79 (0.05)	0.70 (0.04)	n.s.	
	15	0.64 (0.06)	0.61 (0.02)	0.63 (0.03)	n.s.	-
	44	0.72 (0.06)	0.65 (0.14) a	0.78 (0.06) a	**	
Total Proanthocyanidins (g/L)	T= 0	3.2	3.2	3.2	-	
	6	2.8 (0.3)	3.1 (0.3)	3.3 (0.2)	n.s.	
	15	2.9 (0.3) a	3.5 (0.3) a	3.3 (0.2)	*	-
	44	1.3 (0.5)	1.3 (0.1)	0.8 (0.5)	n.s.	
Tannin Specific Activity (NTU/mL)	T= 0	404	404	404	-	
	6	392.1 (10.6) a	360.8 (13.0) a	375.1 (12.5)	**	
	15	361.1 (9.4)	342.1 (12.0)	347.8 (19.3)	n.s.	-
	44	411.1 (17.2) a, b	471.5 (29.2) a	436.3 (15.3) b	***	
Furfural (µg/L)	T= 0	137	137	137	-	
	6	207.6 (73.7)	227.0 (97.8)	308.0 (118.2)	n.s.	Toasty, caramel
	15	298.2 (26.4) a	359.0 (92.2) b	461.4 (43.3) a, b	****	(14 µg/L)
	44	521.4 (90.0) a	471.3 (93.0) b	914.1 (42.7) a, b	****	
5-Methylfurfural (µg/L)	T= 0	NQ	NQ	NQ	-	
	6	NQ	NQ	NQ	-	Spicy, toasty
	15	NQ	NQ	NQ	-	(16 µg/L)
	44	43.5 (2.0) a	42.8 (2.8) b	64.5 (3.9) a, b	****	
Benzaldehyde (µg/L)	T= 0	45	45	45	-	
	6	34.4 (10.4)	35.7 (8.3)	33.9 (8.8)	n.s.	Bitter almonds
	15	16.3 (1.9)	17.4 (1.0) a	15.0 (0.2) a	*	(2 mg/L)
	44	32.7 (4.7) a, b	25.4 (2.9) a, b	28.9 (3.0) a	*	
Phenylethyl acetate (µg/L)	T= 0	NQ	NQ	NQ	-	
	6	NQ	NQ	NQ	-	Floral, sweet
	15	14.6 (1.3)	16.0 (0.8) a	13.2 (1.3) a	**	(250 µg/L)
	44	32.2 (1.1)	32.8 (1.7)	30.8 (1.2)	n.s.	

Results expressed as an average (standard deviation) of three readings for each bottle. Identical letters indicate statistically significant differences among samples stored under different cellar conditions and bottle orientation within the same post-bottling period. n.s.– $p > 0.05$, *– $p \leq 0.05$, **– $p \leq 0.01$, ***– $p \leq 0.001$, NQ–not quantified.

Regarding the impact of cellar conditions on the volatile composition of Vintage Port wine, among the 36 volatile compounds determined (Table S2), five showed significant alterations between the two cellars at 15- or 44-months post-bottling (**Table 2, Figure**

1). At 15 months post-bottling, significant higher levels of furfural and significant lower levels of benzaldehyde and phenylethyl acetate were found in wines stored in cellar B compared with A (**Figure 1a**). The results found at 44 months confirmed the significant increase of furfural in cellar B (Table 2, Figure 1b), in tandem with another furan compound only determined at this time point (5-methylfurfural).

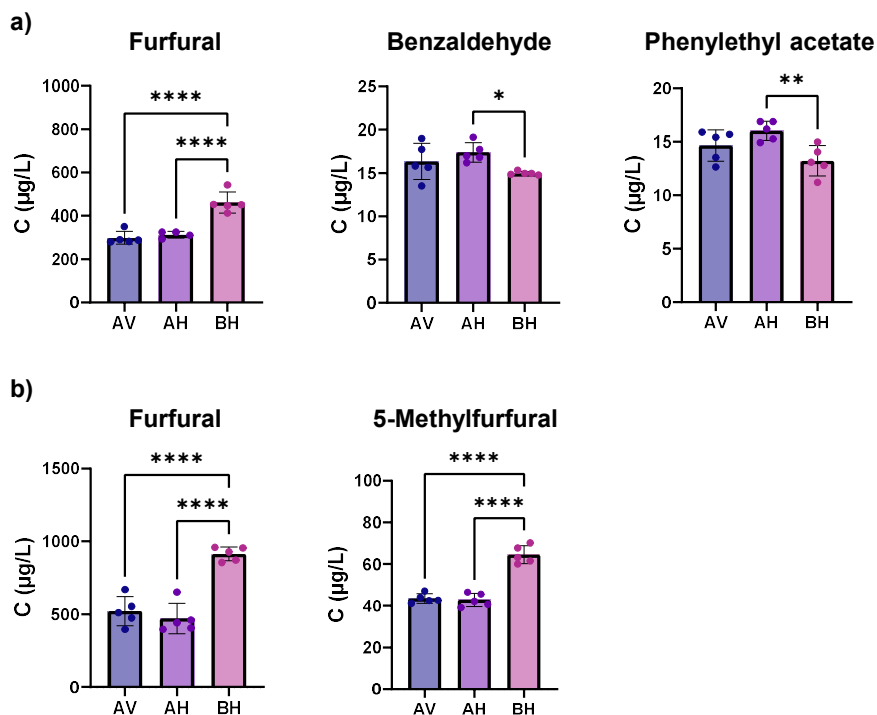


Figure 1. Boxplots illustrating the levels of volatile compounds present in Vintage Port wine that changed with the cellar conditions at a) 15 months and b) 44 months. AV – cellar A vertical position, AH – cellar A horizontal position, BH – cellar B horizontal position. * – $p \leq 0.05$, ** – $p \leq 0.01$, **** – $p \leq 0.0001$.

The remaining 34 volatile compounds showed relatively constant levels between both cellars across the bottle ageing period (Table S2). The increase observed in the levels of furfural and 5-methylfurfural in cellar B may be due to prolonged storage at higher and uncontrolled temperature which can lead to the occurrence of Maillard reaction, caramelization, and an increased susceptibility to oxidation (Escudero, Cacho et al. 2000, Erdal 2022). Furfural and 5-methylfurfural were present in concentrations above the human olfactory perception threshold (**Table 2**) and typically contribute to toasty and caramel aroma in wines (1980, Ferreira, López et al. 2000, Moreno, Zea et al. 2005). The increase in the levels of both furan compounds with temperature was previously observed by Silva Ferreira et al., (Castro, Martins et al. 2014) but considering Port wine under forced ageing conditions (60 °C temperature and different oxygen saturations). The decrease observed in the levels of benzaldehyde may be related with its use in the formation of condensed pigments through the reaction between anthocyanins, flavanols

and benzaldehyde (Pissarra, Mateus et al. 2003). Finally, the decrease of phenylethyl acetate levels with the increase of storage temperature was already reported for Cabernet Sauvignon Wine (Hopfer, Buffon et al. 2013) and may be attributed to hydrolysis.

Effect of the Bottle Storage Position

To study the effect of the bottle storage position on the physical-chemical parameters of Vintage Port wine, the bottles were stored in the cellar A in vertical and horizontal positions. The statistically significant alterations found in Port wine stored with different bottle positions are also presented in **Table 2**. Significant alterations were noted in the total proanthocyanidins at 15 months, tannin specific activity at 6 and 44 months, and benzaldehyde at 44 months. Regarding the color parameters determined by the CIELAB system, the results obtained for the wines showed no significant differences for L^* , a^* , b^* , C^* , H° , Hue and CI parameters (Table S1). For that reason, we can assume that the bottle position didn't have an impact on the final color of wines, at least for 44 months.

At 15 months, the levels of total proanthocyanidins were significant higher in the Porto wine stored in the horizontal position when compared to the wines stored in the vertical position (Table 2). After 15 months and up to 44 months, it was observed an important decrease in proanthocyanins levels, for all wines regardless of the position. The tannin specific activity (TSA) of Porto wine was affected by bottle position at 6 and 44 months showing a contradictory tendency since the TSA was significantly higher in the wine stored in the vertical position at 6 months and significantly higher in the wine stored in the horizontal position at 44 months. These results combined with those of total proanthocyanidins suggest that wines stored in horizontal position may have more complex and astringent structures, and therefore, higher capacity to interact with salivary proteins (Azevedo, Brandão et al. 2020). Moreover, a study investigating the effect of different sealing and storage conditions revealed that white and red wines were better preserved when the bottles were keeping horizontally, according to chemical parameters and sensory analysis (Mas, Puig et al. 2002).

Regarding the volatile composition of Vintage Port, the bottle position only showed an influence in the levels of benzaldehyde which were found significantly lower in wines stored in the horizontal position at 44 months post-bottling (**Table 2**). No significant differences were observed in the levels of the remained 35 volatile compounds between different bottle positions (Table S2). As mentioned above, benzaldehyde is a very reactive molecule that can participate in the formation of condensed pigments by reaction with polyphenols (Pissarra, Mateus et al. 2003). In fact, the horizontal position enables

a direct contact of Vintage Port wine with the natural cork stopper which can promote the occurrence of reactions between aldehydes and phenolic compounds present in cork.

Since previous studies of our group proved that cork compounds can react with main wine constituents, namely (+)-catechin and malvidin-3-O-glucoside giving origin to new compound classes, such as Corklins (Azevedo, Fernandes et al. 2017), the presence of these compounds was investigated in all bottled wine samples studied at 44 months of storage by LC-MS analysis. Indeed, it was possible to detect a compound with an ion mass at m/z 1193 and a fragment at m/z 903 ($M - 290$, loss of a catechin unit) (**Figure 2**) in trace amounts in wines stored in the horizontal position (Table S3). The fragmentation pattern and the retention time of the detected peak agrees with the data previously reported for Corklin (Azevedo, Fernandes et al. 2017). This compound results from the interaction between vescalagin (extracted from cork) ethanol derivative and (+)-catechin present in the wine. These findings suggest that the direct contact between Vintage Port wine and cork during the horizontal storage promotes the formation of Corklins.

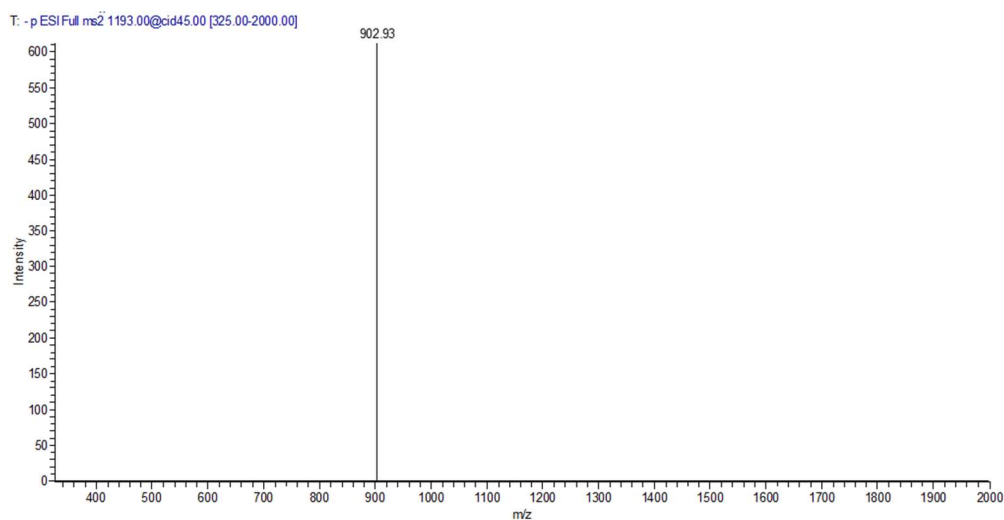


Figure 2: MS² spectrum of Corklin (m/z 1193) obtained by LC-MS analysis of Vintage Port wine stored in the horizontal position, with the main fragment at m/z 903 ($M - 290$, loss of a catechin unit).

Conclusions

This study unveiled that a Vintage Port wine 2014 stored in a traditional cellar (cellar B) under larger thermic amplitudes over the year had more yellow tones (higher hues and b^* values), lower astringency (lower tannin specific activity), lower levels of phenylethyl acetate, and higher levels of oxidation markers (furfural and 5-methylfurfural) contributing for toasty and caramel aromas, when compared with the same Port wine stored in a cellar with controlled temperature (cellar A). Importantly, the impact of larger thermic amplitudes on the tannin specific activity and the phenylethyl acetate levels of Port wine was observed in this work for the first time. Moreover, the Vintage Port stored in the horizontal position showed for the first time, to our knowledge, higher levels of total proanthocyanidins, more complex and astringent structures (higher tannin specific activity), the presence of one compound derived from the reaction of wine and cork components (Corklin) and lower levels of benzaldehyde, when compared with the same wine stored in the vertical position. Overall, these findings were more evident at 44 months post-bottling. The results obtained in this study are of extreme importance for the Port Wine Industry providing new insights for the selection of cellar conditions and bottle orientation according to the desired characteristics for a Vintage Port wine.

Author Contributions: Conceptualization, J.A., J.P., P.G.d.P. and V.d.F.; methodology, J.A., J.P. and N.T.; investigation, J.A., J.P., P.G.d.P., N.M., P.L. and M.C.; writing—original draft preparation, J.A. and J.P.; writing—review and editing, J.O, J.P., P.G.d.P, N.M and V.d.F.; funding acquisition, M.C., P.G.d.P. and V.d.F. All authors have read and agreed to the published version of the manuscript.

Funding: The authors thank the Foundation for Science and Technology (FCT) for financial support of the scholarships SFRH/BD/139709/2018, UIDB/50006/2020 and UIDBP/50006/2020. This research is also supported by AgriFood XXI I&D&I project (NORTE-01-0145-FEDER-000041) co-financed by European Regional Development Fund (ERDF), through the NORTE 2020 (Programa Operacional Regional do Norte 2014/2020). This research was also funded by national funds from FCT in the scope of the project UIDP/04378/2020 and UIDB/04378/2020 of the Research Unit on Applied Molecular Biosciences—UCIBIO, and the project LA/P/0140/2020 of the Associate Laboratory Institute for Health and Bioeconomy—i4HB

Conflicts of Interest: The authors declare no conflict of interest. The funders had no role in the design of the study; in the collection, analyses, or interpretation of data; in the writing of the manuscript, or in the decision to publish the results.

References

- Amaro, F., Almeida, J., Oliveira, A. S., Furtado, I., Bastos, M. d. L., Guedes de Pinho, P., & Pinto, J. (2022). Impact of Cork Closures on the Volatile Profile of Sparkling Wines during Bottle Aging. *Foods (Basel, Switzerland)*, 11(3), 293. <https://www.mdpi.com/2304-8158/11/3/293>
- Azevedo, J., Brandão, E., Soares, S., Oliveira, J., Lopes, P., Mateus, N., & de Freitas, V. (2020). Polyphenolic Characterization of Nebbiolo Red Wines and Their Interaction with Salivary Proteins. *Foods (Basel, Switzerland)*, 9(12). <https://doi.org/https://10.3390/foods9121867>
- Azevedo, J., Fernandes, A., Oliveira, J., Brás, N. F., Reis, S., Lopes, P., Roseira, I., Cabral, M., Mateus, N., & de Freitas, V. (2017). Reactivity of Cork Extracts with (+)-Catechin and Malvidin-3-O-glucoside in Wine Model Solutions: Identification of a New Family of Ellagitannin-Derived Compounds (Corklins). *Journal of Agriculture and Food Chemistry* 65(39), 8714-8726. <https://doi.org/https://doi.org/10.1021/acs.jafc.7b02845>
- Azevedo, J., Fernandes, I., Lopes, P., Roseira, I., Cabral, M., Mateus, N., & Freitas, V. (2014). Migration of phenolic compounds from different cork stoppers to wine model solutions: antioxidant and biological relevance [journal article]. *European Food Research and Technology*, 239(6), 951-960. <https://doi.org/https://doi.org/10.1007/s00217-014-2292-y>
- Bakker, J., & Timberlake, C. (1986). The mechanism of color changes in aging port wine. *American Journal of Enology and Viticulture*, 37(4), 288-292.
- Boulet, J. C., Ducasse, M. A., & Cheynier, V. (2017). Ultraviolet spectroscopy study of phenolic substances and other major compounds in red wines: Relationship between astringency and the concentration of phenolic substances. *Australian Journal of Grape and Wine Research*, 23(2), 193-199.
- Castro, C. C., Martins, R. C., Teixeira, J. A., & Silva Ferreira, A. C. (2014). Application of a high-throughput process analytical technology metabolomics pipeline to Port wine forced ageing process. *Food Chemistry*, 143, 384-391. <https://doi.org/https://doi.org/10.1016/j.foodchem.2013.07.138>
- da Silva Ferreira, A. C., Barbe, J. C., & Bertrand, A. (2002). Heterocyclic acetals from glycerol and acetaldehyde in Port wines: evolution with aging. *J Agric Food Chem*, 50(9), 2560-2564. <https://doi.org/10.1021/jf011391j>
- De Freitas, V., & Mateus, N. (2001). Structural features of procyanidin interactions with salivary proteins [Article]. *Journal of Agricultural and Food Chemistry*, 49(2), 940-945. <https://doi.org/https://doi.org/10.1021/jf000981z>
- de Freitas, V. A. P., Fernandes, A., Oliveira, J., Teixeira, N., & Mateus, N. (2017). A review of the current knowledge of red wine colour. *OENO One*, 51(1). <https://doi.org/10.20870/oeno-one.2017.51.1.1604>
- Díaz-Maroto, M. C., López Viñas, M., Marchante, L., Alañón, M. E., Díaz-Maroto, I. J., & Pérez-Coello, M. S. (2021). Evaluation of the Storage Conditions and Type of Cork Stopper on the Quality of Bottled White Wines. *Molecules*, 26(1), 232. <https://doi.org/https://doi.org/10.3390/molecules26010232>
- Edwin, H. (1980). In vino veritas: Oligomeric procyanidins and the ageing of red wines. *Phytochemistry*, 19(12), 2577-2582. [https://doi.org/https://doi.org/10.1016/S0031-9422\(00\)83922-9](https://doi.org/https://doi.org/10.1016/S0031-9422(00)83922-9)
- Erdal, A. (2022). A Kinetic Approach to Explain Hydroxymethylfurfural and Furfural Formations Induced by Maillard, Caramelization, and Ascorbic Acid Degradation Reactions in Fruit Juice-Based Mediums. *Food analytical methods*, v. 15(no. 5), pp. 1286-1299-2022 v.1215 no.1285. <https://doi.org/10.1007/s12161-021-02214-x>
- Escudero, A., Cacho, J., & Ferreira, V. (2000). Isolation and identification of odorants generated in wine during its oxidation: a gas chromatography–olfactometric study. *European Food Research and Technology*, 211(2), 105-110. <https://doi.org/10.1007/s002179900128>
- Ferreira, V., López, R., & Cacho, J. F. (2000). Quantitative determination of the odorants of young red wines from different grape varieties. *Journal of the Science of Food and Agriculture*, 80(11), 1659-1667. [https://doi.org/https://doi.org/10.1002/1097-0010\(20000901\)80:11<1659::AID-JSFA693>3.0.CO;2-6](https://doi.org/https://doi.org/10.1002/1097-0010(20000901)80:11<1659::AID-JSFA693>3.0.CO;2-6)
- Flanzy, M., & Poux, C. (1958). Les possibilités de la microvinification, application à l'étude de la macération. *Annales de Technologie Agricole*,

- Furtado, I., Lopes, P., Oliveira, A. S., Amaro, F., Bastos, M. d. L., Cabral, M., Guedes de Pinho, P., & Pinto, J. (2021). The Impact of Different Closures on the Flavor Composition of Wines during Bottle Aging. *Foods (Basel, Switzerland)*, 10(9), 2070. <https://doi.org/10.3390/foods10092070>
- Glories, Y. (1984). La couleur des vins rouges. Ire partie : les équilibres des anthocyanes et des tanins. *OENO One*, 18(3), 195-217. <https://doi.org/10.20870/oeno-one.1984.18.3.1751>
- Gonçalves, R., Mateus, N., & de Freitas, V. (2011). Inhibition of α -amylase activity by condensed tannins. *Food Chemistry*, 125(2), 665-672. <https://doi.org/https://doi.org/10.1016/j.foodchem.2010.09.061>
- The Good Scents Company. Flavor and fragrance information catalog.* (1980). Retrieved 27 May from <http://www.thegoodscentscompany.com/>.
- Guerreiro, J. R. L., Teixeira, N., De Freitas, V., Sales, M. G. F., & Sutherland, D. S. (2017). A saliva molecular imprinted localized surface plasmon resonance biosensor for wine astringency estimation. *Food Chemistry*, 233, 457-466. <https://doi.org/https://doi.org/10.1016/j.foodchem.2017.04.051>
- He, F., Liang, N.-N., Mu, L., Pan, Q.-H., Wang, J., Reeves, M. J., & Duan, C.-Q. (2012). Anthocyanins and their variation in red wines. II. Anthocyanin derived pigments and their color evolution. *Molecules (Basel, Switzerland)*, 17(2), 1483-1519. <https://doi.org/10.3390/molecules17021483>
- Hopfer, H., Buffon, P. A., Ebeler, S. E., & Heymann, H. (2013). The Combined Effects of Storage Temperature and Packaging on the Sensory, Chemical, and Physical Properties of a Cabernet Sauvignon Wine. *Journal of Agricultural and Food Chemistry*, 61(13), 3320-3334. <https://doi.org/10.1021/jf3051736>
- Lopes, P., Saucier, C., Teissedre, P.-L., & Glories, Y. (2006). Impact of Storage Position on Oxygen Ingress through Different Closures into Wine Bottles. *Journal of Agricultural and Food Chemistry*, 54(18), 6741-6746. <https://doi.org/10.1021/jf0614239>
- Mas, A., Puig, J., Lladoa, N., & Zamora, F. (2002). Sealing and Storage Position Effects on Wine Evolution. *Journal of Food Science*, 67(4), 1374-1378. <https://doi.org/https://doi.org/10.1111/j.1365-2621.2002.tb10292.x>
- Mateus, N., & de Freitas, V. (2001). Evolution and Stability of Anthocyanin-Derived Pigments during Port Wine Aging. *Journal of Agricultural and Food Chemistry*, 49(11), 5217-5222. <https://doi.org/https://doi.org/10.1021/jf0106547>
- Mateus, N., Proença, S., Ribeiro, P., Machado, J. M., & De Freitas, V. (2001). GRAPE AND WINE POLYPHENOLIC COMPOSITION OF RED Vitis vinifera VARIETIES CONCERNING VINEYARD ALTITUDE COMPOSICIÓN POLIFENÓLICA DE UVAS Y VINO DE VARIEDADES TINTAS DE Vitis vinifera EN FUNCIÓN DE LA ALTITUD DEL VIÑEDO COMPOSICIÓN POLIFENÓLICA DE UVAS E VIÑO DE VARIEDADES TINTAS DE Vitis vinifera EN FUNCIÓN DA ALTITUDE DO VIÑEDO. *Ciencia y Tecnología Alimentaria*, 3(2), 102-110. <https://doi.org/10.1080/11358120109487653>
- Moreira, N., Araújo, A. M., Rogerson, F., Vasconcelos, I., Freitas, V. D., & Pinho, P. G. d. (2019). Development and optimization of a HS-SPME-GC-MS methodology to quantify volatile carbonyl compounds in Port wines. *Food Chemistry*, 270, 518-526. <https://doi.org/https://doi.org/10.1016/j.foodchem.2018.07.093>
- Moreira, N., & Guedes de Pinho, P. (2011). Chapter 5 - Port Wine. In R. S. Jackson (Ed.), *Advances in Food and Nutrition Research* (Vol. 63, pp. 119-146). Academic Press. <https://doi.org/https://doi.org/10.1016/B978-0-12-384927-4.00005-1>
- Moreno, J. A., Zea, L., Moyano, L., & Medina, M. (2005). Aroma compounds as markers of the changes in sherry wines subjected to biological ageing. *Food Control*, 16(4), 333-338.
- Muche, B. M., Speers, R. A., & Rupasinghe, H. P. V. (2018). Storage Temperature Impacts on Anthocyanins Degradation, Color Changes and Haze Development in Juice of “Merlot” and “Ruby” Grapes (Vitis vinifera) [Original Research]. *Frontiers in Nutrition*, 5(100). <https://doi.org/10.3389/fnut.2018.00100>
- Oliveira, A. S., Furtado, I., Bastos, M. d. L., Guedes de Pinho, P., & Pinto, J. (2020). The influence of different closures on volatile composition of a white wine. *Food Packaging and Shelf Life*, 23, 100465. <https://doi.org/https://doi.org/10.1016/j.fpsl.2020.100465>
- Oliveira, J., da Silva, M. A., Jorge Parola, A., Mateus, N., Brás, N. F., Ramos, M. J., & de Freitas, V. (2013). Structural characterization of a A-type linked trimeric anthocyanin derived pigment occurring in a young port wine. *Food Chemistry*, 141(3), 1987-1996. <https://doi.org/https://doi.org/10.1016/j.foodchem.2013.04.091>
- Oliveira, J., de Freitas, V., Silva, A. M. S., & Mateus, N. (2007). Reaction between hydroxycinnamic acids and anthocyanin-pyruvic acid adducts yielding new portisins [Article]. *Journal of Agricultural and Food Chemistry*, 55(15), 6349-6356. <https://doi.org/https://doi.org/10.1021/jf070968f>

- Paula Barros, E., Moreira, N., Elias Pereira, G., Leite, S. G., Moraes Rezende, C., & Guedes de Pinho, P. (2012). Development and validation of automatic HS-SPME with a gas chromatography-ion trap/mass spectrometry method for analysis of volatiles in wines. *Talanta*, *101*, 177-186. <https://doi.org/10.1016/j.talanta.2012.08.028>
- Pinto, J., Oliveira, A. S., Lopes, P., Roseira, I., Cabral, M., Bastos, M. L., & Guedes de Pinho, P. (2019). Characterization of chemical compounds susceptible to be extracted from cork by the wine using GC-MS and ¹H NMR metabolomic approaches. *Food Chem*, *271*, 639-649. <https://doi.org/https://doi.org/10.1016/j.foodchem.2018.07.222>
- Pissarra, J., Mateus, N., Rivas-Gonzalo, J., Santos Buelga, C., & De Freitas, V. (2003). Reaction Between Malvidin 3-Glucoside and (+)-Catechin in Model Solutions Containing Different Aldehydes. *Journal of Food Science*, *68*(2), 476-481. <https://doi.org/https://doi.org/10.1111/j.1365-2621.2003.tb05697.x>
- Ribéreau-Gayon, P., & Stonestreet, E. (1966). Dosage des tanins du vin rouge et détermination de leur structure. *Chimie Analytique*, *48*(4), 188-196.
- Saucier, C., Bourgeois, G., Vitry, C., Roux, D., & Glories, Y. (1997). Characterization of (+)-Catechin-Acetaldehyde Polymers: A Model for Colloidal State of Wine Polyphenols. *Journal of Agricultural and Food Chemistry*, *45*(4), 1045-1049. <https://doi.org/10.1021/jf960597v>
- Scrimgeour, N., Nordestgaard, S., Lloyd, N., & Wilkes, E. (2015). Exploring the effect of elevated storage temperature on wine composition. *Exploring the effects of elevated storage temperature on wine composition*, *21*, 713. <https://doi.org/10.1111/ajgw.12196>
- Somers, T. C., & Evans, M. E. (1977). Spectral evaluation of young red wines: Anthocyanin equilibria, total phenolics, free and molecular SO₂, 'chemical age'. *J. Sci. Food Agric.*, *28*, 279-287.
- Tzachristas, A., Dasenaki, M. E., Aalizadeh, R., Thomaidis, N. S., & Proestos, C. (2021). Development of a Wine Metabolomics Approach for the Authenticity Assessment of Selected Greek Red Wines. *Molecules*, *26*(10). <https://doi.org/10.3390/molecules26102837>

Supplementary Information

Table S1. Color and phenolic parameters of Vintage Port wine stored under different cellar conditions and bottle orientation at 6-, 15- and 44-months post-bottling (n=5 per group at each timepoint).

Compound	T= 0	6 months			15 months			44 months		
		AV	AH	BH	AV	AH	BH	AV	AH	BH
L*	20.2	12.6 (6.7)	12.8 (3.6)	13.4 (3.7)	19.3 (5.9)	20.1 (3.3)	17.6 (0.9)	30.0 (1.7)	30.6 (2.3)	28.1 (5.9)
a*	48.7	36.4 (10.0)	38.2 (4.7)	37.9 (3.9)	47.6 (7.1)	49.3 (3.7)	46.3 (1.3)	48.8 (1.5)	49.8 (2.1)	47.0 (6.6)
b*	28	16.0 (6.6)	19.7 (3.1)	21.1 (3.7)	26.4 (2.6)	26.6 (0.9)	26.4 (1.3)	19.1 (0.7)	18.2 (2.1)	25.1 (13.7)
C*	56	40.9 (12.9)	43.9 (6.6)	43.6 (6.8)	54.9 (8.2)	55.9 (3.5)	52.9 (1.4)	52.3 (7.9)	53.1 (1.8)	50.3 (5.5)
H°	29.6	25.8 (4.7)	27.5 (3.0)	27.9 (2.8)	29.0 (1.7)	28.1 (1.2)	29.7 (0.8)	21.2 (7.8)	20.1 (2.4)	20.6 (1.5)
Chromatic Intensity (CI)	29.7	38.8 (9.5)	38.0 (3.8)	41.3 (4.7)	38.8 (9.5)	38.0 (3.8)	25.9 (1.5)	26.1 (0.5)	28.3 (2.5)	26.6 (1.0)
Hue (Abs 420 nm/ Abs 520 nm)	0.58	0.74 (0.08)	0.79 (0.05)	0.70 (0.04)	0.64 (0.06)	0.61 (0.02)	0.63 (0.03)	0.72 (0.06)	0.65 (0.14)	0.78 (0.06)
Total Phenolic Index (280 nm)	102	91.3 (6.6)	82.7 (5.4)	84.9 (11.4)	77.3 (15.0)	94.1 (23.9)	84.0 (10.6)	68.4 (2.5)	71.2 (2.7)	72.2 (1.1)
Total Proanthocyanidins (g/L)	3.2	2.8 (0.3)	3.1 (0.3)	3.3 (0.2)	2.9 (0.3)	3.5 (0.3)	3.3 (0.2)	1.3 (0.5)	1.3 (0.1)	0.8 (0.5)
Anthocyanins (mg/L)	354	367.8 (36.4)	312.4 (27.2)	344.9 (59.0)	213.8 (20.3)	211.3 (17.4)	186.9 (22.4)	102.2 (29.4)	128.5 (14.7)	113.6 (8.5)
Dialysis Index (g/L)	4.9	5.6 (0.3)	4.9 (0.3)	5.2 (0.9)	4.9 (1.0)	5.4 (1.1)	5.2 (0.8)	5.5 (0.5)	5.2 (0.5)	5.5 (0.3)
Tannin Specific Activity (NTU/mL)	404	392.1 (10.6)	360.8 (13.0)	375.1 (12.5)	361.1 (9.4)	342.1 (12.0)	347.8 (19.3)	411.1 (17.2)	471.5 (29.2)	436.3 (15.3)

AV – cellar A vertical position, AH – cellar A horizontal position, BH – cellar B horizontal position

Table S2. List of the 36 volatile compounds quantified in Vintage Porto wine under different cellar conditions and bottle orientation at 6-, 15- and 44-months post-bottling (n=5 per group at each timepoint).

Compound	RT	m/z	T= 0	6 months			15 months			44 months		
				AV	AH	BH	AV	AH	BH	AV	AH	BH
Alcohols												
Isoamyl alcohol (mg/L)	3.79	55	356	446 (114)	511 (148)	426 (147)	92 (4)	96 (17)	89 (5)	447 (45)	450 (11)	416 (22)
3-Hexen-1-ol (µg/L)	6.24	67	58.6	74.5 (92.7)	88.6 (75.9)	90.3 (78.3)	51.3 (10.3)	50.9 (10.1)	50.7 (9.4)	90.7 (9.7)	95.5 (9.3)	90.6 (10.1)
1-Hexanol (mg/L)	6.60	56	0.62	0.64 (0.79)	0.92 (0.85)	0.93 (0.62)	1.14 (0.11)	1.10 (0.16)	1.08 (0.10)	26.4 (1.9)	26.7 (1.6)	24.7 (0.8)
1-Octanol (µg/L)	12.51	56	18.7	10.3 (12.8)	13.4 (11.9)	16.0 (10.8)	16.0 (1.6)	15.8 (2.5)	15.4 (1.3)	57.7 (2.4)	59.4 (2.8)	58.7 (2.7)
Phenylethyl alcohol (mg/L)	13.77	91	20.5	16.3 (15.0)	17.5 (13.5)	21.2 (11.0)	12.9 (1.6)	13.4 (1.5)	13.0 (2.0)	42.5 (9.7)	49.8 (13.1)	53.8 (3.8)
1-Decanol (µg/L)	18.33	55	1.60	18.9 (6.3)	BLOQ	15.0 (12.6)	3.0 (0.3)	3.3 (0.5)	2.7 (0.2)	67.6 (0.3)	67.2 (0.9)	68.1 (0.6)
Aldehydes												
Furfural (µg/L)	5.66	95	137	207 (74)	227 (98)	308 (118)	298 (26)	359 (92)	461 (43)	521 (90)	471 (93)	914 (43)
5-Methylfurfural (µg/L)	9.24	110	NQ	NQ	NQ	NQ	NQ	NQ	NQ	43.5 (2.0)	42.8 (2.8)	64.5 (3.9)
Benzaldehyde (µg/L)	9.19	77	45.4	34.4 (10.4)	35.7 (8.3)	33.9 (8.8)	16.3 (1.9)	17.4 (1.0)	15.0 (0.2)	32.7 (4.7)	25.4 (2.9)	28.9 (3.0)
Phenylacetaldehyde (µg/L)	11.66	91	64.1	29.7 (8.3)	32.5 (7.5)	28.4 (4.5)	18.6 (3.4)	20.0 (3.0)	18.3 (1.4)	101 (11.1)	98.9 (7.8)	110 (7.0)
Nonanal (µg/L)	13.48	57	0.96	11.3 (4.5)	9.6 (3.0)	7.8 (4.0)	2.7 (1.9)	2.3 (0.6)	2.6 (0.9)	69.1 (5.1)	51.5 (11.6)	72.6 (39.9)
Decanal (µg/L)	16.46	57	3.12	14.5 (23.8)	3.6 (3.0)	5.9 (6.3)	4.0 (2.9)	3.3 (0.4)	3.0 (0.5)	14.9 (4.0)	15.1 (0.9)	23.9 (13.4)
Ethyl esters												
Ethyl isobutyrate (µg/L)	4.06	71	68.9	139 (39)	151 (56)	142 (52)	BLOQ	BLOQ	BLOQ	292 (49)	294 (58)	271 (42)
Ethyl butanoate (µg/L)	4.90	71	258	156 (44)	173 (66)	146 (54)	67 (19)	93 (27)	63 (26)	240 (34)	245 (43)	216 (30)
Ethyl 2-methylbutanoate (µg/L)	6.05	57	9.2	14.5 (4.2)	15.4 (5.3)	15.0 (5.0)	9.9 (2.2)	12.5 (4.0)	9.4 (3.2)	46.0 (6.2)	46.6 (8.3)	51.8 (9.0)
Ethyl isovalerate (µg/L)	6.16	88	9.7	24.7 (7.2)	27.3 (11.0)	25.2 (9.0)	17.8 (3.3)	22.1 (6.0)	18.2 (7.3)	109 (13.4)	111 (24.4)	112 (20.3)
Isoamyl acetate (µg/L)	6.75	70	611	284 (72)	319 (121)	238 (78)	96 (18)	114 (32)	74 (22)	148 (15)	153 (25)	129 (20)
Hexyl acetate (µg/L)	10.69	56	33.8	6.34 (1.31)	7.36 (2.79)	4.96 (1.58)	2.52 (0.42)	3.04 (0.80)	1.92 (0.44)	3.44 (0.31)	3.31 (0.80)	BLOQ
Ethyl hexanoate (mg/L)	10.26	88	0.96	0.42 (0.11)	0.49 (0.19)	0.38 (0.14)	0.19 (0.03)	0.22 (0.06)	0.16 (0.04)	1.16 (0.09)	1.20 (0.22)	1.11 (0.18)
Ethyl heptanoate (µg/L)	13.25	88	2.70	5.23 (1.81)	5.96 (2.63)	4.50 (2.09)	2.41 (0.33)	2.85 (0.64)	2.28 (0.53)	5.77 (0.53)	6.59 (1.40)	5.94 (0.99)
Diethyl succinate (mg/L)	15.71	101	NQ	NQ	NQ	NQ	3.2 (0.4)	3.4 (0.1)	3.9 (0.4)	43.6 (2.0)	44.4 (7.1)	54.5 (3.0)
Ethyl octanoate (mg/L)	16.27	88	NQ	NQ	NQ	NQ	0.60 (0.09)	0.74 (0.28)	0.52 (0.10)	3.66 (0.58)	3.96 (0.87)	3.46 (0.84)
Phenylethyl acetate (µg/L)	17.85	104	NQ	NQ	NQ	NQ	14.6 (1.3)	16.0 (0.8)	13.2 (1.3)	32.2 (1.1)	32.8 (1.7)	30.8 (1.2)
Ethyl nonanoate (µg/L)	18.93	88	1.8	3.0 (1.8)	3.3 (1.8)	2.8 (2.0)	3.6 (0.4)	4.2 (1.3)	3.2 (0.2)	17.7 (2.4)	19.2 (2.5)	18.2 (3.0)
Ethyl decanoate (µg/L)	21.55	88	2042	828 (377)	909 (425)	791 (486)	382 (72)	559 (374)	295 (23)	300 (115)	364 (128)	296 (119)
Ketones												
2-Heptanone (µg/L)	7.10	58	0.66	1.95 (0.20)	2.11 (0.47)	1.87 (0.29)	0.93 (0.16)	1.06 (0.17)	0.93 (0.13)	1.01 (0.09)	1.16 (0.25)	1.03 (0.19)
2-Nonanone (µg/L)	13.04	58	1.82	1.03 (0.61)	1.21 (0.43)	1.05 (0.34)	0.67 (0.04)	0.77 (0.18)	0.63 (0.04)	2.31 (0.20)	2.42 (0.27)	2.27 (0.17)
2-Undecanone (µg/L)	18.85	58	0.972	2.96 (4.32)	1.27 (1.54)	5.28 (5.87)	0.21 (0.05)	0.23 (0.04)	0.18 (0.04)	0.98 (0.31)	1.07 (0.20)	0.74 (0.23)
Isoprenoids												

Compound	RT	m/z	T= 0	6 months			15 months			44 months		
				AV	AH	BH	AV	AH	BH	AV	AH	BH
α -Pinene ($\mu\text{g/L}$)	8.36	93	2.43	1.91 (1.84)	1.21 (0.93)	0.82 (1.55)	BLOQ	BLOQ	BLOQ	ND	ND	ND
Limonene (ng/L)	11.20	68	3.39	7.25 (3.20)	9.90 (4.41)	5.47 (1.14)	NQ	NQ	NQ	31551 (1777)	31363 (2281)	30638 (3031)
Eucalyptol (ng/L)	11.28	81	ND	BLOQ	BLOQ	436 (232)	148 (17)	140 (15)	128 (23)	BLOQ	BLOQ	BLOQ
Linalool oxide ($\mu\text{g/L}$)	12.50	59	15.6	BLOQ	BLOQ	17.1 (14.0)	30.6 (5.5)	33.8 (7.6)	32.1 (3.4)	54.4 (20.9)	59.0 (14.2)	82.8 (15.5)
Linalool ($\mu\text{g/L}$)	13.33	71	30.3	24.6 (2.6)	24.1 (7.1)	18.4 (6.0)	11.2 (0.7)	13.0 (3.9)	9.7 (0.5)	23.6 (2.9)	104 (95)	30.0 (19.7)
β -Cyclocitral (ng/L)	16.84	67	56.6	72.2 (66.6)	147 (124)	11.0 (13.6)	294 (13)	332 (39)	345 (22)	BLOQ	BLOQ	BLOQ
β -Damascenone ($\mu\text{g/L}$)	21.15	69	3.63	3.02 (1.57)	2.98 (1.30)	2.87 (1.20)	1.10 (0.09)	1.36 (0.25)	1.10 (0.10)	0.013 (0.0002)	0.013 (0.0003)	0.013 (0.002)
α -Ionone (ng/L)	22.19	121	81.3	BLOQ	BLOQ	BLOQ	41.6 (2.3)	44.3 (4.9)	45.6 (2.3)	BLOQ	BLOQ	BLOQ

RT – retention time, m/z – mass to charge ratio, T= 0 – sample analysed at the time of bottling, AV – cellar A vertical position, AH – cellar A horizontal position, BH – cellar B horizontal position, BLOQ – below limit of quantification, ND – not detected, NQ – not quantified.

Chapter 2- Identification and structural characterization of a novel (+)-catechin-caffeic acid adduct present in wines

Abstract

A new compound with a molecular ion mass of m/z 467 in the negative ion mode was found to occur in a white wine aged 30 months in bottle. The same ion mass was also detected in a bottling study (wine model solutions with (+)-catechin) closed with a cork stopper. In this latter, fragment ions compatible with the loss of a carboxylic acid (-44 a.m.u.), a caffeic acid unit (-178 a.m.u.), and a Retro-Diels Alder (-152 a.m.u.) were observed. The present work reports the synthesis of a (+)-catechin-caffeic acid adduct resulting from the condensation reaction between caffeic acid and (+)-catechin. The structural characterization by NMR (^1H , COSY, HSQC and HMBC) showed that this adduct is formed by the linkage between carbon 8 at ring A from (+)-catechin and carbon 9 from caffeic acid. In addition, the similarity in the HPLC retention time and UV-Visible spectra of the synthesized compound with the one detected in white wine and the bottling experiments, confirms the presence of this novel (+)-catechin-derived compound in those matrices.

Keywords: wine; caffeic acid; (+)-catechin, catechin-caffeic acid adduct, NMR.

Introduction

The phenolic composition of wine is determined by the grape used as well as the winemaking processes that determine the extraction of phenolic compounds into the must and subsequent reactions (Fulcrand 2006).

In winemaking process and storage, oxidation/reduction reactions take place (OSZMIANSKI, SAPIS et al. 1985, Cheynier and Ricardo da Silva 1991), as well as chemical transformations owing to associations or complexation reactions of phenolic compounds with other compounds such as proteins, polysaccharides, and metals (Edwin 1980, Ricardo-da-Silva, Cheynier et al. 1991, Vasconcelos, Azenha et al. 1999) which leads to their polymerization (Somers 1971, Timberlake and Bridle 1976). Polymerization and/or condensation as a result from interactions between phenolic compounds influence wine color evolution as well as astringency and bitterness (Fulcrand 2006, Monagas, Gómez-Cordovés et al. 2006).

Interactions between wine components and small molecules from oak or cork have also been described (Quideau, Jourdes et al. 2003, Quideau, Jourdes et al. 2005, Glabasnia and Hofmann 2007, Jourdes, Lefeuvre et al. 2009, Azevedo, Fernandes et al. 2017, Azevedo, Jesus et al. 2021). Tannins, phenolic acids and aldehydes such as caffeic and ferulic acids or vanillin are related to participate in polymerization reactions with some wine components resulting in complex structures found in aged wines (Es-Safi, Fulcrand et al. 1999, Es-Safi, Cheynier et al. 2000, Es-Safi, Le Guernevé et al. 2000, Pissarra, Mateus et al. 2003, Lutter, Clark et al. 2007). This diversity of chemical transformations occurs in wine giving rise to more stable compounds.

The propose of this study was to perform, for the first time, the structural characterization by NMR and LC/MS of a new compound resulting from the interaction between (+)-catechin and caffeic acid.

Material and Methods

Reagents

Gallic acid, L-(+)-tartaric acid (99%), (+)-catechin ($\geq 98\%$), and caffeic acid (99%), methanol (p.a.), acetic acid (99%), acetonitrile (for HPLC), ethyl Acetate (99,5%) were obtained from Sigma-Aldrich, Spain. Ellagic acid ($\geq 96\%$, HPCE) was obtained from Fluka Biochemical. Ethanol was purchased from AGA[®] and HCl 37% from Fluka[®].

White wine sample

A commercial white wine (BORBA[®] DOC 2012) from grapes of Roupeiro, Arinto e Antão Vaz grown in Alentejo Region (Portugal) aged in bottle [pH 3.24, 13.1% alcohol (v/v), total acidity 5.2 g/l, total SO₂ 32 mg/l].

The wine was extracted by micro liquid-liquid extraction, performed according to the procedure described by (Yang, Li et al. 2017). For that, 600 μ L of wine, 600 μ L of ethyl acetate, and 300 μ L of acetonitrile were added to a microtube and vortexed for 10 s, and then the samples were centrifuged for 5 min at 5400g. Organic and aqueous phases were separated, and then the same procedure was performed for the remaining aqueous phase. Both organic fractions were combined, and the organic solvent was removed using a CentriVac Concentrator Labconco, Kansas City, MO, USA system and resuspended in 50:50 (v/v) methanol/water. Each wine extraction was performed in duplicate.

Samples were analyzed by HPLC-DAD and LC-ESI- MS.

Bottling study

The bottling experiment was performed by filling 375 mL bottles with a wine-like model solution (12% ethanol at pH 3.2 and 5 g/L tartaric acid) and added 1 g/L (+)-catechin, in triplicate, as described in (Azevedo et al, 2017).

The bottles were sealed with natural cork stopper, provided by Amorim & Irmãos, class “Superior” (44 mm length and 24 mm diameter coated with a mixture of silicone and paraffin coating) and stored at room temperature horizontally to promote the contact between the solution and the cork components. The experimental was analyzed in different periods of time by HPLC-DAD and liquid chromatography– mass spectrometry (LC–MS).

High Pressure Liquid Chromatography-Diode Array Detection (HPLC- DAD) analysis

The samples were analysed by HPLC (Thermo® Scientific Ultimate 3000) on a 150 × 4.6 mm i.d. reversed-phase C18 column (Merck®) thermostated at 25° C (Thermo® Scientific Dionex UltiMate 3000). Detection was carried out at 280 nm using a diode array detector (Thermo® Scientific Dionex UltiMate 3000). Solvents were (A) H₂O/CH₃COOH (99:1; v/v) and (B) CH₃COOH/CH₃CN/H₂O (1:20:79; v/v/v) with the gradient 80-20% A over 55 min, 20-10% A the 55 to 70 min and 10-0% A the 70 to 90 min, at a flow rate of 0.3 mL/min. The sample injection volume was 20 µL. The chromatographic column was washed with 100% B for 10 min and then stabilized with the initial conditions for another 10 min.

Liquid Chromatography-Electro Spray Ionization-Mass Spectroscopy (LC- ESI- MS) analysis

A Finnigan Surveyor series liquid chromatograph, equipped with a Thermo Finnigan (Hypersil Gold®) reversed-phase column (150 mm × 4.6 mm, 5 µm, C18) thermostated at 25° C was used. The samples were analysed using the same solvents, gradients, injection volume, and flow rate referred above for the HPLC analysis. Double-online detection was done by a photodiode spectrophotometer and mass spectrometry. The mass detector was a Finnigan LCQ DECA XP MAX (Finnigan Corp., San Jose, CA) quadrupole ion trap equipped with atmospheric pressure ionization (API) source, using electrospray ionization (ESI) interface. The vaporizer and the capillary voltages were 5 kV and 4 V, respectively. The capillary temperature was set at 325° C. Nitrogen was used as both sheath and auxiliary gas at flow rates of 80 and 30, respectively (in arbitrary units). Spectra were recorded in the negative ion mode between *m/z* 120 and 2000. The mass spectrometer was programmed to do a series of three scans: a full mass, a zoom

scan of the most intense ion in the first scan, and a MS-MS of the most intense ion using relative collision energies of 30 and 60.

Synthesis of (+)-catechin-caffeic acid adduct

(+)-catechin and caffeic acid (1 g/L) were dissolved in 12 % of wine model solution and kept react at 37°C. The effect of pH (3.5, 4.5, 5.5 and 6.5) on the yield of reaction was evaluated over time by HPLC-DAD.

The reaction was stopped by the elimination of ethanol in a rotary evaporator under vacuum and then the reaction was applied on C18 gel in a Buchner and eluted with different percentages of ethanol/water mixtures. The main compound formed was collected in 10% methanol fraction. This latter was isolated by HPLC preparative and characterized by mass spectrometry and NMR.

Preparative HPLC of (+)-catechin-caffeic acid adduct

The isolation of the new compound was performed by preparative HPLC with a fraction collector (Thermo® Scientific Ultimate 3000) using a 250 × 10 mm i.d. reversed-phase C18 column Hypersil GOLD™ (Thermo Scientific®) particle 5 µm, thermostated at 25° C (Thermo® Scientific Dionex UltiMate 3000). Detection was carried out at 280 nm using a variable wavelength (Thermo® Scientific Dionex UltiMate 3000). Solvents were (A) H₂O/CH₃COOH (99:1; v/v) and (B) CH₃COOH/CH₃CN/H₂O (1:20:79; v/v/v) with the gradient 80-20% A over 55 min, 20-10% A the 55 to 70 min and 10-0% A the 70 to 90 min, at a flow rate of 3.0 mL/min. The sample injection volume was 1500 µL. The chromatographic column was washed with 100% B for 10 minutes and then stabilized with the initial conditions for another 10 minutes. The purity of the isolated compound was confirmed by HPLC-DAD and NMR. The compounds were then frozen, freeze-dried, and stored at -20 °C until use.

Nuclear Magnetic Resonance (NMR).

The characterization of (+)-**catechin-caffeic acid** was fully established by ¹H and ¹³C NMR on a Bruker Ascend III 400 9.4 T spectrometer, narrow bore ¹H frequency: 400 MHz; *Console*: 3-channel digital AQS/2 Bruker Avance III HD; *Gradient*: GREAT Z-Gradient; Temperature control BCU-I and probes: PA DUL 400S1 C-H-D-05 Z PLUS; PA BBO 400S1 BBF-H-D-05 Z.

¹H experiments were done at 4.08 s acquisition time and 64 scans at a spectral width of approximately 8013 Hz. Measuring conditions for the ¹H/¹H and 2D spectra (COSY) recorded in the phase-sensitive mode were: 64-12328 scans a total 2K data points in *F2* and 256 data points in *F1* over a spectral width of 4000 Hz.

The assignment of the carbon resonances ($\delta^{13}\text{C}$) was done 2D experiments (HSQC and HMBC).

Results and Discussion

The presence of new phenolic compounds in white wine (30 months) was investigated. For this, two fractions (organic and aqueous) were obtained after ethyl acetate liquid-liquid extraction. The fractions were analyzed by HPLC and LC-MS in the negative ion mode and different families of known polyphenolic compounds were identified, namely Caftaric, Ferularic, Caffeic, Cotaric, *p*-Coumaric, and Gallic acids, methyl Cinnamate, methyl Coumarate, ethyl Cinnamate and others already described in the literature present in wines (Ivanović, Islamčević Razboršek et al. 2016, Gutiérrez-Escobar, Aliaño-González et al. 2021) (data not show).

In this search, it was possible to identify in trace amounts a new compound with m/z 467 in the negative ion mode with the same characteristics found in a previous bottling study. This bottling study was made to understand how compounds that migrate from cork could influence the interaction with wine components, knowing that, when bottles are stored in the horizontal position, compounds from cork are able to be extracted into wine (Azevedo, Fernandes et al. 2014, Azevedo, Fernandes et al. 2017). In this study, it was possible to find the compounds that were identified as a result of the extraction of compounds from cork and their interaction with (+)-catechin.

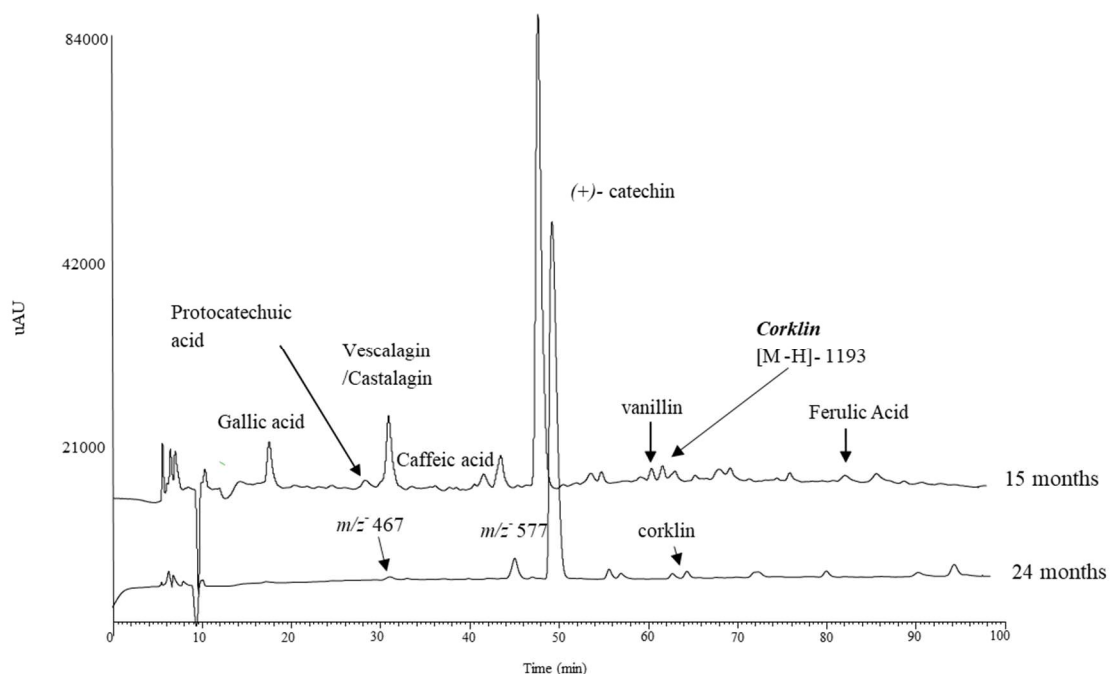


Figure 1: HPLC chromatogram at 280 nm, from bottle with (+)-catechin, after 15 months and 24 months identified compounds that migrate from cork to the wine model solutions.

It was possible to detect by LC-MS after 15 months of storage the appearance of new chromatographic peaks corresponding to gallic acid ($[M-H]^-$ m/z 169) and castalagin ($[M-$

H]⁻ *m/z* 933), vanillin ([M-H]⁻ *m/z* 151), protocatechuic aldehyde ([M-H]⁻ *m/z* 137), ferulic ([M-H]⁻ *m/z* 193), protocatechuic ([M-H]⁻ *m/z* 153), caffeic ([M-H]⁻ *m/z* 179), and Corklin ([M-H]⁻ *m/z* 1193) (Azevedo et al, 2014) (**Figure 1**).

After 24 months, it was possible to detect the appearance of a new chromatographic peak at [M-H]⁻ *m/z* 467. This new compound was observed in the experiment suggesting that it should result from the reaction between (+)-catechin and cork components. However, at the end of this period, the phenolic compounds that were extracted from cork practically did not exist in the solution, probably due to condensation and polymerization reactions that can occur (Vivas et al, 2016).

This newly formed compound was detected and identified in these reactions with an [M-H]⁻ *m/z* 467, with MS² spectrum a fragmentation pattern compatible with the loss of -44 units (carboxylic acid), -178 units (caffeic acid), -152 (Retro Diels Alder, characteristic of catechin). The molecular mass and fragmentation pattern are compatible with a catechin-caffeic acid adduct.

In order to confirm the structure and mechanism of formation of this new compound, the precursors caffeic acid (1 g/L) and (+)-catechin (1 g/L) were incubated in 12% ethanol aqueous solution at pH 3.2 at 35°C and follow daily by HPLC-DAD. After 4 months a new chromatographic peak was formed with the same retention time, molecular mass and fragmentation pattern but in low amounts. To improve the reaction yield, several reactions were performed at different pH values. The greatest increase in Catechin-Caffeic Acid formation was obtained when the pH increased from 3.2 to 6.5, and in 10 days, the maximum product formation was achieved (**Figure 2**).

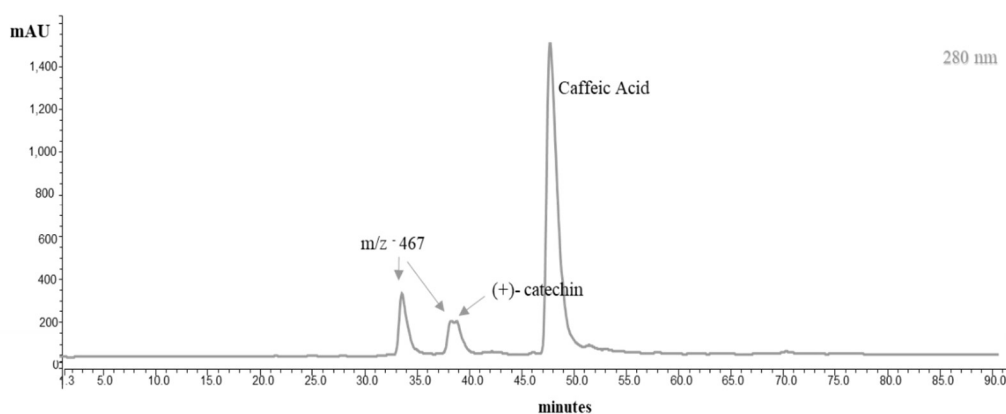


Figure 2: HPLC chromatogram, at 280 nm, at the end of 10 days of reaction between Caffeic acid and (+)- catechin 37°C and pH 6.5

More than one peak with a molecular ion mass at [M-H]⁻ *m/z* 467 was obtained since the formation of different isomers is possible as catechin could make the linkage in carbon C6 or C8. The isomer that was formed in higher amounts was isolated by preparative

HPLC and its structure fully established by mass spectroscopy, 1D and 2D-NMR experiments (**Table 1**).

Table 1. Proton chemical shifts ($\delta^1\text{H}$), coupling constants (J , Hz) and carbon chemical shifts ($\delta^{13}\text{C}$) for (+)-catechin-caffeic acid adduct in deuterated methanol.

Position	$\delta^1\text{H}$ (ppm); J (Hz)	$\delta^{13}\text{C}$ (ppm)	HSQC	HMBC
<i>Catechin moiety</i>				
2C	4.54 <i>d</i> (6.91 Hz)	81.4	C _{2C}	H _{6'B} ; H _{2'B} ; H _{4C}
3C	3.94 <i>dt</i> (7 Hz)	67.4	C _{3C}	H _{2C} ; H _{4C}
4C	α 2.83 <i>dd</i> (5.18 Hz; 16.10 Hz) β 2.58 <i>dd</i> (7.50 Hz; 16.17 Hz)	26.9	C _{4C}	H _{2C}
4a	---	99.84	---	H _{6A} ; H _{4C} ; H _{3C}
5A	---	153.7	---	H _{6A} ; H _{4C}
6A	6.08 <i>s</i>	94.7	C _{6A}	
7A	---	<i>n. a.</i>		
8A	---	106.3	---	H _{5D} ; H _{8D} ; H _{6A}
8a	---	155.2	---	H _{6A} ; H _{4C}
1'B	---	<i>n. a.</i>		
2'B	6.67 <i>d</i> (1.92 Hz)	113.6	C _{2'B}	
3'B	---	131.1	---	H _{5'B} ; H _{2'B} ; H _{2C}
4'B	---	<i>n. a.</i>	---	
5'B	6.63 <i>d</i> (8.20 Hz)	113.6	C _{5'B}	H _{2'B} ; H _{6'B}
6'B	6.58 <i>dd</i> (1.97; 8.20 Hz)	118.2	C _{6'B}	
<i>Caffeic Acid</i>				
1	---	170.7		H ₂ ; H ₃
2	6,15 <i>d</i> (15.80 Hz)	114.0	C ₂	-
3	7,58 <i>d</i> (15,98 Hz)	145.6	C ₃	
4D	---	126.01	---	H ₃ ; H _{5D} ; H _{8D} ; H ₂
5D	7.71 <i>s</i>	111.2	C _{5D}	H ₂ ; H _{8D}
6D	---	144.7	---	H ₃ ; H _{5D}
7D	---	147.6	---	H _{5D} ; H _{8D}
8D	6.64 <i>s</i>	118.6	C _{8D}	H _{5D}
9D	---	129.5	---	H ₃ ; H _{5D} ; H _{8D} ; H _{6A}

s, singlet; *d*, doublet; *dd*, double doublet; *t*, triplet; *, unresolved; *n. a.*, non assigned

The chemical shifts (^1H and ^{13}C) observed for this compound are presented in **Table 1**. NMR data revealed similar signals as those found for the caffeic acid (Papaemmanouil et al, 2020) and catechin (Stark, Wollmann et al. 2010, Azevedo, Fernandes et al. 2017) previously described. These spectra showed an aromatic singlet at 6.08 ppm (H_{6A}) and other three aromatic protons resonating at 6.63, 6.67 and 6.58 ppm (H-2'B, H-5'B, and H-6'B, respectively). In addition, four aliphatic protons were observed (H-4C α and H-4C β ,

H-3C, H-2C) coupling with each other and confirming the presence of a catechin unit (Stark et al, 2010).

In the case of caffeic acid, two characteristics doublets coupling each other at 6.15 and 7.58 ppm corresponding to H-2 and H-3 and two singlet signals corresponding to H-5D (7.71ppm) and H-8D (6.64 ppm) (Papaemmanouil et al, 2020).

In fact, the bond seems to occur at C9 of the D ring (caffeic acid) because if the linkage occurred at C5 or C8, C9 have a proton and for that reason two doublets in the NMR proton should have appeared.

In the NOESY spectra, it is possible to observe (data not shown) a correlation between the H_{8D} proton from caffeic acid with H_{2B} from (+)-catechin (**Figure 3**) showing the proximity of both protons in space, which corroborates with the linkage of the adduct being formed in the C8 position of ring A from (+)-catechin and not in C6 position.

All correlations found in HSQC and HMBC are described in **Table 1** and are in agreement with the structure proposed (**Figure 3**). HSQC spectra allowed the identification of carbons directly linked to protons: C_{2C}, C_{3C}, C_{4C}, C_{6A}, C_{2'B}, C_{5'B}, C_{6'B}, C₂, C₃, C_{5D}, C_{8D}. For HMBC correlations, that described hydrogen bonds related to neighboring carbons, for catechin moiety: the 2C correlates with H_{6'B}, H_{2'B}, and H_{4C}; the 3C correlates with H_{2C}, and, H_{4C}; 4C with the H_{2C}; 4a shows a correlation between H_{6A}, H_{4C}, and, H_{3C}; 5A correlates with H_{6A}, and, H_{4C}; 8A with H_{5D}, H_{8D}, and, H_{6A}; the 8a show a correlation between H_{6A} and, H_{4C}; in case of 3'B with H_{5'B}, H_{2'B}, and, H_{2C}. The 5'B detect H_{2'B}, and, H_{6'B}. Pass to analysis of caffeic acid structure the Carbon 1 correlates with protons H₂ and, H₃; the 4D show a correlation with H₃, H_{5D}, H_{8D}, and, H₂; the 5D with H₂, and, H_{8D}; 6D correlates with H₃, and, H_{5D}; 7D with the H_{5D}, and, H_{8D}; 8D with H_{5D}, and finally the 9D show correlation with H₃, H_{5D}, H_{8D} and, H_{6A}.

Considering all the data obtained from the LC/MS and one- and two-dimensional NMR experiments, the chemical structure of **compound m/z 467** could be unequivocally identified as presented in **Figure 3**, with a single bond between C8 from catechin and C9 of caffeic acid.

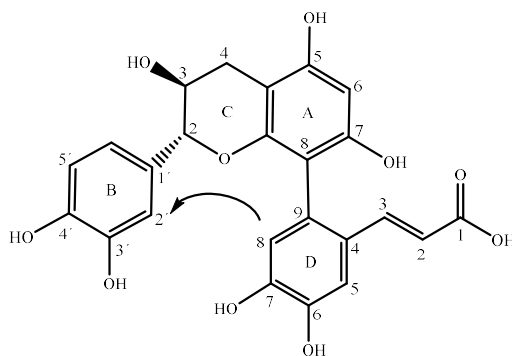


Figure 3. Structure of **compound m/z 467**. Arrow indicates the correlation in the NOESY spectrum.

The mechanism proposed for the formation of **compound *m/z* 467** is presented in **Figure 4**.

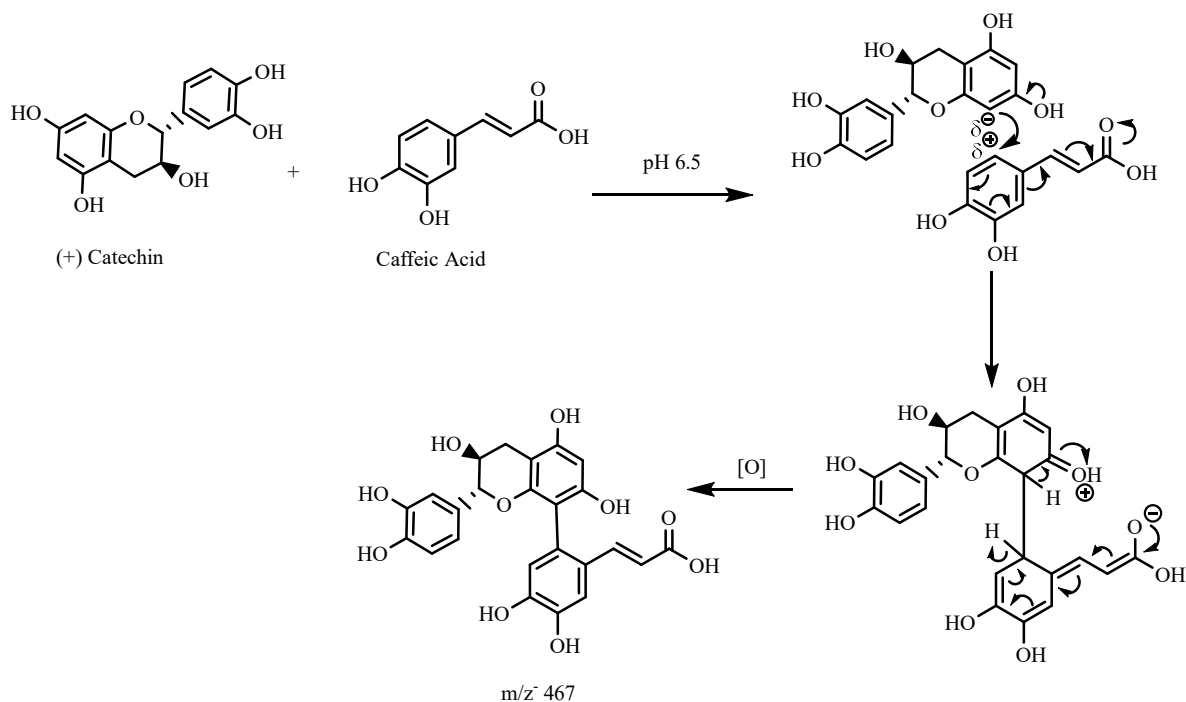


Figure 4: Mechanism proposed to the formation of **new compound**

The proposed mechanism results from the nucleophilic attack of both C6/C8 from A ring of (+)-catechin to the electropositive C9 of caffeic acid arose from the electron-withdrawing carboxylic group. The final C-C bond formation consists in an oxidation step resulting in the new catechin-caffeic acid adduct.

Conclusion

A new catechin-caffeic acid adduct was successfully identified. The full structural characterization of this new compound and studies performed in model solutions revealed that it results from the interaction between caffeic acid and (+)-catechin. Caffeic acid is herein identified in bottling experiment as a compound that migrate from cork stopper but in the case of wines it is known that caffeic acid is a compound that already exists in grapes and that is why this new compound may have even greater importance. Moreover, knowing that wine is a complex matrix other chemical way of formation may exist and new ways still need to be discovered.

References

- Azevedo, J., Fernandes, A., Oliveira, J., Brás, N. F., Reis, S., Lopes, P., . . . de Freitas, V. (2017). Reactivity of Cork Extracts with (+)-Catechin and Malvidin-3-O-glucoside in Wine Model Solutions: Identification of a New Family of Ellagitannin-Derived Compounds (Corklins). *Journal of Agriculture and Food Chemistry*, 65(39), 8714-8726. <https://doi.org/https://doi.org/10.1021/acs.jafc.7b02845>.
- Azevedo, J., Fernandes, I., Lopes, P., Roseira, I., Cabral, M., Mateus, N., & Freitas, V. (2014). Migration of phenolic compounds from different cork stoppers to wine model solutions: antioxidant and biological relevance. *European Food Research and Technology*, 239(6), 951-960. <https://doi.org/https://doi.org/10.1007/s00217-014-2292-y>.
- Azevedo, J., Jesus, M., Brandão, E., Soares, S., Oliveira, J., Lopes, P., . . . de Freitas, V. (2021). Interaction between salivary proteins and cork phenolic compounds able to migrate to wine model solutions. *Food Chemistry*, 130607. <https://doi.org/https://doi.org/10.1016/j.foodchem.2021.130607>.
- Azevedo, J., Oliveira, J., Cruz, L., Teixeira, N., Brás, N. F., De Freitas, V., & Mateus, N. (2014). Antioxidant Features of Red Wine Pyranoanthocyanins: Experimental and Theoretical Approaches. *Journal of Agricultural and Food Chemistry*, 62(29), 7002-7009. <https://doi.org/10.1021/jf404735j>.
- Cheyrier, V., & Ricardo da Silva, J. M. (1991). Oxidation of grape procyanidins in model solutions containing trans-caffeoyltartaric acid and polyphenol oxidase. *Journal of Agricultural and Food Chemistry*, 39(6), 1047-1049.
- Edwin, H. (1980). In vino veritas: Oligomeric procyanidins and the ageing of red wines. *Phytochemistry*, 19(12), 2577-2582.
- Es-Safi, N.-E., Cheyrier, V., & Moutounet, M. (2000). Study of the Reactions between (+)-Catechin and Furfural Derivatives in the Presence or Absence of Anthocyanins and Their Implication in Food Color Change. *Journal of Agricultural and Food Chemistry*, 48(12), 5946-5954. <https://doi.org/https://doi.org/10.1021/jf000394d>.
- Es-Safi, N.-E., Fulcrand, H., Cheyrier, V., & Moutounet, M. (1999). Studies on the Acetaldehyde-Induced Condensation of (-)-Epicatechin and Malvidin 3-O-Glucoside in a Model Solution System. *Journal of Agricultural and Food Chemistry*, 47(5), 2096-2102. <https://doi.org/https://doi.org/10.1021/jf9806309>.
- Es-Safi, N.-E., Le Guernevé, C., Cheyrier, V., & Moutounet, M. (2000). New Phenolic Compounds Formed by Evolution of (+)-Catechin and Glyoxylic Acid in Hydroalcoholic Solution and Their Implication in Color Changes of Grape-Derived Foods. *Journal of Agricultural and Food Chemistry*, 48(9), 4233-4240. <https://doi.org/10.1021/jf000283e>.
- Fulcrand, H. (2006). Structure and properties of wine pigments and tannins. *Am. J. Enol.*
- Glabasnia, A., & Hofmann, T. (2007). Identification and sensory evaluation of dehydro- and deoxyellagitannins formed upon toasting of oak wood (*Quercus alba* L.). *J Agric Food Chem*, 55(10), 4109-4118. <https://doi.org/10.1021/jf070151m>.
- Gutiérrez-Escobar, R., Aliaño-González, M. J., & Cantos-Villar, E. (2021). Wine Polyphenol Content and Its Influence on Wine Quality and Properties: A Review. *Molecules*, 26(3). <https://doi.org/10.3390/molecules26030718>.
- Ivanović, M., Islamčević Razboršek, M., & Kolar, M. (2016). Simultaneous GC-MS Determination of Free and Bound Phenolic Acids in Slovenian Red Wines and Chemometric Characterization. *Acta Chim Slov*, 63(3), 661-669. <https://doi.org/10.17344/acsi.2016.2534>.
- Jourdes, M., Lefeuvre, D., & Quideau, S. (2009). C-Glycosidic Ellagitannins and Their Influence on Wine Chemistry. In (pp. 320-365).
- Lutter, M., Clark, A. C., Prenzler, P. D., & Scollary, G. R. (2007). Oxidation of caffeic acid in a wine-like medium: Production of dihydroxybenzaldehyde and its subsequent reactions with (+)-catechin. *Food Chemistry*, 105(3), 968-975. <https://doi.org/https://doi.org/10.1016/j.foodchem.2007.04.044>.
- Monagas, M., Gómez-Cordovés, C., & Bartolomé, B. (2006). Evolution of the phenolic content of red wines from *Vitis vinifera* L. during ageing in bottle. *Food Chemistry*, 95(3), 405-412.
- OSZMIANSKI, J., SAPIS, J. C., & MACHEIX, J. J. (1985). Changes in grape seed phenols as affected by enzymic and chemical oxidation in vitro. *Journal of Food Science*, 50(5), 1505-1506.
- Papaemmanouil, C., Chatziathanasiadou, M., Chatzigiannis, C., Chontzopoulou, E., Mavromoustakos, T., Grdadolnik, S., & Tzakos, A. (2020). Unveiling the interaction profile of rosmarinic acid and its bioactive substructures with serum albumin. *Journal of Enzyme Inhibition and Medicinal Chemistry*, 35, 786-804. <https://doi.org/10.1080/14756366.2020.1740923>.
- Pissarra, J., Mateus, N., Rivas-Gonzalo, J., Santos Buelga, C., & De Freitas, V. (2003). Reaction Between Malvidin 3-Glucoside and (+)-Catechin in Model Solutions Containing Different Aldehydes. *Journal of Food Science*, 68(2), 476-481. <https://doi.org/https://doi.org/10.1111/j.1365-2621.2003.tb05697.x>.
- Quideau, S., Jourdes, M., Lefeuvre, D., Montaudon, D., Saucier, C., Glories, Y., . . . Pourquier, P. (2005). The Chemistry of Wine Polyphenolic C-Glycosidic Ellagitannins Targeting Human Topoisomerase II. *Chemical European Journal* 11(22), 6503-6513. <https://doi.org/https://doi.org/10.1002/chem.200500428>.

- Quideau, S., Jourdes, M., Saucier, C., Glories, Y., Pardon, P., & Baudry, C. (2003). DNA Topoisomerase Inhibitor Acetaminophen A and Other Flavano-Ellagitannins in Red Wine. *Angew Chemical International Education*, 42(48), 6012-6014. <https://doi.org/https://doi.org/10.1002/anie.200352089>.
- Ricardo-da-Silva, J. M., Cheynier, V., Souquet, J. M., Moutounet, M., Cabanis, J. C., & Bourzeix, M. (1991). Interaction of grape seed procyanidins with various proteins in relation to wine fining. *Journal of the Science of Food and Agriculture*, 57(1), 111-125.
- Somers, T. C. (1971). The polymeric nature of wine pigments. *Phytochemistry*, 10(9), 2175-2186. [https://doi.org/https://doi.org/10.1016/S0031-9422\(00\)97215-7](https://doi.org/https://doi.org/10.1016/S0031-9422(00)97215-7).
- Stark, T., Wollmann, N., Wenker, K., Lösch, S., Glabasnia, A., & Hofmann, T. (2010). Matrix-Calibrated LC-MS/MS Quantitation and Sensory Evaluation of Oak Ellagitannins and Their Transformation Products in Red Wines. *Journal of Agricultural and Food Chemistry*, 58(10), 6360-6369. <https://doi.org/https://doi.org/10.1021/jf100884y>.
- Timberlake, C. F., & Bridle, P. (1976). Interactions Between Anthocyanins, Phenolic Compounds, and Acetaldehyde and Their Significance in Red Wines. *American Journal of Enology and Viticulture*, 27(3), 97-105.
- Vasconcelos, M. T., Azenha, M., & de Freitas, V. (1999). Role of polyphenols in copper complexation in red wines. *Journal of Agricultural and Food Chemistry*, 47(7), 2791-2796.
- Vivas, N., Nonier, M. F. B., Absalon, C., Abad, V. L., Jamet, F., Gaulejac, N. V. D., . . . Fouquet, E. (2016). Formation of Flavanol-aldehyde Adducts in Barrel-aged White Wine Possible Contribution of These Products to Colour. *South African Journal of Enology and Viticulture*, 29, 98-108.
- Yang, P., Li, H., Wang, H., Han, F., Jing, S., Yuan, C., . . . Xu, Z. (2017). Dispersive Liquid-Liquid Microextraction Method for HPLC Determination of Phenolic Compounds in Wine. *Food analytical methods*, 10(7), 2383-2397. <https://doi.org/https://doi.org/10.1007/s12161-016-0781-2>.

Chapter 3- Polyphenolic Characterization of Nebbiolo Red Wines and Their Interaction with Salivary Proteins

Abstract

The present study correlates the polyphenolic composition of two different Nebbiolo red wines from the 2015 vintage (M and P), with the salivary proteins' precipitation process. The work centered on the polyphenolic characterization of Nebbiolo wines and their interaction with different families of salivary proteins. Overall, both wines were found to be very reactive with human saliva which was supposed to contribute to their astringent character. The comparison of both wines showed that the M wine presented higher values of total phenolics, total proanthocyanidins, and tannin specific activity. Moreover, this wine showed a higher interaction with salivary proteins. Altogether, the chemical characterization and reactivity toward human saliva could contribute to the wine astringency.

Keywords: wine; tannins; anthocyanins; proline-rich proteins

Introduction

Polyphenols are the main compounds present in grapes and wines being responsible for some of their organoleptic properties such as colour, bitterness and astringency (Linskens and Jackson 1988, Macheix and Fleuriet 1993, Soares, Brandao et al. 2017). Within these compounds, phenolic acids and derivatives, anthocyanins, flavan-3-ols (catechin monomers and proanthocyanidins) are the main compounds present in red grapes (Roggero, Coen et al. 1986).

The major contributors of red color in wines are anthocyanins or their further derivatives that are extracted or formed during the vinification process (Mazza and Francis 1995, Busse-Valverde, Gomez-Plaza et al. 2011). It is known that the reaction between anthocyanins and proanthocyanidins occurs mainly during conservation and aging. The pigments formed during this period are more stable than their anthocyanin precursors and have different sensory properties (Mateus, Carvalho et al. 2003, Mateus, Silva et al. 2003, Oliveira, da Silva et al. 2013, García-Estévez, Cruz et al. 2017).

Red wines also contain high amounts of tannins (condensed tannins also known as proanthocyanidins) and their content in wines arises mainly from their extraction from

grapes during the winemaking process. On the other hand, tannins such as hydrolysable tannins can also be extracted from oak wood during wine ageing in oak barrels (Puech, Mertz et al. 1999, Glabasnia and Hofmann 2006) or from the use of oenological additives. Moreover, due to their ability to bind proteins (Glabasnia and Hofmann 2006), tannins can directly affect the wine astringency (Glabasnia and Hofmann 2006, Stark, Wollmann et al. 2010, Chira and Teissedre 2015, Soares, Brandao et al. 2017). Astringency is defined as dry, rough, pucker, or grippy and is a tactile sensation that usually persists in the mouth and its intensity may increase depending on the saliva flow rate (Ishikawa and Noble 1995, Kallithraka, Bakker et al. 1997, Kallithraka, Bakker et al. 2001, Soares, Brandao et al. 2017). The constitutive characteristics of tannins and their concentration influence red wine astringency perception. A high mean degree of polymerization and/or a large amount of galloyl groups in the tannin structure, and a high tannin concentration induce a higher intensity of astringency and dryness perception (Vidal, Francis et al. 2003), whereas pigmented tannins seem to reduce it (McRae, Schulkin et al. 2013, Trouillas, Sancho-García et al. 2016, Watrelot, Heymann et al. 2020). It has been reported that the astringency descriptors induced by ellagitannins seem to be different from the ones yielded by condensed tannins (Soares, Vitorino et al. 2011), being described as a rather mellow (Soares, Kohl et al. 2013, Chira and Teissedre 2015) and smooth astringency with a velvety mouth-coating sensation (Stark, Wollmann et al. 2010), with an impact in the roundness and amplitude of red wines (Michel, Jourdes et al. 2011, Michel, Albertin et al. 2016, Soares, Brandao et al. 2017). One of the key mechanisms for astringency perception is the interaction and precipitation of salivary proteins, in particular the proline-rich proteins (PRPs). This family of salivary proteins is characterized by a high content in proline residues and are classically divided into basic PRPs (bPRPs), acidic PRPs (aPRPs) and glycosylated PRPs (gPRPs). Although bPRPs are usually linked to astringency perception, some other studies have shown that aPRPs are significantly precipitated by tannins (Soares, Vitorino et al. 2011). In addition to aPRPs, also mucins, statherin and P-B peptide have been shown to have a significant interaction with tannins.

The present study aims to deepen the polyphenolic composition of two astringent Nebbiolo red wines (P and M) from the 2015 vintage and understand the complexation process with salivary proteins. It is intended to compare these wines in terms of some physical-chemical parameters related to the astringency in order to differentiate them (tannins concentration and salivary protein complexation).

Materials and Methods

Reagents

L-(+)-tartaric acid (99%), Ethyl Acetate, Methanol, Acetonitrile, Acetic Acid, Folin-Ciocalteu Reagent and Sodium Bisulfite were obtained from Sigma-Aldrich, Spain. Ethanol was purchased from AGA® and HCl 37% from Fluka®.

Wine samples

The commercial wine coded as M was produced during the 2015 vintage from 100% Nebbiolo grapes sourced from La Morra and Castiglione Falletto, Barolo, Piedmont (Italy). This wine underwent skins maceration in stainless steel tanks at a controlled temperature for 12 days before pressing and alcoholic and malolactic fermentation for around 20 days.

The wine was aged in small barrels of oak for 24 months. After decanting, the wine was bottled without fining or filtration. The commercial wine coded as P was produced during the 2015 vintage from 100% Nebbiolo grapes sourced predominantly from the Comune di Serralunga d'Alba, Piedmont (Italy). For vinification, the pressed grapes ferment without yeast inoculation and without sulfur for about a month. The wines were left to age during twenty-four months in barrels of 40 hectoliters. The bottles of each wine were sent directly from producers and open in 2019 (4 years old). Both wines were considered very astringent by an expert panel of wine tasters and it was not possible to distinguish both in terms of that sensation.

Total Phenolic Compounds

Total phenolic compounds were determined by the Folin-Ciocalteu assay according to the method described by (Arnous et al, 2001) and adapted as described by (Fernandes et al, 2012). In a microtube, 610 μL of distilled water, 15 μL of wine and 75 μL of Folin–Ciocalteu reagent were mixed. After 30 s, 300 μL of aqueous 20% Na_2CO_3 and 300 μL of distilled water were added, and the mixture was mixed (30 s) and allowed to stand at room temperature in the dark for 30 min. The absorbance at 750 nm was determined, and the total phenolic compounds concentration was calculated accordingly to the calibration curve: $\Delta\text{Abs (750 nm)} = 0.9638 \times \text{concentration (mM)} - 0.0001$, $R^2 = 0.9999$, using gallic acid as standard.

Total Proanthocyanidins

Total proanthocyanidins (condensed tannins) was determined based on Bate-Smith reaction, slightly adapted as describe previously (Gonçalves et al, 2011). This method consisted on the measurements of sample absorbance (at 520 nm) of anthocyanidins resulting from the acidic decomposition of condensed tannins, at 100 °C for 30 min in strongly acidic conditions (Ribéreau-Gayon et al, 1966).

Unknown concentrations of condensed tannins in wines were determined using a calibration curve ($R^2 = 0.9911$) obtained using different concentrations ranging from (0.264–5.92 mg/mL) of a procyanidin fraction composed by dimeric and trimeric procyanidins purified from grape seeds (Gonçalves et al, 2011). Each sample was prepared in duplicate and injected in triplicate and results were expressed as mean \pm standard deviation and presented as $\text{g}\cdot\text{L}^{-1}$ equivalent of total procyanidins.

Identification and Quantification of Phenolic compounds by HPLC-DAD and LC-DAD/ESI-MS analysis

For the phenolic compounds identification and quantification, red wine samples were extracted by micro liquid-liquid extraction performed according to the procedure described by (Yang et al, 2017). For that, 600 μL of wine, 600 μL of ethyl acetate and 300 μL of acetonitrile were added to a microtube and vortexed during 10 s and then the samples were centrifuged during 5 min at 5400 g. Organic and aqueous phases were separated and then the same procedure was performed to the remaining aqueous phase. Both organic fractions were combined, and the organic solvent was removed using a CentriVac Concentrator Labconco system and resuspended in 50/50 (v/v) methanol/water. Each wine extractions were performed in duplicate.

Samples were analyzed by HPLC-DAD follow the method described in (Azevedo et al, 2017) using a HPLC (Merck® Hitachi Elite Lachrom) on a 150 \times 4.6 mm i.d. reversed-phase C18 column (Merck®) thermostated at 25° C (Merck® Hitachi Column Oven L-2300). Detection was carried out at 280 nm using a diode array detector (Merck® Hitachi Diode Array Detector L-2455). Solvents were (A) $\text{H}_2\text{O}/\text{CH}_3\text{COOH}$ (99:1) and (B) $\text{CH}_3\text{COOH}/\text{CH}_3\text{CN}/\text{H}_2\text{O}$ (1:20:79) with the gradient 80-20% A over 55 min, 20-10% A from 55 to 70 min and 10-0% A from 70 to 90 min, at a flow rate of 0.3 mL/min. The sample injection volume was 20 μL . The chromatographic column was washed with 100% B for 10 min and then stabilized with the initial conditions for another 10 min.

The concentration of phenolic compounds in each wine was obtained by applying the calibration curve: $[\text{Phenolic Compound}]_{\text{mM}} = (\text{peak area} + 0.0831) / 329.09$, $R^2 = 0.9999$. This curve was obtained using commercial gallic acid in the range 0.005- 1 mM, and results are expressed in Gallic Acid equivalents. The analysis was made in triplicates.

The identification of the phenolic compounds in all samples was performed by LC-DAD/ESI-MS using the same solvents, gradients, injection volume, and flow rate referred above for the identification and quantification of phenolic compounds by HPLC analysis. Double-online detection was done by a photodiode spectrophotometer and mass spectrometry as described in Azevedo et al. 2017 (Azevedo et al, 2017).

Color Index (RCI and CIELab)

The color characteristics, were evaluated by the red color index (RCI) at A520 nm and CIELab color coordinates (L*, C*, H*), where L* is the lightness, C* the chromaticity and H* hue, measured by direct absorption and determined by Color Win-MSCV® Coordinates software. For that with a 2 mm optical path read absorbance at 450, 520, 570 and 630 nm (Guerreiro et al, 2017).

Anthocyanins and anthocyanin-derived pigments quantification by HPLC-DAD

Anthocyanins and anthocyanin-derived pigments were quantified by HPLC-DAD using the same HPLC equipment described previously for phenolic compounds quantification. In this case a 250×4.6 mm i.d. reversed-phase C18 column (Merck®) was used and the solvents were: (A) 7.5% (v/v) formic acid in water and (B) 7.5% (v/v) formic acid in acetonitrile. The gradient consisted in 97%-70% A during 31 min, the column was washed with 100% solvent B for 10 minutes and equilibrated with the initial conditions for another 10 minutes. The flow rate was 1 mL.min⁻¹ and detection were carried out at 520 and 511 nm. For the quantification of anthocyanins, a calibration curve using different concentrations of malvidin-3-O-glucoside (16.5- 1059.9 mg/L) was used.

$$[\text{Malvidin-3-O-glucoside}]_{\text{mM}} = (\text{peak area} + 874484) / 18687 \quad R^2 = 0.9998$$

For the quantification of anthocyanin-derived pigments, A-type Vitisin (Carboxypyranomalvidin-3-O-glucoside) was used as a standard (2.5- 25 mg/L).

$$[\text{Carboxypyranomalvidin-3-O-glucoside}]_{\text{mM}} = (\text{peak area} + 19302) / 47027 \quad R^2 = 0.996$$

Tannin Specific Activity – TSA

Tannin Specific Activity determines the phenolic compounds capacity to precipitate a protein (bovine serum albumin-BSA) measured by nephelometry as described elsewhere (De Freitas and Mateus 2001). Red wines were diluted 1:50 with a wine model solution (12% ethanol, 5.0 g L⁻¹ tartaric acid, pH 3.20) and filtered (0.45 μm). 4.0 mL of this solution were transferred to a turbidimetry tube and the nephelometry values were recorded in Turbidimeter HACH 2100 N adapted for cells of 100·12 mm. Then, 150 μL of BSA (0.8 mg/mL) was added to each tube and vortexed. The tubes were kept in the dark during 30 min, and then, the maximum turbidity was determined. The TSA was expressed in turbidity units NTU/mL of wine and is determined by the following expression, where 0.08 corresponds to the dilution factor of wine: Turbidity (NTU/mL of wine) = (Turbidity_{after BSA} – Turbidity_{t₀})/0.08

Interaction of wine with human saliva

Human saliva was collected and treated as reported elsewhere (Soares et al, 2011). Briefly, fifteen healthy subjects were instructed to avoid food or beverages intake at least 1 h prior to saliva isolation. Saliva was collected at 2 p.m., pooled together and treated

with TFA (final concentration 0.1%) to precipitate high molecular weight proteins (e.g. mucin and amylase) and to inhibit proteases. After mixing, saliva was centrifuged (8000g, 5 min) and the supernatant, referred as acidic saliva (AS), was recovered. The total protein concentration was assessed by the Bradford assay using BSA as standard and was determined to be 584 µg/mL. This AS was then used for the interactions with wines samples. The interaction with P and M wines was made at a fixed concentration of saliva (438 µg/mL) obtained by mixing AS (90.0 µL) with wine model solution (WMS) and/or wine (30.0 µL). The wines were added at different ratios (saliva: wine, v/v: 10:0.7, 10:2 and 10:3) and the necessary volume of WMS was added to attain a final volume of 30.0 µL. The solutions were mixed and reacted for 5 min at room temperature. After, the solutions were centrifuged (8000g, 5 min) and the supernatant was analysed. Six families of SP were monitored using HPLC-UV: bPRPs, gPRPs, aPRPs, cystatins, statherin and P-B peptide. As statherin and P-B peptide were co-eluted, they were analyzed together. One hundred microliters of each supernatant were analysed on a HPLC Lachrom system (Merck Hitachi, L-7100) equipped with Kinesis C8 column (150×2.1 mm, 5 µm particle diameter) and a UV-vis detector (L-7420). The HPLC conditions were: eluent (A) 0.2% aqueous TFA, eluent (B) 0.2% TFA in acetonitrile/water 80/20 (v/v); linear gradient was 10 to 45% of B in 40 min, followed by a washing step for 10 min with 100% eluent B and stabilization on the initial conditions; flow rate of 0.50 mL/min; detection at 214 nm.

Statistical Analysis

All determinations were conducted in triplicate. Values are expressed as the arithmetic means ± standard deviation. Statistical significance of the difference between the two wines was evaluated by t-test with Welch's correction using the GraphPad Prism. Differences were considered significant when $p < 0.05$.

Results



The main goal of this work was to correlate the phenolic compounds composition of two Nebbiolo red wines from the 2015 vintage with the salivary proteins' complexation process. For that, the phenolic compositions of M and P wines were firstly determined, concerning the total phenolic compounds, the total condensed tannins and the concentration of anthocyanins and anthocyanin-derived pigments. This phenolic composition was then, correlated with the reported wine astringency, as will be further discussed.

Phenolic composition of red Nebbiolo wines

The most abundant phenolics compounds that are described to be present in wines are flavanols, anthocyanins and phenolic acids (Lima, Silani et al. , Van Leeuw, Kevers et al. 2014, Granato, Koot et al. 2015). Anthocyanins are responsible for the color of red wines, especially young red wines and during ageing the concentration of these pigments decreases yielding to the formation of anthocyanin-derivatives and to a color change from red-violet to more red-orange hues.

The chromatic features of M and P wines were evaluated using the CIELab system that uses Cartesian coordinates to calculate color in a color space, determining the lightness (L^*) and the chromaticity (C^*) composed by two parameters: a^* - green for red and b^* - blue for yellow and H° represents the hue. **Table 1** shows the CIELab parameters obtained for both wines and it can be observed that M wine presents lower luminosity (L^*) and higher chromaticity (C^*) values when compared to P wines. Both wines present orange hues which is associated with the age of wines (4-years old).

Table 1. Red wine Color Index absorbance measurement at 520 nm and CIELab parameters obtained by MSCV coordinates program (2 mm glass path cell). Anthocyanins and Carboxypyrananthocyanins concentration obtained by HPLC and express in mg/L.

Wine	M	P
520 nm	0.581 ± 0.006	0.373 ± 0.001
CieLAB color		
L^*	69.04 ± 0.02	78.950 ± 0.001
a^*	23.37 ± 0.03	14.89 ± 0.05
b^*	30.20 ± 0.06	28.4 ± 0.1
C^*	38.21 ± 0.03	32.09 ± 0.09
H°	52.18 ± 0.09	62.4 ± 0.1
[Anthocyanins] mg/L	114 ± 3	151 ± 4
[Carboxypyrananthocyanins] mg/L	5 ± 1	1.4 ± 0.3

Moreover, anthocyanins concentration of M and P wines were determined by HPLC-DAD. As it can be observed in **Table 1**, the concentration of anthocyanins in M wines was significantly lower than in P wines. This result is not correlated with the Absorbance at 520 nm (**Table 1**) observed for both wines, as M wines present a much higher value (0.581) when compared to P wines (0.373). This behavior can be related to the presence of more complex anthocyanin structures in M wines not detected by HPLC. It is well

known that during wine ageing process, the concentration of anthocyanins decreases yielding to the formation of anthocyanin-derived pigments such as A- and B-type vitisins and tannins-anthocyanin condensation products as already reported in the literature (Mateus, Carvalho et al. 2003, Mateus, Silva et al. 2003, Oliveira, da Silva et al. 2013) and that are responsible for wine color stabilization. In fact, **Table 1** shows that along with the lowest concentration of anthocyanins observed in M wines, it is possible to detect a greater amount of A-type vitisins probably resulting from a higher colour evolution comparing to P wine. Moreover, the higher amounts of polyphenols and particularly in condensed tannins present by M wines (**Figure 1**) that can act as copigment and yield to anthocyanins color stabilization by copigmentation may also explain the higher absorbance at 520 nm. On the other hand, M wine is richer in phenolic acids and derivatives and namely in cinnamic acid derivatives that are described to be good copigments toward anthocyanins (**Table 2**) (Trouillas et al, 2016).

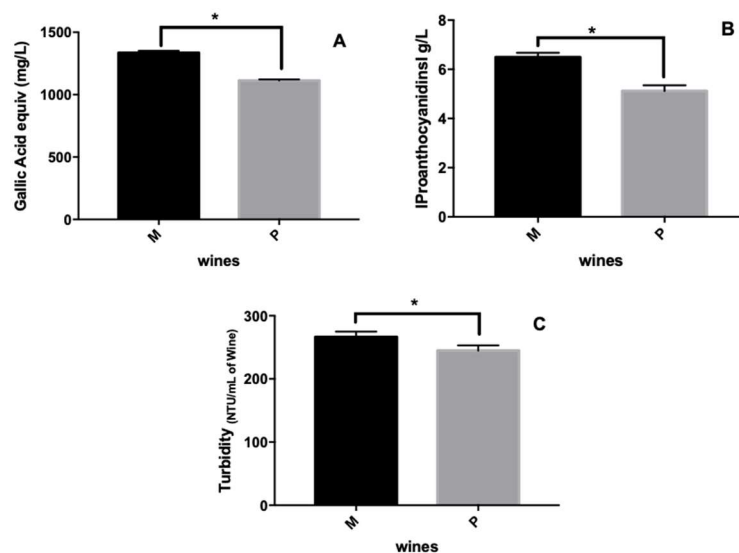


Figure 1. Graphical representation of the quantification of A, Total phenolic compounds (determined by the Folin-Ciocalteu method); B, Total Proanthocyanidins (determined using the Bath-Smith method); C, Tannin Specific Activity for two wines samples. * represent statistically different ($p < 0.0001$).

Regarding the ability of wines to precipitate BSA (**Figure 1C**), although both wines yielded BSA precipitation, M wine shows a higher ability to precipitate BSA. Indeed, the higher level of polyphenols such as anthocyanins, phenolic acid and particularly condensed tannins could explain this behavior. This higher TSA suggests that M wine could present a more astringent character.

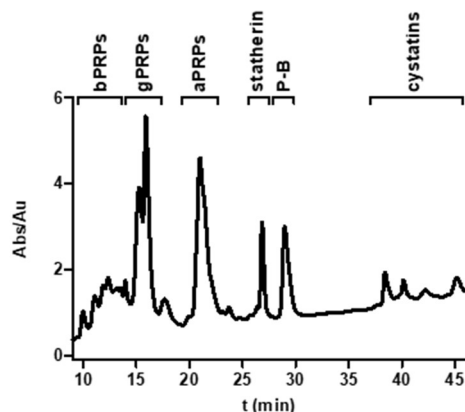
Table 2. HPLC quantification of phenolic acid and derivatives presents in P and M wines. The results were expressed as mean \pm standard deviation and were the result of two extractions of each wine bottle and triplicate injections. The m/z are in the negative ion mode.

Compound / [M - H] ⁻ (m/z)	P wines (μM)	M wines (μM)
Gallic Acid (169)	3459 \pm 186	3059 \pm 46
Methyl Coumarate (177)	146 \pm 32	71 \pm 5
Methyl Cinnamate (161)	129 \pm 28	159 \pm 7
Protocatechuic Acid (153)	141 \pm 15	188 \pm 16
Ethyl Ferulate (221)	75 \pm 3	110 \pm 2
Caftaric acid (311)	638 \pm 25	983 \pm 67
Ethyl Cinnamate (175)	242 \pm 53	335 \pm 9
Coutaric Acid (isomer) (295)	928 \pm 55	716 \pm 46
Coutaric Acid (isomer) (295)	826 \pm 149	130 \pm 40
Fertaric Acid (325)	519 \pm 73	895 \pm 50
Caffeic Acid (179)	405 \pm 60	611 \pm 68
Coumaric Acid (163)	294 \pm 31	528 \pm 21
Syringic Acid (197)	327 \pm 75	278 \pm 29
Ethyl Cinnamate (175)	525 \pm 44	913 \pm 64
Ellagic Acid (301)	173 \pm 4	330 \pm 32
Total Phenolic acids	4100 \pm 280	3855 \pm 123
Total Cinnamic acids	3610 \pm 393	3863 \pm 292

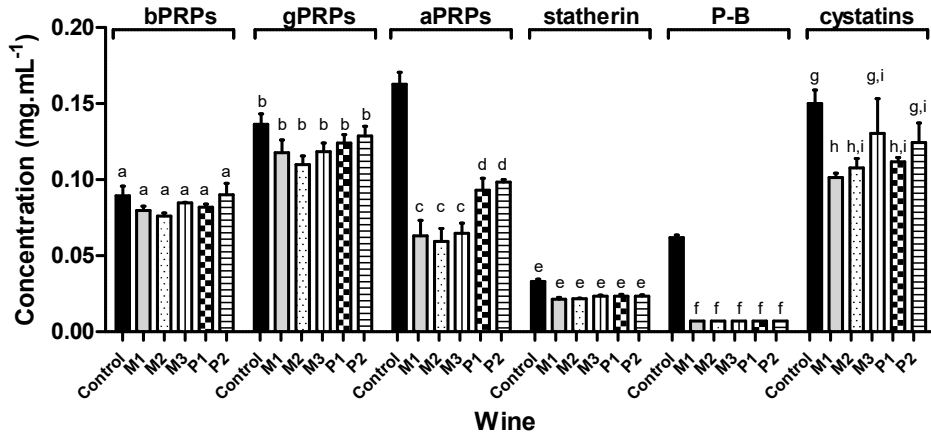
Interaction of wines with salivary proteins

To better understand the chemical differences of M and P wines and to differentiate them in terms of their phenolic composition and respective ability to interact with salivary proteins, studies involving interactions between M and P wines with human saliva were performed. Different saliva: wine ratios (10:0.7, 10:2 and 10:3) were mixed and left to interact for 5 min. Then, a centrifugation was carried out to remove the eventually formed insoluble complexes and the soluble salivary proteins that remained in the supernatant were analyzed by HPLC-UV (**Figure 2**).

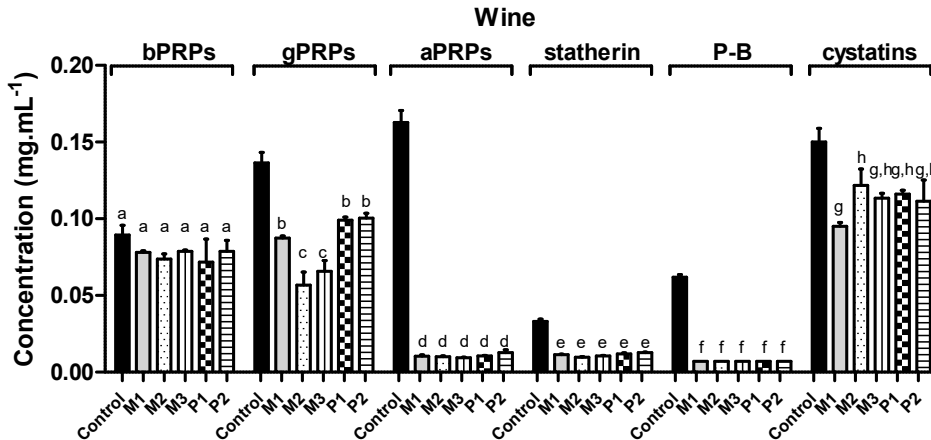
A.



B.
a)



b)



c)

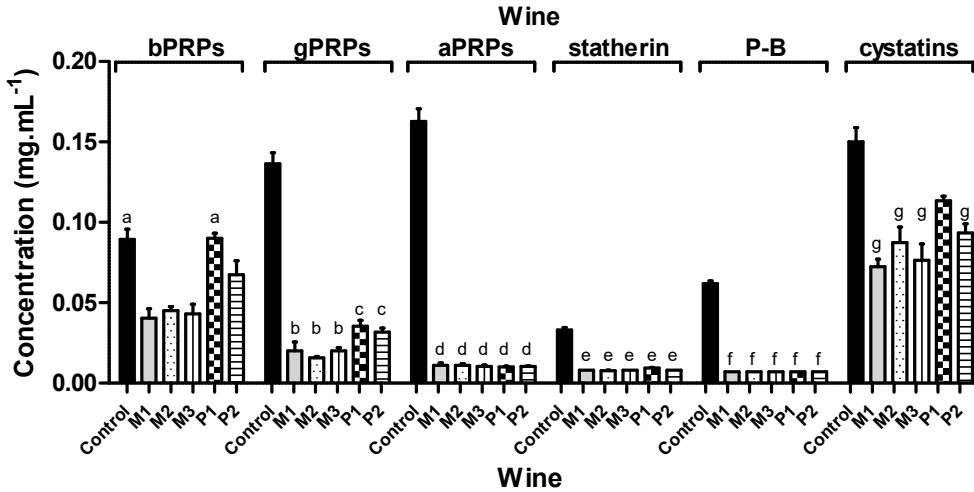


Figure 2. A. Typical salivary protein profile obtained by HPLC analysis with detection at 214nm, and identification of the major families eluted along the chromatogram. B. Modifications in the concentration (mg. mL⁻¹) for each family of salivary proteins upon the interaction with each wine (M and P) at different ratios a) 10:0.7, b) 10:2 and c) 10:3. Control condition is the concentration of each family of salivary proteins in human saliva in absence of wine. Data are presented as mean and SEM of at least three independent experiments (values with the same letter are not significantly different, $p < 0.05$).

From **Figure 2** it is possible to observe that the addition of different volumes of each wine induced significant changes on the concentration of the different salivary protein families.

The lowest saliva: wine ratio (10:0.7) led to a total decrease on the concentration of P-B peptide but also significant decreases were observed for aPRPs and cystatins. On the other hand, bPRPs and gPRPs were not reduced significantly. Besides the total decrease of P-B peptide, the saliva:wine ratio 10:2 led to a total decrease of aPRPs and statherin families. In this case, also gPRPs presented a higher decrease than for the 10:0.7 ratio while the decrease of cystatins was quite similar to the one observed previously. For the highest saliva:wine ratio, it was observed a significant decrease of almost all families of salivary proteins, except for cystatins. In this case, gPRPs were also almost totally decreased and bPRPs were significantly reduced (except for wine P1) (**Figure 2**). For this ratio, cystatins presented a similar decrease than the one observed for the other ratios.

These results are in agreement with previous ones that pointed P-B peptide, aPRPs and statherin as the salivary proteins with highest interaction toward tannins and also with other wines (Soares et al, 2011). Furthermore, these results are also in agreement with *in vivo* studies that showed that these proteins are the first ones to disappear upon the interaction with a grape seed procyanidins extract (Brandão et al, 2014).

Considering the wines effect toward the interaction with salivary proteins, for the saliva:wine ratio 10:0.7, only aPRPs showed a different interaction. In this case, it was observed that all M wines showed a higher reduction than P wines. All the other salivary proteins presented a similar interaction with the different wines at this ratio. For saliva:wine ratio 10:2, gPRPs also showed a higher reduction with M wines than with P wines, while the specificity previously observed for aPRPs disappeared by a total reduction. For the ratio 10:3 this discrimination between wines M and P was additionally observed for the bPRPs.

In summary, bPRPs, gPRPs, and aPRPs seem to have a different interaction with M and P wines when small or medium volumes of wine interact with each family of salivary proteins. When high wine:saliva ratios are used these differences dissipate. This can explain why the sensory analysis panel was not able to discriminate the astringency of both wines, corresponding to the highest wine:saliva ratio.

Considering the results, it was possible to discriminate between M and P wines, being the results in agreement with the wines chemical characterization. In the general characterizations, M wines presented higher total phenolic and total proanthocyanidin content as well as higher performance on the protein precipitation assay. However, when looking at the characterization of the individual phenolic acids composition, it is interesting to observe the content of particular compounds. In M wines, the caffeic acid is present at 610 μM , caftaric acid at 980 μM and cumaric acid at 528 μM , while in P

wines the concentration of these compounds is much lower 405 μM , 638 μM and 293 μM , respectively (**Table 2**). These compounds have been previously linked to puckering astringency and the threshold for astringency has been reported to be 72 μM for caffeic acid, 16 μM for caftaric acid and 139 μM for cumaric acid (Hufnagel and Hofmann 2008). Since these compounds occur in much higher concentrations than their thresholds it is expected that these phenolic acids could contribute to a more pucker sensation of M wine than P wines. As referred, in general, it was observed a higher interaction with salivary proteins of M wines.

In line with what was expected from an Italian wine, the interaction with salivary proteins showed moderate astringency due to an average high concentration of native phenolics and tannins. In chemical terms, M wine seemed a little more evolved and astringent than P wines.

Author Contributions: Conceptualization, J.A.; P.L., S.S. and V.F.; methodology, J.A. and E.B.; investigation, J.A. and E.B.; writing—original draft preparation, J.A. and S.S.; writing—review and editing, J.O, S.S., N.M and V.F.; funding acquisition, S.S. and V.F. All authors have read and agreed to the published version of the manuscript.

Acknowledgments: The authors thank the Science and Technology Foundation (FCT) for financial support the researcher contract, the scholarships SFRH/BD/139709/2018 (J.A.), IF/00225/2015 (J.O.), UIDB/50006/2020 and UIDBP/50006/2020. E.B. thanks the Post-Doctoral fellowship supported by the project ref. 0377_IBERPHENOL_6_E from FEDER-Interreg España-Portugal Programme. This research had financial support by the following projects PTDC/AGR-TEC/6547/2014 and NORTE-01-0145-FEDER-000011 from FCT/MEC through national funds and co-financed by FEDER.

Conflicts of Interest: The authors declare no conflict of interest.

References

- Arnous, A., Makris, D. P., & Kefalas, P. (2001). Effect of principal polyphenolic components in relation to antioxidant characteristics of aged red wines [Article]. *Journal of Agricultural and Food Chemistry*, 49(12), 5736-5742. <https://doi.org/10.1021/jf010827s>
- Azevedo, J., Fernandes, A., Oliveira, J., Brás, N. F., Reis, S., Lopes, P., Roseira, I., Cabral, M., Mateus, N., & de Freitas, V. (2017). Reactivity of Cork Extracts with (+)-Catechin and Malvidin-3-O-glucoside in Wine Model Solutions: Identification of a New Family of Ellagitannin-Derived Compounds (Corklins). *Journal of Agriculture and Food Chemistry* 65(39), 8714-8726. <https://doi.org/https://doi.org/10.1021/acs.jafc.7b02845>
- Azevedo, J., Fernandes, A., Oliveira, J., Brás, N. F., Reis, S., Lopes, P., Roseira, I., Cabral, M., Mateus, N., & de Freitas, V. (2017). Reactivity of Cork Extracts with (+)-Catechin and Malvidin-3-O-glucoside in Wine Model Solutions: Identification of a New Family of Ellagitannin-Derived Compounds (Corklins). *Journal of Agricultural and Food Chemistry*, 65(39), 8714-8726. <https://doi.org/10.1021/acs.jafc.7b02845>
- Brandão, E., Soares, S., Mateus, N., & de Freitas, V. (2014). In Vivo Interactions between Procyanidins and Human Saliva Proteins: Effect of Repeated Exposures to Procyanidins Solution. *Journal of Agricultural and Food Chemistry*, 62(39), 9562-9568. <https://doi.org/10.1021/jf502721c>
- Busse-Valverde, N., Gomez-Plaza, E., Lopez-Roca, J. M., Gil-Munoz, R., & Bautista-Ortin, A. B. (2011). The extraction of anthocyanins and proanthocyanidins from grapes to wine during fermentative maceration is affected by the enological technique. *Journal of Agricultural and Food Chemistry*, 59(10), 5450-5455.
- Chira, K., & Teissedre, P.-L. (2015). Chemical and sensory evaluation of wine matured in oak barrel: effect of oak species involved and toasting process. *European Food Research and Technology*, 240(3), 533-547. <https://doi.org/https://doi.org/10.1007/s00217-014-2352-3>
- De Freitas, V., & Mateus, N. (2001). Structural features of procyanidin interactions with salivary proteins [Article]. *Journal of Agricultural and Food Chemistry*, 49(2), 940-945. <https://doi.org/https://doi.org/10.1021/jf000981z>
- Fernandes, V. C., Domingues, V. F., de Freitas, V., Delerue-Matos, C., & Mateus, N. (2012). Strawberries from integrated pest management and organic farming: phenolic composition and antioxidant properties. *Food Chem*, 134(4), 1926-1931. <https://doi.org/https://doi.org/10.1016/j.foodchem.2012.03.130>
- García-Estévez, I., Cruz, L., Oliveira, J., Mateus, N., de Freitas, V., & Soares, S. (2017). First evidences of interaction between pyranoanthocyanins and salivary proline-rich proteins. *Food Chemistry*, 228, 574-581. <https://doi.org/https://doi.org/10.1016/j.foodchem.2017.02.030>
- Glabasnia, A., & Hofmann, T. (2006a). Sensory-Directed Identification of Taste-Active Ellagitannins in American (*Quercus alba* L.) and European Oak Wood (*Quercus robur* L.) and Quantitative Analysis in Bourbon Whiskey and Oak-Matured Red Wines. *Journal of Agricultural and Food Chemistry*, 54, 3380-3390. <https://doi.org/https://doi.org/10.1021/jf052617b>
- Glabasnia, A., & Hofmann, T. (2006b). Sensory-Directed Identification of Taste-Active Ellagitannins in American (*Quercus alba* L.) and European Oak Wood (*Quercus robur* L.) and Quantitative Analysis in Bourbon Whiskey and Oak-Matured Red Wines. *Journal of Agricultural and Food Chemistry*, 54(9), 3380-3390. <https://doi.org/10.1021/jf052617b>
- Gonçalves, R., Mateus, N., & de Freitas, V. (2011). Inhibition of α -amylase activity by condensed tannins. *Food Chemistry*, 125(2), 665-672. <https://doi.org/https://doi.org/10.1016/j.foodchem.2010.09.061>
- Granato, D., Koot, A., Schnitzler, E., & van Ruth, S. M. (2015). Authentication of geographical origin and crop system of grape juices by phenolic compounds and antioxidant activity using chemometrics. *Journal of Food Science*, 80(3), C584-C593.
- Guerreiro, J. R. L., Teixeira, N., De Freitas, V., Sales, M. G. F., & Sutherland, D. S. (2017). A saliva molecular imprinted localized surface plasmon resonance biosensor for wine astringency estimation. *Food Chemistry*, 233, 457-466. <https://doi.org/https://doi.org/10.1016/j.foodchem.2017.04.051>
- Hufnagel, J. C., & Hofmann, T. (2008). Orosensory-directed identification of astringent mouthfeel and bitter-tasting compounds in red wine. *J Agric Food Chem*, 56(4), 1376-1386. <https://doi.org/https://doi.org/10.1021/jf073031n>
- Ishikawa, T., & Noble, A. C. (1995). Temporal perception of astringency and sweetness in red wine. *Food Quality and Preference*, 6(1), 27-33. [https://doi.org/https://doi.org/10.1016/0950-3293\(94\)P4209-O](https://doi.org/https://doi.org/10.1016/0950-3293(94)P4209-O)
- Kallithraka, S., Bakker, J., & Clifford, M. N. (1997). Effect of pH on Astringency in Model Solutions and Wines. *Journal of Agricultural and Food Chemistry*, 45(6), 2211-2216. <https://doi.org/https://doi.org/10.1021/jf960871i>
- Kallithraka, S., Bakker, J., Clifford, M. N., & Vallis, L. (2001). Correlations between saliva protein composition and some T-I parameters of astringency. *Food Quality and Preference*, 12(2), 145-152. [https://doi.org/https://doi.org/10.1016/S0950-3293\(00\)00040-9](https://doi.org/https://doi.org/10.1016/S0950-3293(00)00040-9)
- Lima, M., Silani, I., Toaldo, I., Corrêa, L., & Biasoto, A. CT, Pereira, GE, & Ninow, JL (2014). Phenolic compounds, organic acids and antioxidant activity of grape juices produced from new Brazilian varieties planted in the northeast region of Brazil. *Food Chemistry*, 161, 94-103.
- Linskens, H., & Jackson, J. (1988). Phenolic composition of natural wine types— Wine analysis. In: Berlin: Springer-Verlag Press.
- Macheix, J., & Fleuriot, A. (1993). Phenolics in fruits and fruit products: progress and prospects.
- Mateus, N., Carvalho, E., Carvalho, A. R. F., Melo, A., González-Paramás, A. M., Santos-Buelga, C., Silva, A. M. S., & de Freitas, V. (2003). Isolation and Structural Characterization of New Acylated

- Anthocyanin–Vinyl–Flavanol Pigments Occurring in Aging Red Wines. *Journal of Agricultural and Food Chemistry*, 51(1), 277-282. <https://doi.org/https://doi.org/10.1021/jf020695j>
- Mateus, N., Silva, A. M. S., Rivas-Gonzalo, J. C., Santos-Buelga, C., & de Freitas, V. (2003). A New Class of Blue Anthocyanin-Derived Pigments Isolated from Red Wines. *Journal of Agricultural and Food Chemistry*, 51(7), 1919-1923. <https://doi.org/https://doi.org/10.1021/jf020943a>
- Mazza, G., & Francis, F. (1995). Anthocyanins in grapes and grape products. *Critical Reviews in Food Science & Nutrition*, 35(4), 341-371.
- McRae, J. M., Schulkin, A., Kassara, S., Holt, H. E., & Smith, P. A. (2013). Sensory Properties of Wine Tannin Fractions: Implications for In-Mouth Sensory Properties. *Journal of Agricultural and Food Chemistry*, 61(3), 719-727. <https://doi.org/https://doi.org/10.1021/jf304239n>
- Messana, I., Cabras, T., Inzitari, R., Lupi, A., Zuppi, C., Olmi, C., Fadda, M. B., Cordaro, M., Giardina, B., & Castagnola, M. (2004). Characterization of the human salivary basic proline-rich protein complex by a proteomic approach. *J. Proteome Res.*, 3(4), 792-800. <http://pubs3.acs.org/acs/journals/doi/lookup?in=doi=10.1021/pr049953c>
- Michel, J., Albertin, W., Jourdes, M., Le Floch, A., Giordanengo, T., Mourey, N., & Teissedre, P.-L. (2016). Variations in oxygen and ellagitannins, and organoleptic properties of red wine aged in French oak barrels classified by a near infrared system. *Food Chemistry*, 204, 381-390. <https://doi.org/https://doi.org/10.1016/j.foodchem.2016.02.129>
- Michel, J., Jourdes, M., Silva, M., Giordanengo, T., Mourey, N., & Teissedre, P.-L. (2011). Impact of Concentration of Ellagitannins in Oak Wood on Their Levels and Organoleptic Influence in Red Wine. *Journal of Agricultural and Food Chemistry*, 59, 5677-5683. <https://doi.org/https://doi.org/10.1021/jf200275w>
- Oliveira, J., da Silva, M. A., Jorge Parola, A., Mateus, N., Brás, N. F., Ramos, M. J., & de Freitas, V. (2013). Structural characterization of a A-type linked trimeric anthocyanin derived pigment occurring in a young Port wine. *Food Chemistry*, 141(3), 1987-1996. <https://doi.org/https://doi.org/10.1016/j.foodchem.2013.04.091>
- Puech, J.-L., Mertz, C., Michon, V., Le Guernevé, C., Doco, T., & Hervé du Penhoat, C. (1999). Evolution of Castalagin and Vescalagin in Ethanol Solutions. Identification of New Derivatives. *Journal of Agricultural and Food Chemistry*, 47(5), 2060-2066. <https://doi.org/https://doi.org/10.1021/jf9813586>
- Ribéreau-Gayon, P., & Stonestreet, E. (1966). Dosage des tanins du vin rouge et détermination de leur structure. *Chimie Analytique*, 48(4), 188-196.
- Roggero, J. P., Coen, S., & Ragonnet, B. (1986). High Performance Liquid Chromatography Survey on Changes in Pigment Content in Ripening Grapes of Syrah. An Approach to Anthocyanin Metabolism. *American Journal of Enology and Viticulture*, 37(1), 77-83.
- Soares, S., Brandao, E., Mateus, N., & de Freitas, V. (2017). Sensorial properties of red wine polyphenols: Astringency and bitterness. *Crit Rev Food Sci Nutr*, 57(5), 937-948. <https://doi.org/https://doi.org/10.1080/10408398.2014.946468>
- Soares, S., Kohl, S., Thalmann, S., Mateus, N., Meyerhof, W., & De Freitas, V. (2013). Different phenolic compounds activate distinct human bitter taste receptors. *J Agric Food Chem*, 61(7), 1525-1533. <https://doi.org/https://doi.org/10.1021/jf304198k>
- Soares, S., Vitorino, R., Osório, H., Fernandes, A., Venâncio, A., Mateus, N., Amado, F., & de Freitas, V. (2011). Reactivity of Human Salivary Proteins Families Toward Food Polyphenols. *Journal of Agricultural and Food Chemistry*, 59(10), 5535-5547. <https://doi.org/https://doi.org/10.1021/jf104975d>
- Stark, T., Wollmann, N., Wenker, K., Lösch, S., Glabasnia, A., & Hofmann, T. (2010). Matrix-Calibrated LC-MS/MS Quantitation and Sensory Evaluation of Oak Ellagitannins and Their Transformation Products in Red Wines. *Journal of Agricultural and Food Chemistry*, 58(10), 6360-6369. <https://doi.org/https://doi.org/10.1021/jf100884y>
- Trouillas, P., Sancho-García, J. C., De Freitas, V., Gierschner, J., Otyepka, M., & Dangles, O. (2016). Stabilizing and Modulating Color by Copigmentation: Insights from Theory and Experiment. *Chemical Reviews*, 116(9), 4937-4982. <https://doi.org/10.1021/acs.chemrev.5b00507>
- Van Leeuw, R., Kevers, C., Pincemail, J., Defraigne, J.-O., & Dommes, J. (2014). Antioxidant capacity and phenolic composition of red wines from various grape varieties: Specificity of Pinot Noir. *Journal of Food Composition and Analysis*, 36(1-2), 40-50.
- Vidal, S., Francis, L., Guyot, S., Marnet, N., Kwiatkowski, M., Gawel, R., Cheynier, V., & Waters, E. J. (2003). The mouth-feel properties of grape and apple proanthocyanidins in a wine-like medium. *Journal of the Science of Food and Agriculture*, 83(6), 564-573. <https://doi.org/10.1002/jsfa.1394>
- Watrelet, A. A., Heymann, H., & Waterhouse, A. L. (2020). Red Wine Dryness Perception Related to Physicochemistry. *Journal of Agricultural and Food Chemistry*, 68(10), 2964-2972. <https://doi.org/https://doi.org/10.1021/acs.jafc.9b01480>
- Yang, P., Li, H., Wang, H., Han, F., Jing, S., Yuan, C., Guo, A., Zhang, Y., & Xu, Z. (2017). Dispersive Liquid-Liquid Microextraction Method for HPLC Determination of Phenolic Compounds in Wine. *Food analytical methods*, 10(7), 2383-2397. <https://doi.org/https://doi.org/10.1007/s12161-016-0781-2>

Final Remarks and Future work

In line with described in the abstract, this work has the main purpose to study the chemical composition of cork which is able to pass for wine, in particular the polyphenolic family and its contribution to wines quality directly or after interactions with compounds in wines.

The work starts with the evaluation, qualitatively and quantitatively, of the migration of cork phenolic compounds to wine model solutions. In this part, cork samples from different geographic origins (Algarve, Badajoz, Cádiz, Douro, Castelo Branco, Alcácer do Sal, Córdoba II, Seville, Toledo, Córdoba I, Évora) were put individually in maceration with wine model solution. The results show that cork obtained from trees from the southern regions of the Iberian Peninsula (warmer climates) have higher amounts of phenolic compounds and antioxidant activity. It is important to emphasize that other factors such as the different ages of the trees, and the way they are oriented in the plantation (North or South) can also influence the discrimination of the samples in addition to geographic regions. It was possible to identify nineteen phenolic compounds, with the amount of each identified compound varies with the cork region, and which comprises different phenolic acids such as gallic acid, protocatechuic acid, caffeic acid, ferulic acid, sinapic acid, ellagic acid, protocatechuic and vanillin aldehydes and ellagic tannins such as castalagin, vescalagin, pentagalloylglucose, between others.

Moving on to optimizing the extraction of phenolic compounds from cork using UAE (ultrasound assisted extraction) and MAE (microwave assisted extraction) techniques, a mixture of cork from different planks was used. For UAE the conditions tested were time (7-30 minutes) and the percentage of ethanol in the solvent (10-90%), in the case of the MAE it was tested time (5-25 minutes), percentage of ethanol in the solvent (10 -90%) and temperature (50-150 °C). The response surface methodology (RSM) and the Desirability function were used to simultaneously maximize the yield and the total phenolic content obtained from the extraction.

The optimal conditions for UAE methodology, were found to be an extraction for 20 min using an ethanol concentration of 75% giving a maximum yield of 23.74 ± 3.71 mg extract/g dw and a total phenolic content (TPC) of 0.69 ± 0.03 mg/g dw. Finally, the application of different UAE extraction cycles, under the best conditions, led to an increase in yield to 32.24 ± 0.82 mg extract/ g dw and in TPC to 0.98 ± 0.015 mg/g dw. For the MAE technique, the maximum extraction conditions found were after 25 min, 150°C and using 90% ethanol/water, allowing a yield of 126.89 ± 6.45 mg extract/g dw

and a TPC of 1.85 ± 0.26 mg/g dw. These results were compared with those found applying the conventional maceration method (cork were placed in glass bottles with hydroalcoholic solution (50% ethanol) at 35 °C for 7 days), and it was concluded that in one hour of extraction by UAE it was possible to obtain almost the same amount of phenolic compounds as obtained in one week of maceration, and in the case of MAE the double the amount in 25 minutes, saving time and solvents. These results show that it is possible to recover bioactive compounds from industrial waste and also contribute to the Circular Economy, based on the reduction, reuse, recovery, and recycling of materials, resources, and energy. After the extraction process, the extract obtained was fractionated in a column, in order to obtain several fractions with different molecular weights (the most representative being: M1- MM average = $165 \text{ g}\cdot\text{mol}^{-1}$; M2- MM average = $483 \text{ g}\cdot\text{mol}^{-1}$; M3- average MM= $933 \text{ g}\cdot\text{mol}^{-1}$). Furthermore, some compounds were isolated such as vanillin, caffeic acid, sinapic acid, ellagic acid, and pentagalloylglucose (PGG).

The tannin/salivary protein (SP) interaction has been referred to as one of the physical-chemical phenomena at the origin of the astringency of wines (sensation of dryness and constriction perceived in the oral cavity when eating foods rich in tannins). The interaction of the three most representative fractions (M1, M2 and M3) of different phenolic compounds extractable from cork with human SP was studied by HPLC-DAD. Changes in the chromatographic profiles of SP families in saliva and phenolic compounds in cork extracts after interaction and removal by centrifugation of the insoluble precipitates formed were evaluated. Within M3, castalagin was the compound that most interacted with SP, mainly aPRPs and P-B peptide. In M2, 4-dehydrocastalagin was the most precipitated compound by all SP families. In the M1 fraction, the caffeic and sinapic compounds were the ones with the greatest interaction with SP, mainly cystatins. In general, castalagin, 4-dehydrocastalagin, caffeic, and ellagic acids shown an effective precipitation equivalent to the concentration of the compound in solution above their reported astringency thresholds, so they may contribute to the perception of astringency. Additionally, there appears to be a matrix effect (due to the presence of other compounds) that can affect the binding of a specific compound. This was observed for castalagin which bound in greater amounts to SP in the presence of other phenolic compounds (in the M2 fraction) than in the M3 fraction. It is possible to conclude that the migration of compounds presents in M2 and M3 fractions to the wine can contribute to the perception of astringency.

It is also known that the phenolic fraction that migrates from the cork stopper to the wine may also contribute to color stabilization through copigmentation phenomena. In this way, the impact of compounds isolated from cork on the phenomena of color stabilization of wine model solutions containing anthocyanins (malvidin-3-O-glucoside) was evaluated. Anthocyanins have the particularity of presenting several structures in a solution whose balance depends on the pH of the medium. In an acid medium (pH ~1) they are mainly present in their red form (flavylium cation, AH⁺), at slightly acidic pH and close to neutrality can be considered a monoprotic acid in equilibrium with its conjugated base (CB) equal to the sum of colorless form (hemiketal, B), and for neutral or higher pH (alkaline media) the formulas appear purple (A) and blue (A-) (quinoidal bases) and *cis* and *trans* chalcones (C). Copigmentation allows for stabilizing the colored forms of anthocyanins and results from the interaction of the colored chemical species of anthocyanins with each other (self-association) or with other colorless compounds called copigments forming anthocyanin-copigment complexes in a colored form. These are charge transfer complexes resulting from the hydrophobic π - π interactions between the aromatic rings of both species also stabilized by hydrogen bonds. These complexes protect the flavylium shape (red color) from the attack of water molecules, prevent the formation of the hemiketal species, and stabilize the red color. It was found that pentagalloylglucose (PGG) and sinapic acid complex with malvidin-3-glucoside, PGG complexes exclusively with flavylium cation (AH⁺), with the copigmentation constant being determined $K_{AH^+CP} = 914 \pm 10 \text{ M}^{-1}$.

For sinapic acid, the copigmentation constant of flavylium cation with the acidic form of the copigment was $K_{CP} = 243 \text{ M}^{-1}$, and no copigmentation with the basic form of the copigment, CP (-), was observed. This was explained by the very small superposition of these two species in the pH domain. The copigmentation constants of CB with the acidic and basic forms of the copigment, calculated from the UV-Vis measurements are respectively $K_{CBCP} = 53 \text{ M}^{-1}$ and $K_{CBCP(-)} = 78 \text{ M}^{-1}$.

The last part of this work, the chemical characterization of red, white and sparkling wines bottled with different types of stoppers were analyzed. These wines were used to search new compounds resulting from the interaction of compounds from cork and wine. Chromatic changes of these wines was studied by measuring the absorbance at different wavelengths defined by the CIELAB system.

The influence of cellar conditions (Cellar A, with controlled temperature and humidity allowed by conditioner air system, and a cellar B, representing a traditional cellar, with uncontrolled temperature and humidity) and bottle orientation on the phenolic and volatile

composition of a 2014 Vintage Port wine, sealed with a natural cork stopper, for 44 months after bottling was studied. This study revealed that a wine stored in a traditional cellar, under greater temperature ranges throughout the year, showed more yellow tones (in hue and b^* values), less astringency (lower specific activity of tannins), lower levels of phenylethyl acetate, and higher levels of oxidation markers (furfural and 5-methylfurfural) contributing to toasted and caramelized aromas, when compared to the same Port wine stored in a temperature-controlled cellar. In addition, Vintage Port wine stored in a horizontal position showed higher levels of total proanthocyanidins, more complex and astringent structures (higher tannin specific activity), the presence of a compound derived from the reaction of wine and cork components (Corklin) and lower levels of benzaldehyde, when compared to the same wine stored in a vertical position. Overall, these characteristics were most evident 44 months after bottling. The results obtained in this study are extremely important for the Port Wine Industry, providing new knowledge for the selection of cellar conditions and bottle orientation according to the desired characteristics of a Vintage Port Wine. In addition to the compound "Corklin" found for the first time in the wine matrix, a new compound was found whose characterization points to an adduct (+)-catechin-caffeic acid resulting from the condensation reaction between caffeic acid and (+)-catechin. The latter was found in a white wine aged 30 months in bottle. Structural characterization by NMR (^1H , COSY, HSQC and HMBC) showed that this adduct is formed by the nucleophilic attack of both C6/C8 from A ring of (+)-catechin to the electropositive C9 of caffeic acid arose from the electron-withdrawing carboxylic group. The final C-C bond formation consists in an oxidation step resulting in the new catechin-caffeic acid adduct. Caffeic acid is identified here in bottling experiments as a compound that migrates from the cork, but in the case of wines it is known that caffeic acid is a compound that already exists in the grapes and therefore this new compound may be even more important in the wines in general. On the other hand, knowing that wine is a complex matrix, other chemical structures may have formed that still need to be identified.

Finally, the polyphenolic composition of two red wines and their ability to interact with salivary proteins were also studied. It was found that both wines were very reactive with saliva proteins, which could explain their high astringent character. The wine that showed greater interaction with salivary proteins also had higher values of total phenolics, total proanthocyanidins and tannin specific activity.

In line with the work developed in this thesis, the search of new ways of extraction of bioactive compounds using a new Accelerated Solvent Extraction (ASE) technique is

expected to be more revolutionary and effective by using organic acids and aqueous solvents, or acids and bases at high temperatures, and pressure conditions that will allow to extract molecules from solid and semi-solid samples in a shorter period of time and using a smaller volume of solvent than any other extraction procedure.

Future work should be continuously addressed in the reactivity studies between cork compounds and the main compounds from wines, since these reactions usually occur at a very slow rate in wine. In fact, considering the high complexity of wine matrix, there are certainly many chemical pathways of formation of new compounds that remain to be discovered.

Considering the reactivity of cork and wine compounds and the characterization of wine astringency over in time, the evolution studies have demonstrated a correlation between the chemical composition of wine, especially in tannins, and the astringency determined by the interaction with salivary proteins. Therefore, concentrating efforts on analyzes over time will allow to obtain more knowledge on the sensory evolution of different cork-bottled wines.